Exploitation of a Marine Bacterial Resource for Drug Lead Discovery

Toyama Prefectural University

Md. Rokon Ul Karim

September 2021

Contents

List of Abbreviations

1-BuOH	1-butanol
CFU	Colony forming unit
DMSO	Dimethyl sulfoxide
EtOAc	Ethyl acetate
HCl	Hydrochloric acid
HEPES	4-(2-hydroxyethyl)-1-piperazineethanesulfonic acid
HPLC	High performance liquid chromatography
HPLC-UV	High performance liquid chromatography-ultraviolet
HR-ESI-TOFMS	High resolution-electrospray ionization-time of flight-mass spectrometry
LC-MS	Liquid chromatography-mass spectrometry
MeCN	Acetonitrile
MeOH	Methanol
MIC	Minimum inhibitory concentration
MTT	3-(4,5-Dimethylthiazol-2-yl)-2,5-diphenyl tetrazolium bromide
NMR	Nuclear magnetic resonance
ODS	Octadecyl-silica
TFA	Trifluoroacetic acid
XTT	Sodium 3′-[1-[(phenylamino)-carbony]-3,4-tetrazolium]-bis(4-methoxy-6-nitro)benzene-sulfonic acid hydrate

CHAPTER 1

Introduction

1-1 Introduction

Natural products are organic molecules usually produced by the natural selection and evolutionary processes that provide unprecedentedly high structural variety and unique pharmacological or potential biological activities [1]. These molecules are commonly known as secondary metabolites produced by living organisms, which are dispensable and not absolutely essential for survival. But they have a wide range of function that is helpful for their producers' evolutionary advantages. It is not easy to explain about all secondary metabolites how they help their producers yet; some of these molecules are produced for specific purposes such as nutrient limitation, signaling and defense [2]. The structural diversity of secondary metabolites far exceeds compared with the synthetic organic molecules, which are synthesized in laboratory. Natural products serve as drug templates which receive synthetic modifications to decrease side effects and increase bioavailability. Until now, approximately half of drugs approved by U.S. Food and Drug Administration (FDA) are discovered from natural products [3].

Natural products are usually obtained from cells, tissues, and secretions of microorganisms, plants and animals. Crude extracts from these sources contain a wide range of structurally diverse bioactive natural products. The biological properties of natural products can be noticed and ascribed to a single molecule or a set of related compounds produced by the organism. These biologically active chemical compounds can be utilized in drug discovery and development [4, 5]. Traditionally, microorganisms, plants and animals are the most valuable source of bioactive natural products. Several number of blockbuster bioactive compounds derived from plants have been utilized as traditional and modern medicines. Plant natural products have provided a variety of medicines including antibiotics, anticancer, immunosuppressants, and so on [6]. Probably the most famous and well-known example is an acetylsalicylic acid (aspirin), potent anti-inflammatory drug derived from the salicin, the natural product originally isolated from the bark of willow trees [7]. Morphine, isolated from the plant *Papaver somniferum*, is an analgesic drug first reported in 1804 [8]. Digitoxin, a cardiotonic glycoside, isolated from plant *Digitalis purpurea*, was found to enhance cardiac conduction and improve the strange cardiac contractibility [9]. Quinine is an anti-malarial drug isolated from the bark of *Cinchona succirubra*. It is also an effective medicine for the treatment of fever, indigestion, mouth and throat diseases [10].

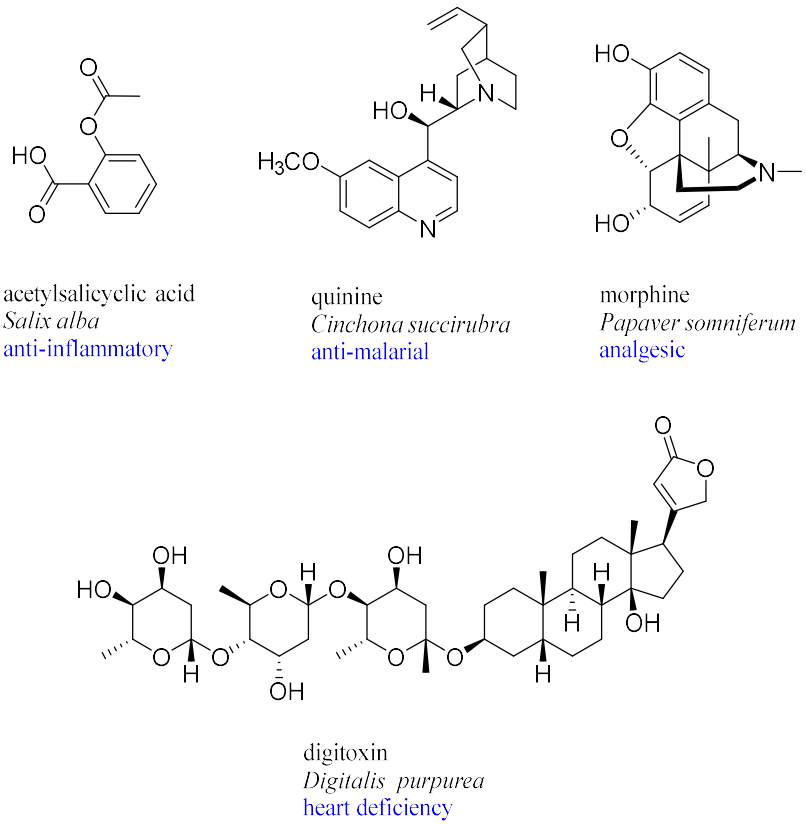

Figure 1-1. Examples of plant-derived drugs.

Natural products from microorganisms are characterized by a broad spectrum of chemical and biological activities and they act as a remarkable class of therapeutics to heal various ailments [11]. These microbial metabolites are responsible not only for the adaptation of microorganisms to their environment but also play an important role in ecological interactions with others. A number of microbial natural products have been developed as new drugs or lead compounds in the pharmaceutical, cosmetic, agrochemical, food industries, and others [12]. Among all microorganisms, fungi have an important role in human life for thousands of years by various prospect including food (mushrooms) and alcoholic beverages (yeasts). Recent developments of biotechnology, fungi are used in biological control, antibiotics and other pharmacologically active products [13]. Penicillin is a well-known antibiotic isolated from the fungus *Penicillium rubens* by Alexander Fleming in the early 20th century. The application of penicillin has effectively controlled a number of bacterial infection diseases such as pneumonia, syphilis and cellulitis [14]. After the first clinical use of penicillin in 1940s, a worldwide search for new bioactive natural products from microorganisms began [15]. Mevastatin, isolated from the fungus genus *Penicillium*, is used as a potent hypolipidemic agent [16].

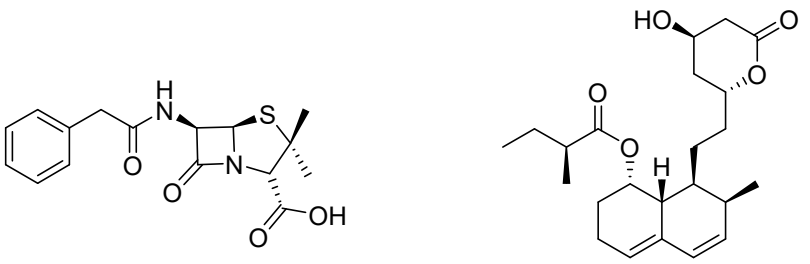

penicillin G
Penicillium
antibacterial

mevastatin
Penicillium
hypolipidemic agent

Figure 1-2. Examples of fungi-derived drugs.

One of the bacterial groups, actinomycetes, is another potential source in terms of producing commercially important bioactive compounds such as enzymes, antibiotics and pigments. Two-third of drugs has been derived from these diverse bacterial taxa [17]. The first aminoglycoside antibiotic designated streptomycin was dicovered from *Streptomyces griseus* by Selman Abraham Waksman in 1943, which is an important milestone in the history of antibiotic [18]. In 1948, the tetracycline antibiotic known as aureomycin was isolated from soil-derived *Streptomyces aureofaciens* [19]. Vancomycin, a glycopeptide antibiotic produced of *Amycolatopsis orientalis* and approved by the FDA in 1958, was first isolated by Edmund Kornfeld in 1953, and are active against a wide range of Gram-positive organisms such as staphylococci and streptococci and against Gram-negative bacteria, mycobacteria and fungi [20]. Erythromycin, a 14-membered macrolide composed entirely of propionate units and being isolated from *Saccharopolyspora erythraea*, is an antibacterial drug that has broad spectrum antibacterial activities against Gram-positive cocci and bacilli [21]. Doxorubicin, a potent chemotherapeutic agent to treat various types of blood and solid tumors, belongs to the anthracycline family of antibiotics originally isolated from *Streptomyces peucetius* from soil of sourthern Italy in 1957 [22, 23].

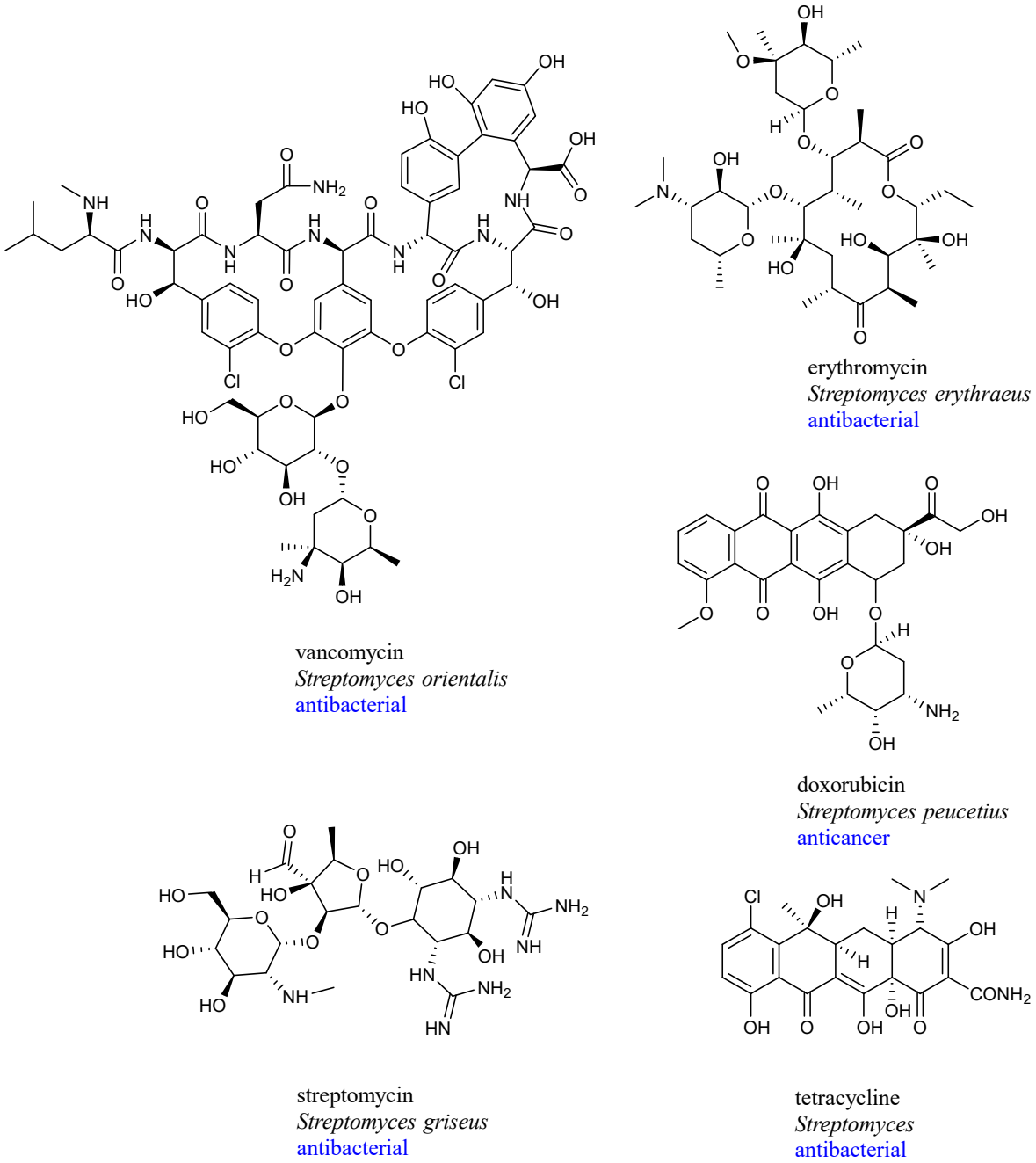

Figure 1-3. Examples of actinomycetes-derived drugs.

Terrestrial ecosystem is considered as a prolific source of diverse chemicals, structurally novel secondary metabolites and unique therapeutic compounds. Metabolites from terrestrial source provided several medicines such as antibiotics, anticancer, and immunosuppressants [24]. Recently, the rate of discovery of novel metabolites from well-established traditional terrestrial ecosystem has diminished dramatically. Therefore, new sources are needed to be explored for the quest of new bioactive compound discovery. In this sense, new, unexplored, unusual and extreme habitat such as marine ecosystems offer a promising opportunity to find

structurally unique compounds with innumerable valuable biological activities [25]. Principally, unexplored organisms from marine environment represent the best way for screening of new metabolites because of divergence of biosynthetic pathways. Overall, marine ecosystems can therefore still be considered as a potential, relatively underappreciated source of novel bioactive compounds that are yet to be discovered.

1-2 Marine Environment as an Unexploited Source for Bioactive Natural Products

The ocean covers more than 70% of our planet and hosts a wide array of species diversity. Approximately, 95% of the biosphere is represented by the sea. Around 34 phyla are found in the marine environment from 35 taxonomically identified animal phyla. Most of these are residing only in marine ecosystem. This biodiversity makes the ocean to be the complex ecosystem on earth. It is an extraordinary habitat for more than 200,000 described species including microorganisms, algae, sponges, bryozoa, mollusks, corals and echinoderms [26].

Thus, the oceans are an unexplored area of searching for the discovery of pharmacologically active compounds, which may provide good results for exploiting and developing valuable marine drugs that can be used against a wide range of human diseases. Marine organisms have been proven to be a very rich source of biological and chemical diversity of bioactive compounds, which have attracted the interest from chemistry and pharmaceutical science [27]. In the last two decades, thousands of compounds have been isolated from marine organisms. On the other hand, literature survey showed that only a small fraction of the total number of marine species has been investigated for their constituent natural products [28].

Secondary metabolites are not essential for the producing organism for basic or primary metabolic processes, but because marine organisms are soft bodied and unmoved, they protect themselves from different threat by producing toxic compounds or obtaining them from symbiotic microorganisms to defense against predator or to paralyze their prey. Other important factors are ecological pressures, including competitions for food and space, fouling of predators, which led to evolution of secondary metabolites with biological activities [29]. Therefore, marine organisms are suitable in the discovery of novel chemicals for the development of new drugs for the treatment of human diseases.

Marine environments are considered to be harsh compared to terrestrial ecosystem with regard to high salinity, low oxygen concentration, extreme temperature (low and high), high hydrostatic pressure, limited light availabity, nutrition, stress and ambient pH. These harsh

conditions are responsible for the production of a great variety of structurally unique compounds in terms of diversity, structural and functional features and also potential bioactivity in relation to natural products from terrestrial life form. Basically, multispecies communities including actinomycetes, fungi and bacteria are residing in marine environment and they must physioloigally and biologically adapted for survival. Such adaptations usually involve modification of metabolic pathways by stimulated signal molecule formation resulting in production of a great variety of molecules bearing unique structures with potent biological activity [30, 31].

Finding new compounds from terrestrial source is now getting more difficult due to rediscovering of the known compounds. In contrast, marine-derived sources are yet to be examined for natural products discovery. The searching of bioactive natural products from marine organisms has started recently later than terrestrial plants and nonmarine microorganisms. Therefore, a large portion of this source is remaining uncultured for new bioactive compound screening program. Over 28,500 marine natural products had been reported and characterized by the end of 2016. Most of them exhibit a wide range of diverse bioactivity such as anticancer and antibacterial [28]. A large number of marine natural products were isolated form marine invertebrates such as corals, tunicates, sponges and molluscs. Many marine organisms have not been studied for new bioactive screening program. Therefore, marine environment could be an unexploited source for new drug discovery. Two arabino-nucleosides, spongothymidine and spongouridine, isolated from the extract of sponge *Tethya crypta* (currently *Tectitethya crypta*) in the early 1950s, are the first marine natural product [32] (Figure 1-4).

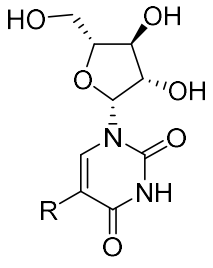

spongothymidine : R= Me
spongouridine : R = H
Tectitethya crypta

Figure 1-4. Structures of arabino-nucleosides.

Marine organisms have been an attractive research topic for scientists all over the world for the past 30-40 years [33]. Every year the number of natural products of marine organism is increasing [34] (Figure 1-5).

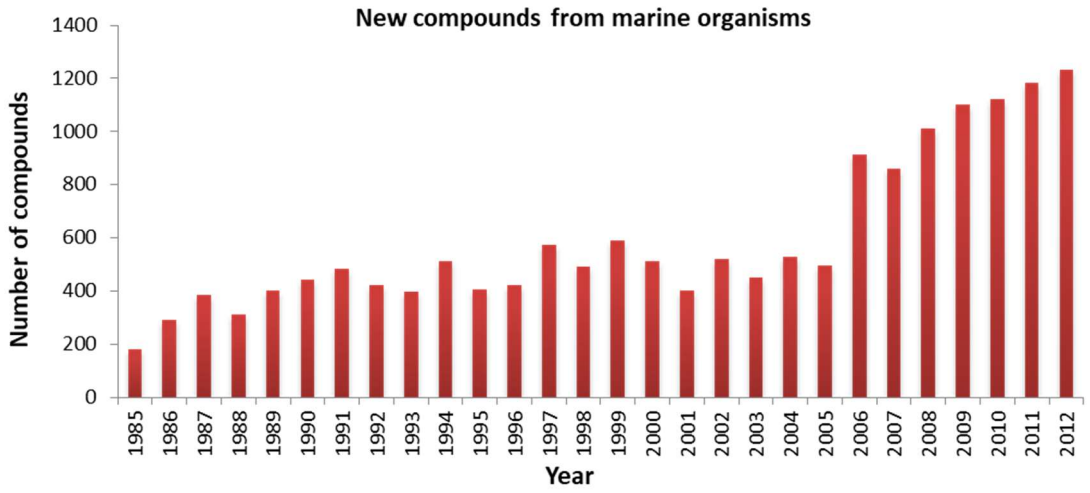

Figure 1-5. Variation in number of new marine natural products for 1985–2012.

1-3 Molecular Targets of Marine Natural Products

Marine natural products have been expected to increase the number of pipelines of drug development. These metabolites possess unique structural architectures and inspire the drug development against a variety of diseases. They are also applied as bioprobes to disclose biological pathways and exploring unconventional biological space for drug discovery. Drugs derived from marine natural product exhibits potential bioactivity by targeting unusual biological space into the cell including lipid membrane component and proteins (enzymes and G protein-coupled receptors). Among them, a few marine natural products such as theonellamide A, merizomib and seriniquinone are the molecular targeting agents against human diseases [35].

Bicyclic dodecapeptide theonellamide A, discovered from the marine sponge *Theonella* sp., shows antifungal activity and mild cytotoxicity against mammalian cells (Figure 1-6). The previous study showed that theonellamide A binds with sterols at the surface of membrane in living cells. After binding, morphological change of the cell membrane occurred by the accumulation of theonellamide A. Because of these unique properties, most of theonellamide-based compounds would enable to bind with sterol-containing domains in living cells that could further unveil the dynamic changes in membrane morphology (Figure 1-7). Another

theonellamide congener derivative, namely, theonellamide F showed chemogenic properties by activating Rho1- dependent 1,3-β-D-glucan synthesis, which was responsible for the membrane damage in living cells [36].

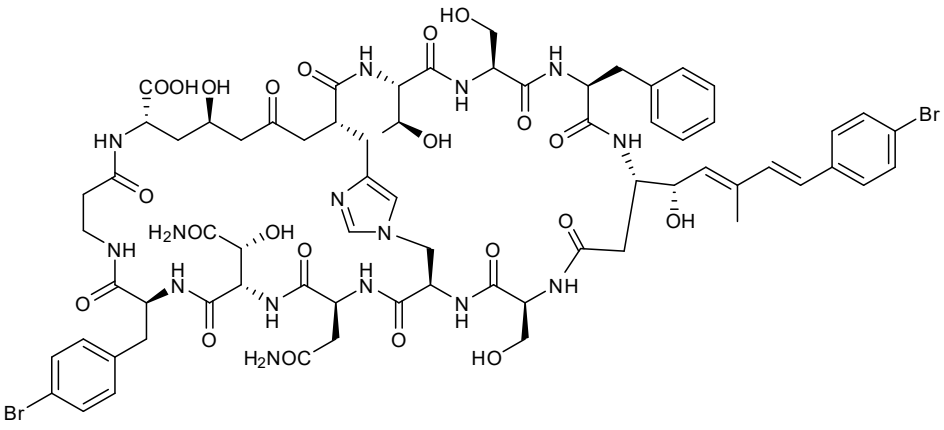

Figure 1-6. Structure of theonellamide A.

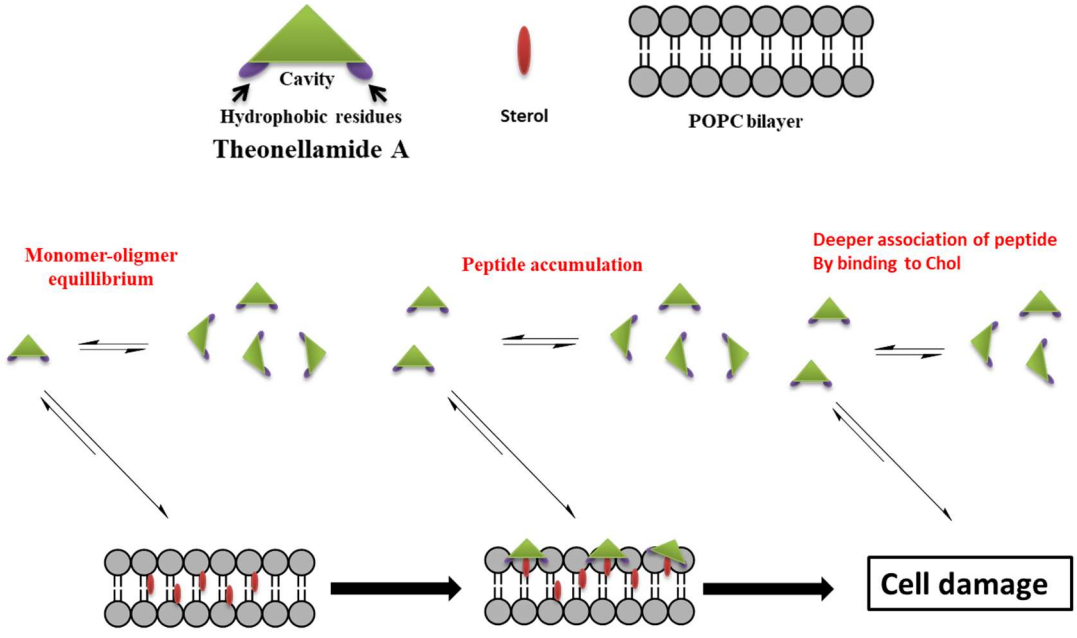

Figure 1-7. Mode of action of theonellamide A.

Marizomib (NPI-0052, salinosporamide A), a second-generation small molecule proteasome inhibitor, was discovered from marine obligate actinobacteria *Salinospora tropica* and *Salinispora arenicola,* which are composed of bicyclic β-lactone γ-lactam ring

(Figure 1-8). The structure of marizomib is different from other peptide-based proteasome inhibitors such as bortezomib and carfilzomib. Marizomib has a broad spectrum of inhibition activity for the 20S proteasome compared with bortezomib and carfilzomib and has been exhibited to inhibit all three active sites including CT-L (β5) CT-T-laspase-like (C-L, β1) and trypsin-like (T-L, β2) of the 20S proteasome in multiple myeloma and in solid tumors. Moreover, marizomib activates several types of caspases (ie, 3, 8, and 9), which is responsible for building up reactive oxygen species (ROS), and thus inhibits tumor cell proliferation [37, 38].

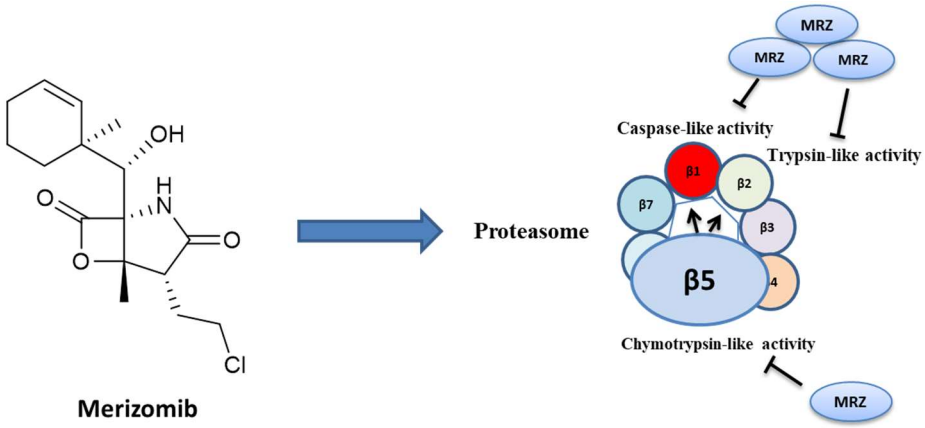

Figure 1-8. Mode of action of marizomib on tumor cell.

Another marine natural product, seriniquinone, was discovered from a marine bacterium *Serinicoccus* and exhibited selective activity against different type of melanoma cell lines in the NCI-60 screen panel (Figure 1-9). This is the first molecule from marine natural product that targets dermcidin and dermcidin-conjugated proteins in tumor cells. Emerging data revealed that seriniquinone binds with dermcidin that plays an important role in stabilizing cancer and provides a new cell-specific process to initiate autophagy and apoptotic cell death [39].

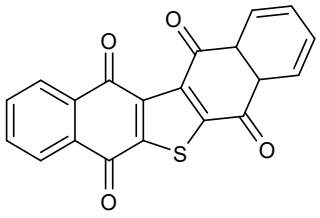

Figure 1-9. Structure of seriniquinone.

1-4 New Therapeutics from Marine Natural Products

Natural products have proven to be a promising source of new therapeutics with diverse and novel structures used against a wide range of human diseases and are a major component of the modern pharmaceuticals. Several new therapeutics have been developed from marine natural products. These marine drugs are being used for the treatment of human diseases including cancer, viral infection, Alzheimer's disease, chronic pain, and hypertriglyceridemia [40].

Untill now, fourteen marine-derived drugs are approved by the FDA (Figure 1-10). For example, two nucleosides, the anticancer cytrabin (ara-C) and antiviral vidarabine (ara-A), sponge derived arabino-nucleosides were approved by FDA in 1969 and 1976, respectively, and firstly introduced as a part of the pharmacopeia which are utilized to treat human disease. Cytarabine (arabinosyl cytosine) is a synthetic pyrimidine nucleoside, developed from spongothymidine, a nucleoside discovered from the Caribbean sponge *Tethya crypta*. Cytarabine is an S-phase specific antimetabolite cytotoxic agent, which showed inhibition of DNA polymerase and DNA synthesis by transferring intracellularly to cytosine arabinoside triphosphate. Cytarabine is used as a drug for the treatment of acute lymphocytic leukemia, acute myelocytic leukemia and blast crisis phase of chronic myelogenous leukemia and meningeal leukemia. Another example of marine-derived approved drug known as vidarabine (arabinofuranosyladenine or adenine arabinoside, Ara-A), a nucleoside originally discovered from the sponge *Tethya crypta*, is currently isolated from *Streptomyces*. It is a synthetic purine nucleoside, which was developed from spongouridine. Vidarabine showed potent anticancer activity which inhibits viral DNA polymerase and DNA synthesis of herpes, vaccinia and varicella zoster viruses [31]. Omega-3 acids are essential drugs for treating human disease, which was approved in 2004. Until now, there are three main types of omega-3 fatty acids, alpha-linolenic acid (ALA), eicosapentaenoic acid (EPA), and docosahexaenoic (DHA). EPA and DHA are found from fish. These drugs are showing effectiveness for reducing hypertriglyceride levels in patients with hypertrig vlyceridemia [41]. A marine depsipeptide, plitidepsin, was isolated from a tunicate *Aplidium albicans*. It is used for the treatment of solid tumors and lymphomas [42]. Lurbinectedin was isolated from a marine-derived species *Ecteinascidia turbinate.* In June 2020, it was first approved in the United States. Lurbinectedin is used for the treatment of adults with metastatic small cell lung cancer (SCLC) [43]. Trabectedin, an antineoplastic agent, was originally isolated from the Caribbean marine tunicate *Ecteinascidia turbinate.* It is used for the treatment of soft-tissue sarcoma and

ovarian cancer. Trabectedin was approved as a potential antineoplastic drug by FDA in 2015 [44].

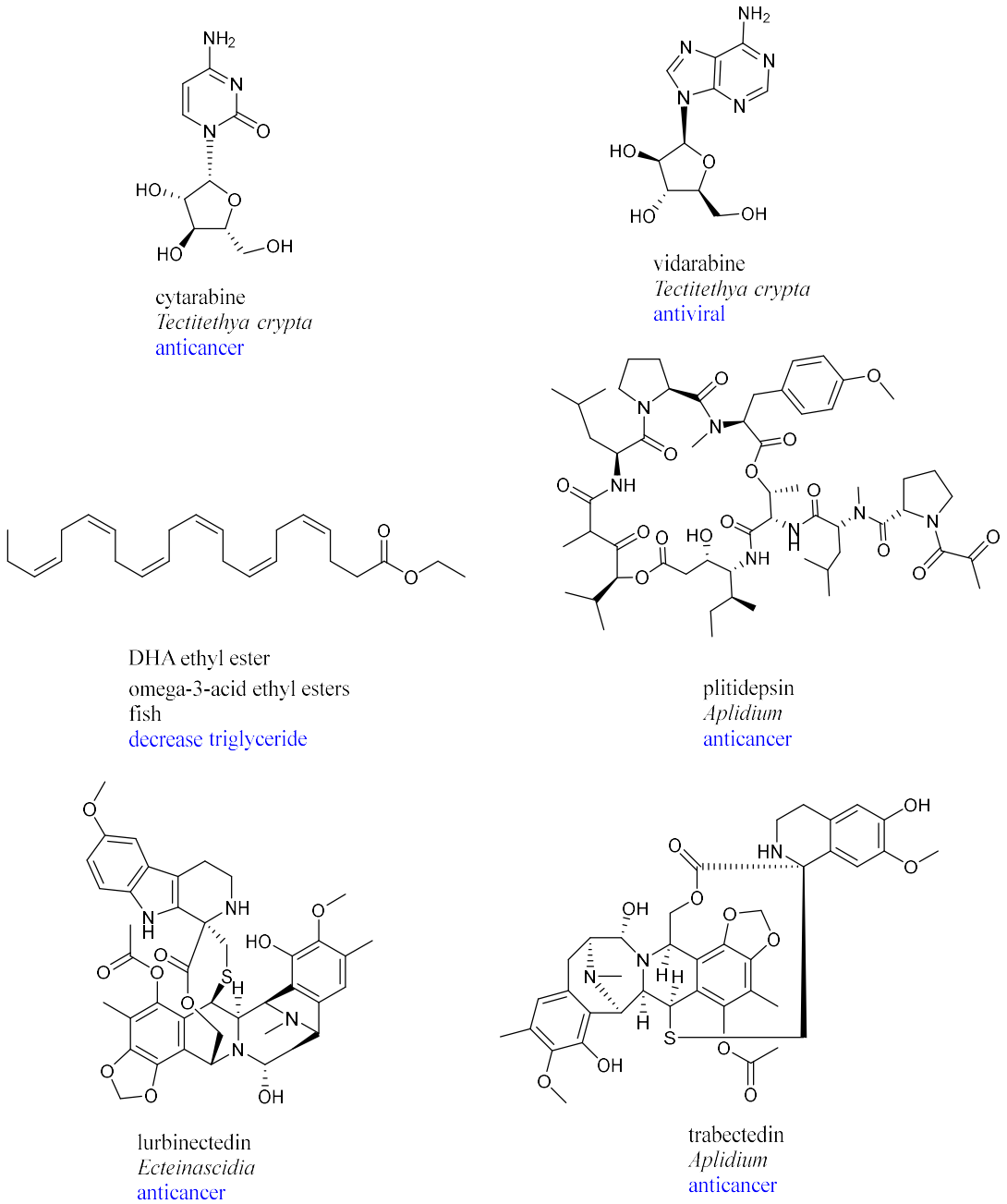

Figure 1-10. Examples of approved drugs from marine natural products.

There are several marine derived natural products tested in different phase of clinical trials. Six compounds are undergoing phase III clinical trials and fourteen other compounds are in phase II clinical trials, and 10 compounds are in phase I and several drugs in preclinical trials (Figure 1-11). Bryostatin, macrocyclic polyketide, was first isolated from the bryozoan *Bugula neritina* in 1968. The main pharmacological mechanism of action of bryostatin is

modulation of protein kinase C (PKC) activity, which was firstly synthesized in 1982. Bryostatin is currently in phase I clinical trial for the Alzheimer's disease [45]. Marizomib (NPI-0052; salinosporamide A), isolated from a marine actinomycete bacteria *Salinospora tropica* and *Salinispora arenicola*, is a proteasome inhibitor which is undergoing phase III clinical trial for the treatment of solid tumors and refractory lymphoma [46]. Plocabulin isolated from the Madagascan sponge *Lithoplocamia lithistoides* is a new polyketide which is currently in phase II trial in patients with advanced malignancies [47]. Plinabulin is a synthetic analogue of halimide, discovered from *Aspergillus* sp. It is now undergoing phase III clinical trials against solid tumors and lymphomas [48]. Monomethyl auristatin E (MMAE) is a synthetic analog of dolastatin 10, originally obtained from the sea hare *Dolabella auricularia*. MMAE, a highly potent microtubule inhibitor, exhibits broad spectrum of anticancer activity against a multitude of lymphomas, leukemia, and solid tumors. It is now undergoing phase III clinical trials [49].

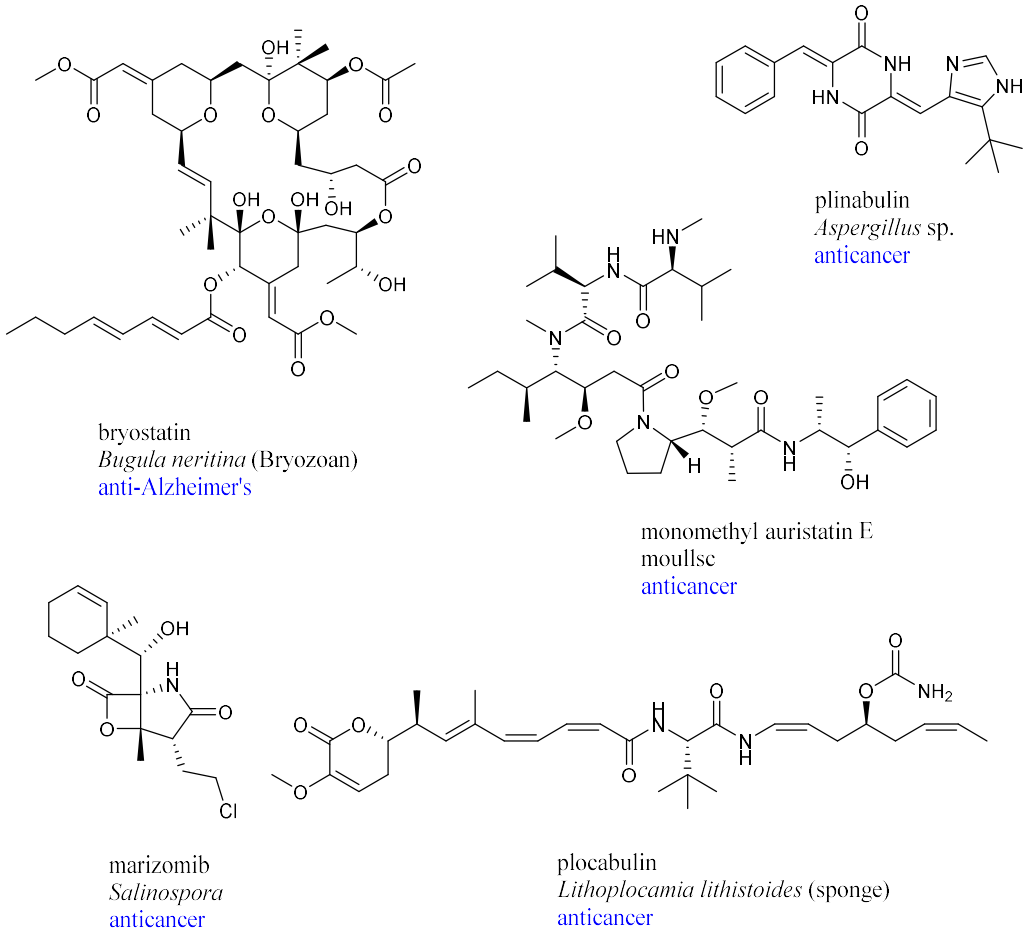

Figure 1-11. Examples of marine natural products in clinical trials.

1-5 Marine Microorganisms are a Reservoir of Bioactive Compounds.

In marine environments, microorganisms occupy nearly 90% of the total biomass. These microbial communities are responsible for up to 98% of primary marine productivity and are important players in mass and energy fluxes in marine environment [50, 51]. Microorganisms live on the oceanic subsurface making complex communities and concentration is up to 3.5×10^{30} [52]. Beside oceanic water surface, microorganisms are also living with marine invertebrates. Corals and sponges are major invertebrates with an immense biodiversity, which can be compared to that of the tropical rain forest and contributes largely to the primary productivity in the sea. Microbial communities interact and establish symbiotic associations at the surface or in the tissue of invertebrates which could be harmful or beneficial depending on its microbial structure and functionality [53]. Therefore, microorganisms have kept an important contribution in their host health by producing secondary metabolites. These marine microbial metabolites have provided diverse types of bioactivities, which can be developed as a new drug candidate.

Marine environment is an untapped source of various types of microbial community and therefore, of new bioactive compounds. Marine microorganisms including bacteria and fungi are the most magnificent source of producing new natural products. The prime species of bacteria found in marine ecosystem contain the genera *Pseudomonas*, *Vibrio*, *Achromobacter*, *Flavobacterium* and *Micrococcus*. However, among all of these marine bacterial genera, actinomycetes are the main providers of novel compounds so far, numerous structurally new compounds with potent bioactivity have been discovered in the past few years. Marine bacteria are considered to possess physiological, biochemical and molecular characteristics that are distinct from their terrestrial ecosystems, which is responsible for producing different compounds. Among them, a few new compounds with rare structure and potent and diverse bioactivity such as lodopyridone, marinomycins and proximicins have been reported.

Lodopyridone, a unique alkaloid, was isolated from a marine *Saccharomonospora* collected from marine sediment. This compound exhibited activity against the human colon adenocarcinoma cell line HCT116 [54]. Proximicins were isolated from the marine *Verrucosispora* strain MG-37, which are composed of unusual structural element of 4-amino-furan-2-carboxylic acid. Proximicins show a strong cytostatic effect to various human tumor cell lines as well as weak antibacterial activity [55]. Marinomycins, unusual macrodiolides composed of dimeric 2-hydroxy-6-alkenyl-benzoic acid lactones with conjugated tetraene-pentahydroxy polyketide chains, were isolated from a marine actinomycete, *Marinispora* sp. [56]. Marinomycins have effective antibacterial activities against drug resistant bacterial

microorganisms and display impressive and selective cancer cell cytotoxicities against six melanoma cell lines. Pteridic acids C-G, five new spirocyclic polyketides, were isolated from *Streptomyces* sp. collected from gorgonian coral *Melitodes squamata* [57]. Pteridic acids C, D and E display weak antibacterial activity against *Bacillus subtilis*. Five novel polyhydroxy polyketides, nahuoic acids B-E, were from the culture broth of *Streptomyces* sp. collected from gorgonian coral *Melitodes squamata*. All compounds exhibited weak antibiofilm activity toward *Shewanella onedensis* biofilm [58]. Octalactin A, an octatomic ring lactone, was isolated from a *Streptomyces* sp. collected from the surface of the gorgonian octocoral *Pacifigorgia* sp. Octalactin A displayed strong cytotoxic activity against human melanoma B-16-F10 and colon carcinoma HCT-116 cell lines [59].

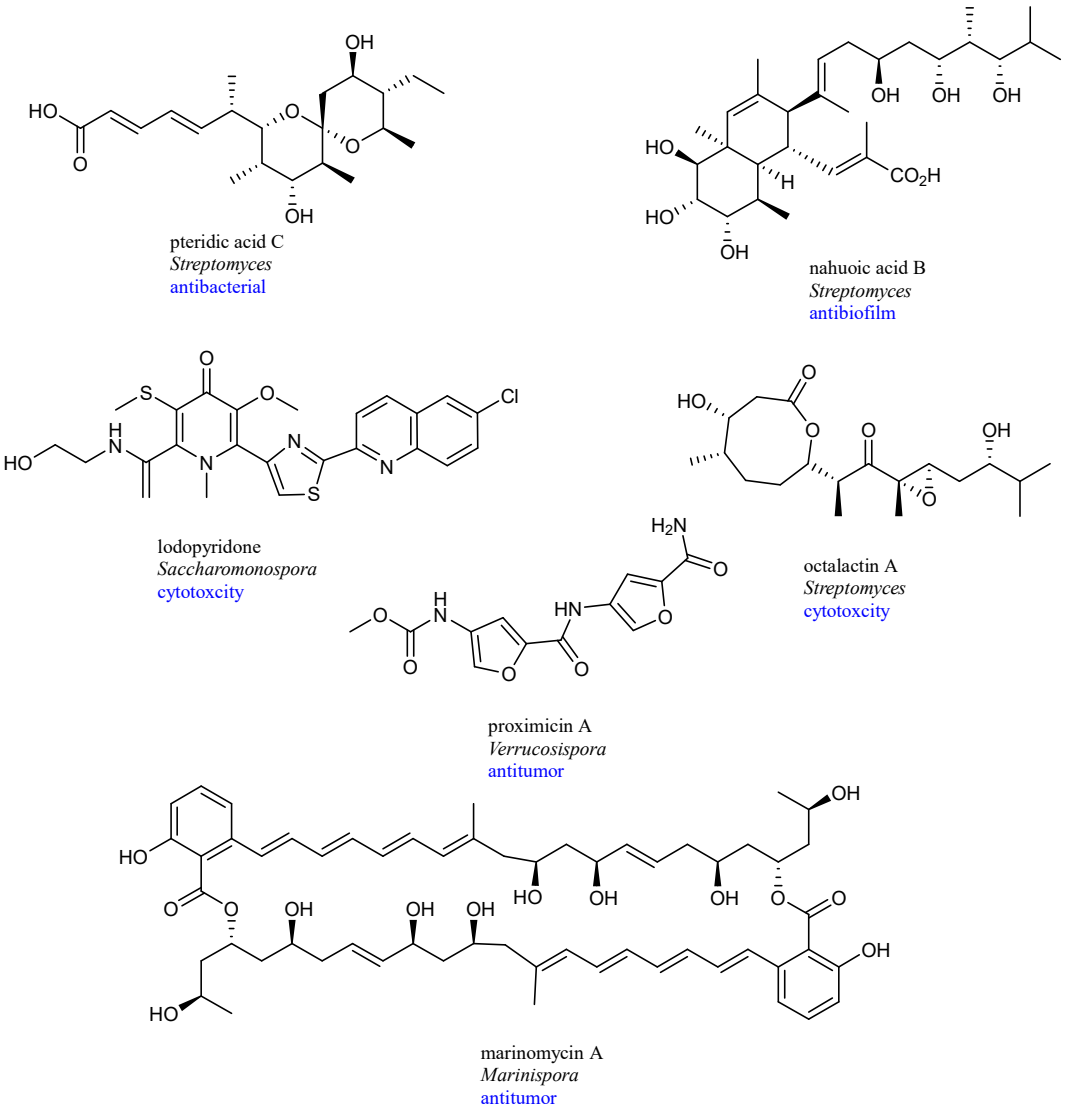

Figure 1-12. Structures of natural products from marine-derived actinomycetes.

Marine fungi are another promising source of new bioactive compounds for the drug discovery. Around 38% of the approximately 22,000 bioactive microbial natural products are reported from fungal origin [60]. A number of bioactive compounds with rare chemical structure have been isolated from marine fungi such as polyketides, alkaloids, terpenes and peptides. These compounds show a range of bioactivities, such as antibacterial, antiviral, and anticancer agents. Penicillanthranin A was isolated from a marine fungus *Penicillium citrinum* and displayed moderate antibacterial activity against both *Staphylococcus aureus* and methicillin-resistant *S. aureus* [61]. Oxalicumones A, dihydrothiophene-condensed chromones, was obtained from a fermentation broth of marine *Penicillium oxalicum* collected from soft coral *Muricella flexuosa* [62]. Versicolactone G was obtained from a marine fungus *Aspergillus terreus* collected from soft coral and showed potent α-glucosidase inhibitory activity [63]. Spirotryprostatin F, a spirocyclic diketopiperazine alkaloid, was isolated from *Aspergillus fumigatus* collected from soft coral *Sinularia* sp. Spirotryprostatin F showed stimulating action on the growth of sprout roots including soy (Glycine max) buckwheat (*Fagopyrum esculentum*), and corn (Zea mays) [64]. Aspernolides A, an aromatic butenolide, was isolated from the culture broth of *Aspergillus terreus* collected from soft coral *Sinularia kavarattiensis*. Aspernolide A exhibited moderate cytotoxicity against cancer cell lines [65]. 4'-*O*-Methyl-asperphenamate, a phenylalanine derivative, was isolated from the culture broth of *Aspergillus elegans* collected from a soft coral *Sarcophyton* sp. This compound exhibited selective antibacterial activity toward *Staphylococcus epidermidis* [66]. Two new benzylazaphilone derivatives with an unusual carbon skeleton, aspergilone A and its symmetrical dimer with a unique methylene bridge, aspergilone B, were isolated from the culture broth of *Aspergillus* sp. obtained from a gorgonian coral *Dichotella gemmacea*. Aspergilone A showed cytotoxicity against HL-60 human promyelocytic leukemia, MCF-7 human breast adenocarcinoma and A-549 human lung carcinoma cell lines [67]. This compound also exhibited potential antifouling activity against the larval settlement of barnacle *Balanus amphitrite*. Anthraquinone derivative, named 8-*O*-methylnidurufin was isolated from culture broth of *Aspergillus* sp. isolated from soft coral *Dichotella gemmacea*. 8-*O*-Methylnidurufin displayed strong antibacterial activity against *Micrococcus luteus* [68]. Aspergillipeptides A-C were obtained from a culture broth of *Aspergillus* sp. isolated from gorgonian coral *Melitodes squamata*. Aspergillipeptide C displayed strong antifouling activity toward *Bugula neritina* larvae [69]. Two prenylated indole alkaloids, 17-epinotoamides Q and M were obtained from static culture of *Aspergillus* isolated from gorgonian coral *Dichotella gemmacea* [70]. Phenalenones, a herqueinone class compounds,

were isolated from a marine-derived fungus *Penicillium*. These compounds displayed moderate anti-angiogenetic and anti-inflammatory activities [71]. Fusaridioic acid A, a new alkenoic acid, was isolated from the fungus *Fusarium solani* collected from mangrove sediments [72].

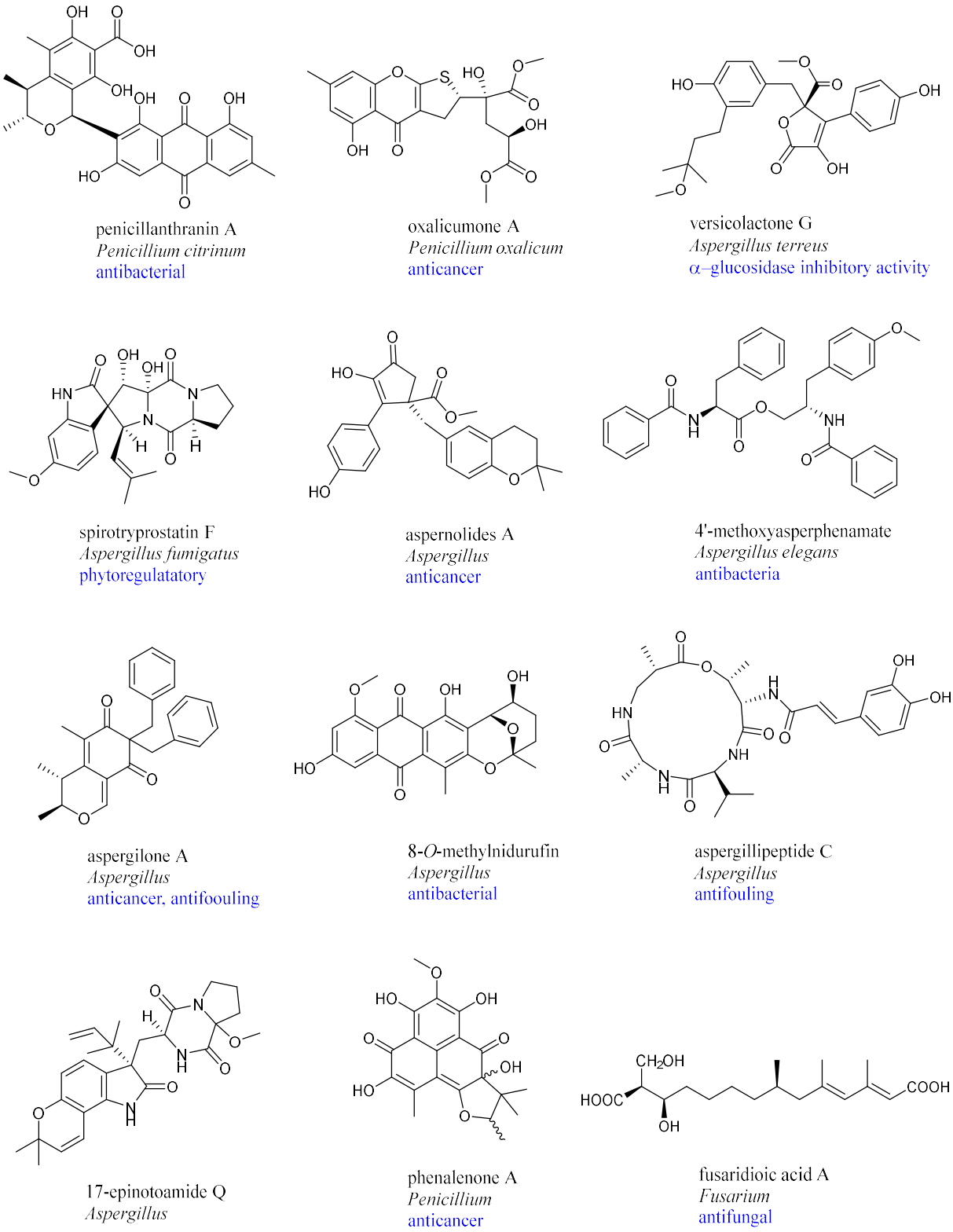

Figure 1-13. Structures of natural products from marine-derived fungi.

In this study, marine bacteria were chosen for the screening of new drug lead discovery. These marine bacteria were isolated from two unexploited or underexplored sources, stony corals and deep-sea water. Stony corals and thire associated microorganisms are largely neglected for new bioactive compound discovery. Marine bacteria commonly inhabit at the surface of stony corals by symbiotic associations. These bacteria can help their host (stony corals) in response to environmental factors such as aging, diseases, and physiological state upon interaction, which may alter the biosynthetic gene clusters responsible for the production of diverse type of structurally new bioactive compounds. Past investigation showed that stony coral-associated microorganisms are not over exploited for screening of new bioactive compounds compared to soft-coral associated bacteria. This may be because limited research has done with respect to new compounds from microorganisms residing stony corals. To the best of our knowledge, a few papers have been published regarding on natural products from stony coral-associated bacteria. In this study, to get bioactive compounds, marine bacteria were isolated from another unexploited source, deep sea water. Still, most of the bacteria from deep sea water have not been cultured yet for new compounds screening. Therefore, there is a high chance to get new bioactive natural products from this unexploited source. This study was conducted to estimate the ability of marine bacteria from both sources such as stony corals and deep-sea water to produce new bioactive compounds.

Literature reviews showed that marine microorganisms are the source of structurally rare metabolites with diverse bioactivities. These compounds are composed of several novel structures including polyketones, pyrones, cyclic peptides, lactones, and alkaloids and exhibit potential activities such as cytotoxicity, antibacterial, antifouling, phytoregulatory, and antiviral etc. This result suggested that bacteria from marine ecosystem can be an important source for getting new compounds with diverse bioactivities. Most of the research have been focused on natural products from marine fungi. The number of natural products from marine bacteria is less compared to terrestrial bacteria because only limited research has been done with bioactive compounds from bacteria obtained from marine environment. Many cultivable microorganisms have not been thoroughly exploited in terms of natural product biosynthesis abilities. Natural products derived from marine bacteria are still representing an unexploited but potential source for new drug discovery.

References

1) Hong, J. *Curr Opin Chem Biol*. **2011**, *15*, 350-354.
2) Iwagawa, T.; Miyazaki, M.; Okamura, H.; Nakatani, M.; Doe, M.; Takemura, K. *Tetrahedron Lett.* **2003**, *44*, 2533-2535.
3) Newman, D. J.; Cragg, G. M. *J. Nat. Prod.* **2020**, *83*, 770–803.
4) Strobel, G.; Daisy, B. *Microbiol. Mol. Biol. Rev*. **2003**, *67*, 491–502.
5) Cushnie, T. P.; Cushnie, B.; Echeverría, J.; Fowsantear, W.; Thammawat, S.; Dodgson, J. L.; Law, S.; Clow, S. M. *Pharm. Res.* **2020**, 3*7*, 125-148.
6) Strobel, G.; Daisy, B. *Microbiol Mol Biol Rev*. **2003**, *67*, 491-502.
7) Ganjehei, L.; Becker, R. C. *J. Thromb. Thrombolysis.* **2015**, *40*, 499-511.
8) Norn, S.; Kruse, P. R.; Dan, K. E. *Medicinhist. Arbog*. **2005**, *33*, 171-184.
9) Der Marderosian, A.; Beutler, J. A. *The Review of Natural Products* **2002**, 13-43.
10) Andrade-Neto, V. F.; Brandão, M. G.; Stehmann, J. R.; Oliveira, L. A.; Krettli, A. U. *J. Ethnopharmacol.* **2003**, *87*, 253-256.
11) Borchardt, J. K. *Drug News Perspect.* **2002**, *15*, 187–192.
12) Sanchez, S.; Guzmán-Trampe, S.; Ávalos, M.; Ruiz, B.; Rodríguez-Sanoja, R.; Jiménez-Estrada, M. "Microbial natural products," in *Natural Products in Chemical Biology*, ed. N. Civjan (Hoboken, NJ: Wiley), **2012**, 65–108.
13) Molitoris, H. P. *Czech. Mycol*. **1995**, *48*, 53-65.
14) Lobanovska M.; Pilla G. *Yale J. Biol. Med.* **2017,** *29*, 135-145.
15) Dias D. A.; Urban S.; Roessner U. *Metabolites.* **2012**, *2*, 303-336.
16) Endo A.; Kuroda M.; Tsujita Y. *J. Antibiot*. **1976**, *29*, 1346–8.
17) Genilloud, O. *Nat. Prod. Rep.* **2017**, *34*, 1203-1232.
18) Wainwright M. *Hist. Philos. Life Sci.* **1991**, *13*, 97-124.
19) Jukes T. H. *Rev. Infect. Dis*. **1985**, *7*, 702–707.
20) Dasgupta A. *Adv. Clin. Chem.* **2012**, *56*, 75-104.
21) Jelić D.; Antolović R. *Antibiotics.* **2016**, *5*, 29.
22) Unverferth D. V.; Magorien R. D.; Leier C. V.; Balcerzak S. P. *Cancer Treat. Rev.* **1982**, *9*, 149-164.
23) Franco, Y. L.; Vaidya, T. R.; Ait-Oudhia, S. *Breast Cancer (Dove Med Press).* **2018**, *10*, 131-141.
24) Nunez-montero, K.; Barrientos, L. *Antibiotics*. **2018**, *7*, 90.
25) Sayed, A. M.; Hassan, M. H. A.; Alhadrami, H. A.; Hassan, H. M.; Goodfellow M.; Rateb M. E. *J. Appl. Microbiol.* **2019**, *51*, 72-80.

26) Donia, M.; Hamann, M. T. *The Lancet Infect. Dis.* **2003**, *3*, 338-348.

27) Costantino, V.; Fattorusso, E.; Menna, M.; Taglialatela-Scafati, O. *Curr. Med. Chem.* **2004**, *11*, 1671-1692.

28) Pereira, R. B.; Andrade P. B.; Valentão, P. *Mar Drugs*. **2016**, *14*, 39-69.

29) Vanisevic, J.; Thomas, O. P.; Pedel, L.; Pénez, N.; Ereskovsky, A. V.; Culioli, G.; Pérez, T. *PloS one*, **2011**, *6*, 28059.

30) Núñez-Montero, K.; Barrientos, L. *Antibiotics.* **2018**, *7*, 90-112.

31) Jiménez, C1. *ACS Med. Chem. Lett.* **2018**, *13*, 959-961.

32) Bergmann, W.; Burke, D. C. *J. Org. Chem.* **1955**, *20*, 1501-1507.

33) Proksch, P.; Edrada-ebel, R.; Ebel, R. *Mar. Drugs*, **2003**, *1*, 5-17.

34) Hu, Y.; Chen, J.; Hu, G.; Yu, J.; Zhu, X.; Lin, Y.; Chen, S.; Yuan, J. *Mar. Drugs* **2015**, *13*, 202-221.

35) Liang, X.; Luo, D.; Luesch, H. *Pharmacol. Res*. **2019**, *147*, 104373-104414.

36) Cornelio, K.; Espiritu, R. A.; Hanashima, S.; Todokoro, Y.; Malabed, R.; Kinoshita, M.; Matsumori, N.; Murata, M.; Nishimura, S.; Kakeya, H.; Yoshida, M.; Matsunaga, S. *Biochimica et Biophysica Acta (BBA) – Biomembranes*, **2019**, *1861*, 228-235.

37) Miller, C. P.; Ban K.; Dujka, M. E.; McConkey, D. J.; Munsell, M.; Palladino, M.; Chandra, J. *Blood*. **2007**, *110*, 267-77.

38) Miller, C. P.; Manton, C. A.; Hale, R.; Debose, L.; Macherla, V. R.; Potts, B. C.; Palladino, M. A. *Chem Biol Interact*. **2011**, *194*, 58-68.

39) Trzoss, L.; Fukuda, T., Costa-Lotufo, L. V.; Jimenez, P.; La Clair, J. J.; Fenical, W. *PNAS*. **2014**, *111*, 14687-14692.

40) Mayer, A. Marine Pharmaceutical: The Clinical Pipeline. Available online: https://www.midwestern.edu/departments/marinepharmacology/clinical pipeline.xml (accessed on 27 May, 2021).

41) Ito, M. K. *PT.* **2015**, *40*, 826-857.

42) Newman, D. J.; and Cragg, G. M. *J. Nat. Prod*. **2004**, *67*, 1216-1238.

43) He, W.; Zhang, Z.; Ma, D. *Angew.Chem. Int.Ed*. **2019**, *58*, 3972-3975.

44) Carter, N. J.; Keam, S. J. *Drugs.* **2007**, *67*, 2257-76.

45) Sun, M. K.; Alkon, D. L.; *CNS Drug Rev.* **2006**, *12*, 1-8.

46) Harrison, S. J.; Mainwaring, P.; Price, T.; Millward, M. J.; Padrik, P.; Underhill, C. R.; Cannell, P. K.; Reich, S. D.; Trikha, M.; Spencer, A. *Clin. Cancer Res.* **2016**, *15,* 4559-4566.

47) Costales-Carrera, A.; Fernández-Barral, A.; Bustamante-Madrid, P.; Guerra, L.; Cantero, R.; Barbáchano, A.; Muñoz, A. *Mar. Drugs.* **2019**, *17*, 648-659.

48) Cimino, P. J.; Huang, L.; Du, L.; Wu, Y.; Bishop, J.; Dalsing-Hernandez, J.; Kotlarczyk, K.; Gonzales, P.; Carew, J.; Nawrocki, S.; Jordan M. A.; Wilson, L.; Lloyd, G. K.; Wirsching, H. G. *Biomed. Rep.* **2019**, *10*, 218-224.

49) Chen, H.; Lin, Z.; Arnst, K. E.; Miller, D. D.; Li, W. *Molecules*. **2017**, *22*, 1281.

50) Caron, D. A.; *Scentia Mar*. **2005**, *69*, 97–110.

51) Sogin, M. L.; Morrison, H. G.; Huber, J. A.; Welch, D. M.; Huse, S. M.; Neal, P. R.; Arrieta, J. M.; Hernd, G. J. *PNAS*, **2006**, *103*, 12115–1212.

52) Grossart, H. P.; Riemann, L.; Tang, K. W. *Front. Microbiol*. **2013**, *4*, 59.

53) Cárdenas, A.; Rodriguez-R, L. M.; Pizarro, V.; Cadavid, L. F.; Arévalo-Ferro, C. *ISME J.* **2012**, *6*, 502–512.

54) Maloney, K. N.; MacMillan, J. B.; Kauffman, C. A.; Jensen, P. R.; DiPasquale, A. G.; Rheingold, A. L.; Fenical, W. *Org. Lett.* **2009**, *11*, 5422–5424.

55) Schneider, K.; Keller, S.; Wolter, F. E.; Röglin, L.; Beil, W.; Seitz, O.; Nicholson, G.; Bruntner, C.; Riedlinger, J.; Fiedler, H. P.; Süssmuth, R. D. *Angew Chem Int Ed Engl.* **2008**; *47*, 3258-61.

56) Kwon, H. C.; Kauffman, C. A.; Jensen, P. R.; Fenical, W. *J. Am. Chem. Soc.* **2006**, *128*, 1622–1632.

57) Nong, X. H.; Wei, X. Y.; Qi S. H. *J. Antibiot*. **2017**, *70*, 1047-1052.

58) Nong, X. H.; Zhang, X. Y.; Xu, X. Y.; Wang J.; Qi S. H. *J. Nat. Prod*. **2016**, *79*, 141-148.

59) Fu, P.; Kong, F.; Wang, Y.; Wang, Y.; Liu, P.; Zuo, G.; Zhu, W. *Chin. J. Chem.* **2013,** *31*, 100-104.

60) Shin, H.J. *Mar. Drugs* **2020**, *18*, 230-233.

61) Khamthong, N.; Rukachaisirikul, V.; Phongpaichit, S.; Preedanon, S.; Sakayaroj, J. *Tetrahedron.* **2012**, *68*, 8245-8250.

62) Zhao, D. L.; Shao, C. L.; Zhang, Q. 1.; Wang, K. L.; Guan, F. F.; Shi, T.; Wang, C. Y. *J. Nat. Prod.* **2015**, *78*, 2310-2314.

63) Liua, M.; Suna, W.; Wanga, J.; Heb, Y.; Zhangb, J.; Lia, F.; Qia, C.; Zhua, H.; Xuea, Y.; Hua, Z.; Zhanga, Y. *Biorg. Chem.* **2018**, *80*, 525-530.

64) Afiyatullov, S. S.; Zhuravleva, O. I.; Chaikina, E. L.; Anisimov, M. M. *Chem. Nat. Compd.* **2012**, *48*, 95-98.

65) Parvatkar, R. R.; D'Souza, C.; Tripathi, A.; Naik, C. G. *Phytochem.* **2009**, *70*, 128-

132.

66) Zheng, C. J.; Shao, C. L.; Wu, L. Y.; Chen, M.; Wang, K. L.; Zhao, D. L.; Sun, X. P.; Chen, G. Y.; Wang, C. Y. *Mar. Drugs.* **2013**, *11*, 2054-2068.

67) Shao, C. L.; Wang, C. Y.; Wei, M. Y.; Gu, Y. C.; She, Z. G.; Qian, P. Y.; Lin, Y. C. *Bioorg. Med. Chem. Lett.* **2011**, *21*, 690-693.

68) Chen, M.; Shao, C. L.; Kong, C. J.; She, Z. G. Wang, C. Y. *Chem. Nat. Compd.* **2014**, *50*, 617-620.

69) Bao, J.; Zhang, X. Y.; Xu, X. Y.; He, F., Nong, X. H.; Qi S. H. *Tetrahedron.* **2013**, *69*, 2113-2117.

70) Chen, M.; Shao, C. L.; Fu, X. M.; Xu, R. F.; Zheng, J. J.; Zhao, D. L.; She, Z. G.; Wang, C. Y. *J. Nat. Prod.* **2013**, *76*, 547-553.

71) Park, S.C.; Julianti, E.; Ahn, S.; Kim, D.; Lee, S.K.; Noh, M.; Oh, D.-C.; Oh, K.-B.; Shin, J. *Mar. Drugs* **2019**, *17*, 176-191.

72) Liu, S.-Z.; Yan, X.; Tang, X.-X.; Lin, J.-G.; Qiu, Y.-K. *Mar. Drugs* **2018**, *16*, 483-493.

CHAPTER 2

Bulbimidazoles A−C, Antimicrobial and Cytotoxic Alkanoyl Imidazoles from a Marine Gammaproteobacterium *Microbulbifer* sp. DC3-6

2-1 Background

Marine microorganisms associating with marine invertebrates are prolific sources of bioactive natural products, but yet underexplored in natural product discovery. The number of new natural products from microorganisms associated with or symbiotic to the host invertebrates is still limited, compared to the marine animals including sponges, tunicates and corals [1]. However, marine animal-bacterial symbioses are attracting attention because of the accumulating evidence that bacteria possess a diverse type of unknown biosynthetic gene clusters, which are responsible for the production of a number of marine natural products [2]. An anticancer cyclic depsipeptide didemnin B is one of the prime examples of marine natural products isolated from both invertebrates and bacteria (Figure 2-1). This compound belongs to a class of cyclic depsipeptides and first isolated from Caribbean tunicates of the family *Didemnidae* and was reisolated from a marine α-proteobacterium *Tistrella*, obtained from a sediment sample [3, 4]. Didemnin B demonstrated significant *in vitro* cytotoxicity and *in vivo* antitumor activity and is the first marine natural product to enter phase II clinical trials as an anticancer agent [5].

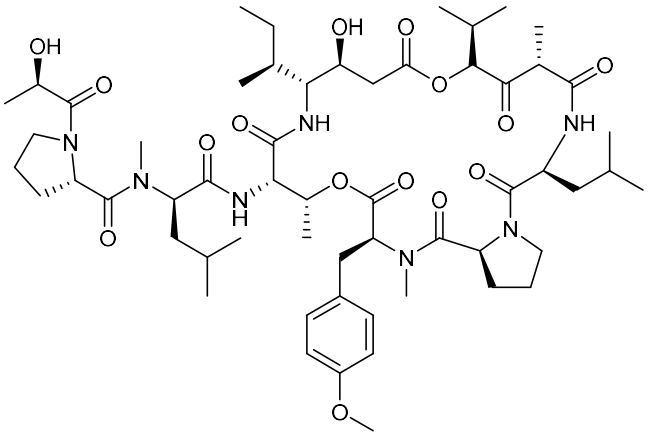

Figure 2-1. Structure of didemnin B.

Marine organisms usually adjust themselves to the most diverse ecosystems on the earth such as marine environment which differs from terrestrial ecosystem in many points of view and represents a complex set of extremely fascinating habitats that are referred by a broad range of temperature, hydrostatic pressure, salinity and eukaryotic predation or viral attacks. These harshfull marine environmental factors drive the adaptation of marine organisms that may involve in the modification of metabolic pathways of organisms as well as the utilization

of marine specific secondary metabolites [6]. Thus, marine bacteria associating with invertebrates become the most promising source of novel bioactive compounds. It is reported that most of bioactive medicinal compounds have been isolated from a range of marine organisms such as sponges, tunicates and bryozoans. Besides sponges and tunicates, corals are another rich source of natural products [7]. Natural products discovered from corals bear unique structures in terms of structural diversity and functional features as well as various types of biological activities [8]. Several bioactive compounds with novel structures have been isolated from corals. For example, sarcodictyin B [9], pseudopterosin A [10], hippuristanol [11], tubastraine [12] and montipyridine [13] were isolated from corals (Figure 2-2).

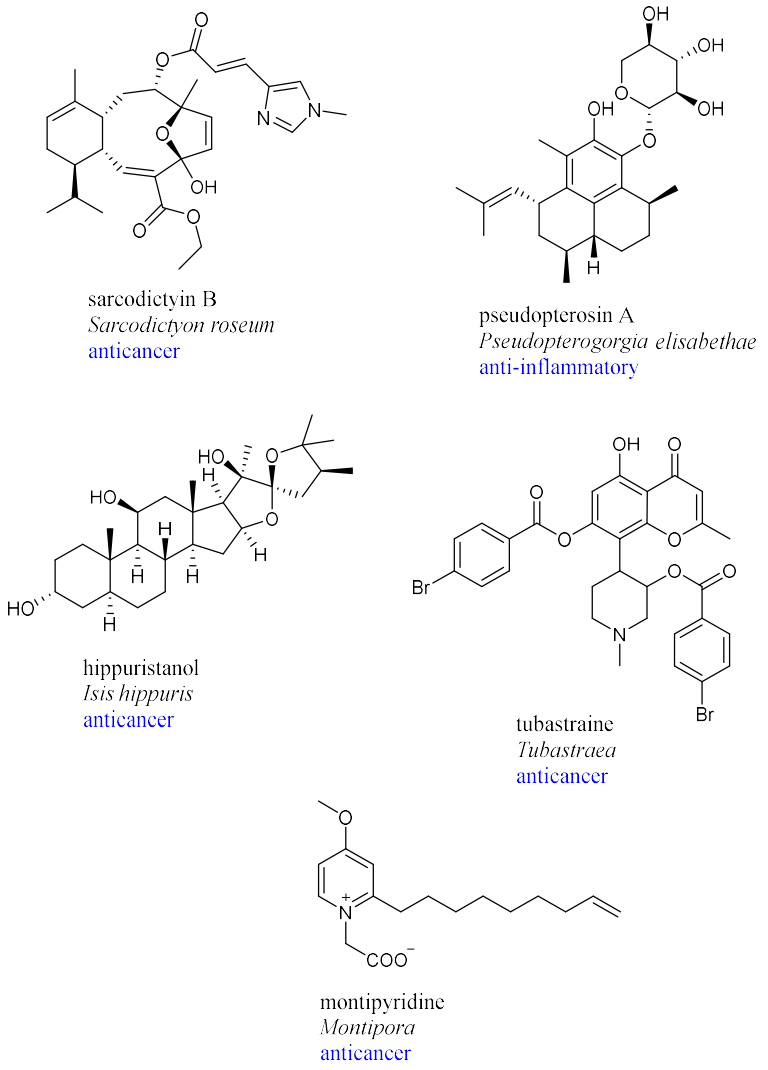

Figure 2-2. New bioactive compounds from corals.

On the other hand, some bioactive compounds with unique structures have been discovered from soft corals and their associated bacteria. A few examples of natural products have been

reported from bacteria from soft corals such as pseudoalteromones A and B [14, 15], and macrolactin V [16] (Figure 2-3). Bacteria from stony corals are still an underestimated source in natural product screening and have received less attention compared with other invertebrate associated bacteria [17].

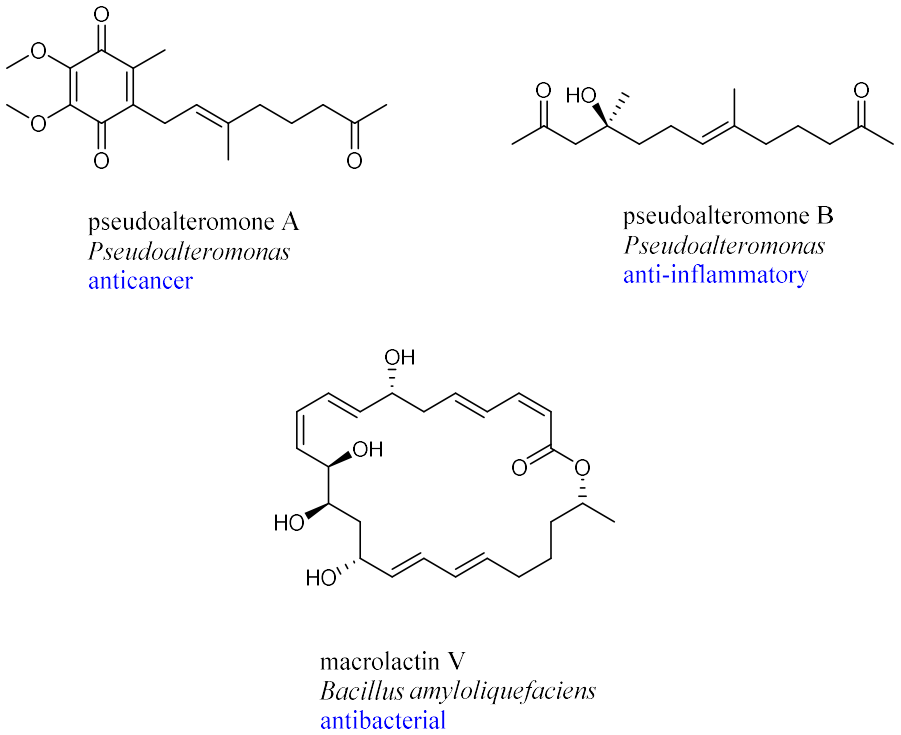

Figure 2-3. New bioactive compounds from soft coral-associated bacteria.

Only a few numbers of natural products from stony coral-associated bacteria have been reported. Recently, three new bioactive compounds such as labrenzbactin [18], an unsaturated fatty acid [19] and two new keto fatty acids [20] were discovered from stony coral-associated bacteria *Labrenzia*, *Microbulbifer* and *Micrococcus* by our research group (Figure 2-4). These results indicate that marine bacteria have potential ability to produce new natural products with bioactivity. Like marine obligate bacteria such as *Labrenzia* and *Microbulbifer*, it would be possible to isolate new bacterial taxa from underexploited source like stony corals which may contain biosynthetic gene clusters for new bioactive natural products. Therefore, there is still a chance to get more bioactive compounds from these less exploited marine bacteria.

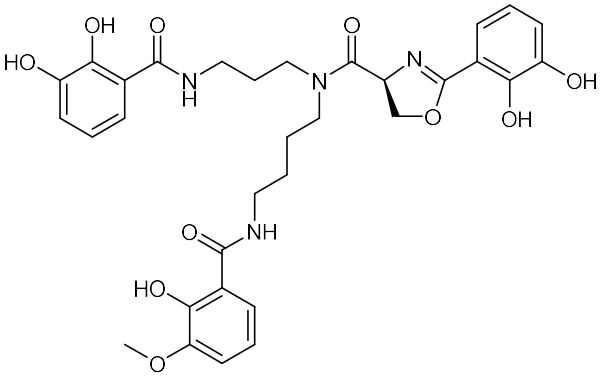

labrenzbactin
Labrenzia
anticancer

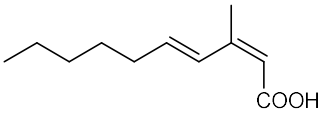

(2*Z*,4*E*)-3-methyl-2,4-decadienoic acid
Microbulbifer
antibacterial activity

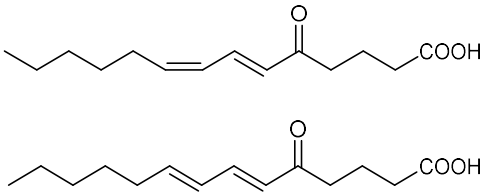

(6*E*,8*Z*)- and (6*E*,8*E*)-5-oxo-6,8-tetradecadienoic acids
Micrococcus
antibacterial, PPARs agonist

Figure 2-4. New bioactive compounds from stony coral-associated bacteria found in our laboratory.

In this study, the search for new secondary metabolites produced from a group of coral-associated bacterial strains were conducted by HPLC/UV-based spectroscopic analysis. Firstly, bacterial strains were grown at 30ºC on Marine Agar for 2 days. Then, a loopful of bacterial culture was inoculated into 500 mL K-1 flask containing 100 mL of Marine Broth (Difco) (equivalent to sea water) as seed medium for increasing the number of bacterial cells and the flask was placed on a rotary shaker (200 rpm) at 30ºC for 2 days. Then, 3 mL of seed culture was inoculated into 500 mL K-1 flasks each containing 100 mL of A3M, A11M and A16 production medium prepared in natural seawater collected from Toyama Bay, Toyama, Japan. The composition of these production medium is shown in Table 2-1.

Table 2-1. Composition of seed culture and production culture media

Media	Composition
Marine Broth	peptone 0.5%, yeast extract 0.1%, and major consitutents of inorganic salts present in seawater
A3M	glucose 0.5%, glycerol 2%, soluble starch 2%, Pharmamedia (Traders Protein) 1.5%, yeast extract 0.3% and Diaion HP-20 (Mitsubishi Chemical, Japan) 1%
A11M	glucose 0.2%, soluble starch 2.5%, yeast extract 0.5%, polypeptone (Wako Pure Chemical Industries, Ltd.) 0.5%, NZ-amine (Wako Pure Chemical Industries, Ltd.) 0.5%, $CaCO_3$ 0.3%, and Diaion HP-20 (Mitsubishi Chemical Co.) 1%
A16	glucose 2%, Pharmamedia (Traders Protein) 1%, $CaCO_3$ 0.5%, and Diaion HP-20 (Mitsubishi Chemical, Japan) 1%

The pH of the medium was adjusted to 7.0 before sterilization. The inoculated flasks were incubated at 30ºC on a rotary shaker at 200 rpm for 2 days. Finally, 1-butanol was selected as an ideal solvent for the extraction of all unknown secondary metabolites produced in the fermentation medium, because 1-butanol has a wide solubility range from hydrophilic to hydrophobic compounds. After fermentation, 100 mL of 1-butanol was added to each flask, and the flasks were shaken for 1 h. The mixture was then centrifuged at 6,000 rpm for 10 min, and the organic layer was separated from the aqueous layer. The organic layer was concentrated *in vacuo* and subjected to HPLC-UV spectroscopy to analyze the unknown secondary metabolites produced by the bacterial strains. For this purpose, two milliliter of 1-butanol extract was dried by vacuum centrifugation. Dried extract was dissolved in 200 µL DMSO and filtered using 0.45 µm membrane filter and then HPLC-DAD analysis was performed. The secondary metabolites in the extract of bacterial strain were separated using reversed-phase HPLC, and photodiode array detector (DAD, 200-600 nm) was used to record their characteristic UV spectra. To screen unknown secondary metabolites, the following conditions for the HPLC analysis were applied: Varian Microsorb C18 column (4.6 x 100 mm) on an Agilent HP1100 system with a binary pump equipped with DAD for 200 to 600 nm. The mobile phase used the following stepwise gradient of acetonitrile (MeCN) and 0.1% formic acid at pH 2.7: 15% MeCN for 0-3 min, 15-85% MeCN for 3-25 min, 85% MeCN for 25-29 min and 85-15% MeCN for 29-32 min, with a flow-rate of 1.2 mL/min.

In my study, chemical screening as described was employed to discover new bioactive compounds from eighty-four marine bacterial strains, which were isolated from eight stony corals. These coral samples were collected as fishery waste at −10 to −15 m near the coast of Minami-Ise, Mie Prefecture, Japan, and were obtained through a local aquarium vendor.

After a successful spectroscopic screening process using HPLC/UV analysis in combination with our in-house UV database, I selected seven bacteria as candidate strains for further isolation of unknown secondary metabolites (Table 2-2).

Table 2-2. Selection of seven candidate strains

No	Candidate strains	Coral genus	Compounds
1	DC1-1	*Acropora*	known (fatty acid)
2	DC1-2	*Acropora*	known (diketopiperazine)
3	DC1-6	*Acropora*	not identified (future study)
4	DC1-9	*Acropora*	known (diketopiperazine)
5	DC2-3	*Cyathelia*	not identified (future study)
6	**DC3-6**	***Tubastraea***	**new (alkanoylimidazole)**
7	DC4-3	*Dendrophyllia*	not identified (future study)

The DC3-6, one of the selected seven bacterial strains, was isolated from a scleractinian coral *Tubastraea* sp. After chemical screening performed by HPLC/UV spectroscopy, I found strain DC3-6 produced secondary metabolites only in A11M seawater-based medium. In the solvent extract of culture broth of DC3-6 in A11M showed three major peaks with retention times 10.5, 11.2 and 15.5 min. The UV spectrum of each peak was similar and showed absorption maximum at 254 nm (Figure 2-5). The pattern of UV spectra was not found when I searched in our in-house UV database. Actually, UV spectra can be used to predict the overall structure and the presence of chromophore in the compounds. Therefore, I decided to work with this strain obtained from an unexplored source which may still contain new biosynthetic pathway for producing novel secondary metabolites.

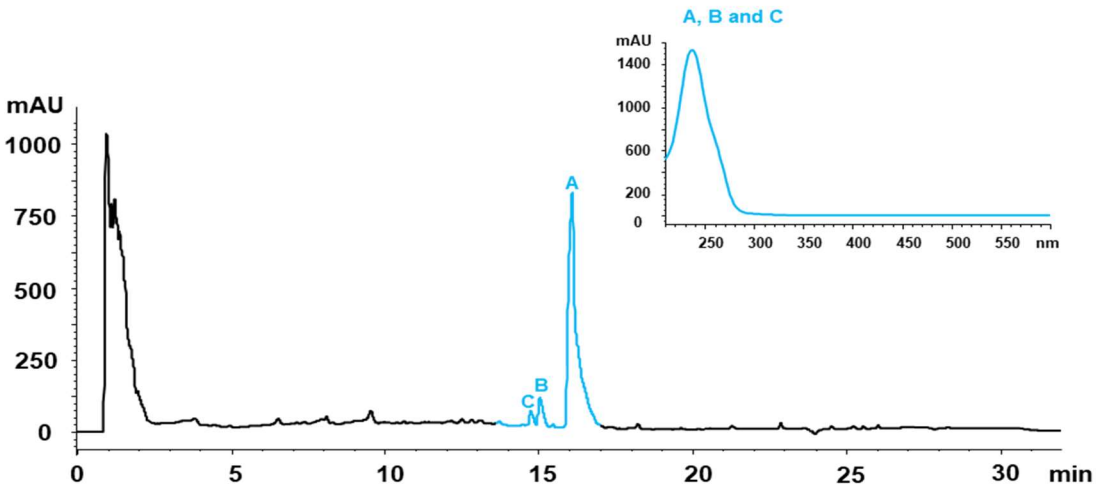

Figure 2-5. HPLC chromatogram of 1-butanol extract of *Microbulbifer* sp. DC3-6.

The producing bacterial strain DC3-6 was identified as a member of the genus *Microbulbifer* on the basis of 99.3% similarity in the 16S rRNA gene sequence (1,455 nucleotides; DDBJ accession number LC498626) to *Microbulbifer echini* AM134^{T} (accession number KJ789957). The genus *Microbulbifer* is a Gram-negative, strictly aerobic, rod-shaped bacterium belonging to the class gammaproteobacteria [21]. Members of this genus are obligate marine strains because sea-salt based medium is required for their growth (Figure 2-6). *Microbulbifer* are commonly found in marine habitats such as salt marshes, intertidal sediments, solar salterns, marine sediments, and marine algae [22]. According to the latest genomic data, the *Microbulbifer* species possess biosynthetic genes for the production of nonribosomal peptides and siderophores but very little is known about their secondary metabolites [23]. Up to date, there are merely two bioactive compounds have been reported from this genus. Benzoate derivatives known as bulbiferates A and B were isolated from culture broth of *Microbulbifer* collected from marine sediment [24]. These compounds showed moderate antibacterial activity against different Gram-positive bacteria (Figure 2-7). Similarly, chemical investigation of fermentation broth of *Microbulbifer* isolated from stony coral led to the discovery of an unsaturated fatty acid [19]. This compound exhibited moderate antibacterial activity.

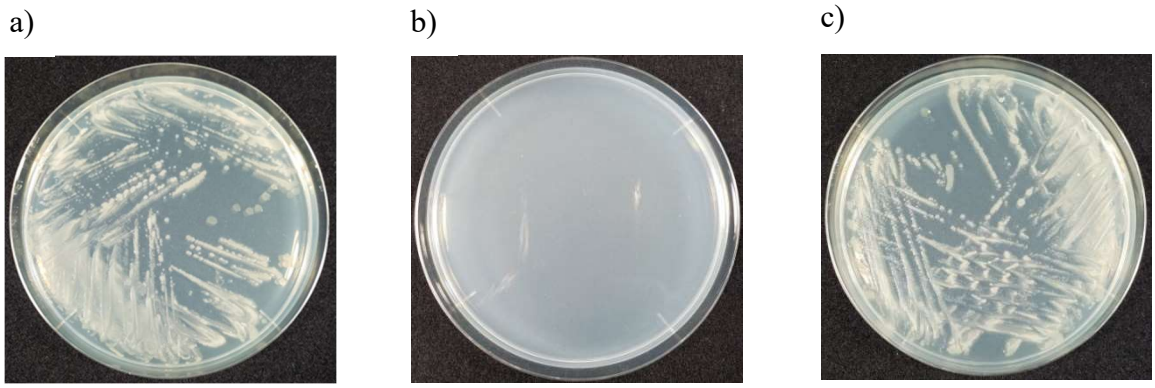

Figure 2-6. Colony morphology of *Microbulbifer* sp. DC3-6 on a) Marine Agar, b) YP medium (yeast extract 0.1% and peptone 0.5%) in distilled water, c) YP medium in natural seawater.

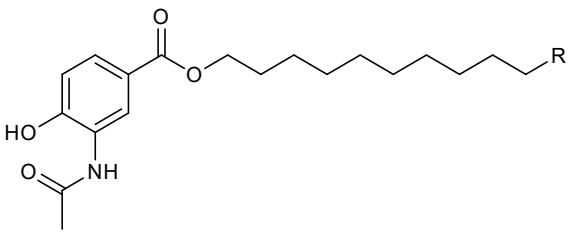

bulbiferate A : R = H
bulbiferate B : R = CH_3
antibacterial

Figure 2-7. Bulbiferates A and B, the first compounds reported from *Microbulbifer* sp.

In the screening for novel bioactive compounds with therapeutic potential from marine microbes, the genus *Microbulbifer* was found to produce unknown metabolites. This strain was isolated from a scleractinian (stony) coral *Tubastraea* sp. collected off the south shore of central Japan. HPLC peaks of secondary metabolites produced by this marine strain displayed UV absorption maximum around 254 nm, which was not present in the in-house UV database in our laboratory. HPLC/UV-guided purification was conducted from the culture extract resulting in the isolation of three new alkanoyl imidazoles designated bulbimidazoles A−C (**1**−**3**) (Figure 2-8) were identified. These compounds are the deamino congeners of nocarimidazoles A and B previously isolated from a marine actinomycete of the genus *Nocardiopsis* [25]. In this chapter, I describe the isolation, structure determination, and biological activities of **1**, **2**, and **3** as well as the absolute configuration of the *anteiso*-methyl substituent of **1**.

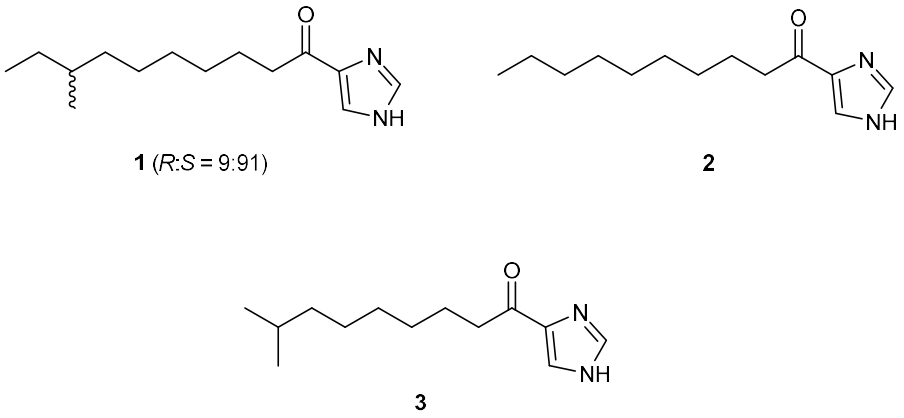

Figure 2-8. Structures of bulbimidazoles A−C (**1**−**3**).

2-2 Results and Discussion

2-2-1 Fermentation and isolation

The producing strain DC3-6 was isolated from a scleractinian (stony) coral *Tubastraea* collected near the coast of Mie Prefecture, Japan, and identified as a member of the genus *Microbulbifer* by phylogenetic analysis based on the 16S rRNA gene sequence similarity. Large scale fermentation of this strain was carried out in A11M seawater medium at 30 °C for five days. The crude extract was obtained by 1-butanol extraction. After evaporation, the whole culture broth was subjected to consecutive fractionation using silica gel and ODS column chromatographies and final purification was achieved by reversed-phase HPLC purification, yielding bulbimidazoles A (**1**, 11.3 mg), B (**2**, 3.2 mg), and C (**3**, 2.5 mg) from 3 L of culture of strain DC3-6 which was sufficient amount to determine full chemical structure as well as biological characterization (Scheme 2-1).

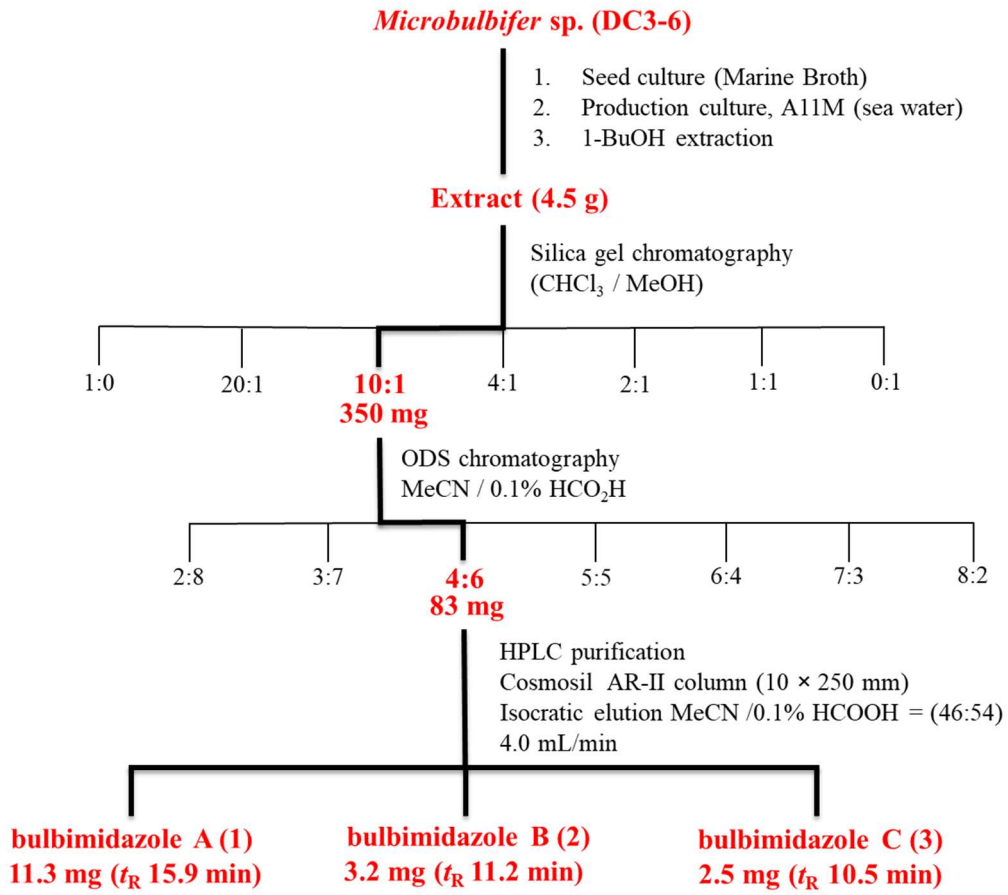

Scheme 2-1. Isolation of bulbimidazoles A-C (**1-3**).

2-2-2 Structure determination

Bulbimidazole A (**1**) was obtained as a yellow amorphous solid. The molecular formula of **1** was established to be $C_{14}H_{24}N_2O$ based on a protonated molecule $[M + H]^+$ at *m/z* 237.1964 by HR-ESITOFMS measurement, indicating four degrees of unsaturation. The UV spectrum in methanol displayed an absorption band at 253 nm and the IR spectrum indicated the presence of an OH or NH group and a carbonyl functionality with absorption bands around 3300 and 1665 cm^{-1}. The ^1H NMR spectroscopic data showed characteristic resonances of two distinctive doublet resonances of sp^2 protons (δ_H 8.55 and 9.15), one doublet and one triplet methyl proton (δ_H 0.79 and 0.80), one aliphatic methine (δ_H 1.26), and several methylene multiplets confirmed the presence of a methyl-branched alkyl chain and an aromatic group in **1**. However, only 10 aliphatic carbons were detected in a ^{13}C NMR spectrum recorded in DMSO-d_6, having failed to detect the rest of the resonances (Figure S6), which were expected to be of the sp^2 carbons. The presence of unseen carbons were noticed in HSQC and HMBC spectra as cross peaks from the aforementioned undetectable sp^2 and

some of the aliphatic protons (Figures S9 and S11). I suspected that this undetectability of sp^2 carbons in the ^{13}C NMR spectrum was due to the signal broadening and splitting caused by tautomeric property of the unidentified functional group present in **1**. A trace amount of trifluoroacetic acid (TFA) was added to the NMR solvent to improve the spectrum quality and convert the envisaged tautomers into a few resonating structures. Fortunately, in the ^{13}C NMR spectrum showing clearer resonances for four anticipated sp^2 carbons at δ_C 125.2, 131.8, 137.5, and 190.6. In combination with HSQC data, 14 carbon signals were assigned as one deshielded carbonyl carbon, one nonprotonated sp^2 carbon, two sp^2 methines, seven sp^3 methylenes, one sp^3 methine, and two methyl groups (Table 2-3). Analysis of COSY and HMBC spectroscopic data defined the structure of **1** that comprised two structural units, an aliphatic chain part and an imidazole moiety. COSY analysis elucidated the connectivity among three methylenes, (H_2-7−H_2-8−H_2-9) and a six-carbon fragment with an anteiso-branching (H_3-15−H_2-14−H-13(H_3-16)−H_2-12−H_2-11) (Figure 2-9). A series of HMBC correlations from H_2-8 to C-10 and H_2-9 to C-10 and C-11, confirming the connection of those aliphatic fragments via a methylene group at C-10. Furthermore, long range correlations were observed from H_2-7 and H_2-8 to the carbonyl carbon (C-6), thereby determining an 8-methyldecanoyl moiety. The COSY correlation was found between two sp^2 aromatic protons H-2 and H-4 protons, which were long-range coupled with J = 0.6 Hz, analysis of HMBC correlations were detected from H-2 to C-4 and C-5 and from H-4 to C-2 and C-5, together with the molecular formula $C_3H_3N_2$ for the remaining structural part, suggested the presence of an imidazole ring. Finally, the connection between alkanoyl moiety and imidazole were established by HMBC correlations from the imidazole protons H-2 and H-4 to the carbonyl carbon C-6 and from the alkanoyl α-proton H_2-7 to the imidazole carbon C-5, to complete the planar structure of **1**. The carbon chemical shifts of C-2, C-4, C-5, and C-6 as well as the UV maximal absorption were in good accordance with those reported for synthetic alkanoyl imidazoles [26, 27].

Table 2-3. ^{1}H and ^{13}C spectroscopic data for bulbimidazole A (**1**) in DMSO-d_6 with TFA

	1		
no.	δ_C[a]	δ_H mult (*J* in Hz)[b]	HMBC[b,c]
2	137.6, CH	9.15, d (0.6)	4, 5, 6
4	125.2, CH	8.55, d (0.6)	2, 5, 6
5	131.8, C		
6	190.6, C		
7	38.6, CH_2	2.89, t (7.3)	5, 6, 8, 9
8	23.5, CH_2	1.59, quint (7.3)	6, 7, 9, 10
9	28.6, CH_2	1.29, m	8, 10
10	29.2, CH_2	1.23, m	
11	26.4, CH_2	1.22, m	13
12	36.0, CH_2	1.05, m; 1.24, m	11, 13
13	33.8, CH	1.26, m	12, 15, 16
14	29.0, CH_2	1.09, m; 1.27, m	12, 13, 15, 16
15	11.3, CH_3	0.80, t (7.3)	13, 14
16	19.1, CH_3	0.79, d (6.7)	12, 13, 14

[a] Recorded at 125 MHz (reference δ_C 39.5).

[b] Recorded at 500 MHz (reference δ_H 2.49).

[c] HMBC correlations are from proton(s) stated to the indicated carbon.

[d] Assignment may be interchanged.

[e] Overlapping signals.

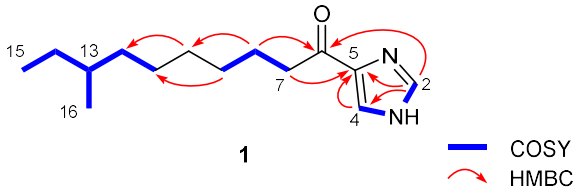

Figure 2-9. COSY and key HMBC correlations for **1**.

Bulbimidazole B (**2**) was obtained as a pale yellow, amorphous solid. The molecular formula of **2**, $C_{14}H_{22}N_2O$, determined by HR-ESITOFMS ($[M + H]^+$ at *m/z* 223.1809) indicated that one methylene (14 amu) was fewer in **2** than **1**. UV and IR spectra showed almost the same absorption bands as **1**. As expected from the molecular formula 1D and 2D NMR spectral data were in overall similarity to those for **1**, except for the absence of the doublet methyl and a methine (H_3-16 and H-13 in **1**) resonance and the presence of one additional methylene resonance (δ_C 31.3/δ_H 1.22, CH_2-13).

Table 2-4. ^{1}H and ^{13}C spectroscopic data for bulbimidazole B (**2**) in DMSO-d_6 with TFA

	2		
no	δ_C[a]	δ_H mult (*J* in Hz)[b]	HMBC[b,c]
2	137.5, CH	9.24, d (0.6)	4, 5
4	125.1, CH	8.61, d (0.6)	2, 5
5	131.5, C		
6	190.5, C		
7	38.5, CH_2	2.89, t (7.3)	6, 8, 9
8	23.5, CH_2	1.60, quint (7.2)	6, 7, 9, 10
9	28.5, CH_2	1.22-1.30[e]	8, 10, 11
10	28.7,[d] CH_2	1.22-1.30[e]	
11	28.8,[d] CH_2	1.22-1.30[e]	
12	28.9,[d] CH_2	1.22-1.30[e]	
13	31.3, CH_2	1.22, m	14
14	22.1, CH_2	1.23, m	13
15	14.0, CH_3	0.83, t (6.9)	13, 14

[a] Recorded at 125 MHz (reference δ_C 39.5).

[b] Recorded at 500 MHz (reference δ_H 2.49).

[c] HMBC correlations are from proton(s) stated to the indicated carbon.

[d] Assignment may be interchangeable.

[e] Overlapping signals

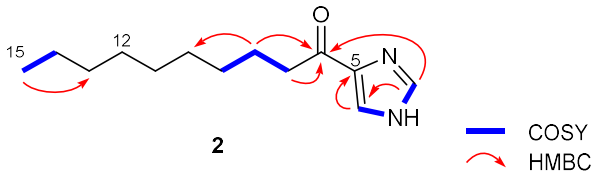

Figure 2-10. COSY and key HMBC correlations for **2**.

COSY cross peaks between neighboring protons in a *n*-propyl spin-system H_3-15–H_2-14–H_2-13 and HMBC correlations from H-15 to C-13 and C-14 and H-14 to C-12 and C-13 established the non-branching linear alkyl chain structure in **2** (Table 2-4, Figure 2-10). The ^{1}H and ^{13}C NMR chemical shifts for the imidazole ring were mostly the same as those found for **1** (Table 2-4).

Bulbimidazole C (**3**) was also obtained as a pale yellow, amorphous solid. Its molecular formula $C_{14}H_{22}N_2O$ determined by HR-ESITOFMS ($[M + H]^+$ at *m/z* 223.1809) was same as **3**, indicative of the isomeric relationship between **2** and **3**.

Table 2-5. ^{1}H and ^{13}C spectroscopic data for bulbimidazole C (**3**) in DMSO-d_6 with TFA

	3		
no	δ_C[a]	δ_H mult (*J* in Hz)[b]	HMBC[b,c]
2	137.5, CH	9.20, d (0.6)	4, 5
4	125.1, CH	8.57, d (0.6)	2, 5
5	131.5, C		
6	190.5, C		
7	38.5, CH_2	2.89, t (7.3)	6, 8, 9
8	23.5, CH_2	1.60, quint (7.3)	6, 7, 9, 10
9	28.5, CH_2	1.28, m	10
10	29.0, CH_2	1.24, m	12
11	26.7, CH_2	1.24, m	10
12	28.9,d CH_2	1.11, m	10, 11, 13, 14, 15
13	27.4, CH	1.47, sept (6.7)	12, 14, 15
14	22.5, CH_3	0.82, d (6.7)	12, 13, 15
15	22.5, CH_3	0.82, d (6.7)	12, 13, 14

[a] Recorded at 125 MHz (reference δ_C 39.5).

[b] Recorded at 500 MHz (reference δ_H 2.49).

[c] HMBC correlations are from proton(s) stated to the indicated carbon.

[d] Assignment may be interchangeable

[e] Overlapping signals

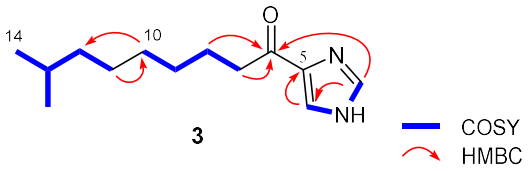

Figure 2-11. COSY and key HMBC correlations for **3**.

A doublet methyl resonance (δ_H 0.82 d, J = 6.7 Hz) accounting for six protons was observed in the ^{1}H NMR spectrum, and this methyl group was joined with a septet methine proton (δ_H 1.47, J = 6.7 Hz) in the COSY spectrum, confirming the appearance of an isopropyl group. The methylene chain part and the imidazole moiety were connected by COSY and HMBC correlations to establish the structure of **3** (Table 2-5, Figure 2-11).

2-2-3 Absolute configuration

In order to determine the absolute configuration of the single stereogenic center C-13 of bulbimidazole A, the Ohrui−Akasaka method was applied (Figure 2-14) [28]. This method is a few analytical procedures for determining the absolute configuration of branched chain

fatty acids which have chiral center more than three bonds aparts from their carboxyl groups. Past investigation attemted, several chiral derivatization reagents but failed to separate the diastereomeric derivatives of branched chain fatty acids. Based on Ohrui−Akasaka method, firstly, a highly reactive and sensitive nonchiral fluorescent reagent was developed such as 2-(anthracene-2,3-dicarboximido)ethyl trifluoromethanesulfonate (AE-OTf), for the carboxylic acid group. The separation of okadaic acid (OA), dinophysis toxins-1 (DTX-1) and dinophysis toxins-3 (DTX-3) in scallops and mussels was successfully performed by using an LC-LC system after labeling with AE-OTF (Figure 2-12) [28].

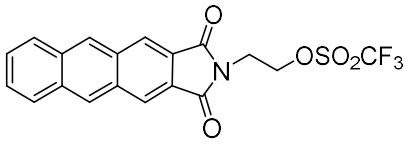

AE-OTf

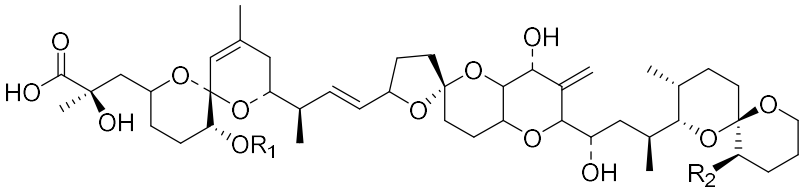

Okadaic acid : $R_1 = R_2 = H$
DTX-1 : $R_1 = H$, $R_2 = -CH_3$
DTX-3 : $R_1 = Acyl$, $R_2 = -CH_3$

Figure 2-12. Structures of AE-OTF and dinophysis toxins-3 (DTX-3)

Although a highly sensitive nonchiral fluorescent reagent was synthesized such as AE-OTf for the separation of polyethers have been known as diarrhetic shellfish toxins, but it was unable to determine the absolute configuration of branched chain fatty acids. Therefore, a very potent fluorescent chiral labeling reagents including (*S*)-(+)-2-(anthracene-2,3-dicarboximido)-l-propyl trifluoromethanesulfonate (AP-OTf) was developed. By labeling with this reagent, the enantiomaric discrimination of 18 kinds of long-chain fatty was achived, including polyunsaturated fatty acids, which was analyzed on a low- temperature HPLC with an isocratic elution mode. According to this mehod, the chiral fluorescent derivatization reagent AP-OTf react with branched long-chain chain fatty acids by forming AP-O-esters bond. This ester bond constracted by hydrophobic interaction. The hydrophobic characteristic of synthesized compounds was responsible for the formation of bent

conformation took place at the amino ethanol moiety of the reagent. Analysis of ^{1}H NMR spectrum also demonstrated that the existence of the bent conformation between chiral reagent and long chain branched fatty acid (Figure 2-13). A low temperature ODS column based HPLC analysis will be performed for the separation of the diastereomeric derivatives of long chain fatty acids. The bent conformer of synthesized AP-O-esters could be existed as a more stable phase at low temperature. On the other hand, the synthesized compounds will be broken down with increasing temperature. Therefore, high temperature will not be suitable condition for HPLC analysis.

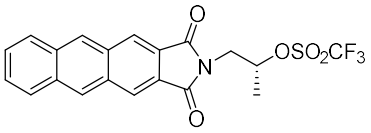

AP-OTf

Figure 2-13. Possible conformers of (*R*) and (*S*)-4-methylhexanoate derivatized with (*S*)-AP-OTF

To generate a carboxyl group for derivatization, the imidazole ring of **1** was oxidatively degraded by the treatment with $RuCl_3$–$NaIO_4$ in a biphasic solvent system CCl_4–MeCN–H_2O, which yielded 8-methyldecanoic acid (*nat*-**4**) (Scheme 2-3). This anteiso-fatty acid was then derivatized with a chiral anthracene reagent (*R*)-2-(anthracene-2,3-dicarboximido)propanol [(*R*)-2A1P] to give ester nat-**4**-(*R*)- 2A1P (Scheme 2-2). (*S*)-8-methyldecanoic acid [(S)- 4] was synthesized from commercially available (S)-6-methyloctanol, which was used to prepare the authentic (*S*)-**4**-(*R*)-2A1P and (*S*)-**4**- (*S*)-2A1P in four steps (Scheme 2-3). Retention times of these reference compounds were 243 min for (*S*)-**4**-(*R*)-2A1P and 234 min for (*S*)-**4**-(*S*)-2A1P, which is chromatographically equivalent to (*R*)-**4**-(*R*)-2A1P, whereas *nat*-**4**-(*R*)-2A1P showed two peaks for (*R*)-**4**-(*R*)-2A1P and (*S*)-**4**-(*R*)-2A1P in a ratio of 9.1:90.9 (Figure 2-14). Therefore, **1** was concluded to be an

enantiomeric mixture consisting of 9% (*R*)- and 91% *(S)*- isomers.

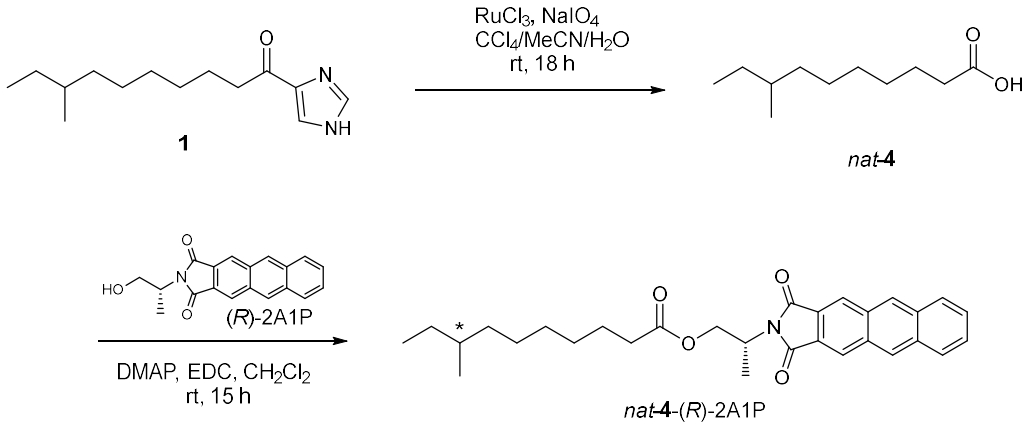

Scheme 2-2. Oxidative degradation of **1** and derivatization with (*R*)-2A1P for Ohrui-Akasaka Analysis

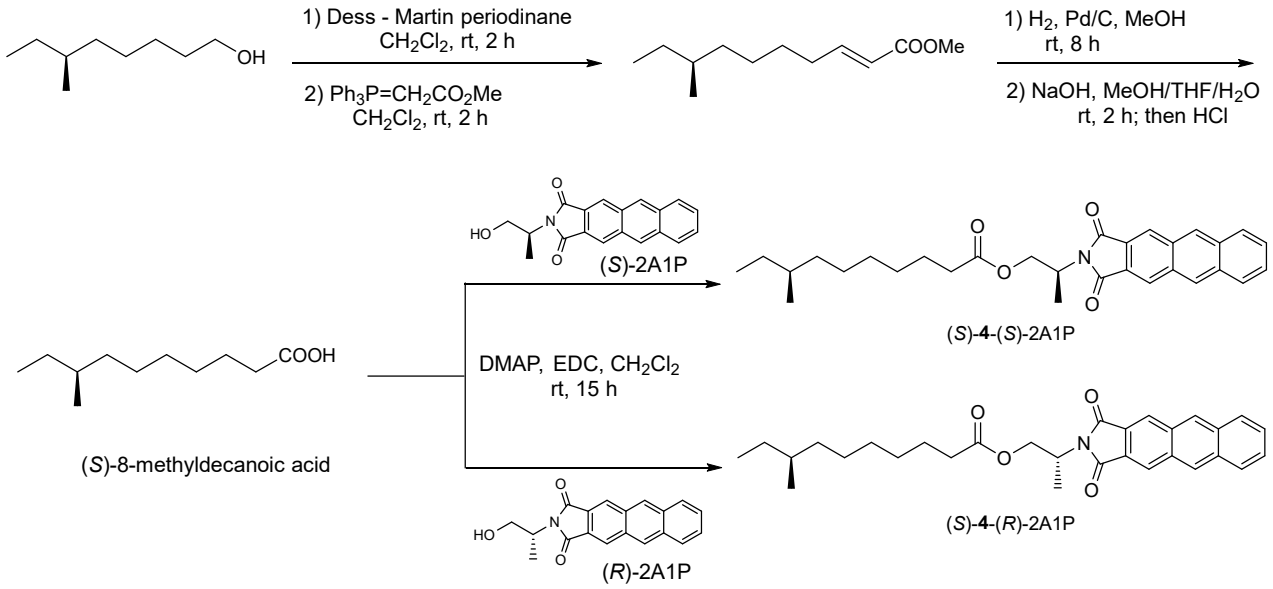

Scheme 2-3. Synthesis of (*S*)-8-methyldecanoic acid and derivatization with (*S*)-2A1P and (*R*)-2A1P for Ohrui-Akasaka analysis.

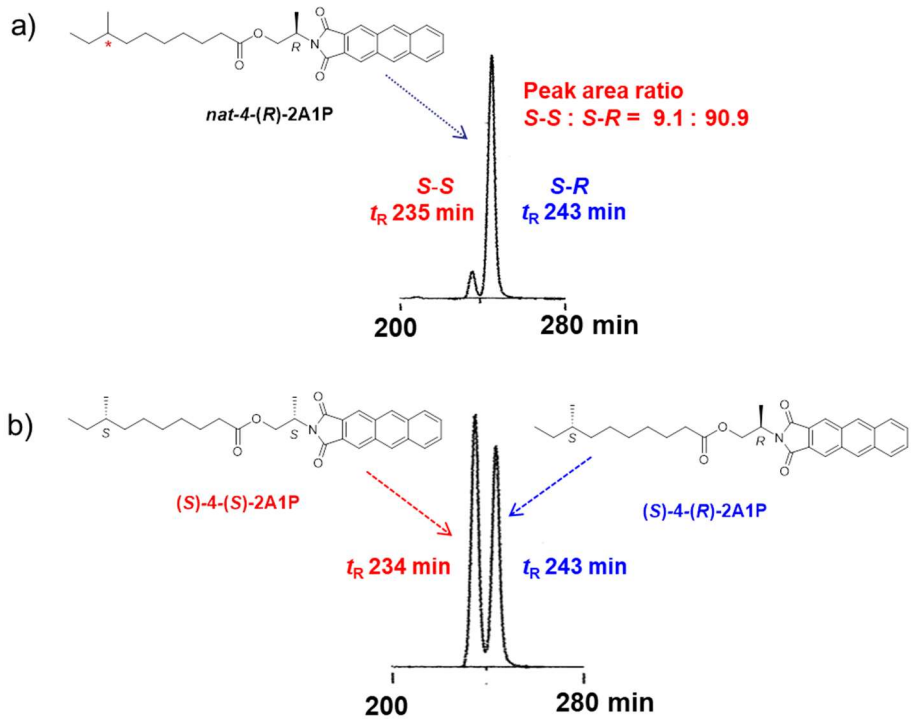

Figure 2-14. Absolute configuration of **1** determined by using chiral anthracene derivatives. (a) HPLC chromatogram of nat-4-(*R*)-2A1P.; (b) HPLC chromatogram of standard (*S*)-**4**-(*R*)-2A1P and (*S*)-**4**-(*S*)-2A1P

HPLC conditions
Develosil ODS HG-3 [3.0 mm id x (250 +150) mm]
MeCN/MeOH/THF (3:1:1, v/v/v)
0.075 mL/min, -42.5 ℃
Fluorometry: Ex. 298 nm, Em. 460 nm

The enantiometric discrimination existing in both natural and synthetic compounds has received much attention due to enantiomers would have different types of biological activities [29]. Therefore, determination of absolute stereochemistry of compound is very important for evaluating their biological properties. Ohrui−Akasaka method is one few analytical procedure for determining the absolute configuration of branched chain fatty acid which had chiral center more than three bonds remote from their carboxyl groups [28]. In particular, it is very difficult or almost impossible to determine the chiral discrimination of such kind of branched chain fatty acid by chromatographic or by spectrometric methods such as NMR of circular dichroism (CD) [30]. Therefore, Ohrui−Akasaka have been used to solve this issue by labeling the branched chain chiral fatty acids with a highly sensitive chiral fluorescent

conversion reagent such as (*S*, *R*)-2-(anthracene-2,3- dicarboximido)propanol. This method consists of four steps; 1) the natural or synthetic compounds must be converted into fatty acid by chemical degradation (if there have other group except carboxyl acid in the long fatty chain). 2) The carboxyl group of branched chain fatty acid is derivitized with chiral fluorescent conversion reagent such as, (*S)* or (*R*)-2-(anthracene-2,3-dicarboximido)propanol. 3) the neutralized derivatized analyte is subjected to HPLC analysis 4) HPLC retention times of derivatized baranched chain fatty acid residue in the analyte is compared with (*S*) and (*R*)- fatty acid standards derivatized with fluorescent conversion reagent [30].

According to Ohrui−Akasaka method, the relationship between (*R*)-2-(anthracene-2,3-dicarboximido)propanol derivative produce diastereomaers of (*S*)-fatty acid (*S*-*R* type) and that of (*R*)-fatty acid (*R*-*R* type) and this pair of diastereoisomers has different retention times on chromatogram (Scheme 2-4). Therefore, these diastereoisomers easily separated by HPLC under the special condition. Column: tandemly connected Develosil ODS-HG-3 (3.0 mm i.d. × (250 + 150) mm; mobile phase: MeCN−MeOH−THF; column temperature: low temperature like −42.5 °C; flow rate: 0.10 mL/min. HPLC peaks detected by monitoring fluorescence intensity detector.

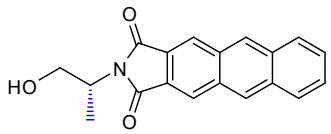

(*R*)-2-(anthracene-2,3- dicarboximido)propanol [(*R*)-2A1P]

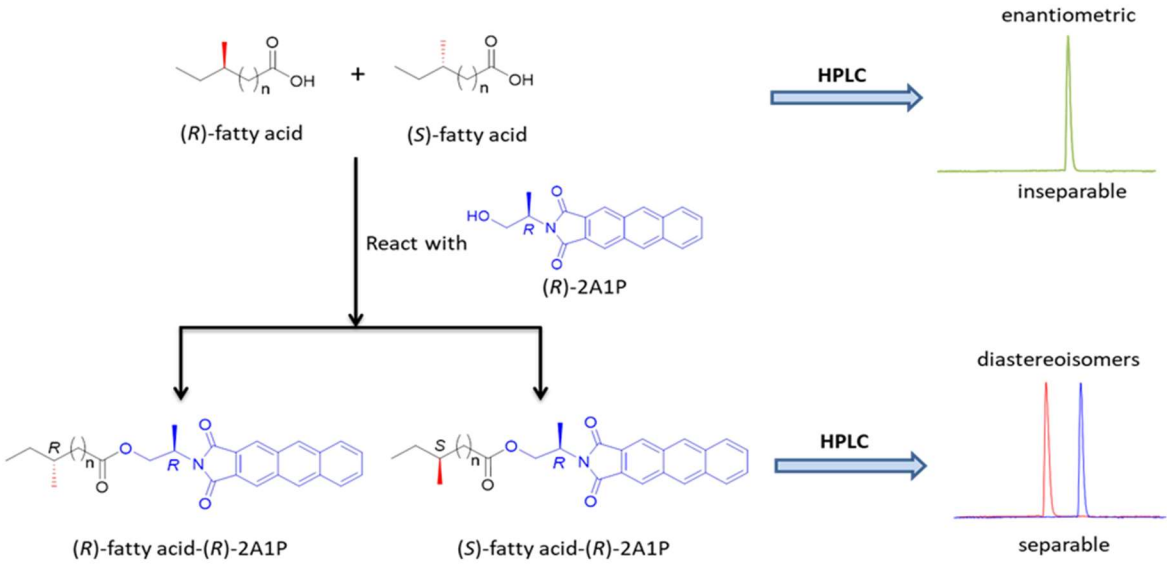

Scheme 2-4. Principle of Ohrui−Akasaka analysis.

2-2-4 Bioactivity

Biological activity of bulbimidazoles A–C (**1**–**3**) was evaluated in antimicrobial and cytotoxic assays. Antimicrobial activity was examined against two Gram-positive bacteria (*Kocuria rhizophila* ATCC9341 and *Staphylococcus aureus* FDA209P JC-1), three Gram-negative bacteria (*Escherichia coli* NIHJ JC-2, *Rhizobium radiobacter* NBRC14554, and *Tenacibaculum maritimum* NBRC16015), and three fungi (*Candida albicans* NBRC0197, *Glomerella cingulata* NBRC5907, and *Trichophyton rubrum* NBRC5467). Bulbimidazoles A–C (**1**–**3**) exhibited strong activity against *K. rhizophila* and *S. aureus* with MICs of 0.78−3.12 μg/mL. They did not show activity against *E. coli* and *R. radiobacter*, but were effective against *T. maritimum*, a causative agent of fish skin ulcer, with a minimum inhibitory concentration (MIC) ranging from 3.12 to 12.5 μg/mL. Compounds **1–3** also exhibited relatively potent activity against yeast and fungi tested in this study with MIC values ranging from 0.78 to 12.5 μg/mL. Overall, compound **3** showed better antimicrobial activity compared with compounds **1** and **2**. In addition, **1–3** showed moderate cytotoxicity against P388 murine leukemia cells with IC_{50} values of 5.0, 5.8, and 7.0 μM, respectively.

Table 2-6. Antimicrobial activity of bulbimidazoles A–C (**1–3**)

	MIC (μg/mL)		
Microorganisms	**1**	**2**	**3**
Kocuria rhizophila ATCC9341	0.78	0.78	1.56
Staphylococcus aureus FDA209P JC-1	1.56	1.56	3.12
Escherichia coli NIHJ JC-2	>100	>100	>100
Rhizobium radiobacter NBRC14554	>100	>100	>100
Tenacibaculum maritinum NBRC16015	3.12	6.25	12.5
Candida albicans NBRC0197	6.25	12.5	6.25
Glomerella cingulata NBRC5907	1.56	1.56	3.12
Trichophyton rubrum NBRC5467	0.78	1.56	3.12

2-3 Conclusion

In summary, HPLC-UV based chemical investigation of unknown secondary metabolites from a marine derived bacterium belonging to the genus *Microbulbifer* led to the discovery of three new alkanoyl imidazoles designated bulbimidazoles A–C (**1–3**). These compounds are structurally rare and new members of imidazole-containing natural products. Compounds **1–3**

consist of an alkyl chain and an imidazole ring coupled through a ketone group. Similar natural products known as nocarimidazoles A and B were discovered from a marine-derived actinomycete *Nocardiopsis,* which possess a primary amine group at 4-position of the imidazole ring [25]. Several key drugs such as HIV-1 protease inhibitor and aromatase inhibitor were synthesized from alkanoyl imidazoles used as an intermediate, but nocarimidazoles and bulbimidazoles are the only examples of this class of compounds obtained from nature [27, 31].

Heterocyclic compounds receive a central attention in medicinal chemistry and valuable importance in the search for new drug candidate in the pharmaceutical industry [32]. Particularly, nitrogen containing heterocyclic compounds are getting more consideration due to their diverse range of biological activities [33]. Imidazole is a five-membered aromatic heterocyclic ring consisting of two nitrogens, which are major components of a large number of highly significant biomolecules, such as amino acid histidine, histamine, purines, and biotin [34]. Imidazole is also used as privileged scaffolds for the development of new drugs in many areas of clinical field. Compounds with imidazole ring are amphoteric in nature possessing both acidic and basic characteristics and also exist in two equivalent tautomeric forms, in which the hydrogen atom can be located on either of the two nitrogen atoms. Therefore, the electron-rich nitrogen in imidazole ring cannot accept or donate protons and form a weak bond [35, 36]. This special feature of imidazole ring makes them ready to bind with a variety of therapeutic targets and exhibit broad pharmacological activities [37, 38]. The imidazole scaffolds are extremely versatile and have wide range of biological activity such as antibacterial, antifungal, antiparasitic, antiemetic and anticancer. For example, clotrimazole [39], phenethylimidazole [40] and miconazole [41] are imidazole-derived compounds used as antifungal drugs. Many imidazole-containing anticancer drugs such as dacarbazine [42], zoledronic acid [43] and azathioprine [44] have been developed (Figure 2-15). Most of imidazole-derived drugs are synthetic compounds. Bulbimidazoles are the example of natural products that contains important class of heterocycles imidazole ring with alkanoyl chain. This is notable that marine bacterial genus *Microbulbifer* have biosynthetic genes for the production of such structurally unique chemical entities which may offer new hope for researchers to discover new drug candidates from unexploited sources. From this study, I can conclude that bacterial strains isolated from unexplored sources such as a stony coral can be the suitable source for finding novel bioactive compounds and marine bacteria have great potential in the natural product drug discovery.

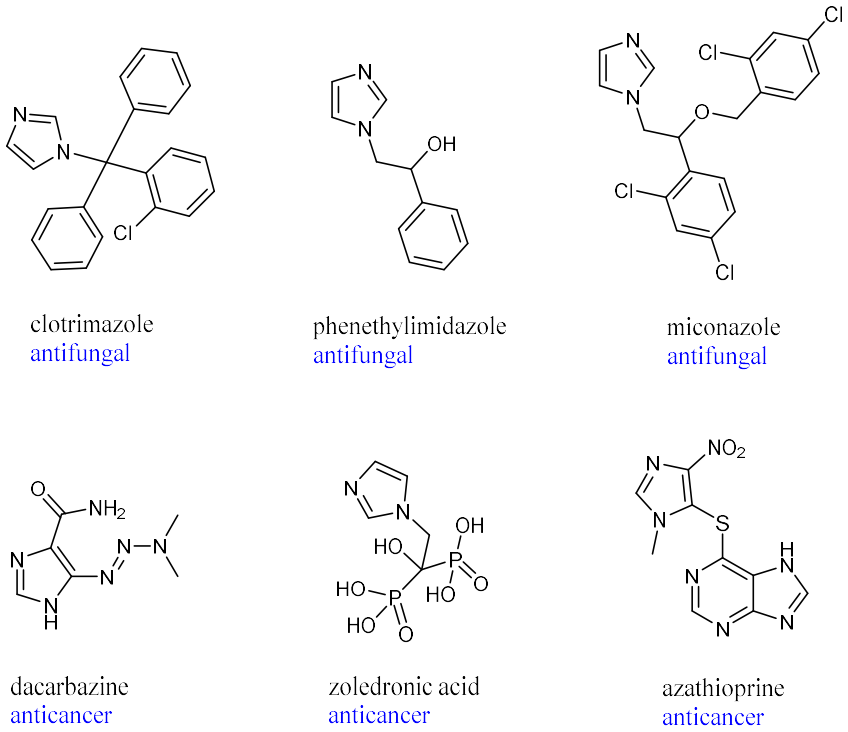

Figure 2-15. Chemical structures of imidazole-based antifungal and anticancer drugs.

The absolute configuration of anteiso-fatty acids from bacteria have been regarded to have an (*S*)-configuration. According to the biosynthesis of the fatty acids, the starter unit 2-methylbutanoyl-CoA is derived from L-isoleucine [45, 46]. However, this idea seems not always true for secondary metabolites. For example, nocapyrone L is a mixture of (*R*)- and (*S*)-enantiomers in a ratio of 2:3 from marine derived *Nocardiopsis* [47]. Bulbimidazole A is the second example of this kind, which also showed a mixture of (*R*)- and (*S*)-enantiomers in a ratio of 9:91. The absolute configurations of both of these compounds were unambiguously determined by a sound analytical technique. The inconsistency of absolute configuration of anteiso-methyl group could be explained by the acceptance of both (*R*)- and (*S*)-2-methylbutanoyl CoA as starter units by chain elongation enzymes [46]. In the upstream pathway, conversion of L-isoleucine into both of the enantiomers of 2-methylbutanoyl CoA takes place in *Streptomyces* [48, 49], rat skin [50] and apple [51] (Scheme 2-5). It is no wonder that the downstream pathway is also shaped to accept and process both enantiomers.

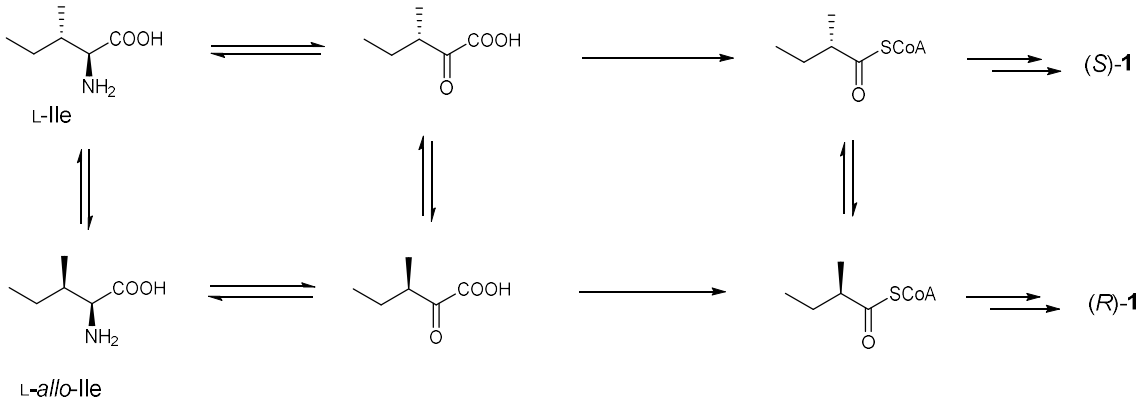

Scheme 2-5. Possible biosynthetic routes to (*R*)- and (*S*)-2-methylbutanoyl CoA from L-isoleucine.

Literature survey shows that a few natural products which have characteristic of enantiomeric mixtures. Most of them are discovered from marine environment. Trichodenone A is an (*R*)- and (*S*)-enantiomeric mixture, which was an antitumor metabolite of *Trichodermamha zianum* isolated from marine sponge [52]. Pericosines B and C are also enantiomeric mixtures, containing four chiral centers, a metabolite of *Periconia byssoide* isolated from sea hare *Aplysia kurodai* [53]. Therefore, marine microorganisms have a distinct type of biosynthetic genes to produce such natural products which possess enantiomaric mixture characteristic (Figure 2-16).

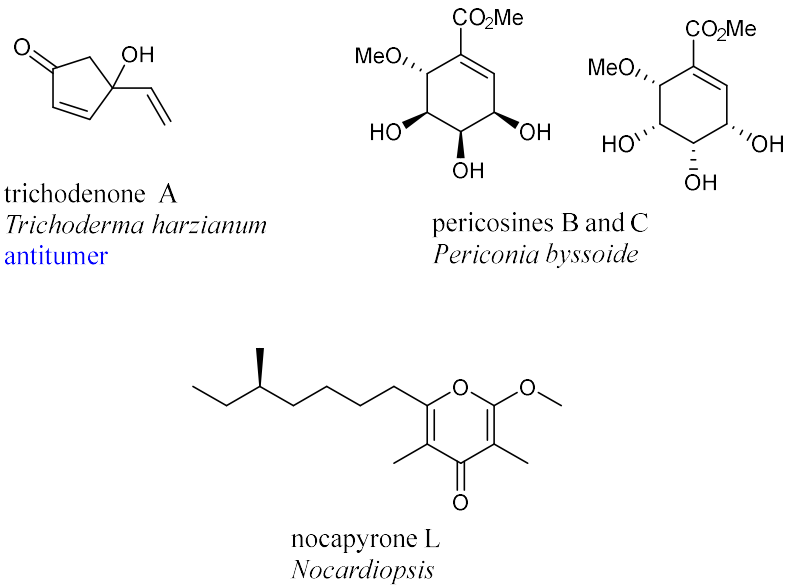

Figure 2-16. Natural products existing as a mixture of enantiomers.

Still a large portion of bacteria in marine environment are neglected in natural product screening compared with other microorganisms such as actinomycetes and fungi. In this

study, I discovered three structurally rare natural products from marine bacterial genus *Microbulbifer*, from which only two classes of compounds are known to date [24]. Additionally, it is notable that phylogenetically distinct species, *Microbulbifer* and *Nocardiopsis*, both obtained from marine environment, have ability to produce structurally similar compounds in terms of the acquisition and evolution of biosynthetic genes for secondary metabolites.

Proteobacteria is the most abundant phylum in marine pelagic systems and contains a wide array of Gram-negative marine bacteria that encompasses a number of medically important species, such as the genera *Neisseria*, *Yersinia*, and *Bortadella.* Biotechnologically important genera such as *Agrobacterium* and *Escherichia* are member of this phylum [54]. Moreover, many well-known pathogens from Vibrionaceae, Enterobacteriaceae and Pseudomonadaceae, also belong to Proteobacteria [55]. In marine environment, most of the species of proteobacteria inhabit by forming symbiotic associations with corals, sponges, and mollusks. Many bioactive compounds such as antibiotics have been discovered from Gram-positive bacteria, actinobacteria or filamentous fungi but very little attention have been paid to Gram-negative bacteria. However, in recent years, the number of bioactive natural products with novel structures from marine proteobacteria has increased significantly with the development of modern technology associated with functional genomics, such as computational sequence analysis, targeted DNA manipulation, and heterologous expression [56, 57]. With the aid of these technologies, it is becomeing easier to probe the mechanisms of biosynthetic gene cluster which are responsible for natural product production. It is revealed that marine proteobateria possess biosynthetic mechanism which are able to produce a distinct class of secondary metabolites including halogenated, sulfur-containing heterocycles, non-ribosomal peptides, and polyketides [56]. For example, a halogenated natural products pentabromopseudillin (Figure 2-17) was first isolated from a marine *Pseudoalteromonas* in the 1960, is composed of a brominated phenol coupled to a bromopyrrole and displayed potential broad-spectrum antimicrobial activity due to their ability to inhibit DNA and protein synthesis in both Gram-positive and Gram-negative pathogens as well as some cytotoxic effect in mammalian cells [58]. Up to date, a few natural products have been reported from this group of bacterial taxa, because most of them have not been studied extensively or remain uncultured for natural products screening program. Examples of a few bioactive compounds from marine proteobacteria are shown in Figure 2-17 [59-67].

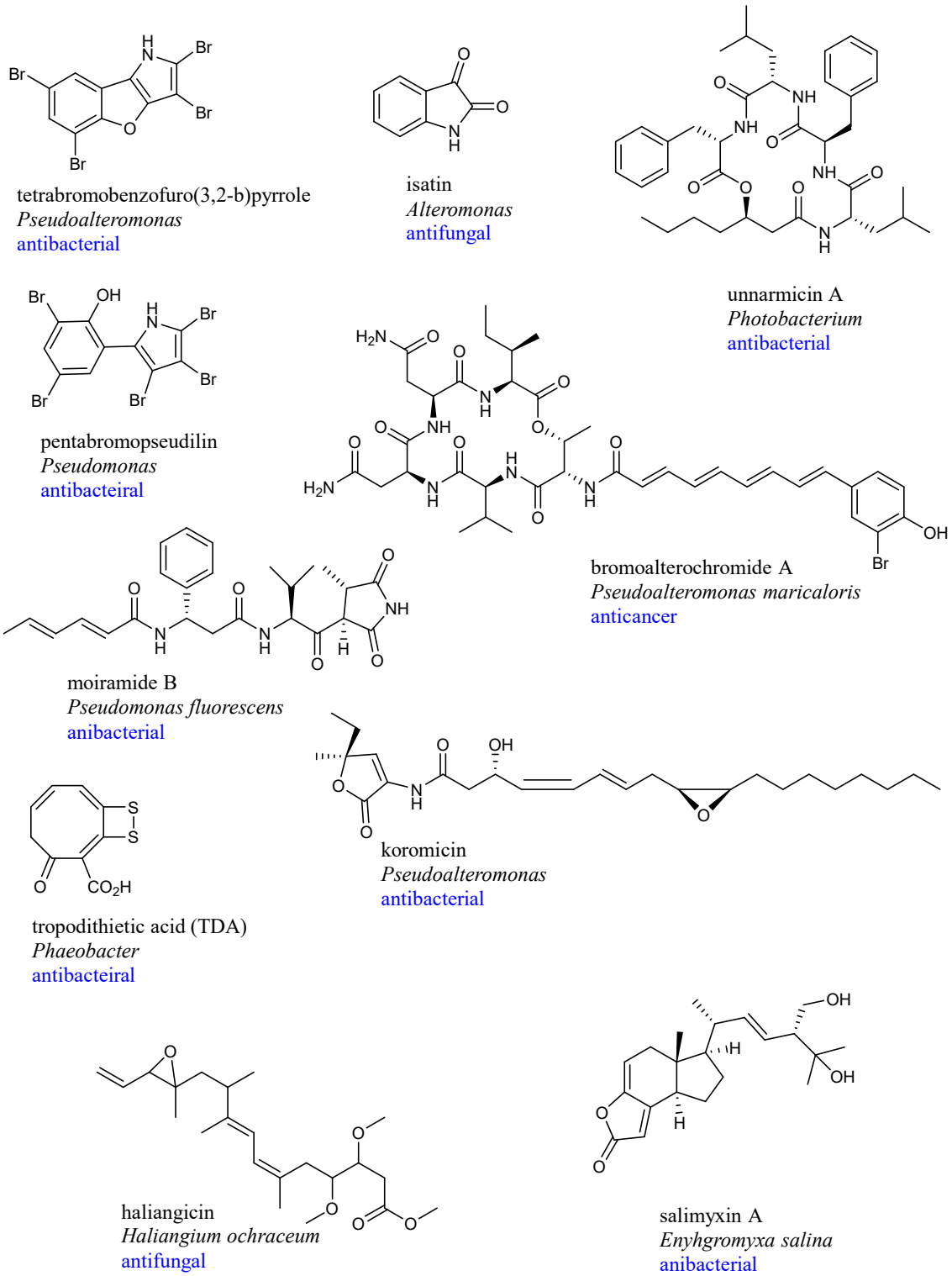

Figure 2-17. Structures of compounds isolated from marine proteobacteria

About 55% of marine bacterial species belong to the phylum proteobacteria which are considered to be a potential source of bioactive natural products because two important

factors involved behind this [68]. Firstly, most of marine proteobacteria inhabit with invertebrates in symbiotic interaction and produce secondary metabolites as a chemical defense to protect their host organisms from predators, pathogen, and the encroachment of competitors. This symbiotic relationship may alter their biosynthetic mechanisms for the production of new compounds in proteobacteria [56]. Secondly, bacteria of phylum proteobacteria are a dominant group in marine environment, because they evolved diverse metabolic and biosynthetic strategies in order to adapt to extremely harsh marine ecosystems [68]. Both factors make marine proteobacteria as an attractive reservoir of unknown bioactive molecules as well as more reasonable candidate group for natural products discovery program.

2-4 Experimental Section

General Experimental Procedures. The specific rotation was measured on a JASCO P-1030 polarimeter. UV spectra were obtained on a Shimadzu UV-1800 spectrophotometer. IR spectra were recorded on a PerkinElmer Spectrum 100 spectrophotometer. NMR spectra were obtained on a Bruker AVANCE 500 spectrometer in DMSO-d_6 supplemented with or without a trace amount of trifluoroacetic acid, using the signals of the residual solvent protons (δ_H 2.49) and carbons (δ_C 39.5) as internal standards for compounds **1**−**3** or in $CDCl_3$ using the signals of the residual solvent protons (δ_H 7.27) and carbons (δ_C 77.0) as internal standards for other compounds. HR-ESITOFMS spectra were recorded on a Bruker micrOTOF focus. An Agilent HP1200 system equipped with a diode array detector was used for analysis and purification.

Microorganism. The coral sample *Tubastraea* sp., collected as fishery waste at −10 to −15 m near the coast of Minami-Ise, Mie Prefecture, Japan, was obtained through a local aquarium vendor. Strain DC3-6 was isolated according to the method described previously and was identified as a member of genus *Microbulbifer* on the basis of 99.3% similarity in the 16S rRNA gene sequence (1,455 nucleotides; DDBJ accession number LC498626) to *Microbulbifer echini* AM134^T (accession number KJ789957).

Fermentation. Strain DC3-6 was maintained on Marine Agar 2216 (Difco). A loopful of strain DC3-6 was inoculated into a 500 mL K-1 flask containing 100 mL of Marine Broth 2216 as a seed culture. The seed culture was incubated at 30 °C on a rotary shaker at 200 rpm for 2 days. Then 3 mL each of seed culture was inoculated into 30 500 mL K1 flasks

containing 100 mL of A11M production medium, which consists of glucose 0.2%, soluble starch 2.5%, yeast extract 0.5%, polypeptone (Wako Pure Chemical Industries, Ltd.) 0.5%, NZ-amine (Wako Pure Chemical Industries, Ltd.) 0.5%, $CaCO_3$ 0.3%, and Diaion HP-20 (Mitsubishi Chemical Co.) 1% in natural seawater (collected from Toyama Bay, Japan). The pH of the medium was adjusted to 7.0 before sterilization. The inoculated flasks were incubated at 30 °C for 5 days with rotational shaking at 200 rpm.

Extraction and Isolation. After fermentation, 100 mL of 1-butanol was added to each flask, and the flasks were shaken for 1 h. The emulsified mixture was centrifuged at 6000 rpm for 10 min, and the organic layer was separated from the aqueous layer. Then, the organic layer was concentrated in vacuo to afford 4.3 g of extract from 3 L of production culture. The extract was chromatographed on a silica gel column with $CHCl_3$−MeOH (1:0, 20:1, 10:1, 4:1, 2:1, 1:1, and 0:1 v/ v). Fraction 3 (10:1) was concentrated to provide 0.35 g of brown oil, which was then fractionated by ODS column chromatography with a gradient of MeCN−0.1% HCO_2H aqueous solution (2:8, 3:7, 4:6, 5:5, 6:4, 7:3, and 8:2 v/v). Fraction 4 (5:5) was concentrated in vacuo, and the remaining aqueous layer was extracted with EtOAc. The organic layer was dried over anhydrous Na_2SO_4, filtered, and concentrated to give 83 mg of semipure material. Final purification was achieved by preparative HPLC (Cosmosil AR-II, Nacalai Tesque Inc., 10 × 250 mm, 4 mL/min, UV detection at 254 nm) with an isocratic elution of MeCN/0.1% HCO_2H aqueous solution (46:54) to afford **1** (11.3 mg, t_R 15.9 min), **2** (3.2 mg, t_R 11.2 min), and **3** (2.5 mg, t_R 10.5 min).

Bulbimidazole A (**1**): pale yellow, amorphous solid; $[\alpha]^{23}_D$ +1.2 (c 0.10, MeOH); UV (MeOH) λ_{max} (log ε) 253 (4.32) nm; IR (ATR) ν_{max} 3125, 2957, 2925, 1665 cm^{-1}; ^1H and ^{13}C NMR data, Table 1; HR-ESITOFMS *m*/*z* 237.1964 $[M + H]^+$ (calcd for $C_{14}H_{25}N_2O$, 237.1961).

Bulbimidazole B (**2**): pale yellow, amorphous solid; UV (MeOH) λ_{max} (log ε) 254 (4.32) nm; IR (ATR) ν_{max} 3127, 2957, 2925, 1667 cm^{-1}; ^1H and ^{13}C NMR data, Table 1; HR-ESITOFMS *m*/*z* 223.1809 $[M + H]^+$ (calcd for $C_{13}H_{23}N_2O$, 223.1804).

Bulbimidazole C (**3**): pale yellow, amorphous solid; UV (MeOH) λ_{max} (log ε) 254 (4.28) nm; IR (ATR) ν_{max} 3260, 2958, 2929, 1668 cm^{-1}; ^1H and ^{13}C NMR data, Table 1; HR-ESITOFMS *m*/*z* 223.1809 $[M + H]^+$ (calcd for $C_{13}H_{23}N_2O$, 223.1804).

Synthesis of (S)-8-Methyldecanoic Acid (**4**). To a solution of (*S*)-6- methyl-1-octanol (50 mg, 0.35 mmol, Wako Pure Chemical Industries, Ltd.) in dry CH_2Cl_2 (5 mL) was added Dess-

Martin periodinane (200 mg, 0.47 mmol) at room temperature (rt), and the resultant mixture was stirred for 2 h. The reaction mixture was quenched by adding saturated a $NaHCO_3$ solution and Na_2SO_3 solution and extracted with EtOAc. The organic layer was washed with H_2O and brine, dried over anhydrous Na_2SO_4, and concentrated in vacuo to afford (*S*)-6-methyloctanal (30 mg), which was used for the next reaction without further purification. (*S*)-6-Methyloctanal (30 mg, 0.21 mmol) was then reacted with methyl (triphenylphosphoranylidene)acetate (140 mg, 0.42 mmol) in dry CH_2Cl_2 (1 mL) at rt. After stirring for 2 h, ice−water was added to the reaction mixture, which was then extracted with EtOAc. The organic layer was washed with H_2O and brine, dried over anhydrous Na_2SO_4, and concentrated under reduced pressure. The residue was chromatographed over a silica gel column (*n*-hexane−EtOAc = 1:0− 1:1) to give methyl (*S*,*E*)-8-methyl-2-decenoate (12 mg, 17% yield): ^{1}H NMR ($CDCl_3$, 500 MHz) δ 0.83 (3H, d, *J* = 6.3 Hz), 0.85 (3H, t, *J* = 7.2 Hz), 1.08−1.15 (2H, m), 1.24−1.37 (5H, m), 1.40−1.45 (2H, m), 2.20 (2H, ddt, *J* = 1.7, 7.1, 7.1 Hz), 3.72 (3H, s), 5.81 (1H, dt, *J* = 15.6, 1.7 Hz), 6.97 (1H, dt, *J* = 15.6, 7.0 Hz); ^{13}C NMR ($CDCl_3$, 125 MHz) δ 167.2, 149.8, 120.8, 51.4, 36.3, 34.3, 32.3, 29.4, 28.3, 26.6, 19.2, 11.4; HR-ESITOFMS *m*/*z* 221.1648 $[M + Na]^+$ (calcd for $C_{12}H_{22}O_2Na$, 221.1644).

A solution of methyl (*S,E*)-8-methyl-2-decenoate (12 mg, 60 μmol) in MeOH (3 mL) was vigorously stirred with Pd/C (20 mg) under a H_2 atmosphere at rt. After stirring for 8 h, the reaction mixture was passed through Celite and the eluent was concentrated under reduced pressure to give methyl (*S*)-8-methyldecanoate (10 mg, 50 μmol), which was further subjected to hydrolysis in MeOH−THF (2 mL each) containing 1 M NaOH (2 mL). After stirring at rt for 12 h, the solution was acidified with 2 M HCl and extracted with EtOAc. The EtOAc layer was washed with H_2O and brine, dried over anhydrous Na_2SO_4, and concentrated in vacuo. The residue was purified on a silica gel column (*n*-hexane−EtOAc = 1:0−1:1) to afford (*S*)-8-methyldecanoic acid (10 mg, 88% yield): ^{1}H NMR ($CDCl_3$, 500 MHz) δ 0.83 (3H, d, *J* = 6.3 Hz), 0.85 (3H, t, *J* = 7.2 Hz), 1.06−1.16 (2H, m), 1.24− 1.37 (9H, m), 1.63 (2H, quint, *J* = 7.6 Hz), 2.34 (2H, t, *J* = 7.6 Hz); ^{13}C NMR ($CDCl_3$, 125 MHz) δ 179.2, 36.5, 34.3, 33.9, 29.5, 29.4, 29.0, 26.8, 24.6, 19.1, 11.3.

Preparation of (*R*)- and (*S*)-2-(Anthracene-2,3- dicarboximido)propyl ester of (*S*)-8-Methyldecanoic acid [(*S*)- 4-(*R*)-2A1P and (*S*)-4-(*S*)-2A1P]. (*S*)-8-Methyldecanoic acid (**4**, 5.0 mg, 26 μmol) was treated with (*R*)-2-(anthracene-2,3-dicarboximido)-propanol [(*R*)-2A1P] (8.0 mg, 26 μmol), EDAC (6.0 mg, 34 μmol), and DMAP (trace amount) in dry CH_2Cl_2 (4 mL) at rt for 17 h. The reaction was quenched with ice−water, and the mixture was

extracted with EtOAc. The organic layer was concentrated in vacuo, and the residue was chromatographed over a silica gel column (*n*-hexane−EtOAc = 1:0−1:1) to give (*R*)-2-(anthracene-2,3-dicarboximido)- propyl ester of (*S*)-8-methyldecanoic acid [(*S*)-**4**-(*R*)-2A1P, 3.5 mg]: ^{1}H NMR ($CDCl_3$, 500 MHz) δ 0.74 (3H, d, *J* = 6.3 Hz), 0.78 (3H, t, *J* = 7.3 Hz), 0.98−1.22 (9H, m), 1.49 (2H, m), 1.57 (3H, d, *J* = 7.1 Hz), 2.22 (2H, t, *J* = 7.5 Hz), 4.43 (1H, dd, *J* = 11.2, 5.0 Hz), 4.63 (2H, dd, *J* = 11.2, 9.8 Hz), 4.74 (1H, m), 7.63 (2H, m), 8.09 (2H, m), 8.51 (2H, s), 8.64 (2H, s); HR-ESITOFMS m/z 496.2451 $[M + Na]^+$ (calcd for $C_{30}H_{35}NO_4Na$, 496.2458). (*S*)-**4**-(*S*)-2A1P was prepared from (*S*)-**4** and (*S*)-2A1P in a similar manner to that described above: ^{1}H NMR ($CDCl_3$, 500 MHz) δ 0.73 (3H, d, *J* = 6.3 Hz), 0.78 (3H, t, *J* = 7.3 Hz), 0.98−1.25 (9H, m), 1.49 (2H, m), 1.57 (3H, d, *J* = 7.2 Hz), 2.22 (2H, t, *J* = 7.6 Hz), 4.43 (1H, dd, *J* = 11.2, 4.9 Hz), 4.63 (1H, dd, *J* = 11.2, 9.7 Hz), 4.74 (1H, m), 7.63 (2H, m), 8.09 (2H, m), 8.50 (2H, s), 8.64 (2H, s); HR-ESITOFMS *m*/*z* 496.2454 $[M + Na]^+$ (calcd for $C_{30}H_{35}NO_4Na$, 496.2458).

Oxidative Degradation of 1 and Derivatization with (*R*)-2A1P. A solution of bulbimidazole A (**1**, 0.5 mg, 2 μmol) in a mixture of MeCN (80 μL) and deionized H_2O (60 μL) was stirred with $NaIO_4$ (4.8 mg, 22 μmol) until the salt was dissolved. To this solution were added CCl_4 (80 μL) and a solution of $RuCl_3$ hydrate in 0.1 M sodium phosphate buffer (1 mg/mL, 60 μL, pH 7.6), and the biphasic mixture was vigorously stirred at rt for 18 h. The reaction mixture was passed through Celite, and the filter cake was washed with MeCN. After evaporation of the organic solvent from the filtrate, the aqueous solution was acidified with 2 M HCl and extracted with EtOAc. The EtOAc layer was washed with H_2O and brine, dried over anhydrous Na_2SO_4, and concentrated in vacuo to give (*S*)-8-methyldecanoic acid (0.8 mg), which was reacted with (*R*)-2A1P in a similar manner to that described for (*S*)-**4**-(*R*)-2A1P to give the ester derivative of 8- methyldecanoic acid derived from **1** [*nat*-**1**-(*R*)-2A1P, 0.4 mg]: HR-ESITOFMS m/z 496.2457 $[M + Na]^+$ (calcd for $C_{30}H_{35}NO_4Na$, 496.2458).

Determination of the Absolute Configuration at the anteiso-Methyl Branching in 1. *nat*-4-(*R*)-2A1P and synthetic (*S*)-**4**-(*R*)-2A1P and (*S*)-**4**-(*S*)-2A1P were analyzed by HPLC under the following conditions. Column: tandemly connected Develosil ODS-HG-3 (3.0 mm i.d. × (250 + 150) mm, Nomura Chemical); mobile phase: MeCN−MeOH−THF = 3:1:1; column temperature: −42.5 °C; flow rate: 0.10 mL/min. The column was cooled by using Cryocool CC-100 (Neslab Instruments Inc.). HPLC peaks were detected by monitoring fluorescence intensity at 460 nm with the excitation at 298 nm by using an FP-4025 fluorescence detector

(JASCO Corporation). Retention times were 234 min for (*S*)-4-(*S*)-2A1P and 243 min for (*S*)-4-(*R*)- 2A1P, while nat-4-(*R*)-2A1P gave peaks at 235 and 244 min in a ratio of 9.1:90.9.

Antimicrobial Activity. Antimicrobial activity was evaluated by the liquid microculture method using round-bottomed 96-well microtiter plates against five bacteria, *Kocuria rhizophila* ATCC9341, *Staphylococcus aureus* FDA209P JC-1, *Escherichia coli* NIHJ JC-2, Rhizobium *radiobacter* NBRC14554, and *Tenacibaculum maritimum* NBRC16015, and three fungi, *Candida albicans* NBRC0197, *Glomerella cingulata* NBRC5907, and *Trichophyton rubrum* NBRC5467, as indication strains. Mueller-Hinton broth (Difco), Sabouraud dextrose broth (Difco), and Marine Broth (Difco) were used for bacteria, fungi, and *T. maritimum* NBRC16015, respectively. Compounds **1**−**3**, reference drugs kanamycin sulfate for bacteria, sulfamethoxazole for *R. radiobacter* NBRC14554 and *T. maritimum* NBRC16015, and amphotericin B for fungi were made in 2-fold dilution series along the longer side of the plates by sequential transfer of 100 μL aliquots between the adjacent wells, to which the same amount of medium was predispensed. To each well was added a 100 μL suspension of the indication strains prepared at 1×10^4−10^5 cfu/mL from a culture at the logarithmic growth phase. The solvent vehicle added to the top rows was set at 0.5% of the final culture volume to avoid the effect on the growth of microbes. The plates were incubated at 37 °C for 20 h for bacteria, at 24 °C for *T. maritimum* NBRC16015, and at 25 °C for fungi. The experiments were done in triplicate, and the absorbance at 650 nm was measured using a microplate reader.

Cytotoxicity Assay. P388 murine leukemia cells were maintained in RPMI-1640 medium containing L-glutamine (product no. 186- 02155) supplemented with 10% fetal bovine serum and 0.1 mg/mL gentamicin sulfate. Compounds **1**−**3** and doxorubicin as a reference were used to validate cytotoxicity in a 96-well round-bottom microtiter plate. To each well were seeded the cells at a final density of 1×10^4 cells/well, and 200 μL cultures thus made were incubated for 72 h at 37 °C in an atmosphere of 5% CO_2 in air with 100% humidity. Viability of the cells was visualized by addition of 50 μL of medium containing XTT (1 mg/mL) and PMS (40 μg/mL) to each well. After incubating for 4 h at 37 °C, medium was carefully removed by a suction aspirator, and formazan dye formed by respiratory reduction by living cells was quantified by measurement of absorption at 450 nm and read by a microplate reader to calculate the rate of cell growth inhibition at each concentration. The results of triplicate experiments were plotted on a graph to deduce IC_{50} values.

References

1) Rizzo, C.; Giudice, A. L. *Diversity* **2018**, *10*, 52-87.

2) Tobias A. M. Gulder, T. A. M.; Moore, B. S. *Curr. Opin. Microbiol.* **2009**, *12*, 252–260.

3) Hossain, M. B.; Helm, D. V. D.; Antel. J.; Sheldrick, G. M.; Sanduja, S. K.; Weinheimer, A. J. *Proc. Natl. Acad. Sci. USA*, **1988**, *85*, 4118-4122.

4) Tsukimoto, M.; Nagaoka, M.; Shishido, Y.; Fujimoto, J.; Nishisaka, F.; Matsumoto, S.; Harunari, E.; Imada, C.; Matsuzaki, T. *J. Nat. Prod.* **2011**, *74*, 2329−2331.

5) Simmons, T. L.; Andrianasolo, E.; McPhail, K.; Flatt, P.; Gerwick, W. H. *Mol. Cancer Ther*. **2005**, *3*, 333−342.

6) Jimenez C. *ACS Med. Chem. Lett.* **2018**, *13,* 959-961.

7) Van de Water, J. A.; Allemand, D.; Ferrier-Pagès, C. *Microbiome* **2018**, *6*, 64-91.

8) Gonzalez, J. M.; Mayer, F.; Moran, M. A.; Hodson, R. E.; Whitman, W. B. *Int. J. Syst. Bacteriol.***1997**, *47*, 369–376.

9) D'Ambrosio M.; Guerriero A.; Pietra F. *Helv. Chim. Acta.* **1987**, *70*, 2019-2027.

10) Look S. A.; Fenical W.; Jacobs R. S.; Clardy J. *Proc. Natl. Acad. Sci. U. S. A.* **1985**, *83*, 6238-6240.

11) Bordeleau M. E.; Mori A.; Oberer M.; Lindqvist L.; Chard L. S.; Higa T.; Belsham G. J.; Wagner G.; Tanaka J.; Pelletier J. *Nat. Chem. Biol.* **2006**, *2*, 213-220.

12) Alam, M.; Sanduja, R.; Sanduja, M.; Wellington, G. *Heterocyclic* **1998**, *27*, 719-724.

13) Alam, N.; Hong, J.; Lee, C. O.; Im, K. S.; Son, B. W.; Choi, J. S.; Won Chul Choi, W. C.; Jung, J. H. *J. Nat. Prod.* **2001**, *64*, 956-957.

14) Chen Y. H.; Lu M. C.; Chang Y. C.; Hwang T. L.; Wang W. H.; Weng C. F.; Sung K. J. *Tetrahedron Lett.* **2012**, *53*, 1675-1677.

15) Chen Y. H.; Kuo J; Su J. H.; Hwang T. L.; Chen Y. H.; Lee C. H.; Weng C. F.; Sung P. J. *Mar. Drugs.* **2012**, *10*, 1566-1571.

16) Gao C. H.; Tian X. P.; Qi S. H.; Luo X. M.; Wang P; Zhang S. *J. Antibiot.* **2010**, *63*, 191-193.

17) Raimundo, I.; Silva, S. G.; Costa. R.; Keller-Costa. T. *Mar. Drugs* **2018**, *16*, 485-509.

18) Sharma, A. R.; Zhou, T.; Harunari, E.; Oku, N.; Trianto, A.; Igarashi, Y. *J.*

Antibiot. **2019**, *72*, 634-639.

19) Sharma, A. R.; Harunari, E.; Zhou, T.; Trianto, A.; Igarashi, Y. *Beilstein J. Org. Chem.* **2019**, *15*, 2327–2332.

20) Sharma, A. R.; Harunari, E.; Oku, N.; Matsuura, N.; Trianto, A.; Igarashi, Y. *Beilstein J. Org. Chem.* **2020**, *16*, 297–304.

21) Gonzalez, J. M.; Mayer, F.; Moran, M. A.; Hodson, R. E.; Whitman, W. B. *Int. J. Syst. Bacteriol.***1997**, *47*, 369–376.

22) (a) Yoon, J.-H.; Kim, I.-G.; Shin, D.-Y.;1, Kang, K. H.; Park, Y.-H. *Int. J. Syst. Evol. Microbiol.* **2003**, *53*, 53–57; (b) Yoon, J.-H; Kim, I.-G.; Oh, T.-K.; Park, Y.-H. *Int. J. Syst. Evol. Microbiol*. **2004**, *54*, 1111–1116; (c) Yoon, J.-H.; Jung, S.-Y.; Kang, S.-J.; Oh, T.-K. *Int. J. Syst. Evol. Microbiol.* **2007**, *57*, 2365–2369; (d) Zhang, D.-S.; Huo, Y.-Y.; Xu, X.-W.; Wu, Y.-H.; Wang, C.-S.; Xu, X.-F.; Wu, M. *Int. J. Syst. Evol. Microbiol.* **2012**, *62*, 505–510; (e) Nishijima, M.; Takadera, T.; Imamura, N.; Kasai, H.; An, K.-D.; Adachi, K.; Nagao, T.; Sano, H.; Yamasato, K. *Int. J. Syst. Evol. Microbiol.* **2009**, *59*, 1696–1707.

23) https://antismash.secondarymetabolites.org (accessed on Apr. 21, 2021)

24) Jayanetti, D. R.; Braun, D. R.; Barns, K. J.; Rajski, S. R.; Bugni, T. S. *J. Nat. Prod.* **2019**, *82*, 1930–1934.

25) Leutou, A. S.; Yang I.; Kang, H.; Seo, E. K.; Nam, S. J.; Fenical W. *J. Nat. Prod.* **2015**, *25*, 2846-2849.

26) Kawakami, J.-I.; Kimura K.; Yamaoka, M. *Synthesis* **2003**, *5*, 677-680.

27) Iwasaki, S. *Helv. Chim. Acta.* **1976**, *59*, 2738-2752.

28) Akasaka, K.; Meguro, H.; Ohrui, H. *Tetrahedron Lett.* **1997**, *38,* 6853-6856.

29) Foster, R. T.; Jamail, F. *J. Chromatogr*. **1987**, *416*, 388-393.

30) Akasaka, K.; Ohrui, H. *Biosci. Biotechnol. Biochem.* **1999**, *63*, 1209–1215.

31) Thompson, S. K.; Murthy, K. H. M.; Zhao, A.; Winborne, E.; Green, A. W.; Fisher, S. M.; DesJarlais, R. L.; Tomaszek, T. A.; Jr.; Meek, T. D.; John G. Gleason, J. G.; Abdel-Meguid S. S. *J. Med. Chem.* **1994**, *37*, 3100-3107.

32) Gaba, M.; Singh, S.; Mohan, C. *Eur. J. Med. Chem*. **2014**, *76*, 494–505.

33) De Simone, R. W.; Currie, K. S.; Mitchell, S. A.; Darrow, J. W.; Pippin, D. A. *Comb. Chem. High T. Scr.* **2004**, *7*, 473–494.

34) Fei, F.; Zhou, Z. *Expert. Opin. Ther. Pat.* **2013**, *23*, 1157–1179.

35) Wright, J. B.; *Chem. Rev*. **1951**, *48*, 397–541.

36) Bhatnagar, A.; Sharma, P. K.; Kumar, N. *Int. J. Pharm. Tech. Res*. **2011**, *3*, 268–

282.

37) Gaba, M.; Singh, D.; Singh, S.; Sharma, V.; Gaba, P. *Eur. J. Med. Chem.* **2010**, *45*, 2245–2249.

38) Ingle, R. G.; Magar, D. D. *Int. J. Drug. Res. Tech*. **2011**, *1*, 26–32.

39) Sheehan, D. J.; Hitchcock, C. A.; Sibley, C. M. *Clin. Microbiol. Rev.* **1999**, *12*, 40–79.

40) Bossche, H. V. *Biochem Pharmacol*. **1974**, *23*, 887–899.

41) Heel, R. C.; Brogden, R. N.; Parke, G. E.; Speight, T. M.; Avery, G. S. *Drugs* **1980**, *19*, 7–30.

42) Pectasides, D.; Yianniotis, H.; Alevizakos, N.; Bafaloukos, D.; Barbounis,V.; Varthalitis, J.; Dimitriadis, M.; Athanassiou, A. *Br. J. Cancer.* **1989**, *60*, 627–629.

43) Li, E. C.; Davis, L. E. *Clin. Ther*. **2003**, *25*, 2669–2708.

44) Hawwa, A. F.; Millership, J. S.; Collier, P. S.; Vandenbroeck, K.; McCarthy, A.; Dempsey, S.; Cairns, C.; Collins, J.; Rodgers, C.; McElnay, J. C. *Br. J. Clin. Pharmacol*. **2008**, *66*, 517–528.

45) Kaneda, T. *Microbiol. Rev*. **1991**, *55*, 288-302.

46) Challis, G. L. *Microbiology* **2008**, *154*, 1555-1569.

47) Kim, Y.; Ogura, H.; Akasaka, K.; Oikawa, T.; Matsuura, N.; Imada, C.; Hisato Yasuda, H.; Igarashi, Y. *Mar. Drugs* **2014**, *12*, 4110-4125.

48) Yajima, T.; Mason, K.; Katz, E. *Antimicrob. Agents Chemother*. **1976**, *9*, 224-232.

49) Oku, H.; Sakihama, T.; Chinen, I. *Biosci. Biotech. Biochem*. **1996**, *60*, 1724-1725.

50) Matich, A.; Rowan, D. *J. Agric. Food Chem.* **2007**, *55*, 2727−2735.

51) Li, Q.; Qin, X.; Liu, J.; Gui, C.; Wang, B.; Li, J.; Ju, J. *J. Am. Chem. Soc.* **2015**, *138*, 408-415.

52) Usami, Y.; Ikura, T.; Amagata, T.; Numata, A. *Tetrahedron Asymmetry* **2000**, *11*, 3711–3725.

53) Usami, Y.; Okada, Y.; Yamada, T. Natural pericosines B and C. *Chirality* **2001**, *23*, 7–11.

54) Gupta, R.S. *FEMS Microbiol. Rev.* **2000**, *24*, 367–402.

55) Williams, K.P.; Gillespie, J.J.; Sobral, B.W.; Nordberg, E.K.; Snyder, E.E.; Shallom, J.M.; Dickerman, A.W. *J. Bacteriol*. **2010**, *192*, 2305–231.

56) Timmermans, M. L.; Paudel, Y. P.; Ross A. C. *Mar. Drugs*. **2017**, *15*, 235-270.

57) Hsu, P. D.; Lander, E. S.; Zhang F. *Cell*. **2014**, *157*, 1262–1278.

58) Bowman, J. *Mar. Drugs* **2007**, *5*, 220-241.

59) Fehér, D.; Barlow, R.; McAtee, J.; Hemscheidt, T. K. *J. Nat. Prod.* **2010**, *73*, 1963-1966.

60) Gil-Turnes, M. S.; Hay, M. E.; Fenical, W. *Science.* **1989**, *246*, 116-118.

61) Oku, N.; Kawabata, K.; Adachi, K.; Katsuta, A.; Shizuri, Y. *J. Antibiot.* **2008**, *61*, 11-17.

62) Speitling, M.; Smetanina, O. F.; Kuznetsova, T. A.; Laatsch, H. *J. Antibiot*. **2007**, *60*, 36-42.

63) Needham, J.; Kelly, M. T.; Ishige, M.; Andersen, R. J. *J. Org. Chem*. **1994**, *59*, 2058-2063.

64) Yoshikawa, K.; Takadera, T.; Adachi, K.; Nishijima, M.; Sano, H. *J. Antibiot.* **1997**, *50*, 949-953.

65) Brinkhoff, T.; Bach, G.; Heidorn, T.; Liang, L.; Schlingloff, A.; Simon, M. *Appl. Environ. Microbiol.* **2004**, *70*, 2560-2565.

66) Fudou, R.; Iizuka, T.; Sato, S.; Ando, T.; Shimba, N.; Yamanaka, S. *J. Antibiot.* **2001**, *54*, 149-152.

67) Felder, S.; Kehraus, S.; Neu, E.; Bierbaum, G.; Schäberle, T. F.; König, G. M. *Chem. Bio. Chem.* **2013**, *14*, 1363-1371.

68) Buijs, Y.; Bech, P. K.; Vazquez-Albacete, D.; Bentzon-Tilia, M.; Sonnenschein, E. C.; Gram, L.; Zhang, S. D. *Nat. Prod. Rep.* **2019**, *36*, 1333-1350.

2-5 Spectral Data

Table of Contents

Figure S26. ^{1}H NMR spectrum of *nat*-**4**-(*R*)-2A1P (500 MHz, $CDCl_3$)

Figure S27. ^{1}H NMR spectrum of synthetic (*S*)-**4**-(*S*)-2A1P (500 MHz, $CDCl_3$)

Figure S28. ^{1}H NMR spectrum of synthetic (*S*)-**4**-(*R*)-2A1P (500 MHz, $CDCl_3$)

Figure S1. UV spectrum of bulbimidazole A (**1**)

(MeOH)

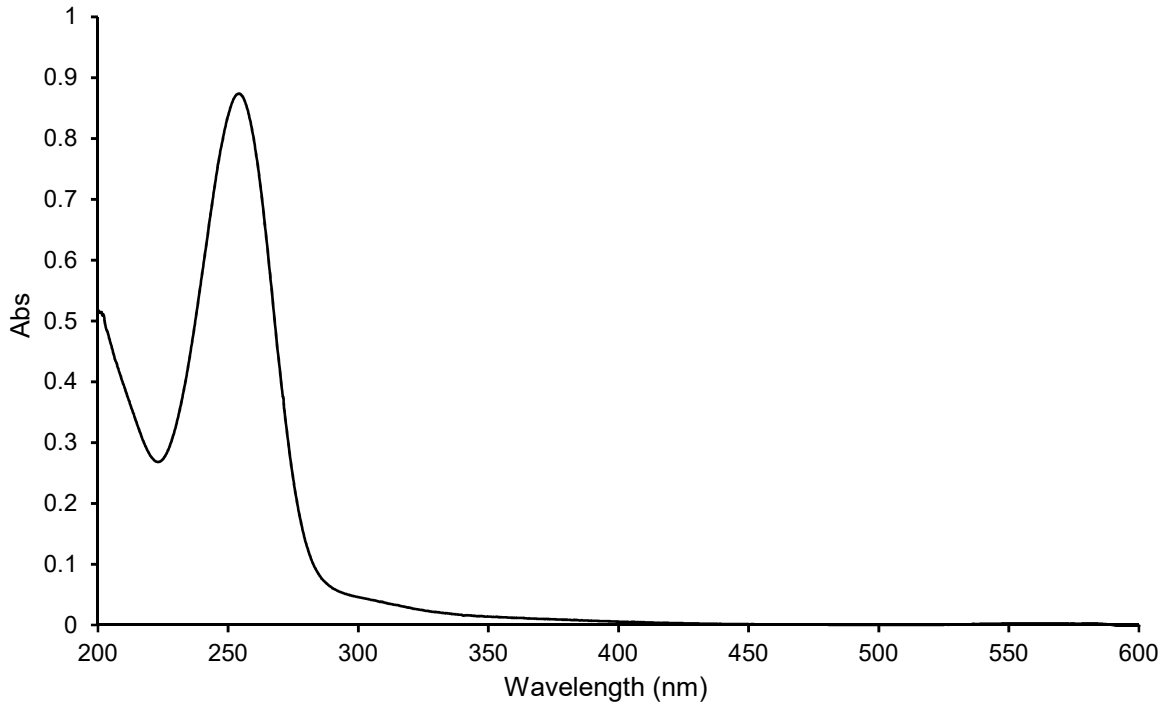

Figure S2. IR spectrum of **1**

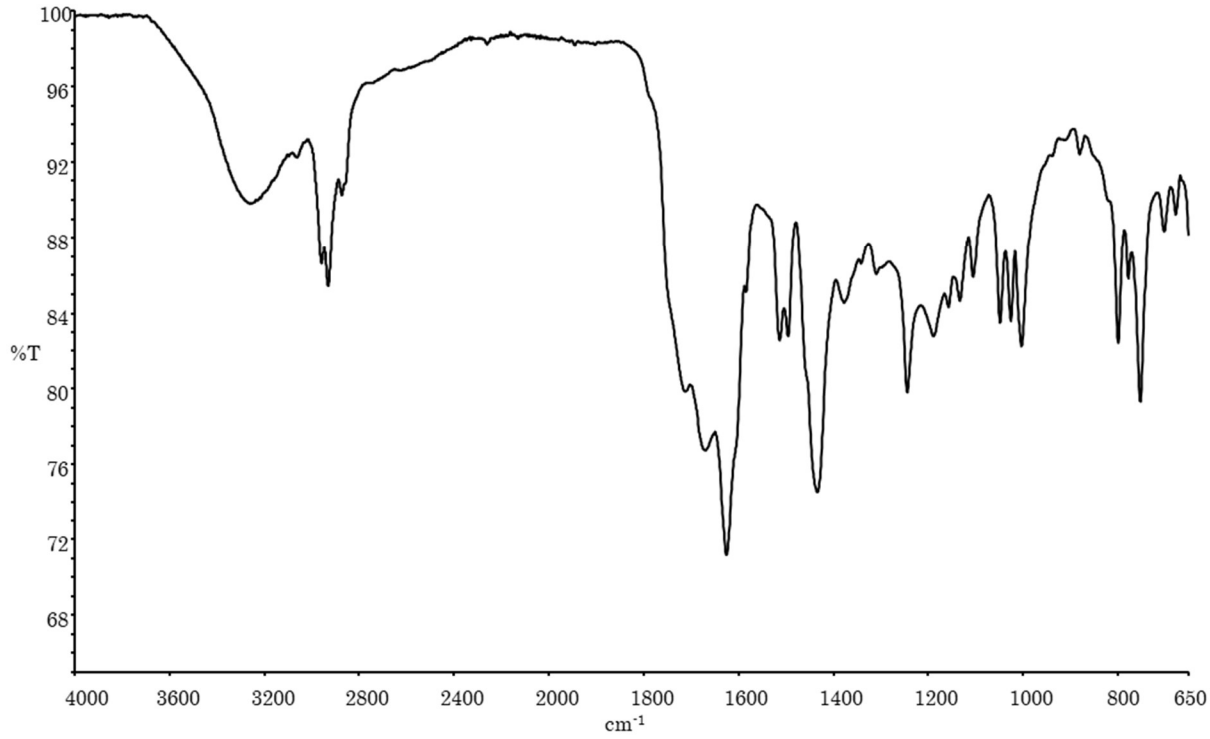

Figure S3. ^{1}H NMR spectrum of **1** (500 MHz, DMSO-d_6 with TFA)

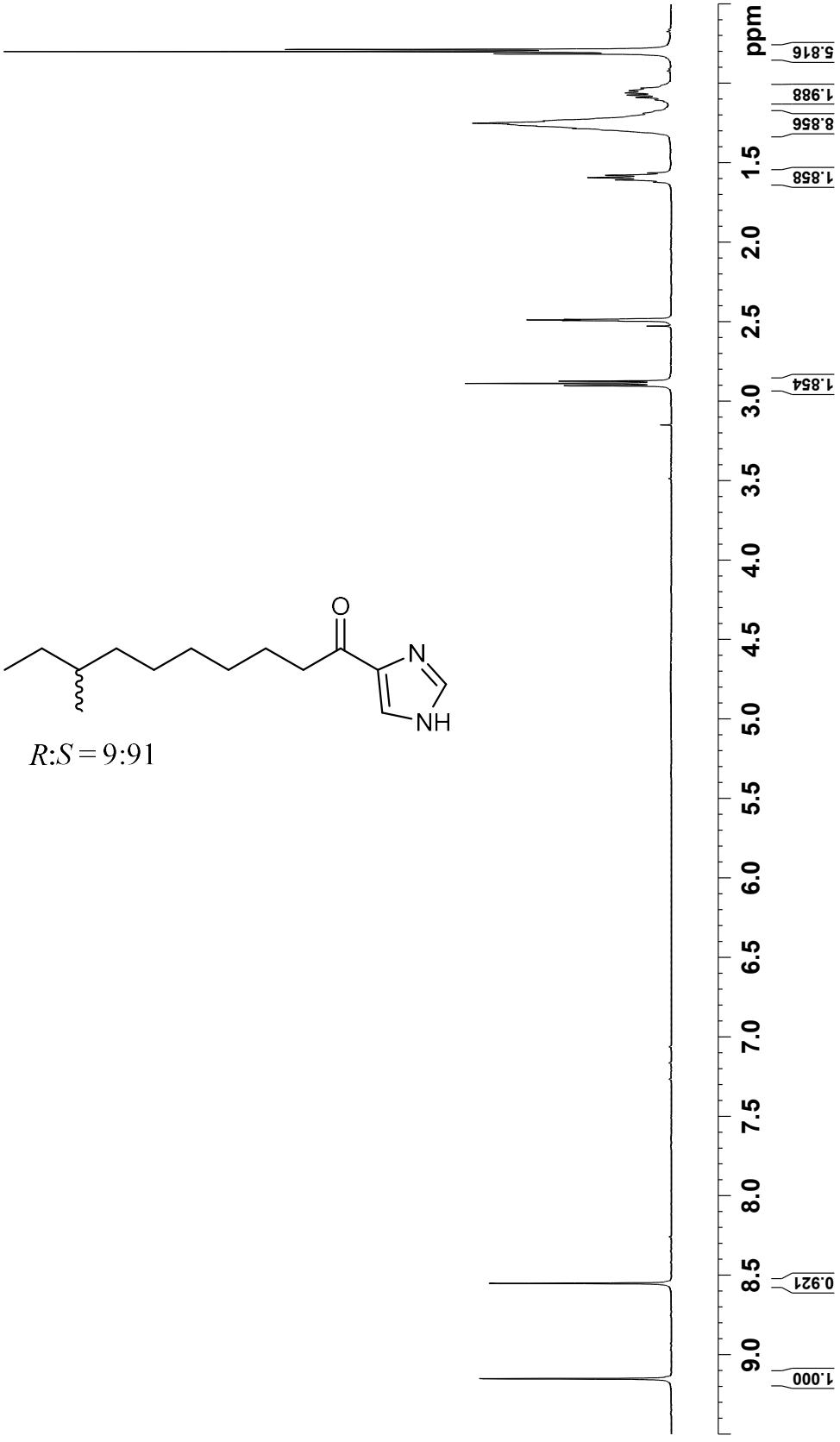

Figure S4. ^{1}H NMR spectrum of **1** (500 MHz, DMSO-d_6 without TFA)

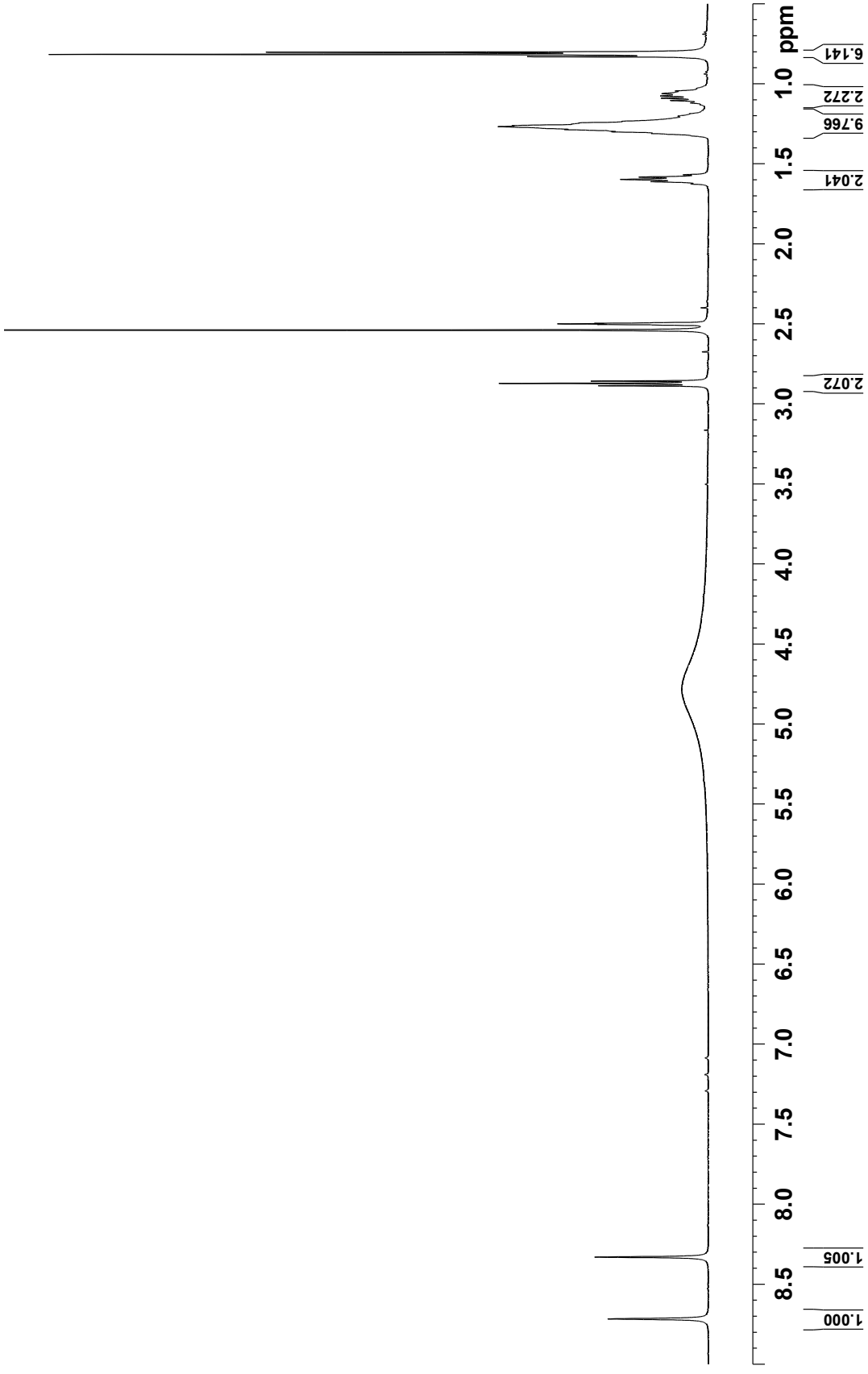

Figure S5. ^{13}C NMR spectrum of **1** (500 MHz, DMSO-d_6 with TFA)

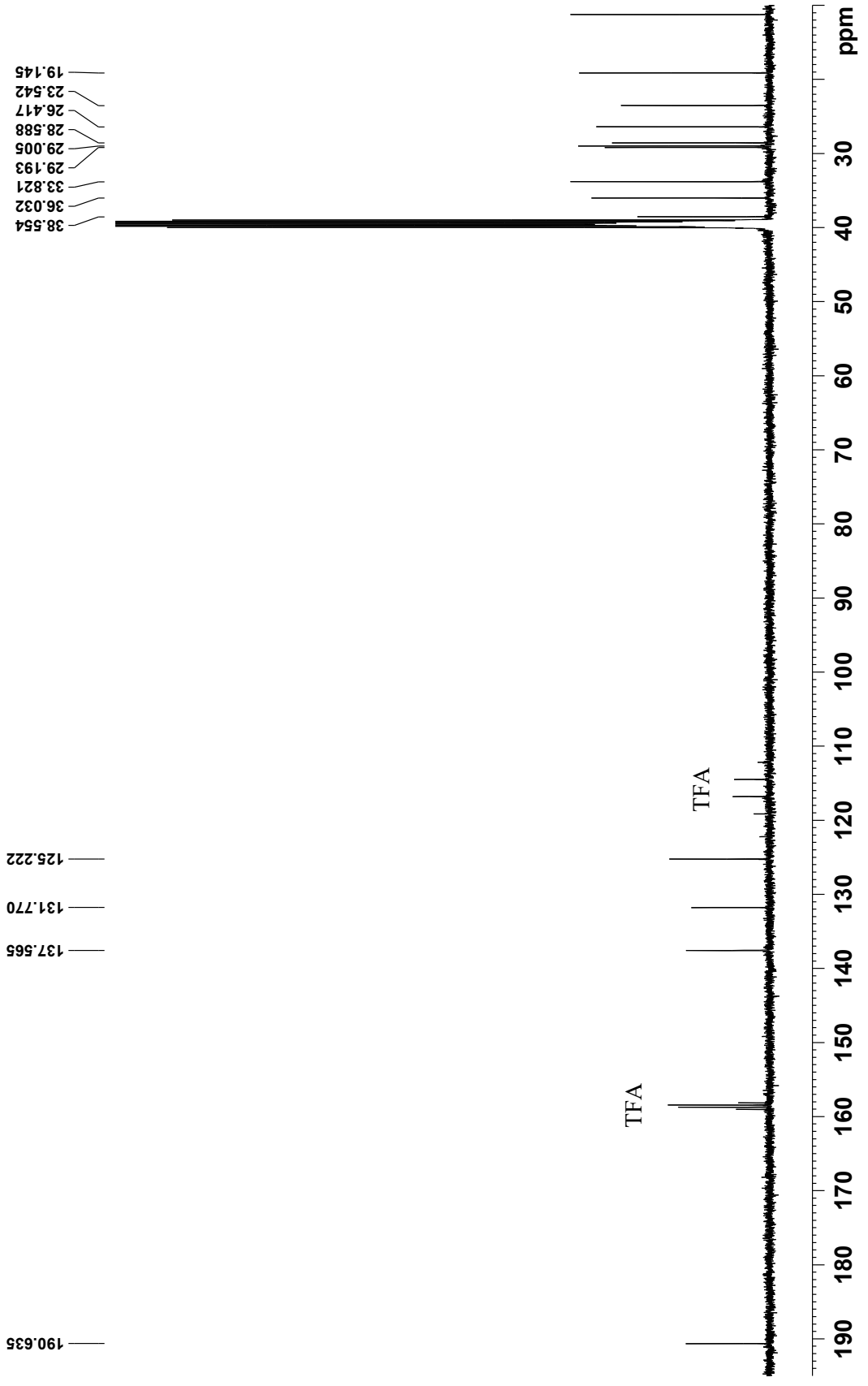

Figure S6. ^{13}C NMR spectrum of **1** (125 MHz, DMSO-d_6 without TFA)

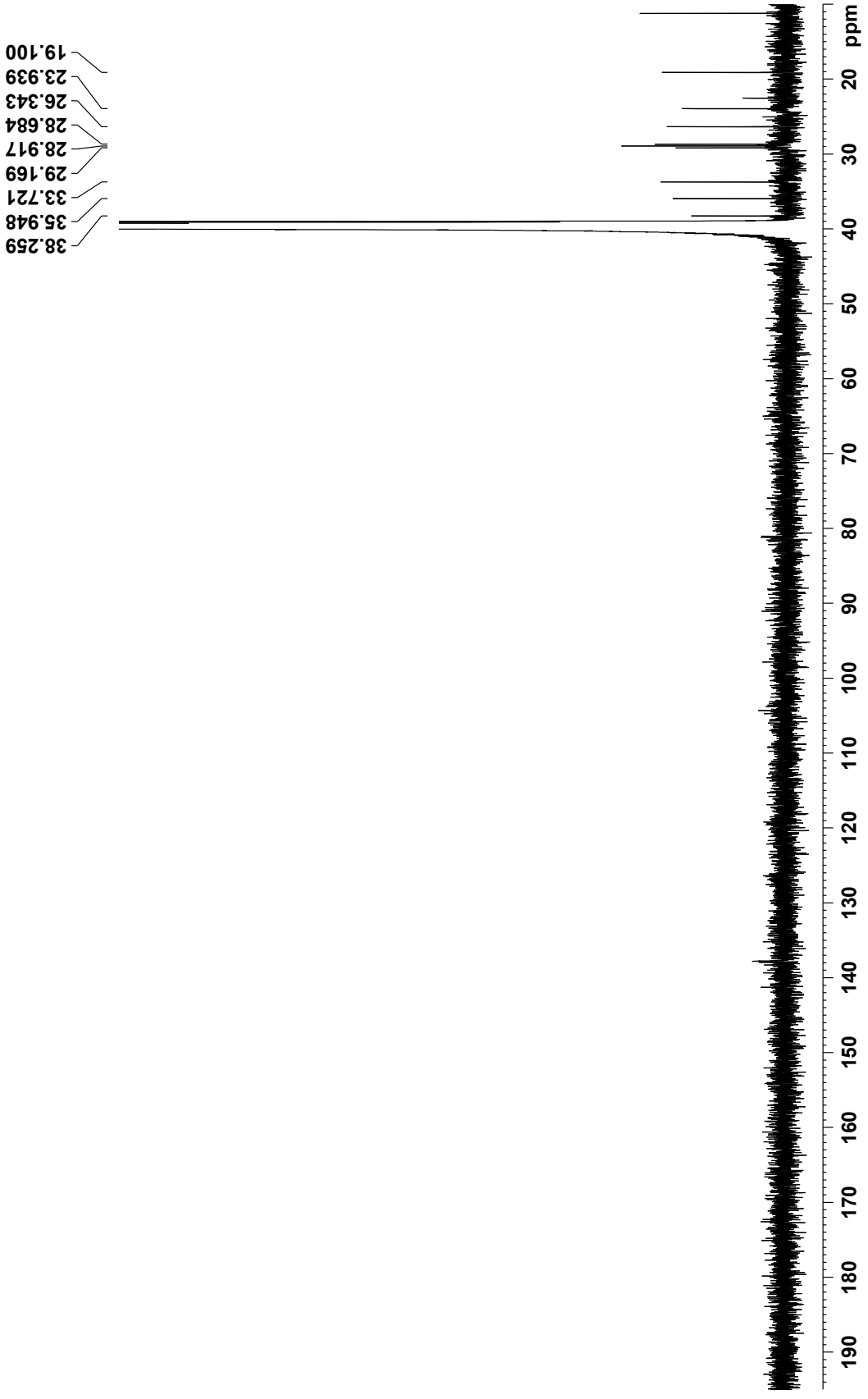

Figure S7. COSY spectrum of **1** (500 MHz, DMSO-d_6 with TFA)

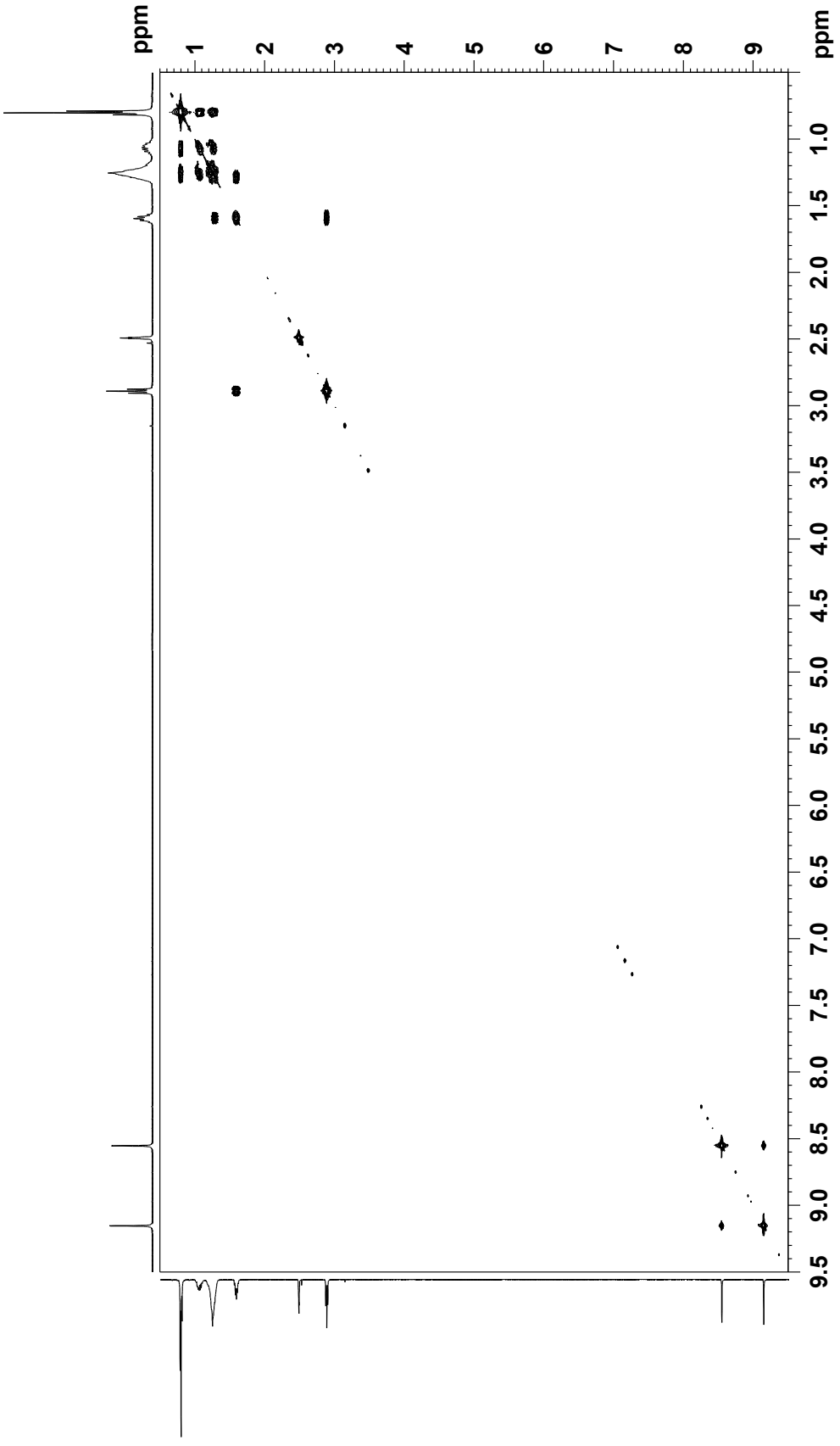

Figure S8. HSQC spectrum of **1** (500 MHz, DMSO-d_6 with TFA)

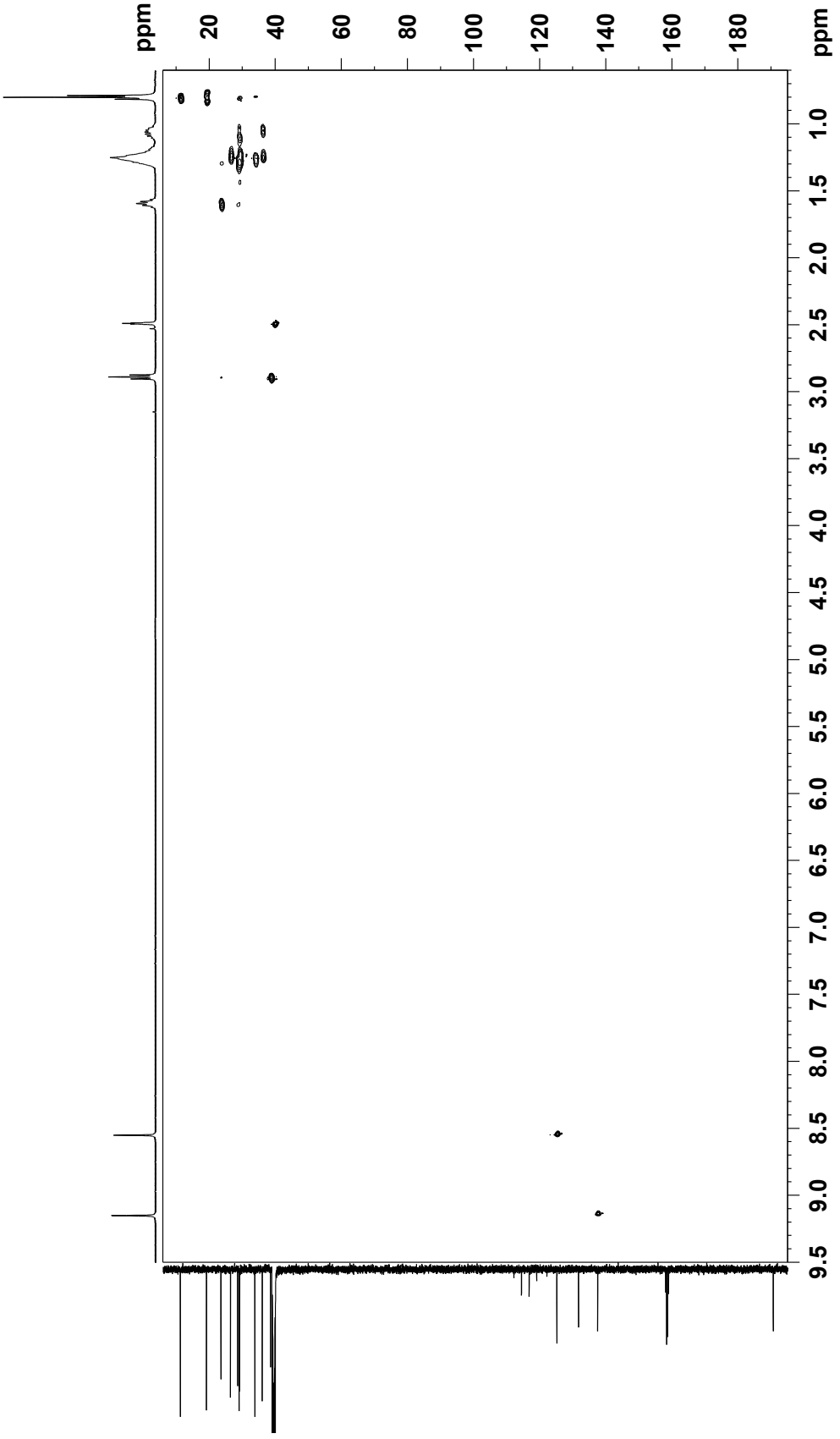

Figure S9. HSQC spectrum of **1** (500 MHz, DMSO-d_6 without TFA)

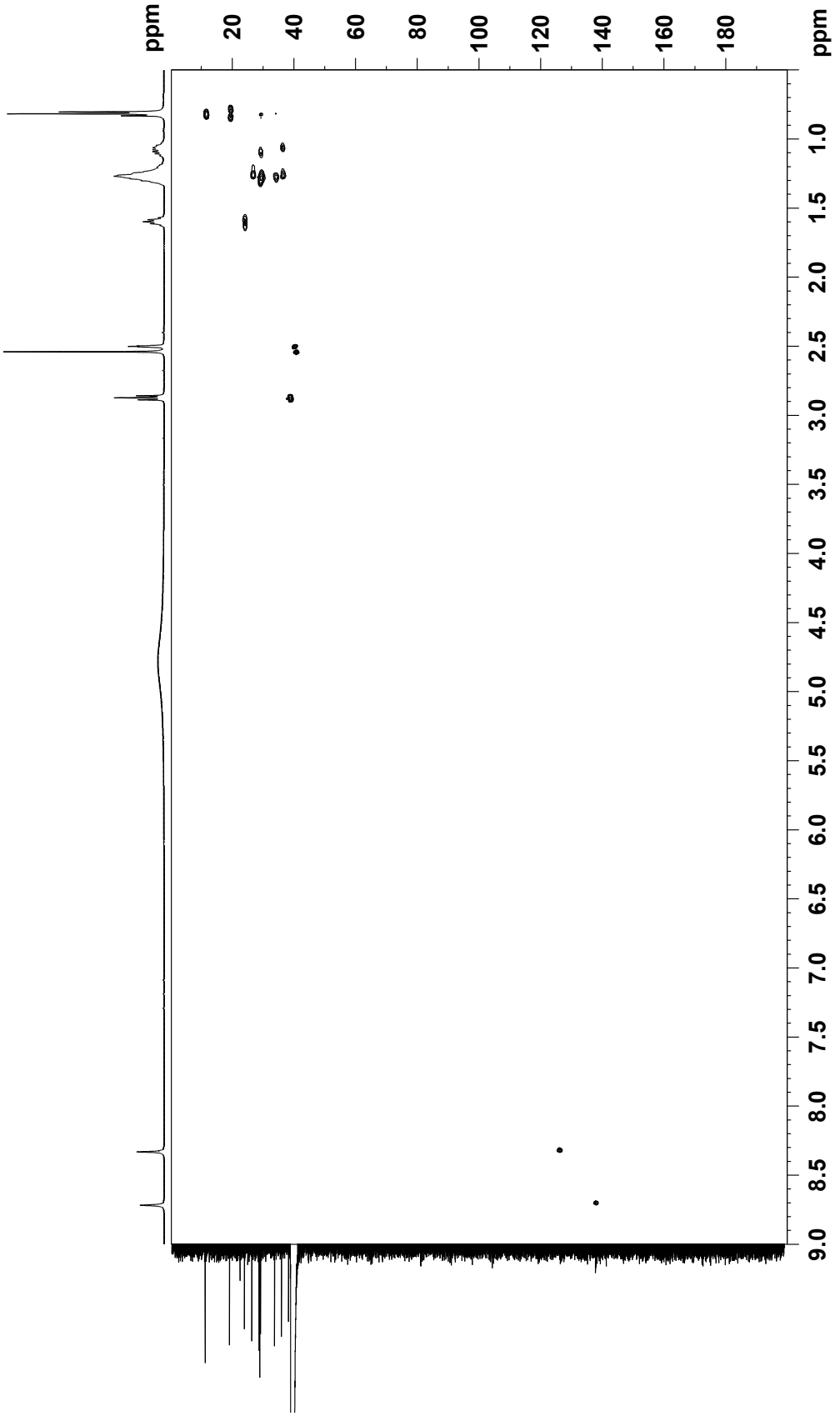

Figure S10. HMBC spectrum of **1** (500 MHz, DMSO-d_6 with TFA)

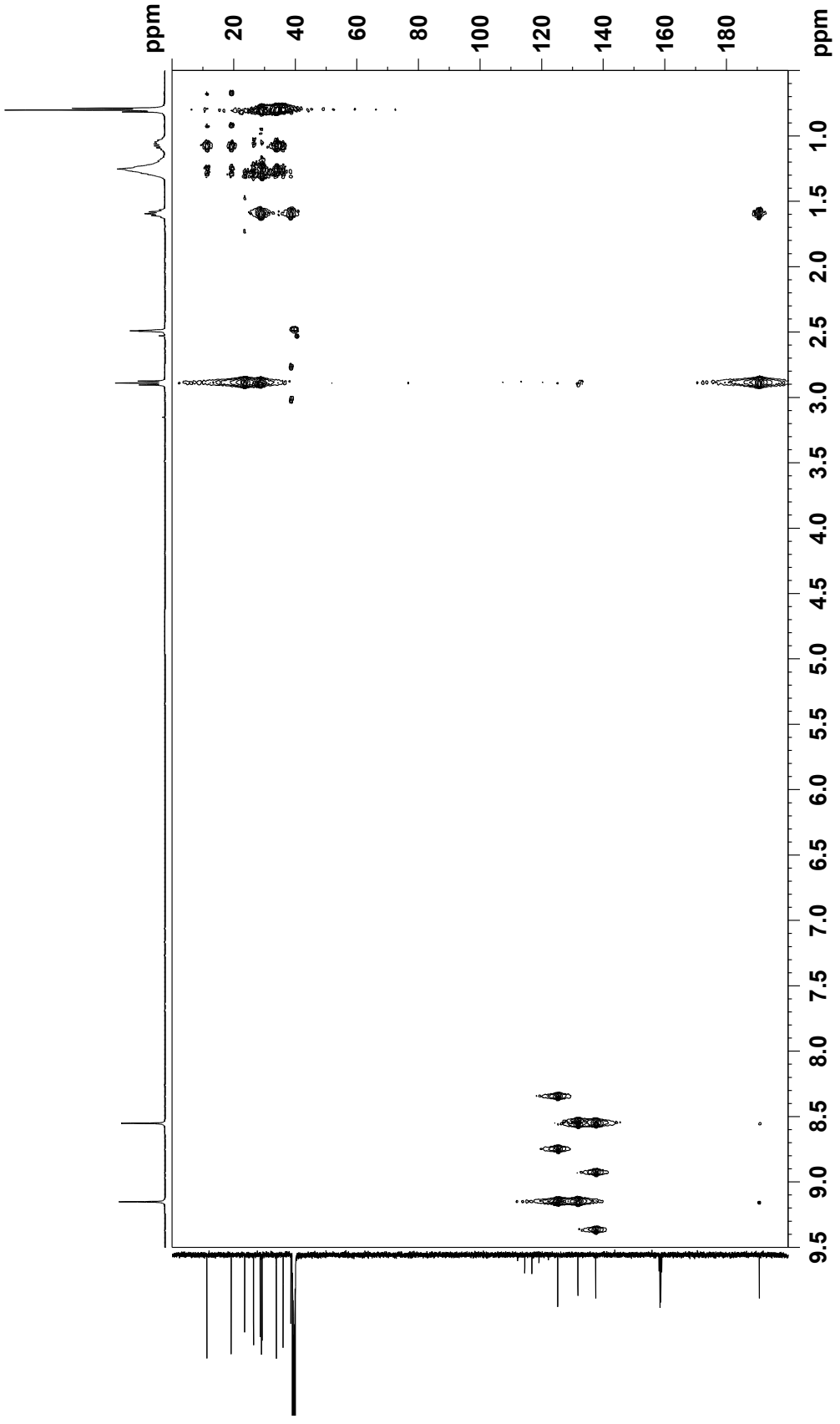

Figure S11. HMBC spectrum of **3** (500 MHz, DMSO-d_6 without TFA)

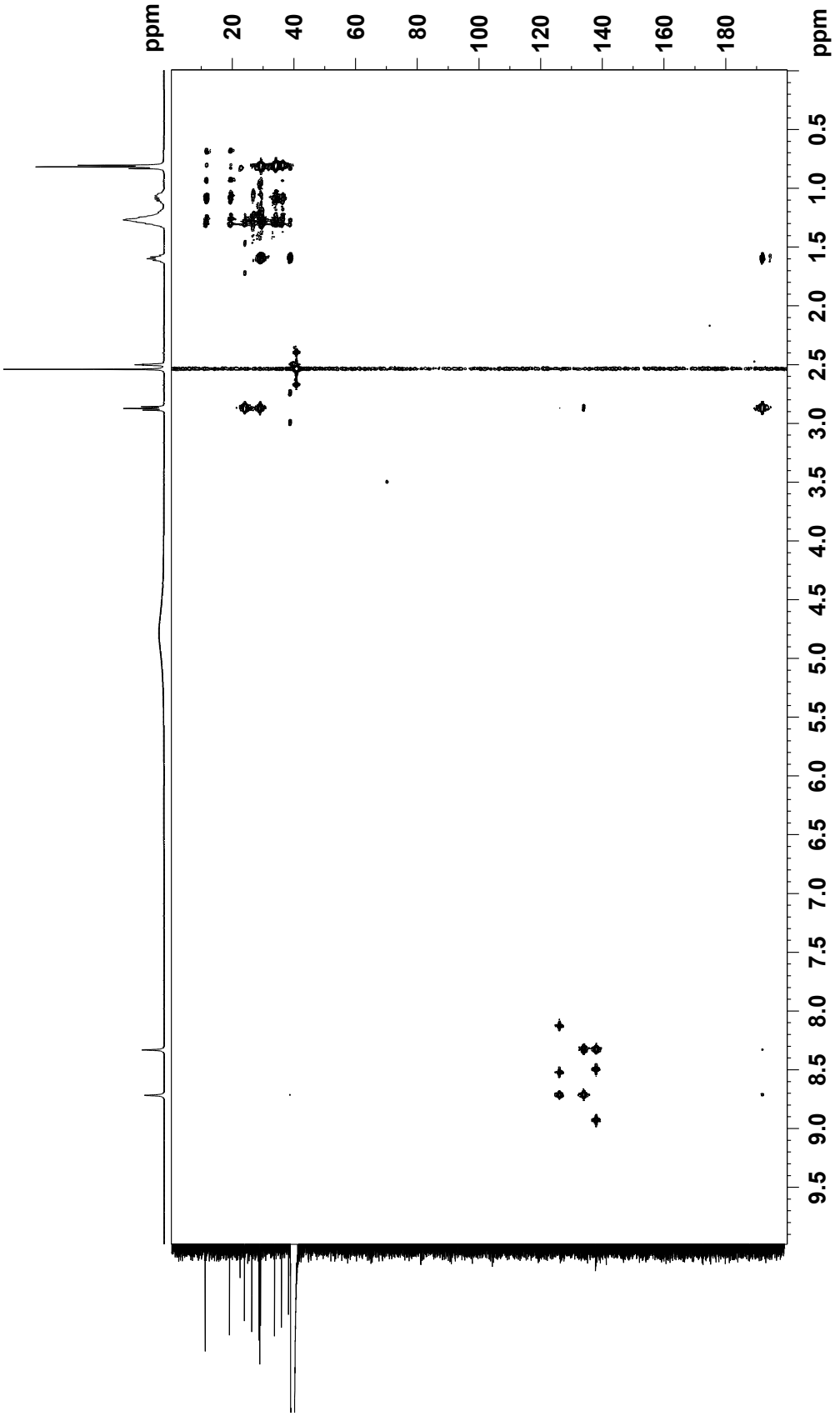

Figure S12. UV spectrum of bulbimidazole B (**2**)

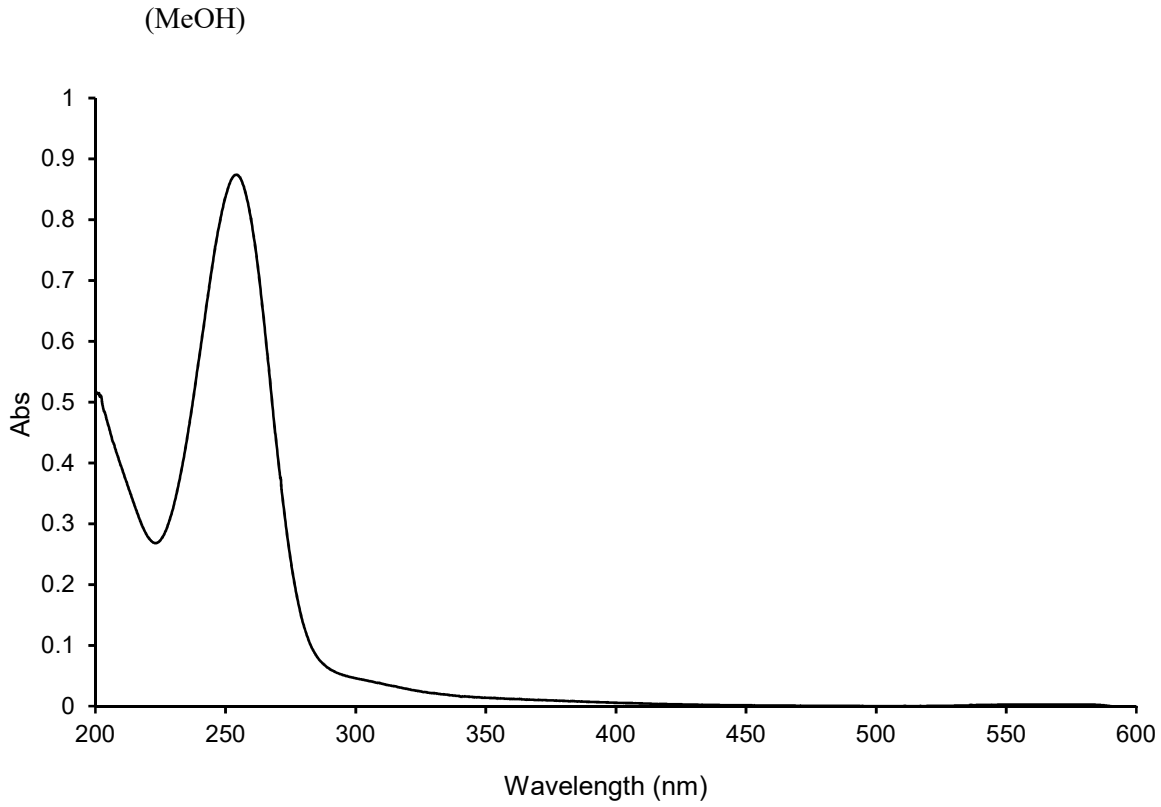

Figure S13. IR spectrum of **2**

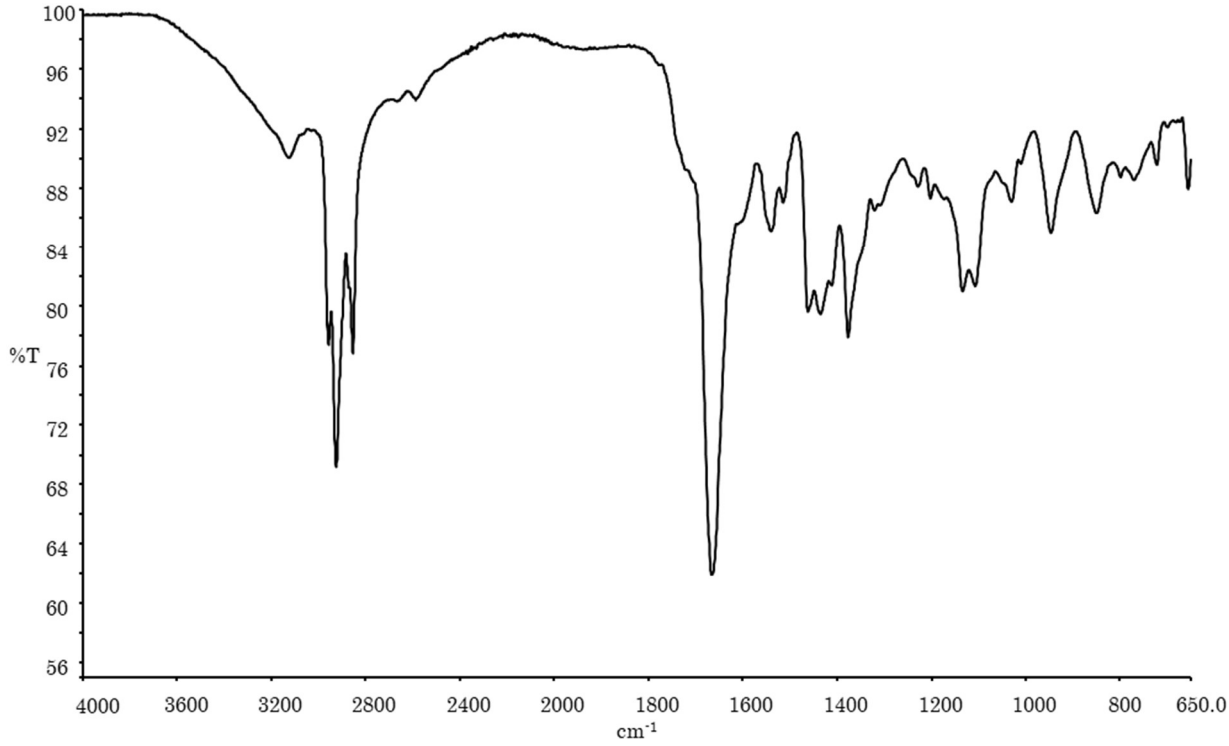

Figure S14. ^{1}H NMR spectrum of **2** (500 MHz, DMSO-d_6 with TFA)

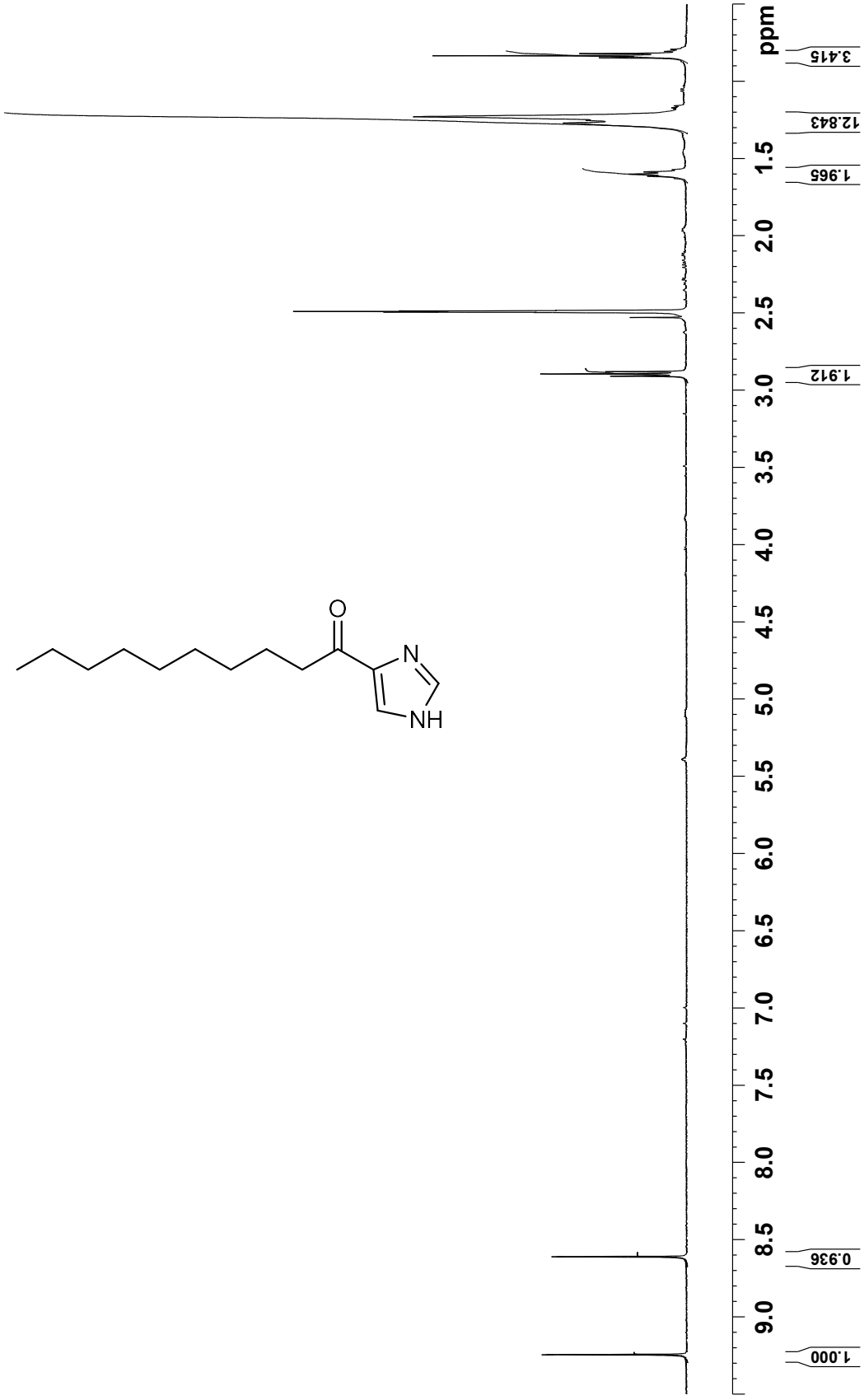

Figure S15. ^{13}C NMR spectrum of **2** (125 MHz, DMSO-d_6 with TFA)

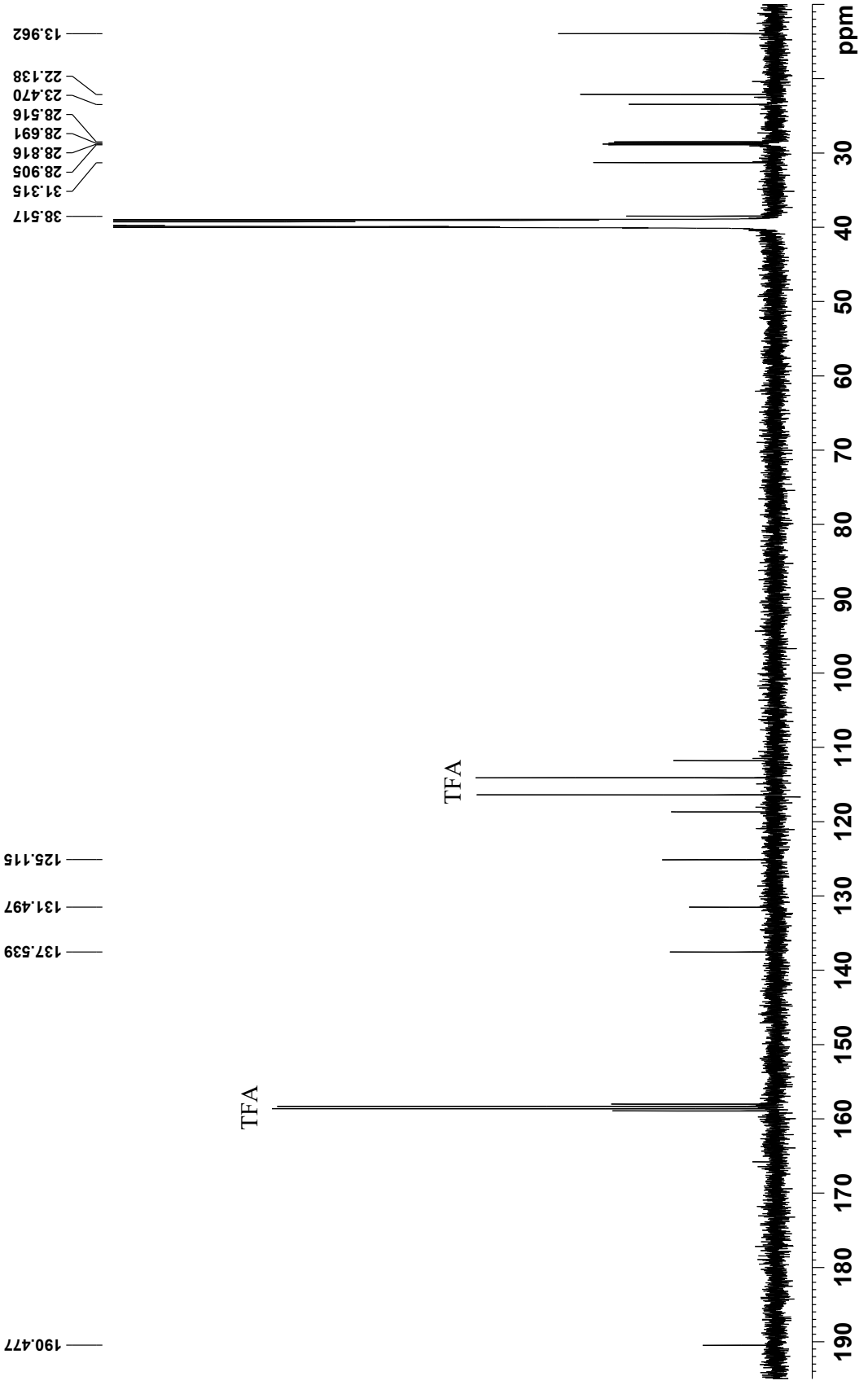

Figure S16. COSY spectrum of **2** (500 MHz, DMSO-d_6 with TFA)

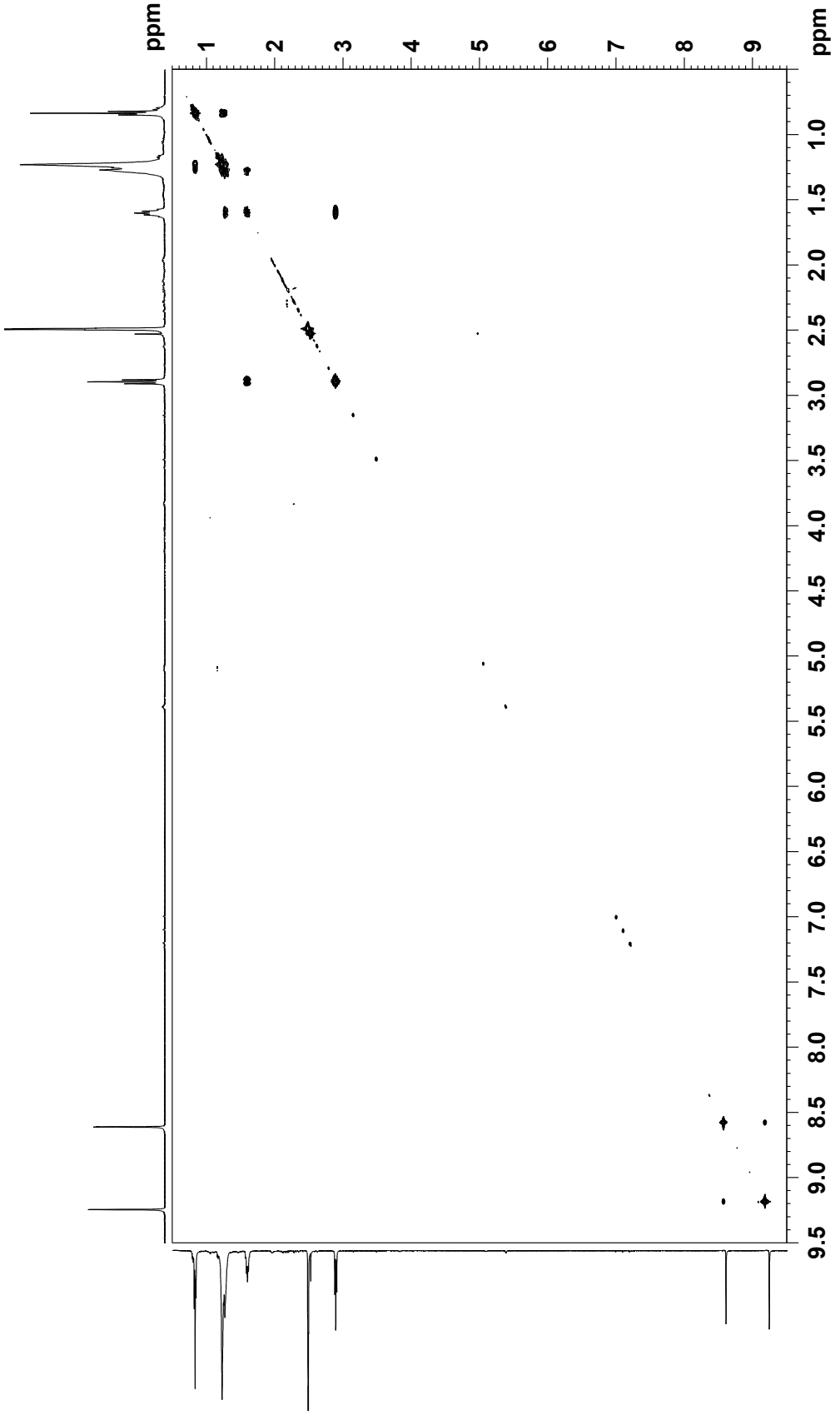

Figure S17. HSQC spectrum of **2** (500 MHz, DMSO-d_6 with TFA)

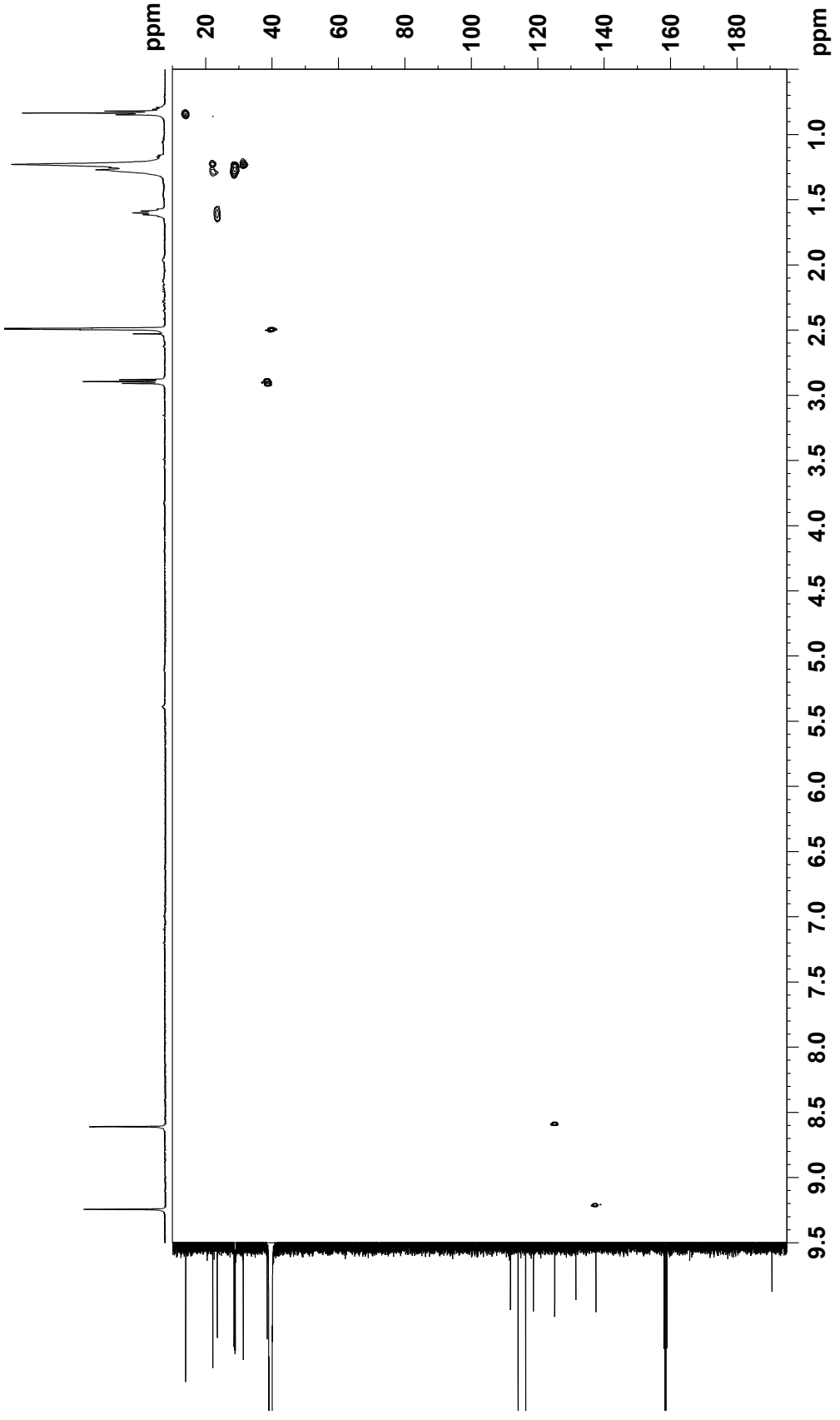

Figure S18. HMBC spectrum of **2** (500 MHz, DMSO-d_6 with TFA)

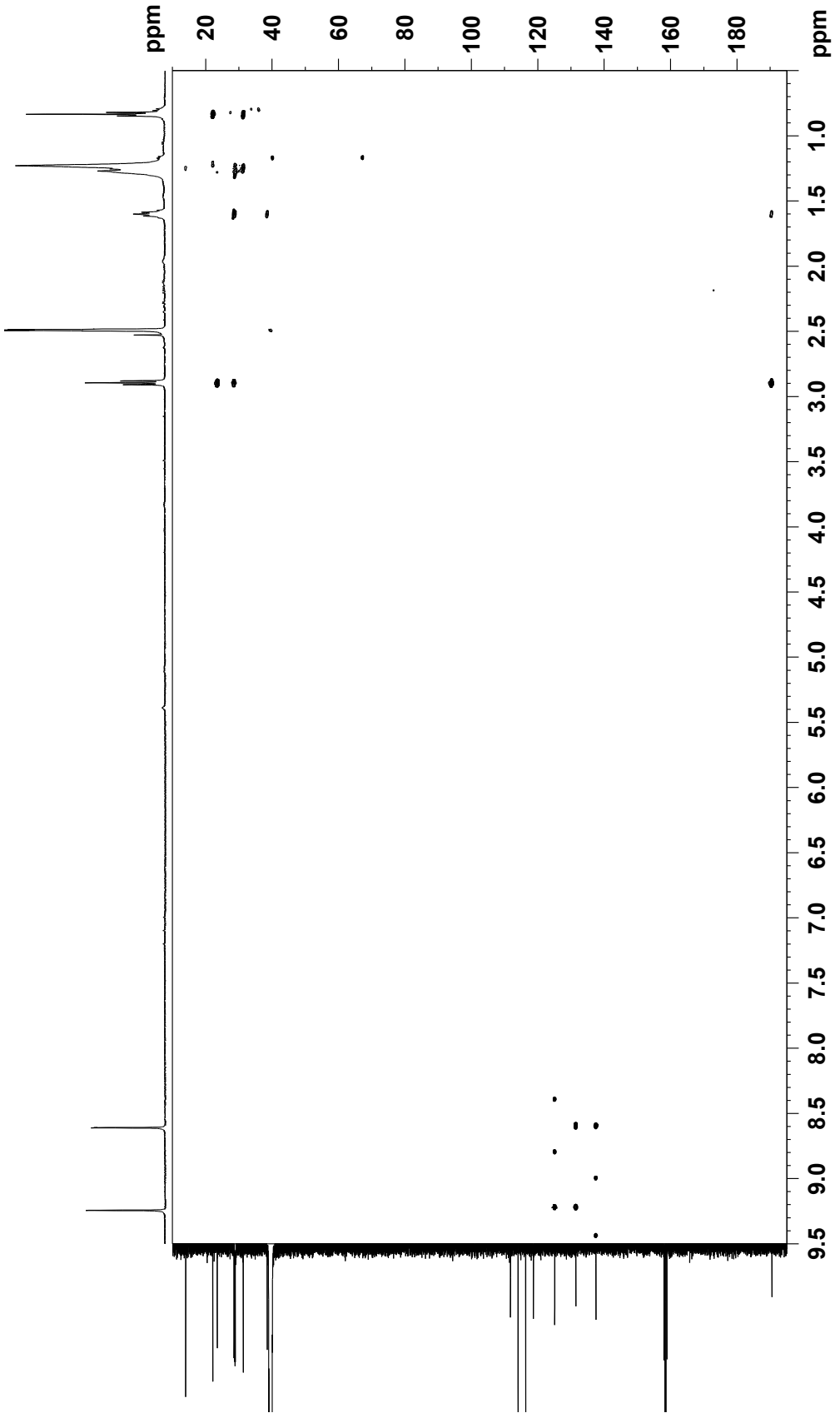

Figure S19. UV spectrum of bulbimidazole C (**3**)

(MeOH)

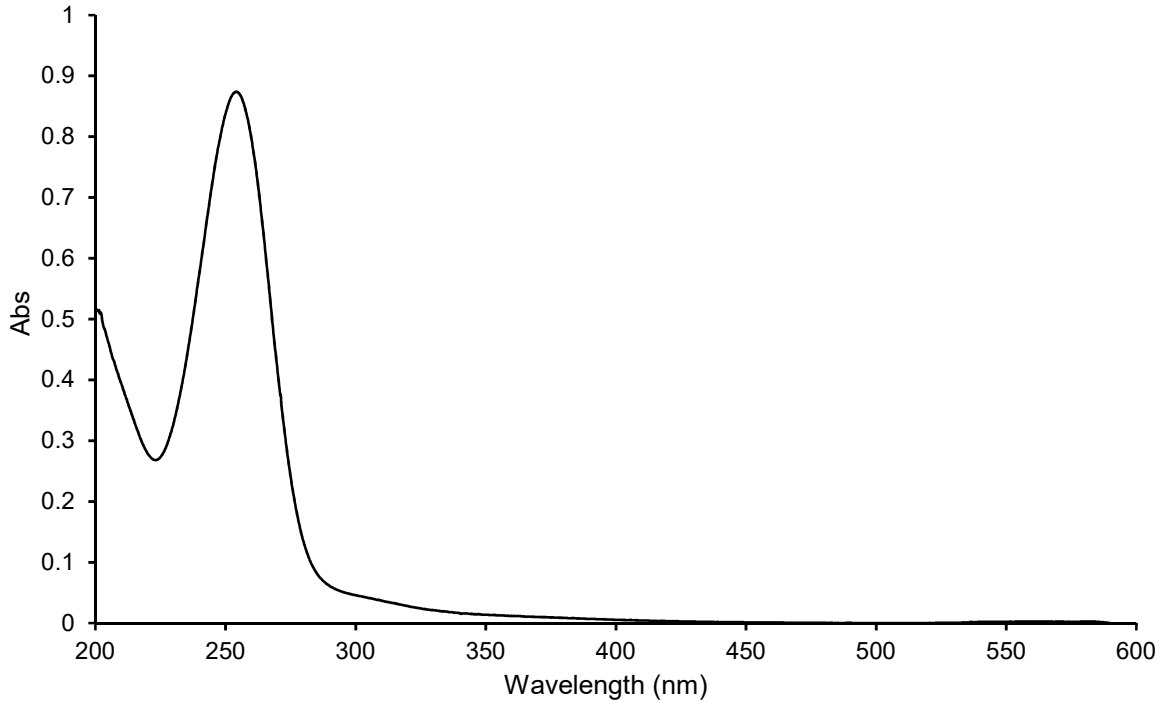

Figure S20. IR spectrum of **3**

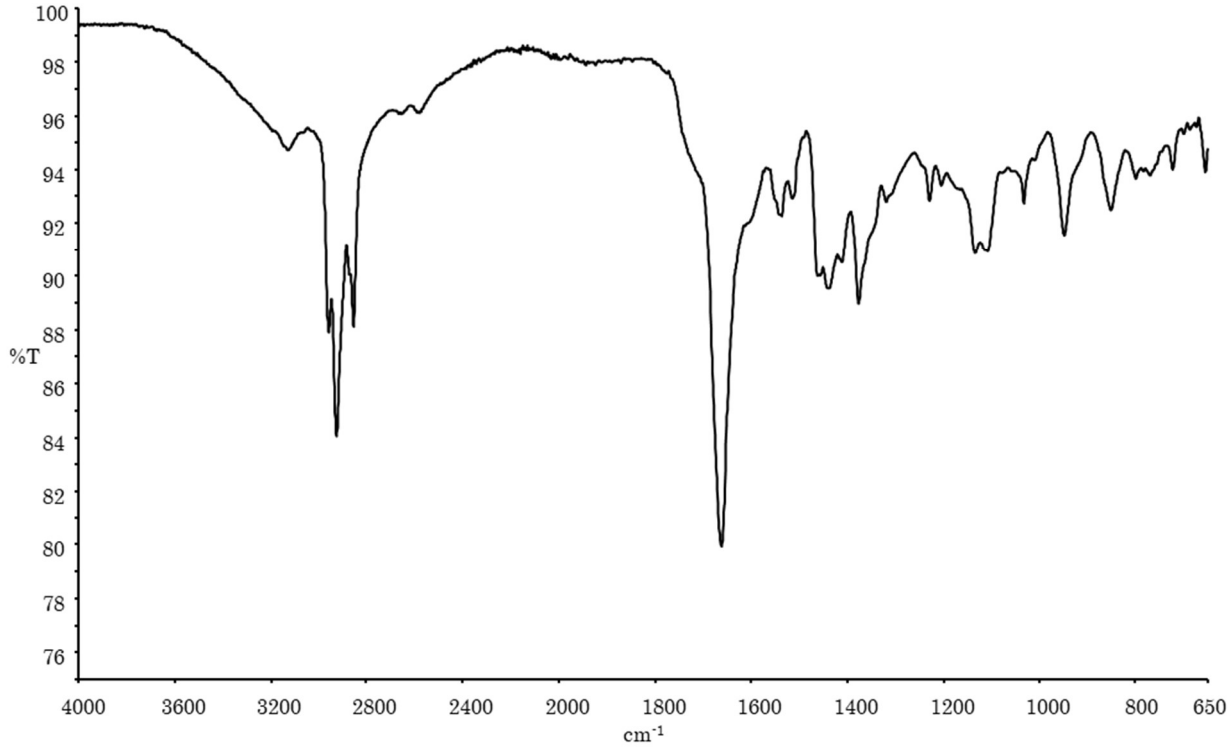

Figure S21. ^{1}H NMR spectrum of **3** (500 MHz, DMSO-d_6 with TFA)

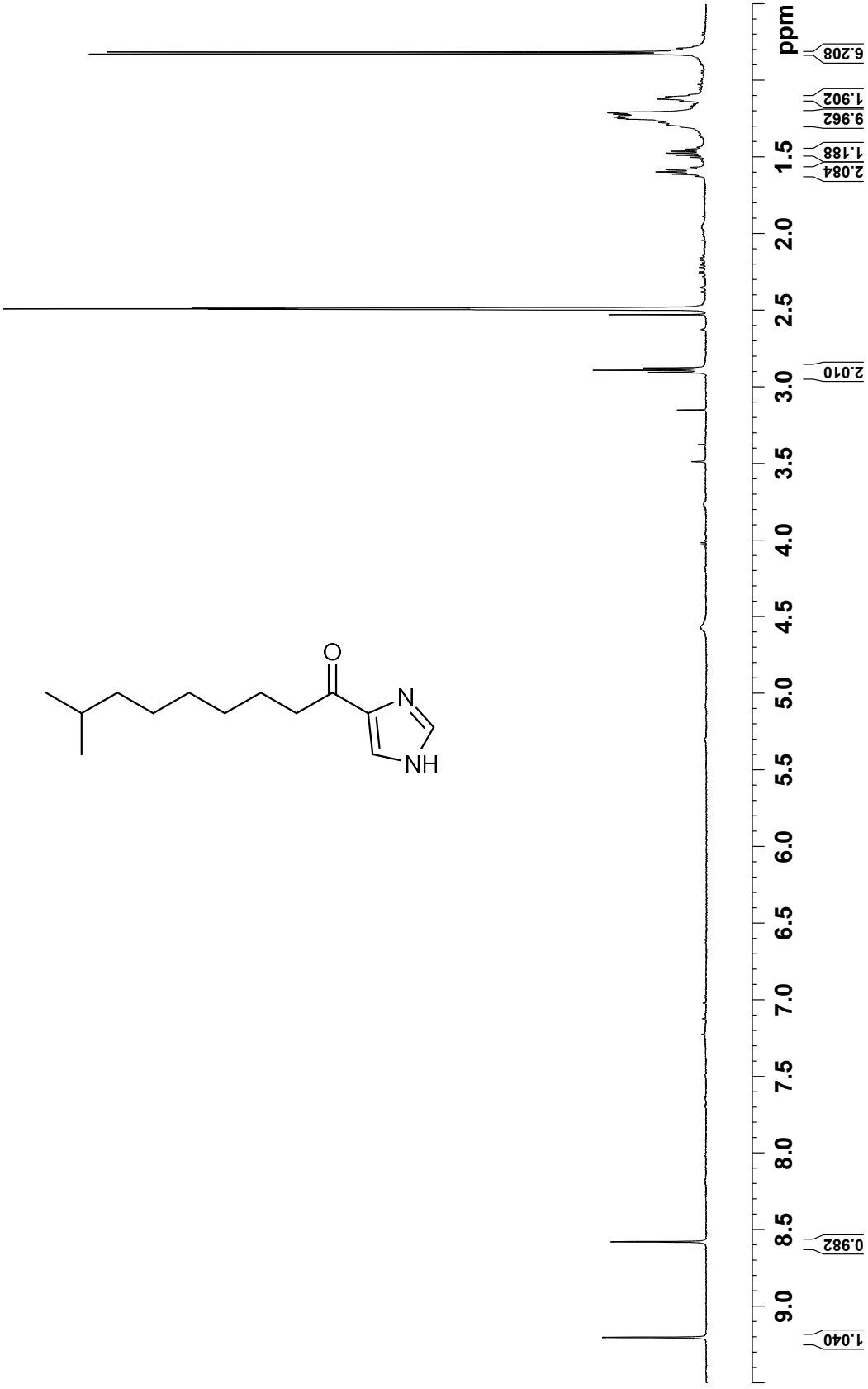

Figure S22. ^{13}C NMR spectrum of **3** (500 MHz, DMSO-d_6 with TFA)

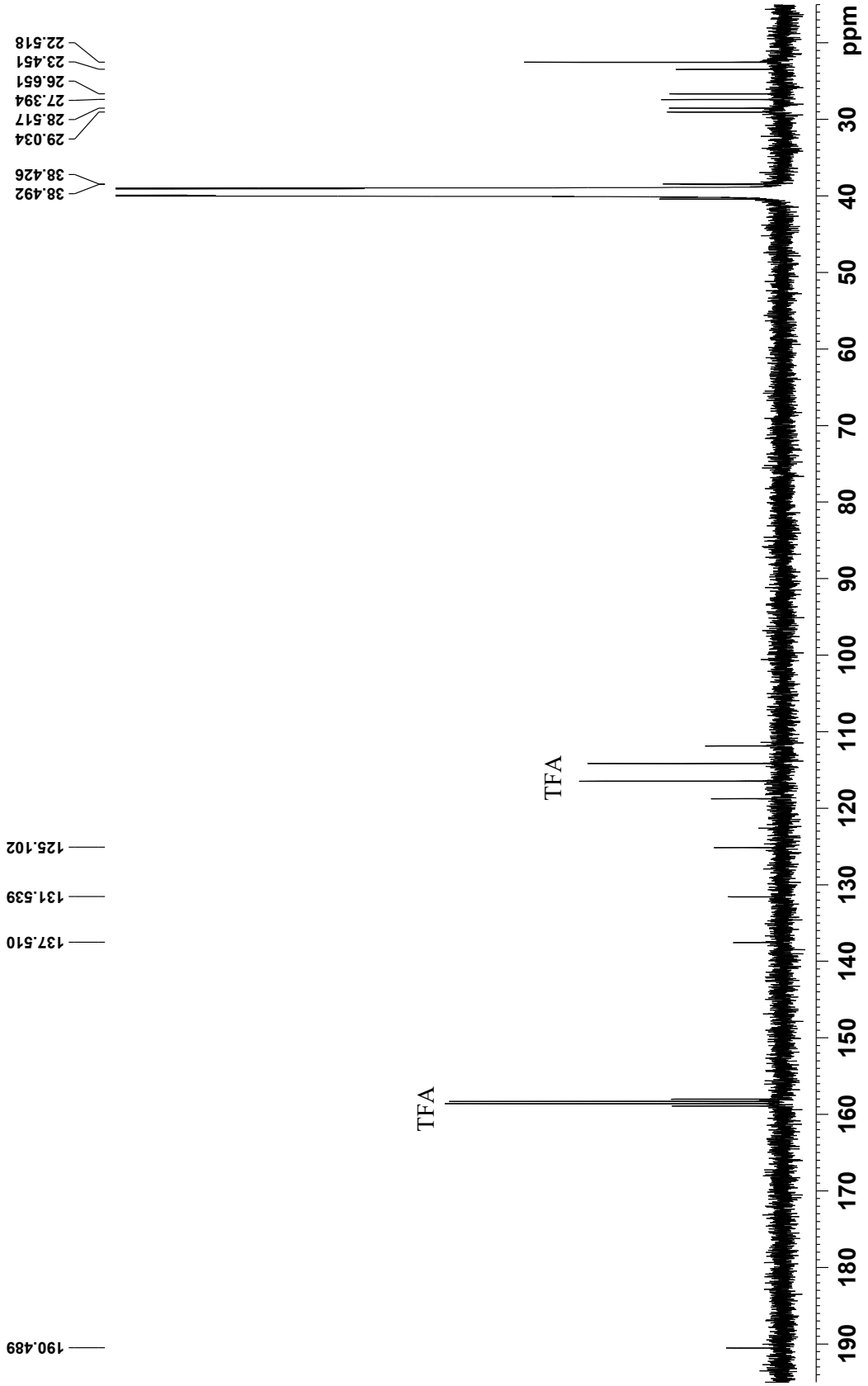

Figure S23. COSY spectrum of **3** (500 MHz, DMSO-d_6 with TFA)

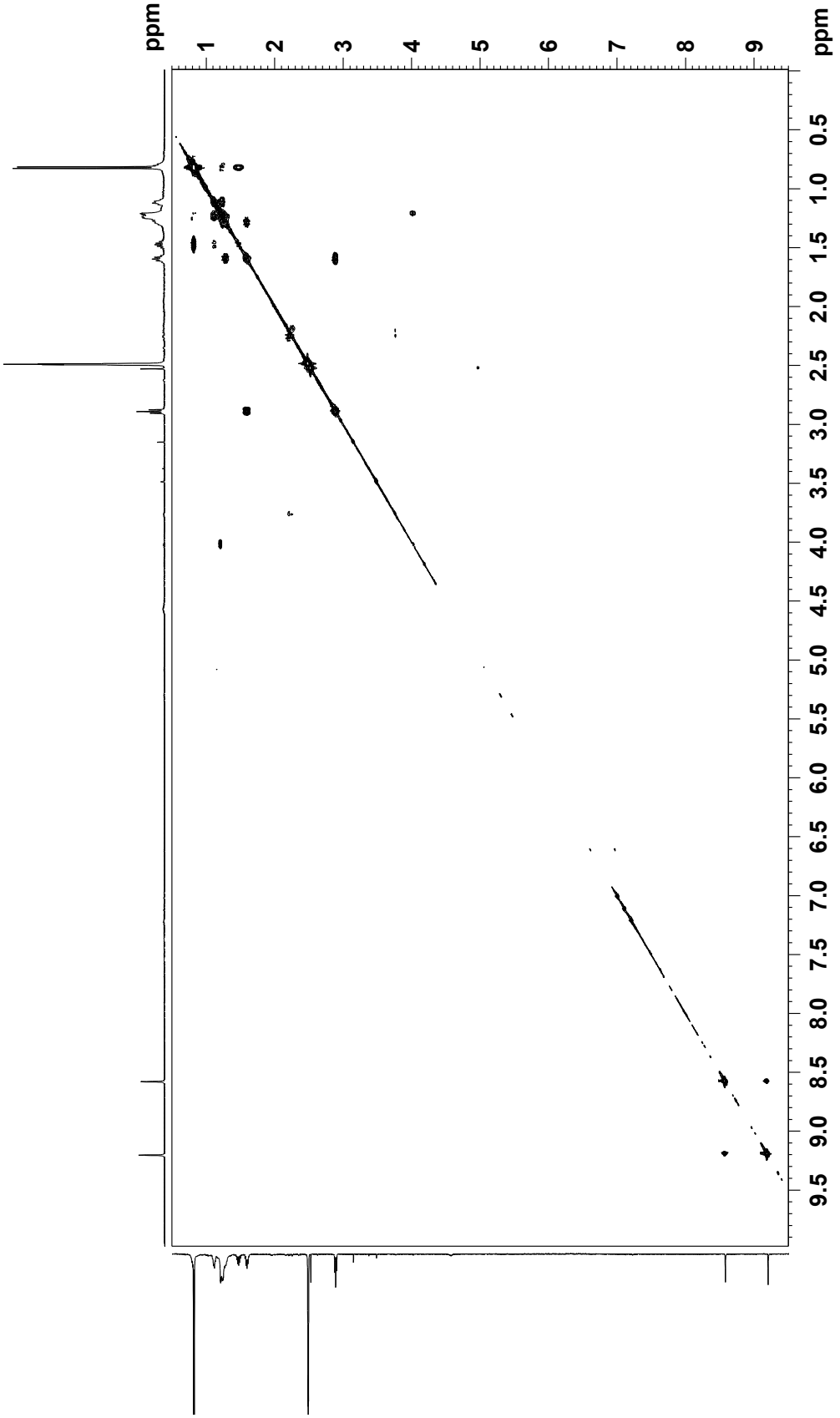

Figure S24. HSQC spectrum of **3** (500 MHz, DMSO-d_6 with TFA)

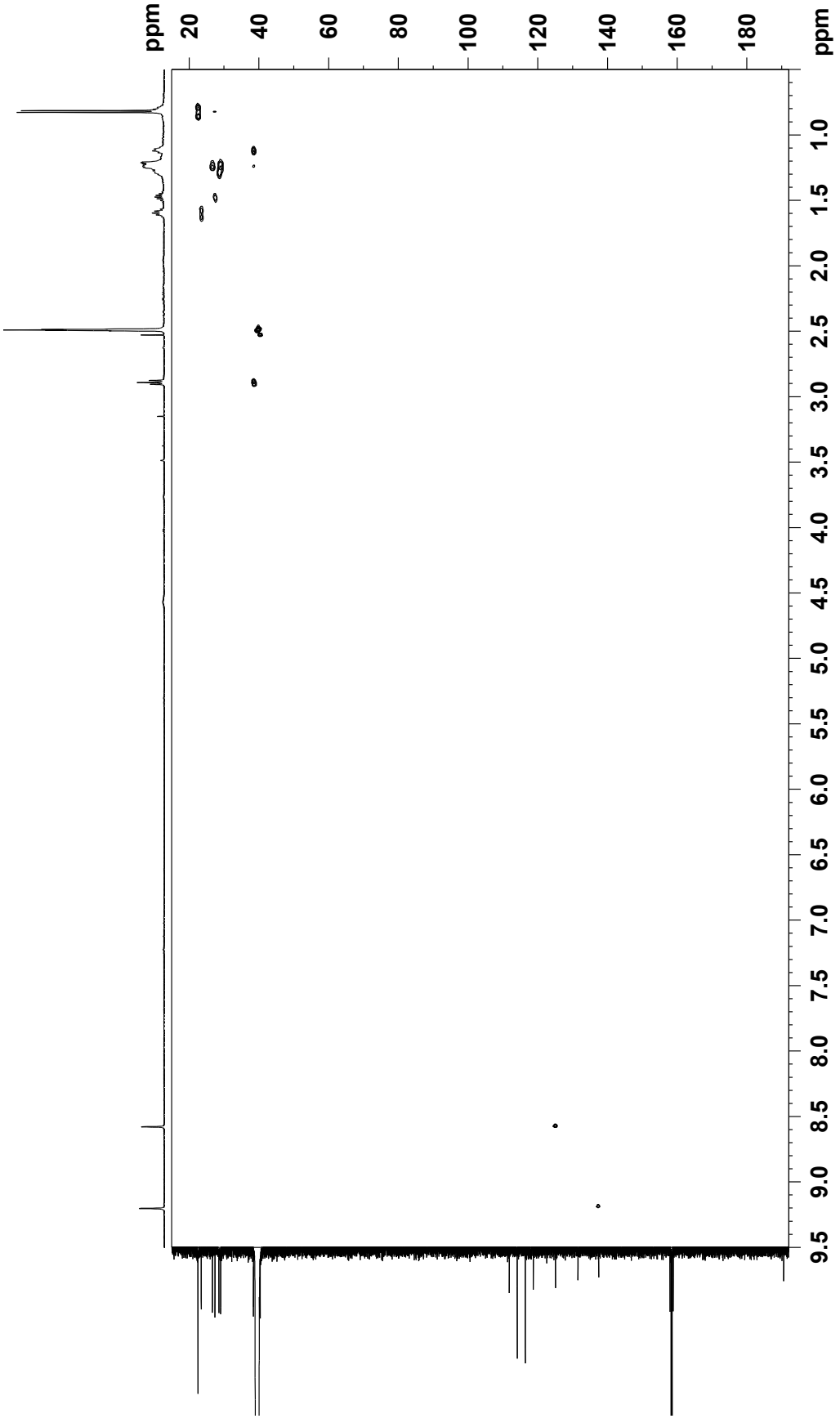

Figure S25. HMBC spectrum of **3** (500 MHz, DMSO-d_6 with TFA)

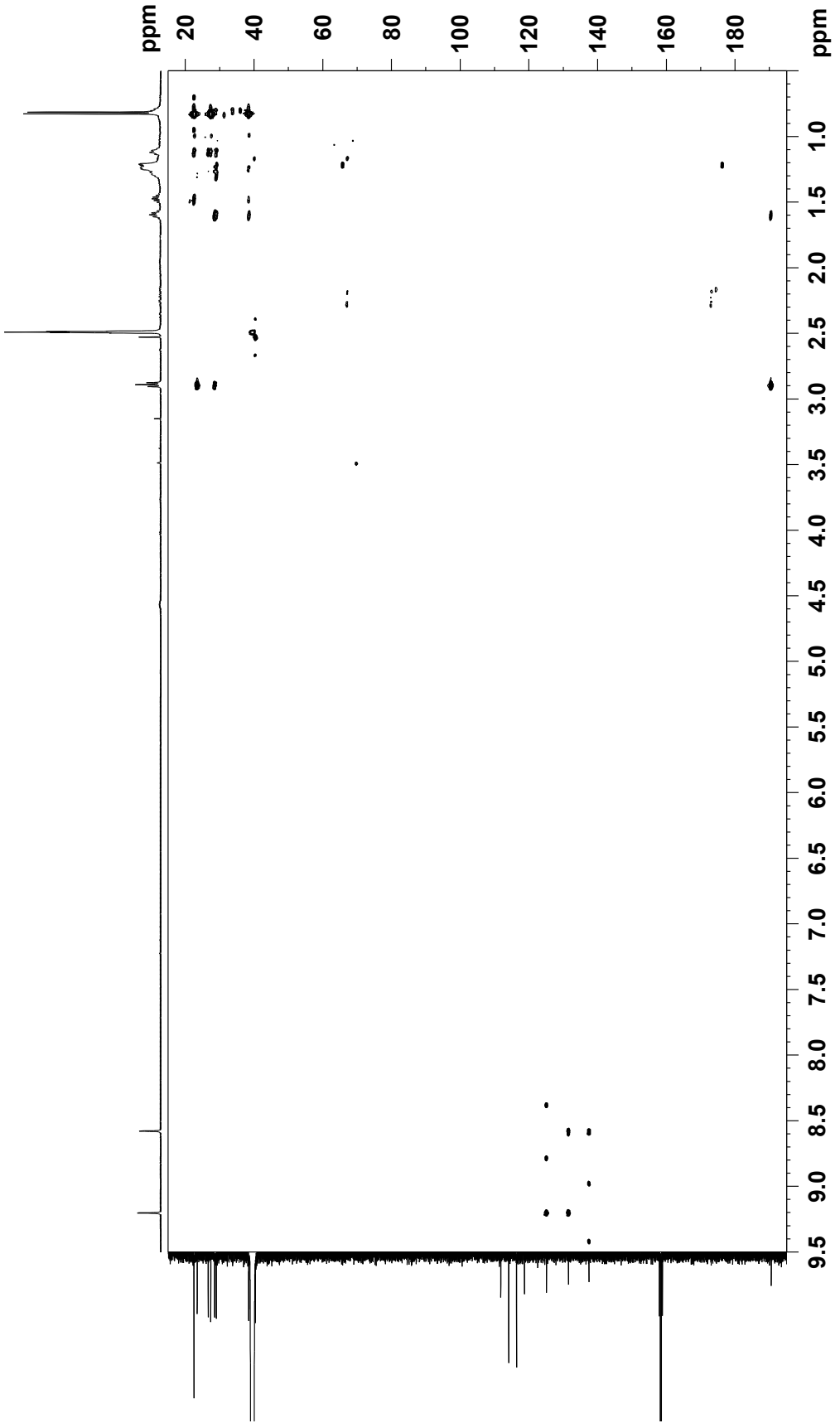

Figure S26. ^{1}H NMR spectrum of *nat*-**4**-(*R*)-2A1P (500 MHz, $CDCl_3$)

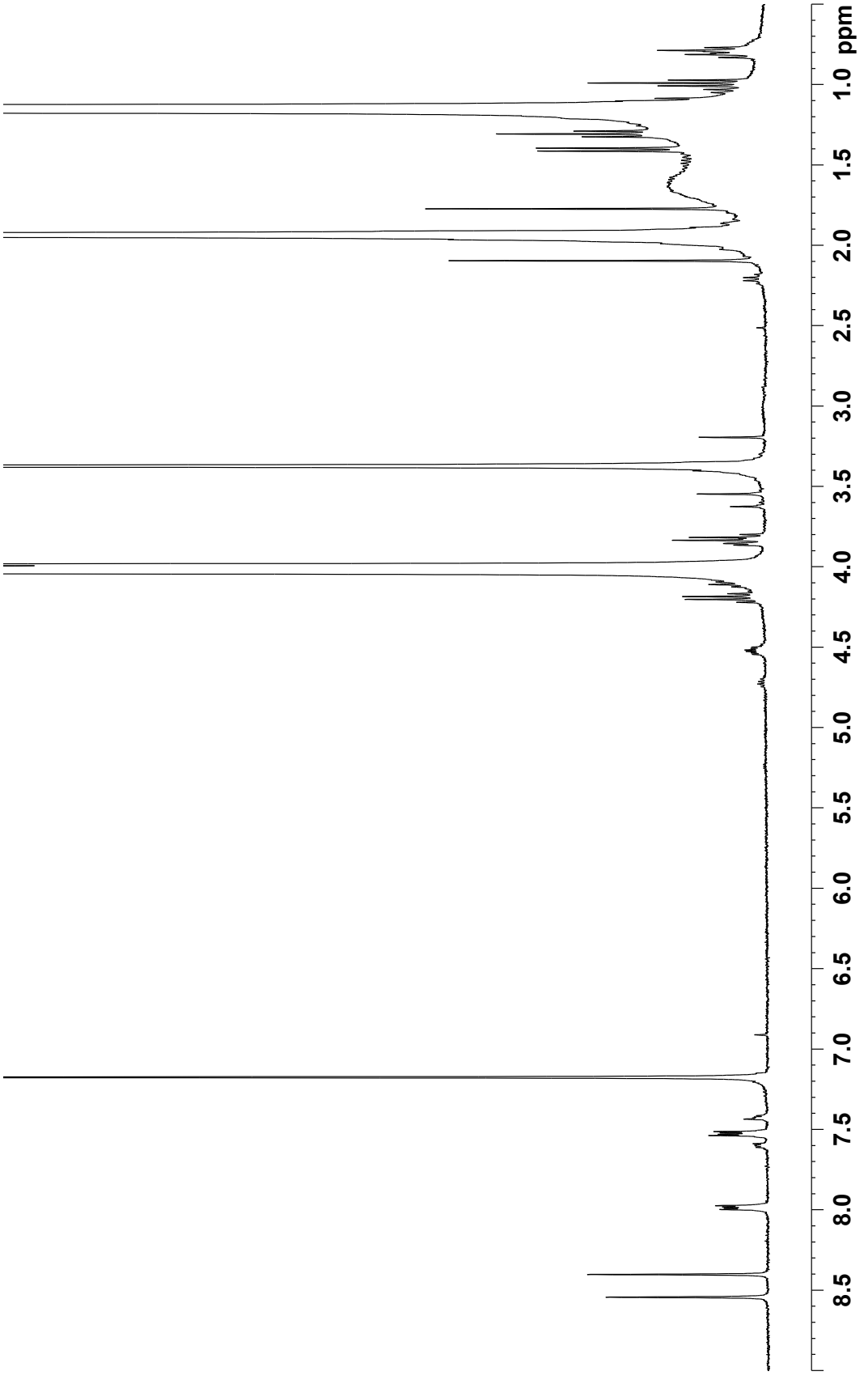

Figure S27. ^{1}H NMR spectrum of synthetic (*S*)-**4**-(*S*)-2A1P (500 MHz, $CDCl_3$)

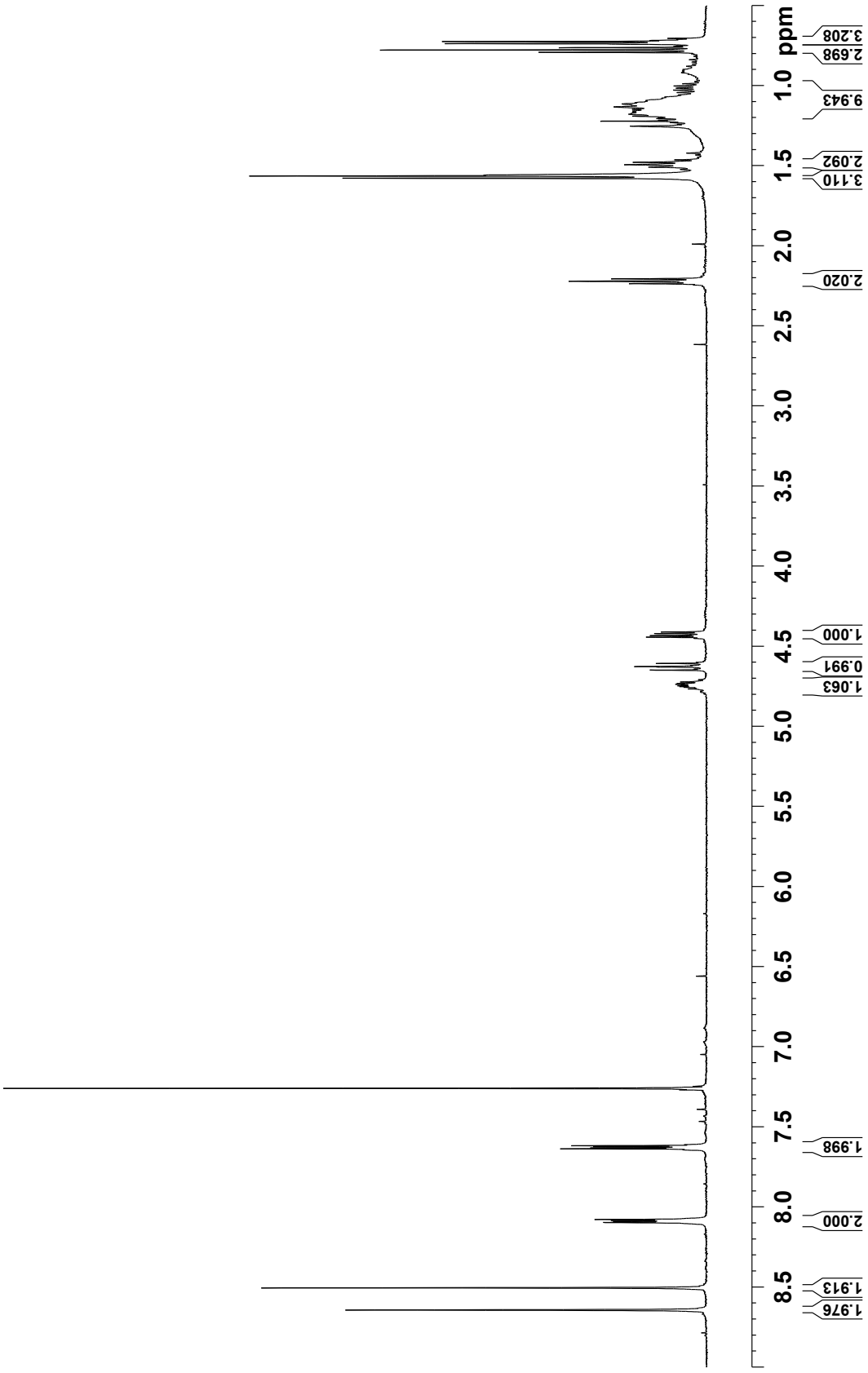

Figure S28. ^{1}H NMR spectrum of synthetic (*S*)-**4**-(*R*)-2A1P (500 MHz, $CDCl_3$)

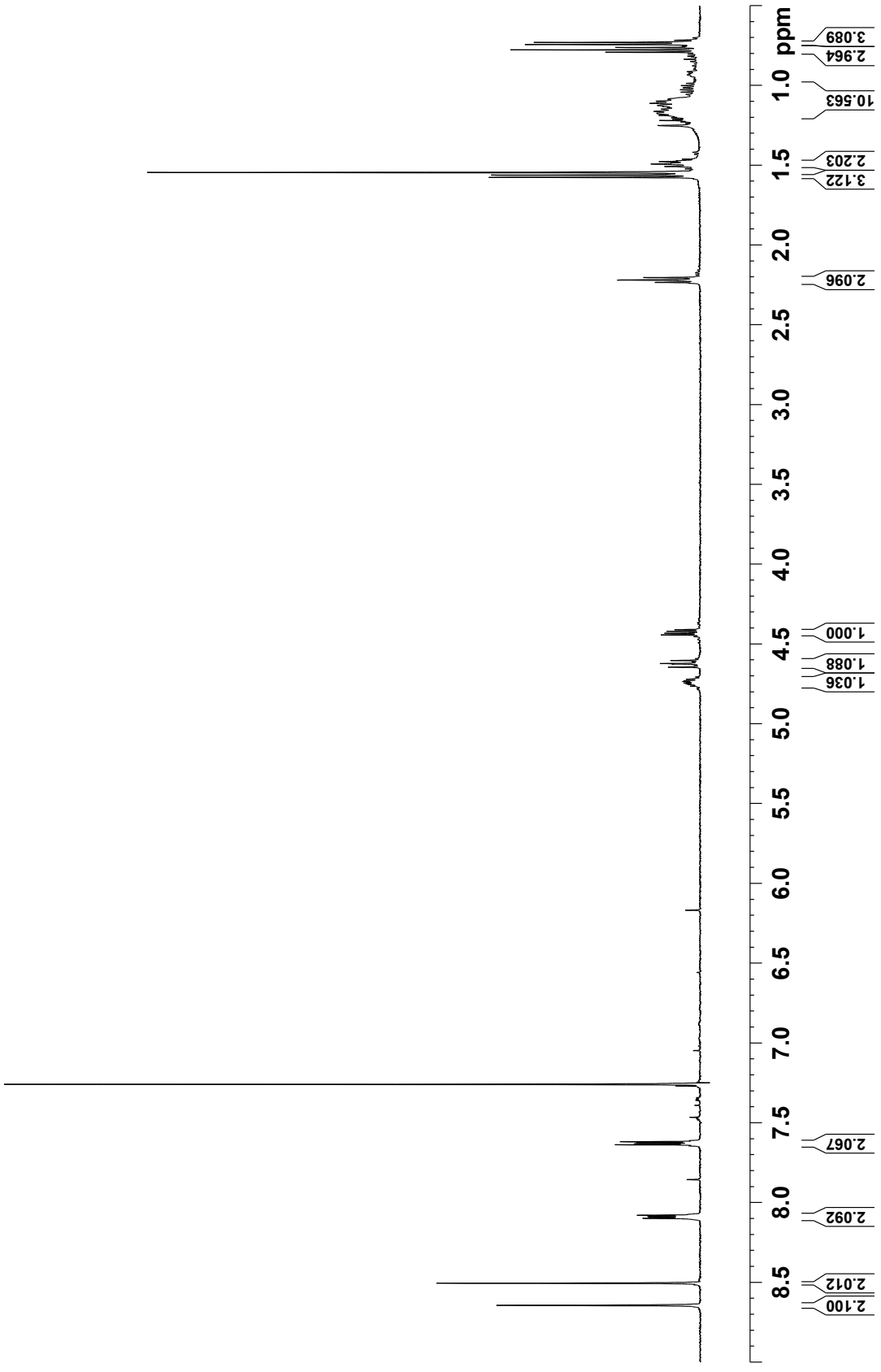

CHAPTER 3

Nocarimidazoles C and D, Antimicrobial Alkanoylimidazoles from a Coral-derived Actinomycete *Kocuria* sp. T35-5

3-1 Background

In Chapter 2, I discussed the isolation and characterization of three new alkanoyl imidazoles named bulbimidazoles A−C. All of these secondary metabolites were isolated from a marine bacterial strain of the genus *Microbulbifer* collected from a stony coral and exhibited potential antimicrobial activities against different pathogenic microorganisms. So, I found that stony coral-associated or symbiotic marine bacteria have the ability to produce new compounds with potent bioactivity. However, the number of new natural products from terrestrial microorganisms is decreasing day by day, compared with marine sources. A large fraction of new types of bacterial strains in marine environment have not been screened for natural product discovery. This unexploited bacterial group may contain genomes for new type of biosynthetic pathways, responsible for producing structurally and biologically diverse new compounds. For this reason, I decided to work with marine bacteria associated with stony corals to get new bioactive compounds. In this study, marine bacterial genus *Kocuria*, formerly categorized in the genus *Micrococcus*, collected from a stony coral *Mycedium* was selected as a candidate strain to isolate new bioactive compounds. Although I worked with common genus *Kocuria* which also isolated form non-marine source and a few number of natural products have already been reported, but I decided to undertake HPLC-UV screening of secondary metabolites from this strain by using three different types of fermentation media because I think there still have possibility to get new compounds because they are isolated from unexploited source like stony corals which are less exploited compared with soft coral associated microorganisms in natural product discovery. This is not true that common bacterial taxa always produce known type of compounds but could be an interesting source in natural product screening program. In this chapter, I will discuss about the isolation and characterization of two new alkanoyl imidazoles from *Kocuria* associated with an underexploited stony coral. HPLC-UV guided fractionation was also conducted in this study as described in Chapter 2.

Corals are taxonomically and biologically diverse and possess numerous physiological and structural characteristics [1]. Unique properties of corals make them to live under harsh chemical and physical circumstance in the marine environment such as hydrostatic pressure, salinity, and temperature [2]. Due to these environmental factors, corals are promising producers of bioactive compounds and can be obtained substantial attention. Many bioactive compounds have been discovered from soft corals with distinctive structures including terpenoids, diterpenoids, sesquiterpenoids, steroids, and other chemical types [3]. Corals are

known to be a host of diverse and highly abundant microbial communities. Highly specific and diverse microorganisms make various forms of interconnection and communication with corals in marine environment [4]. Actually, coral microbes play a prime role to keep their hosts healthy from the appearance of signs of diseases and bleaching, resistance to stressors, and the stability of reef ecosystems by producing chemical compounds [5]. Previous investigations revealed that microorganisms in coral have ability to protect their coral hosts by making a defense substance against predators, competitors, fouling organisms, and pathogenic microorganisms by inhibiting catabolic enzymes or disrupting cell-to-cell communication in pathogens, which led to the development of structurally unique compounds with a wide range of bioactivities [6-9]. Thus, not only corals, but also microorganisms from corals, are being extraordinary sources of novel bioactive compounds [10]. Among the microbial communities in corals, fungi have been the focus of previous researches for secondary metabolites [10]. Several structurally unique compounds, obtained from fungi from soft corals, have rare structures such as acetonide group (cochliomycins A) [11], complex spiro skeleton (spiroxins A) [12], and rare amino acid residues (toquinazolines D) (Figure 3-1) [13].

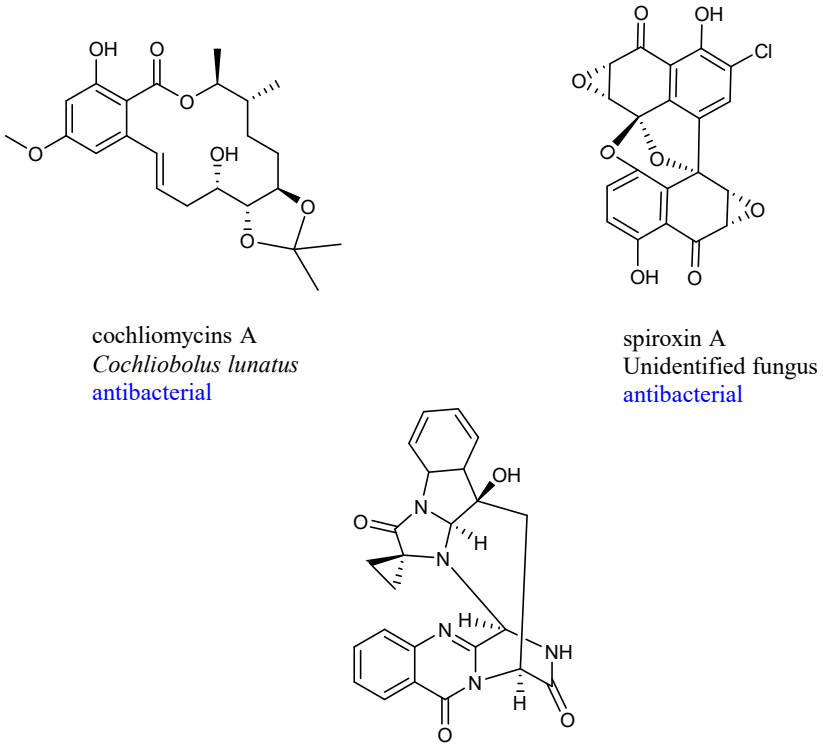

Figure 3-1. Structures of natural products from soft coral-associated fungi.

Only a few natural products have been reported from actinomycetes isolated from soft corals but very few reports on new compounds from stony coral associated actinomycetes except two compounds including (6*E*,8*Z*)- and (6*E*,8*E*)-5-oxo-6,8-tetradecadienoic acids (Figure 3-2) discovered from stony coral-associated *Micrococcus* by our group [14]. Therefore, I selected marine actinomycete strain *Kocuria* from stony corals, for screening new natural products.

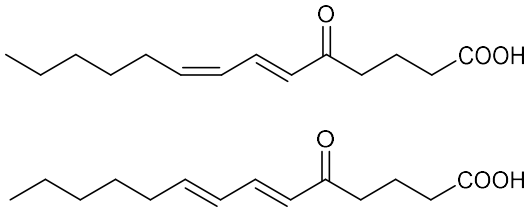

(6*E*,8*Z*)- and (6*E*,8*E*)-5-oxo-6,8-tetradecadienoic acids
Micrococcus
antibacterial, PPARs agonist

Figure 3-2. Structures of natural products obtained from stony coral-associated actinomycete *Micrococcus.*

The producing strain T35-5 was identified as a member of the genus *Kocuria* on the basis of 100.0% similarity in the 16S rRNA gene sequence (1381 nucleotides; DDBJ accession number LC556325) to *Kocuria palustris* DSM 11925^{T} (accession number Y16263). The genus *Kocuria*, formerly categorized in the genus *Micrococcus*, belongs to the family *Micrococcaceae* and encompasses Gram-positive, aerobic, and non-motile cocci bacterium [15]. *Kocuria* is ubiquitous in distribution and commonly inhabited with diverse marine environments such as seawater [16, 17], sediments [18], and deep-sea hydrothermal plumes [19]. The average genome size of the genus *Kocuria* is around 2.7 to 3.0 Mbp, which is one of the smallest among actinomycetes. Although the species of *Kocuria* possess biosynthetic genes for nonribosomal peptides and type III polyketides [20], to date, only a few limited number of metabolites including polyamine-derived siderophores and modified peptides have been reported from *Kocuria* and *Micrococcus* (Figure 3-3) [21, 22].

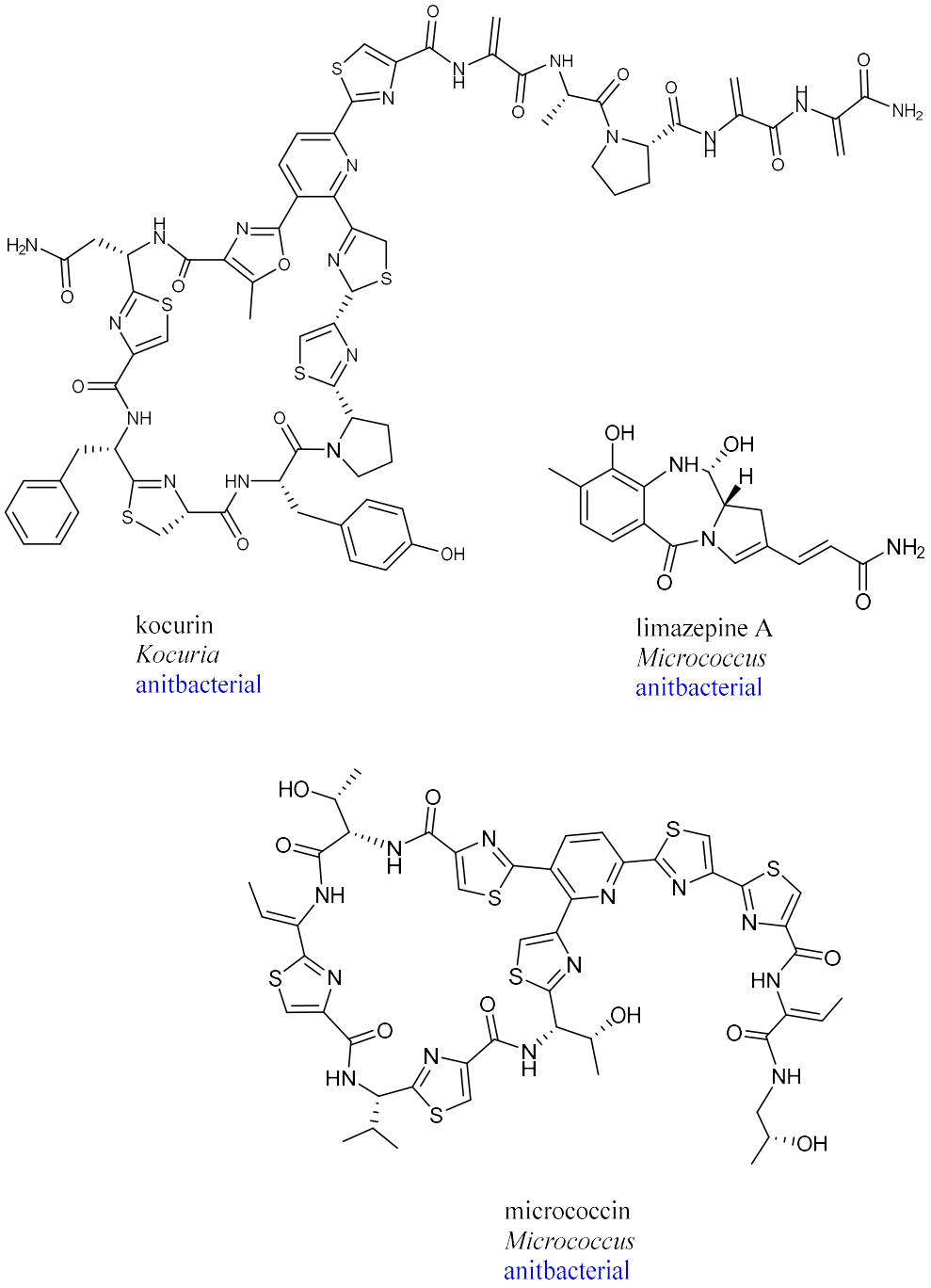

Figure 3-3. Structures of natural products from *Kocuria* and *Micrococcus.*

In this study, HPLC-UV screening on secondary metabolites from marine bacteria led to discovery of five alkanoylimidazoles from the culture extract of a *Kocuria* strain collected from a stony coral *Mycedium*. Alkanoylimidazole is a new and rare class of natural products. The first alkanoylimidazoles were discovered from *Nocardiopsis* collected from marine sediment [23]. The second were recently found as bulbimidazoles A-C from a marine obligate bacterium *Microbulbifer* as described in Chapter 2 [24]. In this chapter, I describe

the isolation, structure determination, and biological activities of two new alkanoylimidazoles, nocarimidazoles C (**4**) and D (**5**), along with three known compounds, nocarimidazoles A (**6**) and B (**7**) and bulbimidazole A (**1**) (Figure 3-4).

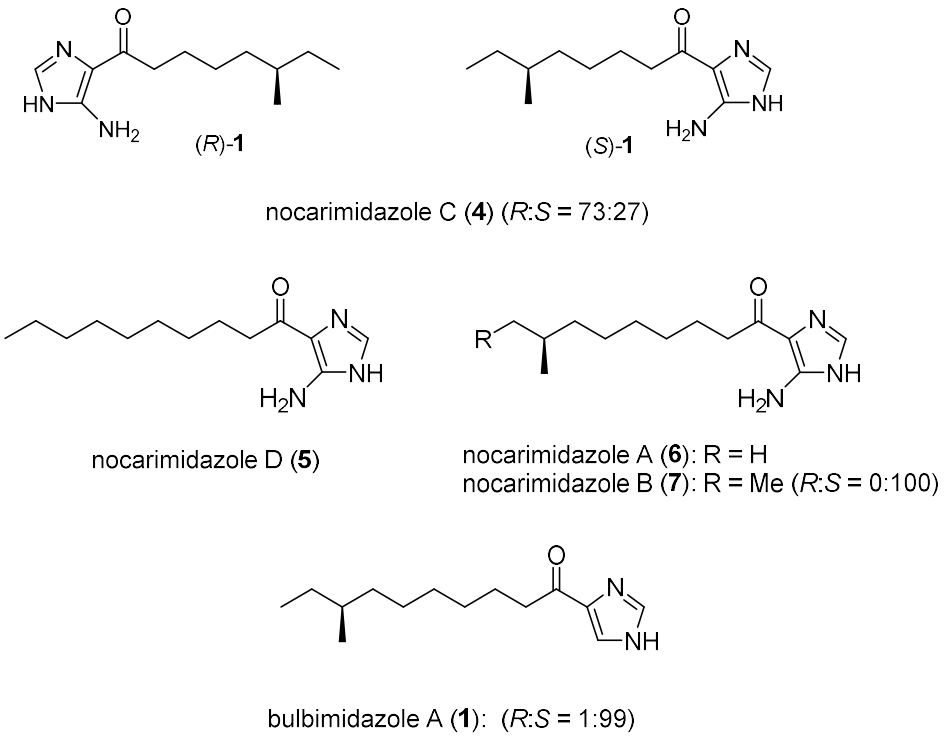

Figure 3-4. Structures of nocarimidazoles (**4**–**7**) and bulbimidazole A (**1**).

3-2 Results and Discussion

In this study, firstly, twenty-six bacterial strains were isolated from two stony corals and were subjected to examine new bioactive compounds. Twenty-one and five bacterial strains were isolated from two coral samples of the genus *Acropora* and *Mycedium*. Stony corals were collected at −15 to −20 m from Tanjung Gelam, Karimunjawa National Park, Jepara, Central Java, Indonesia. The secondary metabolites produced by these strains were analyzed by HPLC/UV-based spectroscopy analysis. The overall process of chemical screening performed by HPLC-UV analysis is described in Chapter 2. For this purpose, three types of fermentation media (A3M, A11M and A16) composed of different nutritional ingredients which were used for screening of unknown secondary metabolite production. In the HPLC-UV chemical screening, I found two bacterial strains T35-5 and T36-16 produced unknown secondary metabolites in the culture extract. Therefore, I selected these two bacteria as candidate strains for further study. After UV-chemical screening of three production media, a candidate strain T35-5 produced metabolites only in A11 medium. Therefore, this media was

selected for further large-scale culture. HPLC/UV analysis showed five major peaks in A11 medium produced by this strain. After chromatographic purification, I collected five peaks in sufficient amounts for structure determination and bioactivity assays. The UV spectra of four peaks A, B, C and D were similar each other with absorption maxima at 200, 226 and 296 nm, respectively. These peaks were eluted at 13.8, 12.5, 12.9 and 10.9 min, respectively (Figure 3-5). Peak E was eluted at 15.6 min and showed UV absorption maximum at 254 nm that was similar to bulbimidazole A described in Chapter 2 (Figure 3-5).

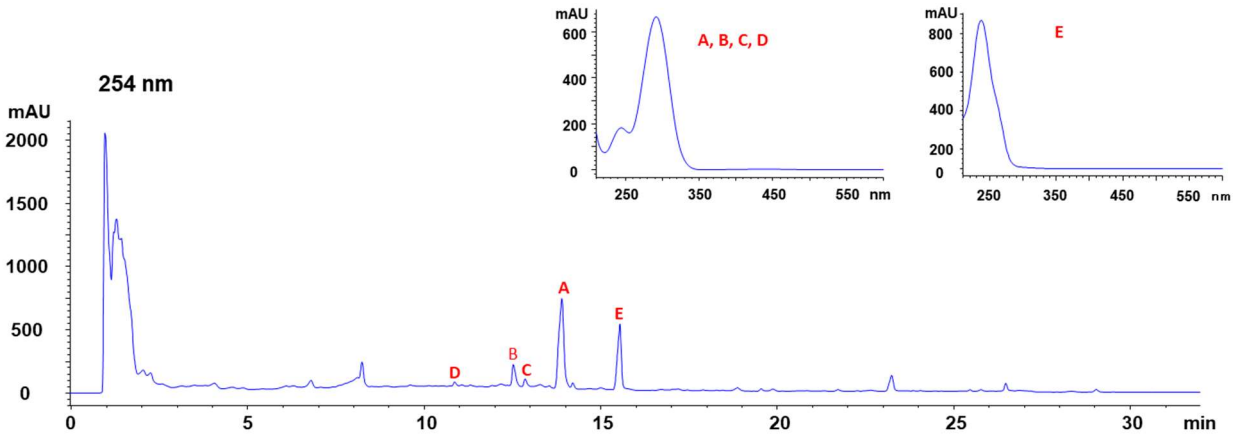

Figure 3-5. HPLC analysis of 1-butanol extract of *Kocuria* sp. T35-5.

The producing strain T35-5 readily grew on Marine Agar but not on the medium without NaCl such as YP (yeast extract 0.1% and peptone 0.5%) Agar prepared in distilled water, indicating that this strain is obligate marine origin (Figure 3-6). *Kocuria* sp. is commonly halotolerant, but in this study, I found this strain was not able to grow on agar medium without sea water (Figure 3-6). I decided to work with this strain for my study because this strain was collected from a stony coral, which is an unexplored source for new bioactive compounds.

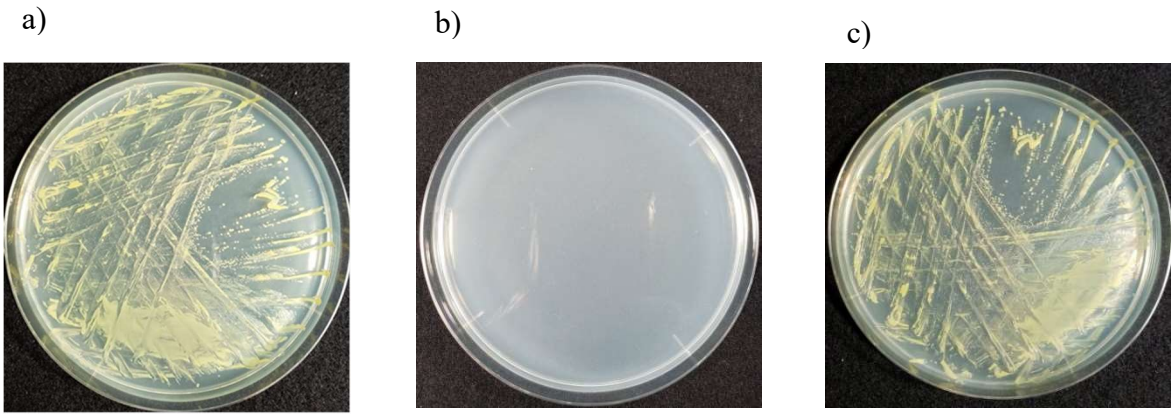

Figure 3-6. Colony morphology of *Kocuria* sp. T35-5 on a) Marine Agar, b) YP medium (yeast extract 0.1% and peptone 0.5%) in distilled water, c) YP medium in natural seawater.

3-2-1 Fermentation and Isolation

The producing strain T35-5 was isolated from the scleractinian (stony) coral of the genus *Mycedium,* which was collected near the coast of Karimunjawa, Central Java, Indonesia. The whole culture broth of *Kocuria* sp. T35-5 cultivated in A11M seawater medium at 30 °C for five days. 1-Butanol was used to extract all unknown secondary metabolites. After evaporation, the extract was fractionated by a sequence of chromatographies and the final purification was achieved by reversed-phase HPLC, yielding two new alkanoylimidazoles, nocarimidazoles C (**4**) and D (**5**), along with three known congeners, nocarimidazoles A (**6**) and B (**7**) and bulbimidazole A (**1**) (Scheme 3-1).

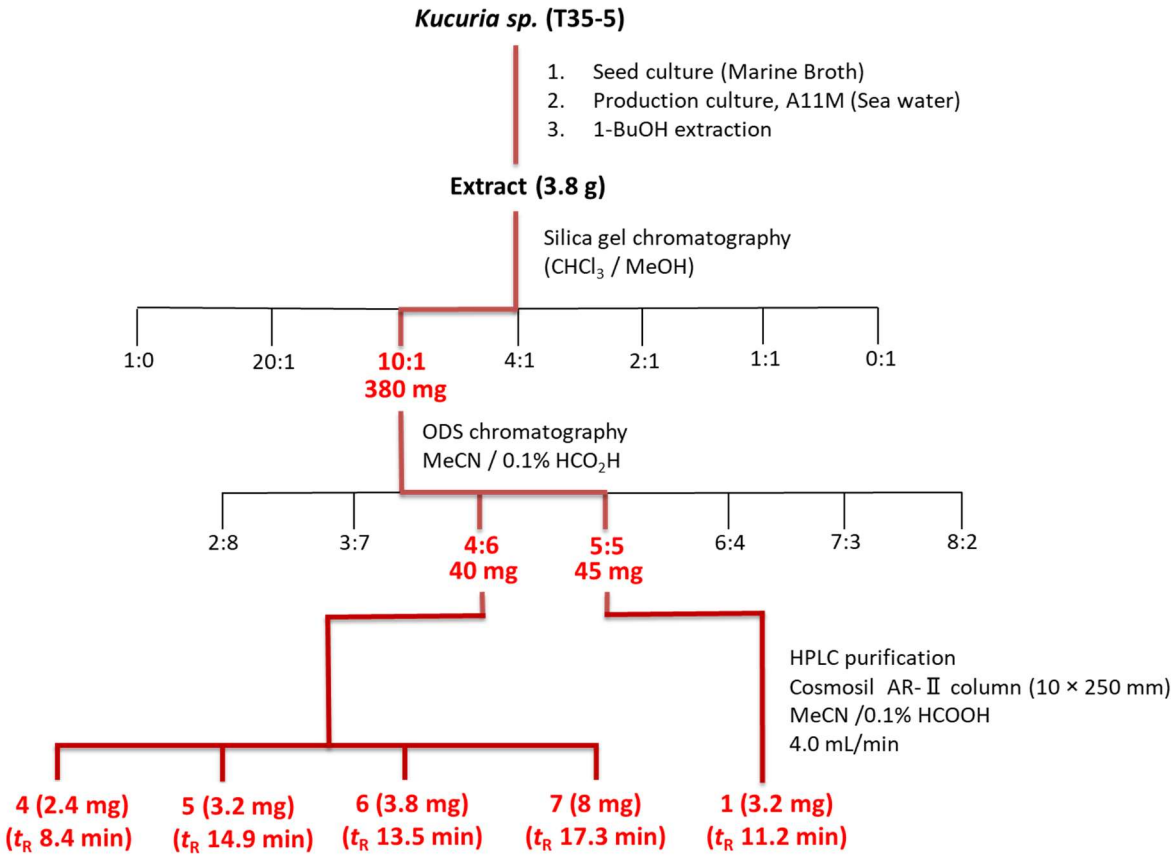

Scheme 3-1. Isolation of nocarimidazoles (**4–7**) and bulbimidazole (**1**).

3-2-2 Structure Determination

Nocarimidazole C (**4**) was obtained as a pale yellow amorphous solid. The molecular formula of **4** was established as $C_{12}H_{21}N_3O$ with four degrees of unsaturation on the basis of its NMR and HR-ESITOFMS (*m/z* 224.1763 $[M + H]^+$; calcd for $C_{12}H_{21}N_3O$ 224.1757) data. The UV spectrum of **1** in methanol exhibited the absorption band at 296 nm, indicating the presence of a conjugated system in this molecule. Moreover, the IR spectrum showed absorption bands at 3127 and 1664 cm^{-1}, corresponding to NH/OH and carbonyl functionality, respectively. The ^1H NMR spectroscopy revealed only six proton signals: a deshielded proton singlet resonance at δ_H 8.62, three isolated aliphatic methylene unit resonances, a methylene envelope signal, and a doublet and a triplet methyl group resonance overlapping. Based on the ^{13}C NMR spectrum only exhibited nine sp^3 carbons signals at 10–40 ppm. No signal was shown for sp^2 carbon atoms in $CDCl_3$, CD_3OD, or DMSO-d_6 (data not shown). The same incident was noticed during the study of bulbimidazole A (**1**), which showed lack of resonances for sp^2 carbon signals in neutral solutions due to the presence of multiple resonance structures for the imidazole moiety [24]. I anticipated that owing to the

existence of an imidazole ring, the UV spectra of **4** and **1** would obviously be different, and as expected, a trace amount of trifluoroacetic acid (TFA) was supplemented to DMSO-d_6, incorporated with a longer relaxation delay (*d1* = 30 sec) for the ^{13}C NMR experiment, which significantly improved the detectability of sp^2 carbon resonances. Combination of the ^{13}C and HSQC spectra collected in this solvent mixture permitted the assignment of 12 carbon signals to one deshielded carbonyl carbon at δ_C 189.4, two nonprotonated sp^2 carbons at δ_C 109.7 and 144.6, one sp^2 methine unit at δ_C 130.9, one sp^3 methine carbon, five sp^3 methylene units, and two methyl moieties (Table 3-1).

The interpretation of the ^1H, ^{13}C, COSY, HSQC, and HMBC NMR spectra revealed that **4** was composed of two partial structures, an alkanone side chain and an 5-aminoimidazole unit. From the COSY spectrum, three isolated spin-systems were established: H-7/H-8/H-9, H-11/H-14 and H-12/H-13. Meanwhile, HMBC correlations from the two methyl protons (H-13 and H-14) to well-resolved C-11, and C-12, along with a correlation from H-14 to C-10, permitted the establishment of an anteisomethyl terminus from C-10 to C-14. The connectivity between C-9 and C-10 was established by a series of HMBC correlations from H-8 to C-10 and H-10 to C-9. Furthermore, long range correlations were found from H-7 and H-8 to a down fielded carbonyl carbon at δ_C 189.4 (C-6), thereby establishing a 6-methyloctanoyl substructure. The remaining structural unit has the composition formula $C_3H_4N_3$ with three double bond equivalents, consisting of the two nonprotonated sp^2 carbon atoms C-4 (δ_C 109.7) and C-5 (δ_C 144.6) and a sp^2 methine unit (CH-2) and exhibiting HMBC correlations from H-2 to C-4 and C-5. These requirements were only satisfied by a 5-aminoimidazole moiety.

Table 3-1. ^{1}H and ^{13}C NMR spectroscopic data for nocarimidazoles C (**4**) and D (**5**) in DMSO-d_6 with TFA.

	4			**5**		
No	δ_C[a]	δ_H mult (*J* in Hz)[b]	HMBC[b,c]	δ_C[a]	δ_H mult (*J* in Hz)[b]	HMBC[b,c]
2	130.9, CH	8.62, s	4, 5, 6	130.9, CH	8.59, s	4, 5, 6
4	109.7, C			109.7, C		
5	144.6, C			144.7, C		
6	189.4, C			189.3, C		
7	38.3, CH_2	2.66, t (7.4)	6, 8, 9	38.3, CH_2	2.66, t (7.4)	4, 6, 8, 9
8	23.9, CH_2	1.55, quint (7.2)	6, 10	23.6, CH_2	1.54, quint (7.3)	6, 7, 9, 10
9	26.2, CH_2	1.27[e]	11	28.76, CH_2	1.22-1.26[e]	7
10	35.9, CH_2	1.07, m	9, 11	29.1, CH_2	1.22-1.25[e]	8
		1.27[e]	9, 11			
11	33.8, CH	1.27[e]	9, 13, 14	29.0,[d] CH_2	1.22-1.25[e]	9, 10, 12
12	29.0, CH_2	1.08, m	11, 13, 14	28.83,[d] CH_2	1.22-1.26[e]	
		1.26[e]	11, 13, 14			
13	11.3, CH_3	0.80, t (7.4)	11, 12	31.4, CH_2	1.21,[e] m	14
14	19.2, CH_3	0.79, d (6.7)	10, 11, 12	22.3, CH_2	1.21-1.25[e]	13, 15
15				14.0, CH_3	0.83, t (6.8)	13, 14

[a] Recorded at 125 MHz (reference δ_C 39.5).

[b] Recorded at 500 MHz (reference δ_H 2.49).

[c] From proton stated to the indicated carbon(s).

[d] Assignment may be interchangeable.

[e] Overlapping signals.

Nocarimidazole D (**5**) was obtained as a pale yellow amorphous solid. Its molecular formula was established as $C_{13}H_{23}N_3O$, based on the HRESITOFMS data ($[M + H]^+$ at *m/z* 238.1915, Δ +0.2 mmu), implying four degrees of unsaturation. The molecular weight displayed that **5** had one more methylene (14 amu) than **4**. The UV and IR spectra displayed almost identical as those for **4**. Combination analysis of the ^{1}H, ^{13}C, and HSQC spectra data of **5** was almost similar to that of **4** revealed the appearance of three additional methylene groups and the absence of one doublet methyl and one methine signal. Based on COSY correlation data, two aliphatic spin system were elucidated, a trimethylene unite (H-7/H-8/H-9) and a two carbon fragments (H-14/H-15). These two-alkyl chain were then connected into a nonbranching linear fragment by HMBC correlations from H-15/C-13 and H-8/C-10, but no assignable cross peaks were noticed from H-11to C-11 and H-12 to C-12 due to a severe signal overlapping, thereby confirming the decanoyl moiety. This alkyl chain and imidazole

ring was linked via a carbonyl carbon atom C-6 based on the HMBC correlations from H-7 and H-2 to C-6 (Figure 3-7). ^{1}H and ^{13}C NMR chemical shifts for the imidazole moiety of **5** were mostly the same as those observed for **4** (Table 3-1).

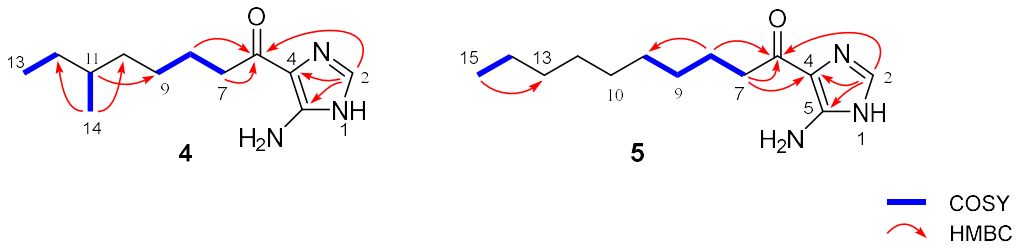

Figure 3-7. COSY and key HMBC correlations for **4** and **5**.

3-2-3 Determination of Amino Substitution

The remaining question was whether the amino group is bound to C-2 or C-5 in the imidazole ring. The correct position of amino group in imidazole ring was not possible to establish by 2D NMR spectroscopy. There had no signal from exchangeable proton of NH_2 group in the ^{1}H NMR spectrum. Therefore, no HMBC cross peaks were observed from this group. Firstly, MS data revealed the presence of amino group in **4**, but it was difficult to assign the position of amino group in imidazole ring. In previous study, methylation chemistry was applied to assign aminoimidazole ring structure in **7**. Two methylation reactions were occurred in **7**; firstly, monomethyl derivative was synthesized by treating with diazomethane in dilute MeOH. Based on HMBC correlation methylation, of N-1 was established in **7**. Secondly, dimethyl derivative displayed two methyl groups by reacting with iodomethane and K_2CO_3 in DMF. HMBC cross peaks indicated that methylation had occurred at N-3 and N-5a. Thus, these two methylated derivatives established the structure of the aminoimidazole functionality in **7** (Figure 3-8) [23].

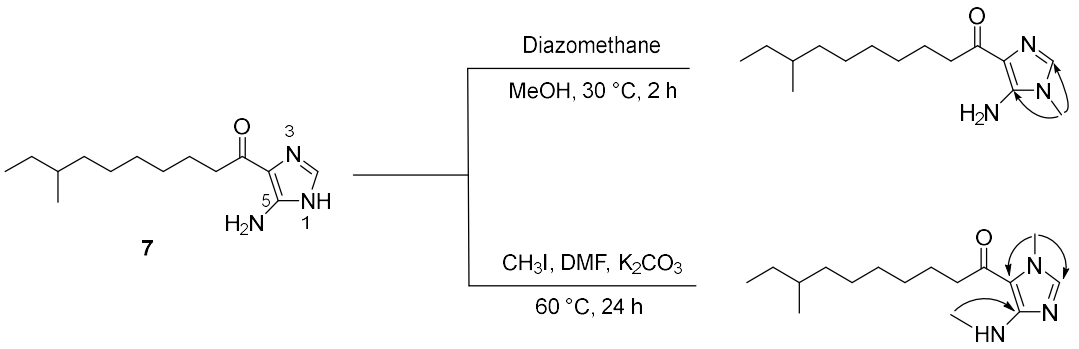

Figure 3-8. Methyl derivatives of nocarimidazole B (**7**).

In contrast, in this study, new approach using $^{1}J_{CH}$ coupling constants was applied to determine the amino group in imidazole ring. Literature survey suggested a diagnostic use of $^{1}J_{CH}$ coupling constants in L-histidine [25].

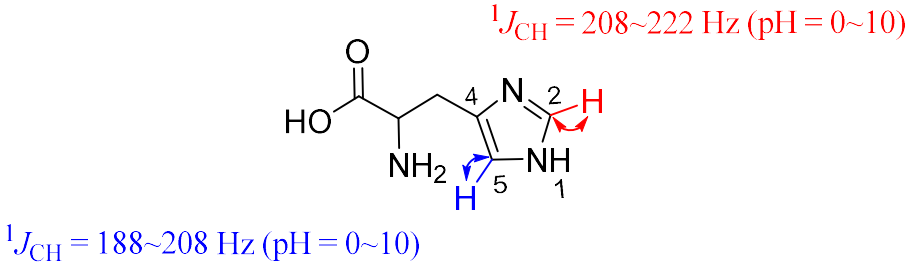

Figure 3-9. $^{1}J_{CH}$ coupling constants for imidazole ring of L-histidine.

I found that the $^{1}J_{CH}$ values for H-2/C-2 (208 to 222 Hz) to be always larger by at least 15 ppm than those for H-4/C-4 (188 to 208 Hz) at any pH condition below 11 (Figure 3-9) in imidazole of L-histidine [26]. The value of the sp^2 methine group in **4** showed $^{1}J_{CH}$ = 221 Hz in a coupled HSQC experiment, which was assignable to the imidazole 2-position based on this criterion, and hence a C-5 amino substitution (Figure 3-10). Additionally, $^{1}J_{CH}$ measurements of bulbimidazole A (**1**) gave 221 Hz for H-2/C-2 and 204 Hz for H-4/C-4, which supported the assignment (Figure 3-11). To finally resolve this matter, two aminoimidazoles **8** and **9** were synthesized for comparison, possessing 4-acetyl and 5- or 2-amino substitutions, respectively, according to the reported procedures (Scheme 3-2) [27-29]. Compound **8** is known as a photolysis product of 6-methylpurine 1-oxide, but I prepared it by the Grignard reaction of a commercially available imidazole derivative, 4-isocyano-1*H*-imidazol-5-amine, with MeMgBr [30]. On the other hand, three steps reaction were performed to synthesize **9** from pyrimidin-2-amine. An *N*,*N*-dimethylformimidamide derivative was synthesized by imidation reaction of starting material 1,1-dimethoxy-*N*,*N*-dimethylmethylamine, which was cyclized with 1-chloropropan-2-one to give 3-acetylimidazo[1,2-*a*]pyrimidine, followed by degradation of the pyridimine ring with hydrazine, yielding **9**. The coupled HSQC experiments measured $^{1}J_{CH}$ = 215 Hz for the H-2/C-2 pair in **8** (Figure 3-12) and 201 Hz for H-5/C-5 in **9** (Figure 3-13). Thus, the amino substitution at C-5 in **4** was unequivocally established (Figure 3-10).

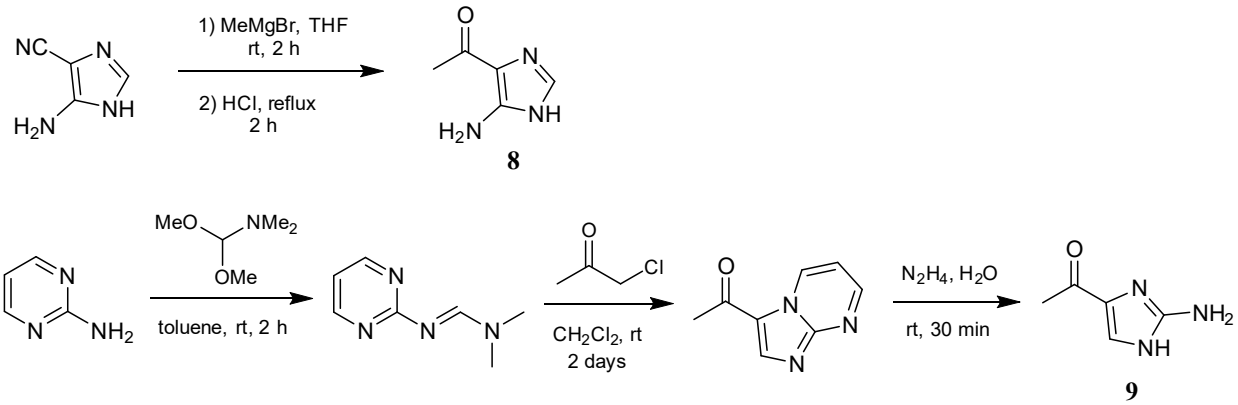

Scheme 3-2. Synthesis of model compounds **8** and **9**.

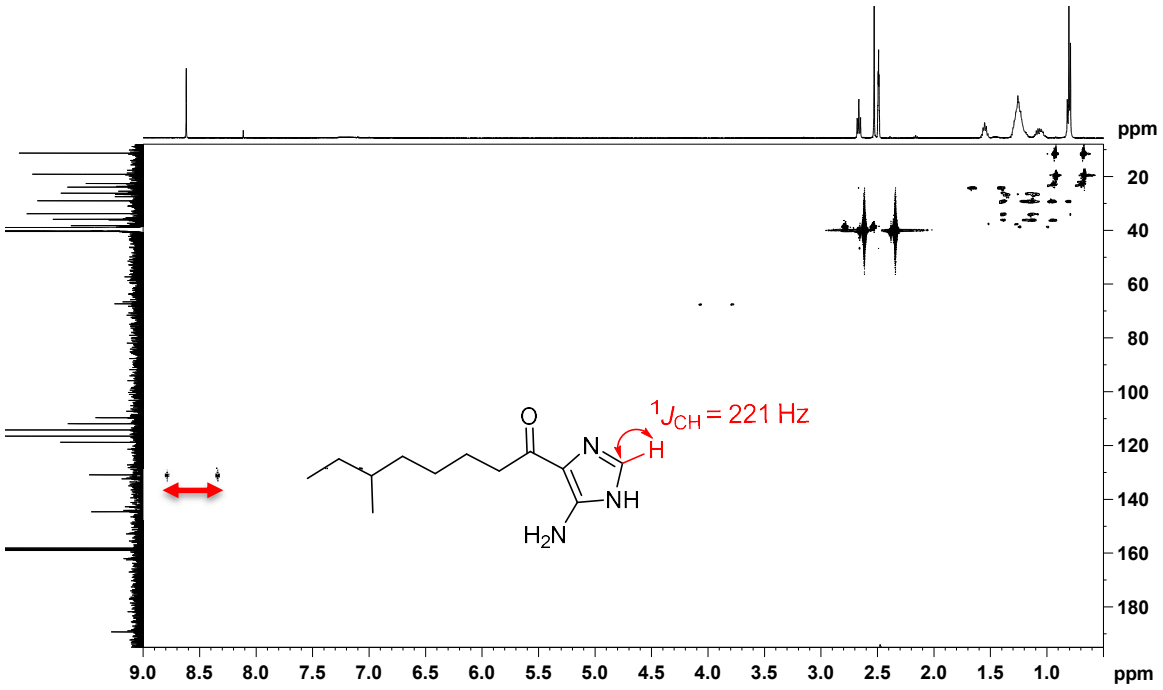

Figure 3-10. $^{1}J_{CH}$ coupling constant for imidazole ring of **4**.

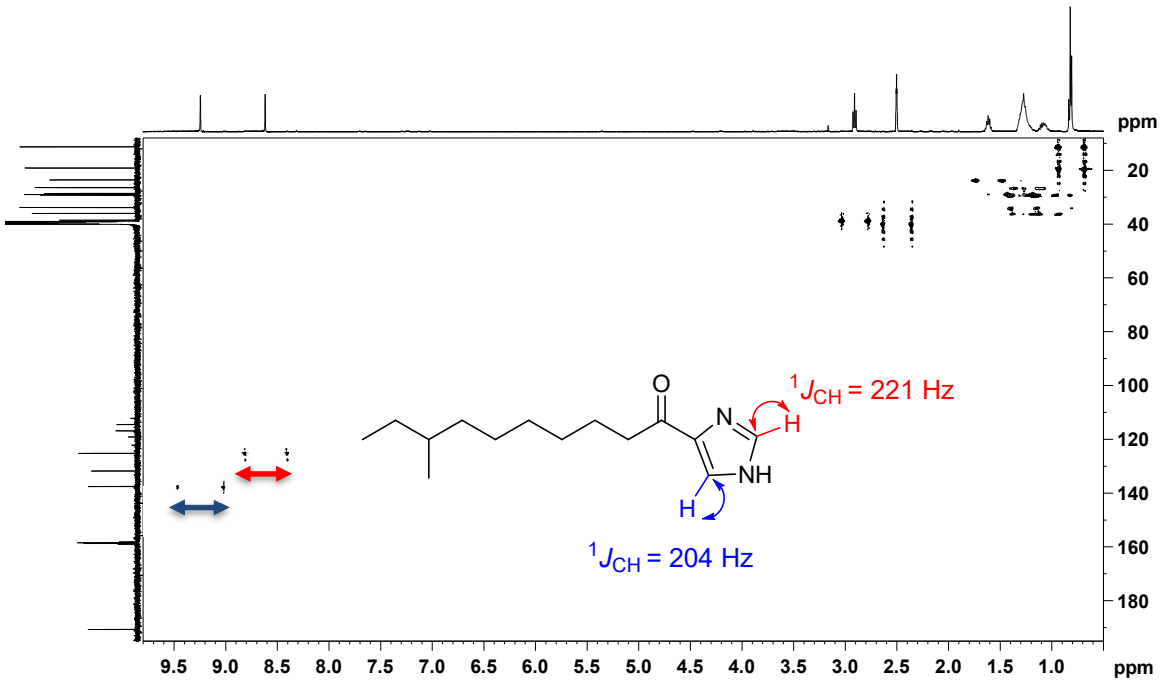

Figure 3-11. $^1J_{CH}$ coupling constants for imidazole ring of **1**

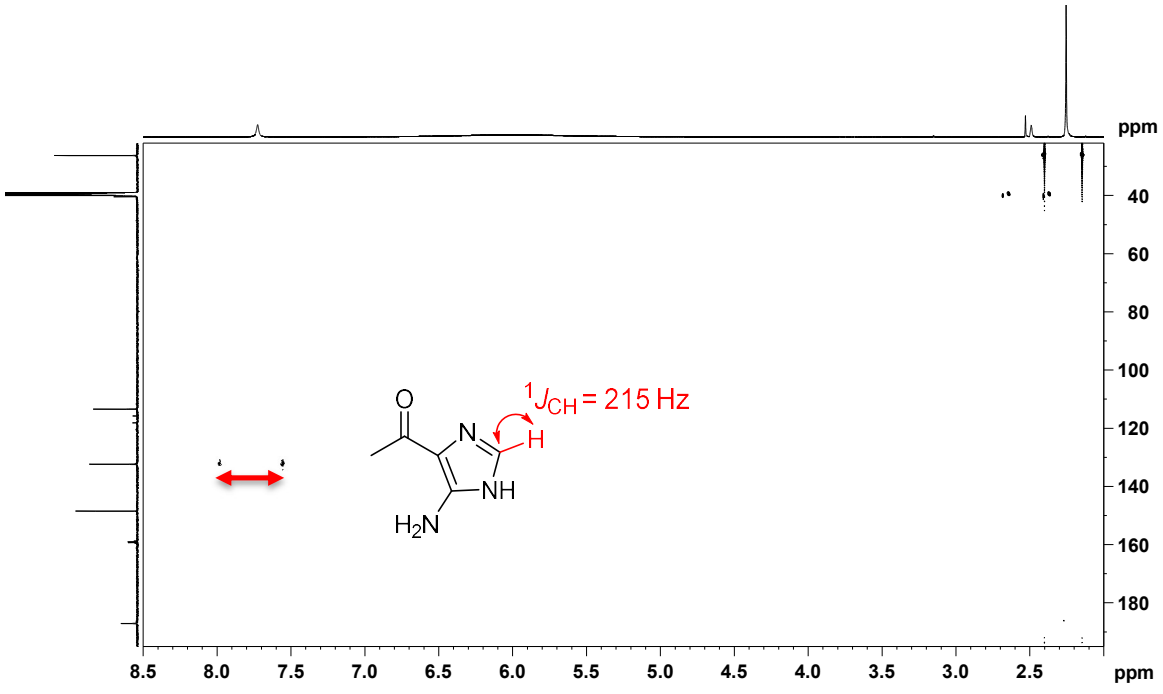

Figure 3-12. $^1J_{CH}$ coupling constant for imidazole ring of model compound **8**.

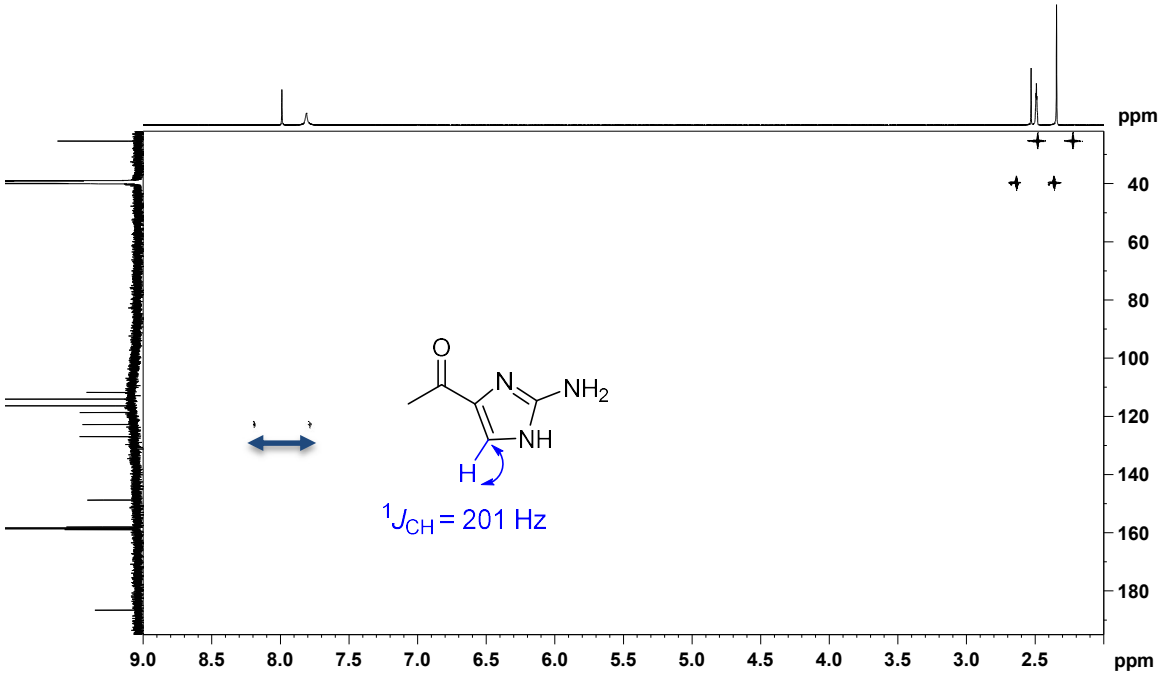

Figure 3-13. $^{1}J_{CH}$ coupling constant for imidazole ring of model compound **9**.

3-2-4 Absolute Configuration

The absolute configurations of **4, 7,** and **1** were determined by the Ohrui–Akasaka method [31]. The brief explanation of this method was described in Chapter 2. To generate a carboxy group for derivatization, the imidazole ring of **4** was oxidatively degraded by the treatment with ruthenium tetraoxide and sodium periodate in a biphasic solvent mixture (CCl_4/MeCN/H_2O), which gave 6-methyloctanoic acid (*nat*-**10**). This anteiso-fatty acid was then esterified with a chiral anthracene reagent, (*R*)-2-(anthracene-2,3-dicarboximido)propanol [(*R*)-2A1P], to give *nat*-**10**-(*R*)-2A1P (Scheme 3-3). The authentic (*S*)-**10**-(*R*)-2A1P and (*S*)-**10**-(*S*)-2A1P) was synthesized from (*S*)-6-methyldecanoic acid [(*S*)-**10**], which was prepared from commercially available (*S*)-6-methyloctanol in two steps. (Scheme 3-4) [32].

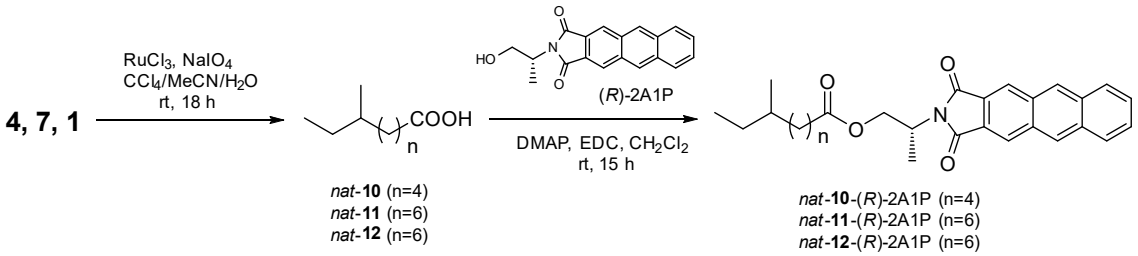

Scheme 3-3. Oxidative degradation of **4**, **7**, and **1**, and derivatization with (*R*)-2A1P for Ohrui-Akasaka Analysis.

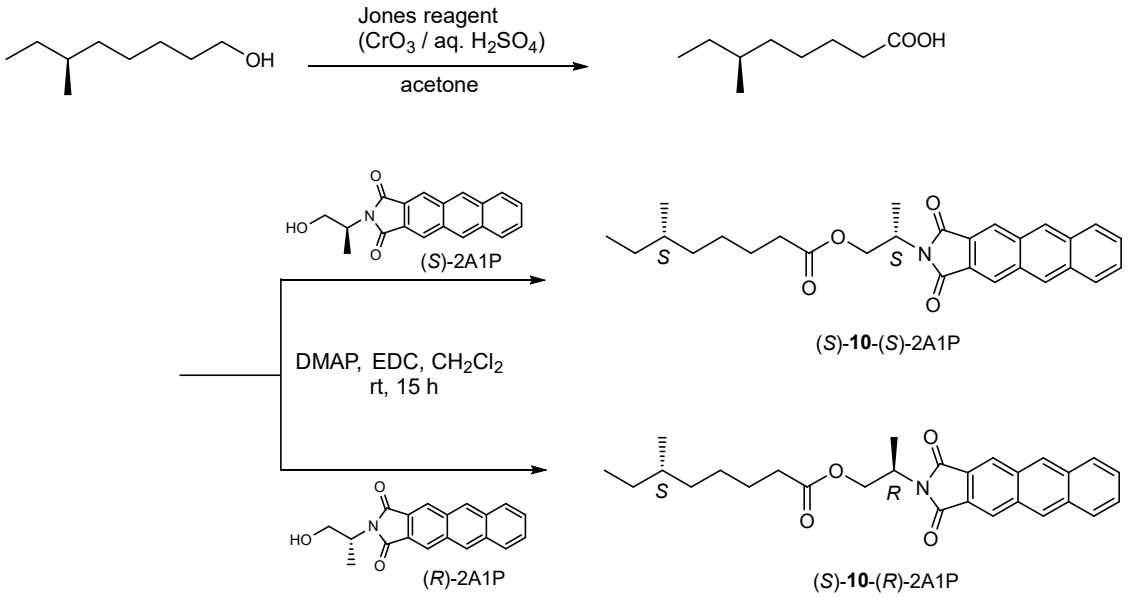

Scheme 3-4. Synthesis of (*S*)-6-methyldecanoic acid and derivatization with (*S*)-2A1P and (*R*)-2A1P for Ohrui-Akasaka analysis.

These three synthesized compounds (*nat*-**10**-(*R*)-2A1P, (*S*)-**10**-(*R*)-2A1P, and (*S*)-10-(*S*)-2A1P) were subjected to HPLC analysis for comparison. The retention times of the standard samples were 177 min for (*S*)-**10**-(*S*)-2A1P (chromatographically equivalent to (*R*)-**10**-(*R*)-2A1P) and 184 min for (*S*)-**10**-(*R*)-2A1P, and *nat*-**10**-(*R*)-2A1P gave both peaks with the area ratio of 72.9:27.1 (Figure 3-14). Therefore, **1** was established as an enantiomeric mixture comprising 73% of the *R*- and 27% of the *S*-enantiomer.

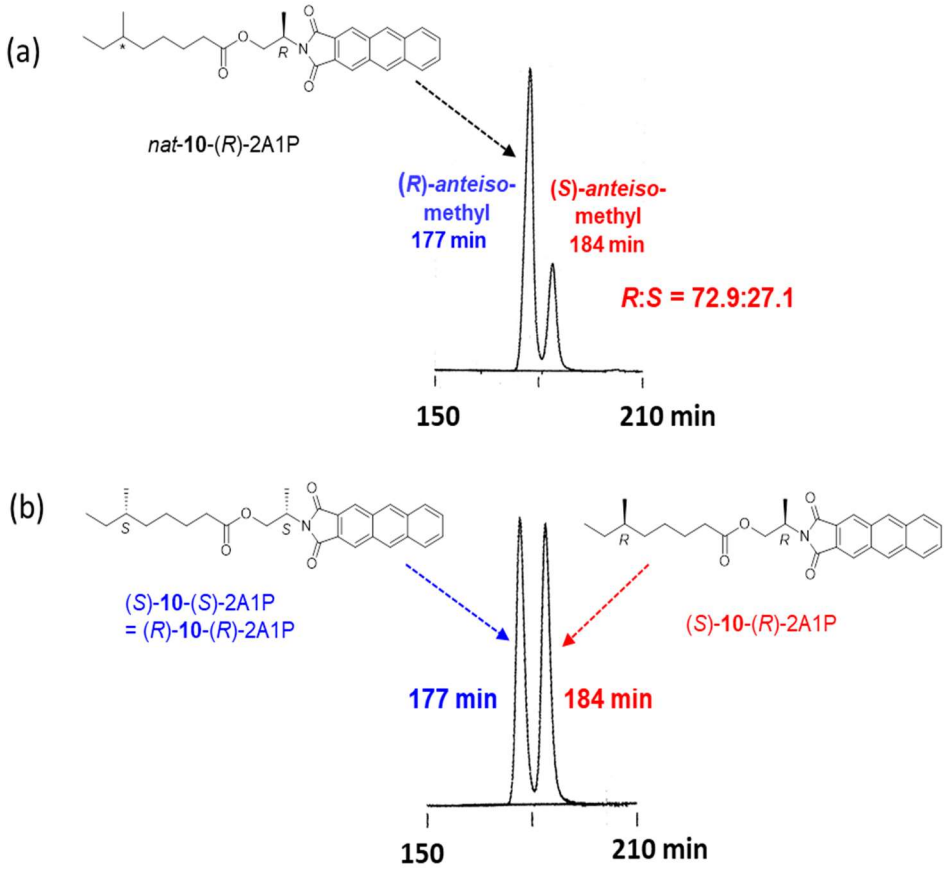

Figure 3-14. Absolute configuration of **1** determined by using chiral anthracene derivatives. (a) HPLC chromatogram of *nat*-**10**-(*R*)-2A1P; (b) HPLC chromatogram of standard (*S*)-**10**-(*S*)-2A1P and (*S*)-**10**-(*R*)-2A1P

HPLC conditions

Develosil ODS HG-3 [3.0 mm id x (250 +150) mm]

MeCN/MeOH/THF (3:1:1, v/v/v)

0.075 mL/min, -48.5 ℃

Fluorometry: Ex. 298 nm, Em. 460 nm

Nocarimidazole B (**4**) was originally produced by marine *Nocadiopsis*, but in the previous study, the absolute configuration was not determined [23]. In this study, the same compound was isolated from strain T35-5 and the configuration was determined by Ohrui–Akasaka method as same as **1** [31]. The conversion of **4** into the derivative *nat*-**11**-(*R*)-2A1P was carried out in a similar manner as described for **1** (Scheme 3-3). The preparation of authentic (*S*)-**11**-(*R*)-2A1P, and (*S*)-**11**-(*S*)-2A1P) were explained in the previous Chapter [24]. HPLC analysis showed that the retention times of the standard samples were 234 min for (*S*)-**11**-(*S*)-2A1P (chromatographically equivalent to (*R*)-**11**-(*R*)-2A1P) and 244 min for (*S*)-**11**-(*R*)-

2A1P, and 244 min for *nat*-**11**-(*R*)-2A1P. Therefore, **4** was determined to be an enantiomerically pure *S*-enantiomer (Figure 3-15).

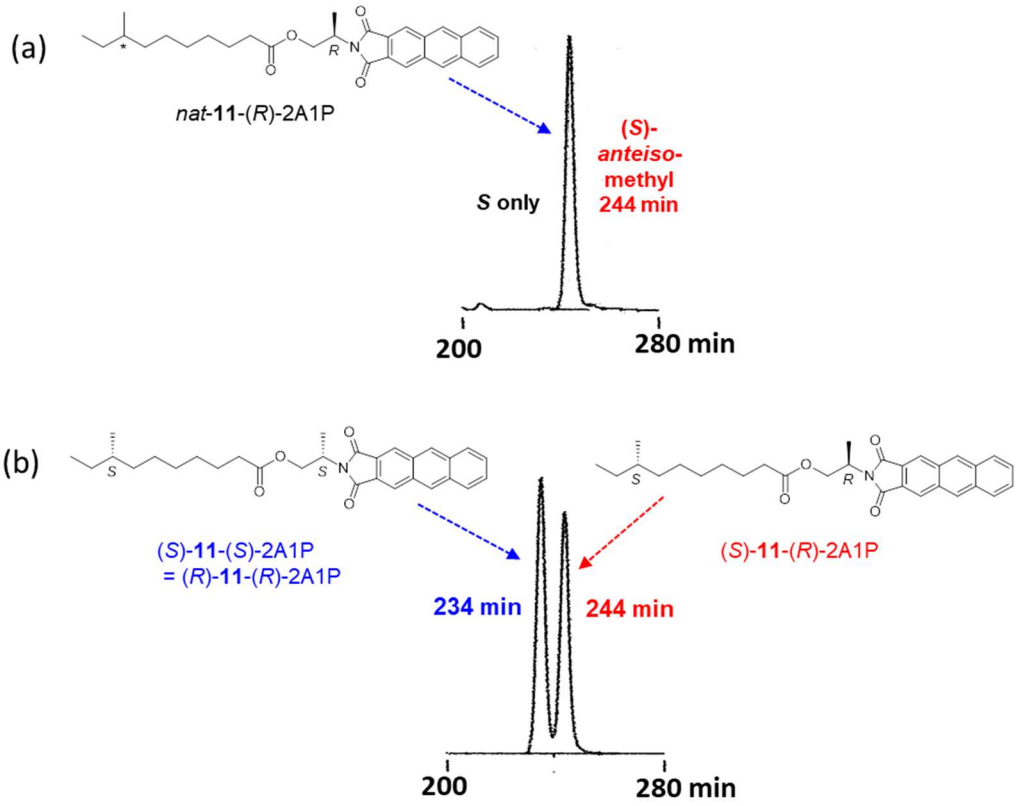

Figure 3-15. Absolute configuration of **4** determined by using chiral anthracene derivatives. (a) HPLC chromatogram of *nat*-**11**-(*R*)-2A1P; (b) HPLC chromatogram of standard (*S*)-**11**-(*S*)-2A1P and (*S*)-**11**-(*R*)-2A1P

HPLC conditions

Develosil ODS HG-3 [3.0 mm id x (250 +150) mm]

MeCN/MeOH/THF (3:1:1, v/v/v)

0.10 mL/min, -42.5 ℃

Fluorometry: Ex. 298 nm, Em. 460 nm

Bulbimidazole A (**1**) was firstly isolated from a marine bacterium *Microbulbifer* and was an enantiomeric mixture of (*R*)-and (*S*)-isomers in a ratio of 9:90 as described in Chapter 2 [24]. The same compound was obtained from a different microorganism, actinomycete *Kocuria.* Therefore, it might be possible to have different absolute configuration. In this study, to determine the configuration, the same chiral analysis was employed for bulbimidazole A (**1**) [31]. The *nat*-**12**-(*R*)-2A1P was synthesized as described for **4** (Scheme 3-3). The

authentic (*S*)-**11**-(*R*)-2A1P, and (*S*)-**11**-(*S*)-2A1P were used for comparison because both **7** and **1** consist of the same number of carbon in their fatty acid chain. HPLC analysis showed that the retention times of the standard samples were 312 min for (*S*)-**11**-(*S*)-2A1P (chromatographically equivalent to (*R*)-**11**-(*R*)-2A1P), 324 min for (*S*)-**11**-(*R*)-2A1P, and *nat*-**12**-(*R*)-2A1P gave both peaks with an enantiomeric ratio of *R*/*S* = 1.4:98.6 (Figure 3-16). Therefore, **1** was established as an enantiomeric mixture comprising 1% of the *R*- and 99% of the *S*-enantiomer. In this study, the same authentic compounds were used for both **7** and **1.** But, their retention times were not the same due to the analysis performed in a different HPLC condition.

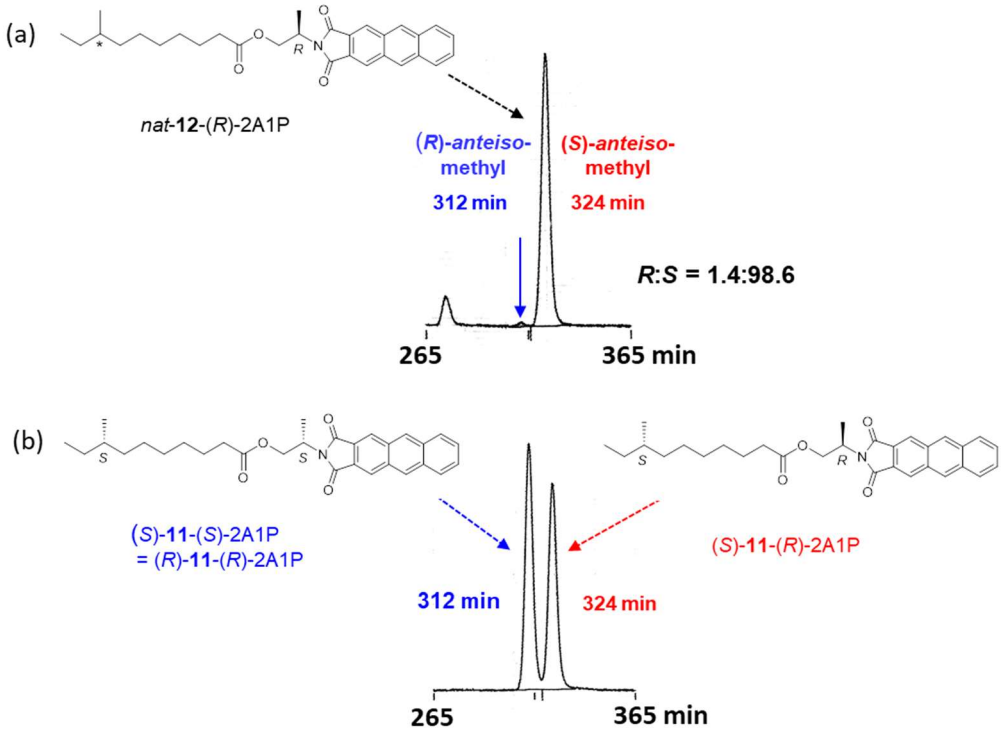

Figure 3-16. Absolute configuration of **5** determined by using chiral anthracene derivatives. (a) HPLC chromatogram of *nat*-**12**-(*R*)-2A1P; (b) HPLC chromatogram of standard (*S*)-**11**-(*S*)-2A1P and (*S*)-**11**-(*R*)-2A1P

HPLC conditions

Develosil ODS HG-3 [3.0 mm id x (250 +150) mm]

MeCN/MeOH/THF (3:1:1, v/v/v)

0.075 mL/min, -42.5 °C

Fluorometry: Ex. 298 nm, Em. 460 nm

3-2-5 Bioactivity

Biological activity of nocarimidazoles (**4**–**7**) was evaluated in antimicrobial and cytotoxicity assays. The antimicrobial activity of **4**–**7** was examined against two Gram-positive bacteria *Kocuria rhizophila* and *Staphylococcus aureus*, two Gram-negative bacteria *Escherichia coli* and *Rhizobium radiobacter*, a yeast *Candida albicans*, and two filamentous fungi *Glomerella cingulata* and *Trichophyton rubrum* (Table 3-2). All compounds showed moderate antibacterial activity against Gram-positive bacteria with a minimum inhibitory concentration (MIC) of 6.25–12.5 μg/mL but no appreciable activity against Gram-negative bacteria. Compounds **4–7** were also active against the yeast and fungi with MIC values ranging from 6.25–25 μg/mL. In addition, compounds **4** and **7** showed weak cytotoxicity against P388 murine leukemia cells with IC_{50} values of 38 and 33 μM (IC_{50} of a reference drug doxorubicin: 0.02 μM), respectively.

Table 3-2. Antimicrobial activity of nocarimidazoles (**4**–**7**).

	MIC (μg/mL)			
microorganism	**4**	**5**	**6**	**7**
Kocuria rhizophila ATCC9341	6.25	12.5	6.25	6.25
Staphylococcus aureus FDA209P JC-1	12.5	25	12.5	25
Escherichia coli NIHJ JC-2	>100	>100	>100	>100
*Rhizobium radiobacter*NBRC14554	>100	>100	>100	>100
Candida albicans NBRC0197	25	25	12.5	12.5
Glomerella cingulata NBRC5907	12.5	12.5	25	25
Trichophyton rubrum NBRC5467	6.25	6.25	25	6.25

3-3 Conclusion

In summary, chemical investigation of new secondary metabolites from a marine bacterium, I selected marine bacterial strain T35-5 through a successful spectroscopic screening process using HPLC/UV analysis in combination with the in-house UV database. The strain was obtained from the stony coral of the genus *Mycedium* collected near the coast of Karimunjawa, Central Java, Indonesia. This producing strain was identified as a member of the genus *Kocuria* by analysis of 16S rRNA gene sequence. I isolated five secondary metabolites from this strain by using different chromatographic techniques and the structures of all compounds were established by NMR, MS and IR spectroscopic data. All compounds are the members of rare class of marine natural products belonging to alkanoylimidazoles. These compounds are 4-acylated imidazoles joined with alkayl chains difference of varying

chain length and terminal branching. The imidazole ring substitution at C-5 by an amino group make them an emerging class of marine-derived bioactive compounds. Until now, only two natural products in this class have been isolated from nature. The first members known as nocarimidazoles A (**4**) and B (**5**) were discovered from a marine actinomycete *Nocardiopsis* [23]; on the other hand, bulbimidazoles A–C are the second example, isolated from a marine gammaproteobacterium *Microbulbifer* [24]. In this study, nocarimidazoles C (**4**) and D (**5**) were discovered from a marine-derived actinomycete of the genus *Kocuria* as two new additional members of alkanoylimidazoles.

I also analyzed the chirality of three compounds including nocarimidazole C (**4**), nocarimidazole B (**7**) and bulbimidazole A (**1**), which possess the *anteiso*-branched alkanoyl chain. The absolute configurations of the *anteiso*-branched metabolites are in general believed to be *S*, because they are biosynthesized from L-isoleucine [33, 34]. However, our laboratory has shown that the absolute configuration of *anteiso*-branched natural products from marine bacteria such as nocapyrone L and bulbimidazole A (**1**) are an enantiomeric mixture of (*R*)- and (*S*)-isomers in a ratio of 2:3 and 9:91, respectively [32, 24], as determined by Ohrui−Akasaka method [31]. Therefore, this method was employed to determine the absolute configuration for **4**, **7**, **1** and reveal enantiomeric mixture of (*R*)-and (*S*)-isomers in **4** and **1** but at the same time purely *S*-configured in **7.** However, I found that **4** is an enantiomeric mixture of (*R*)-and (*S*)-isomers in a ratio of 73:27. It should be acclaimed that the *R*-enantiomer-rich anteisoalkyl group is extremely rare. Up to date, only two examples were reported such as ceramides, each from the dinoflagellate *Coolia monotis* [35] and the sponge *Ephydatia syriaca* [36]. Interestingly, the same chemistry is seen among related compounds which have the common planar structure from different organisms such as bulbimidazole A isolated from two different marine bacteria *Microbulbifer* and *Kocuria* that have enantiomeric mixture of (*R*)- and (*S*)-isomers in a ratio of 9:91 and 1:99, respectively and even though the same compounds are discovered from the same organism (e.g., nocarimidazole C, nocarimidazole B and bulbimidazole A). Bulbimidazoles A–C, nocarimidazoles C–D and nocarimidazoles A–B are only three examples of alkanoylimidazole found in nature, isolated from three different marine bacteria *Microbulbifer*, *Kocuria* and *Nocardiopsis*, suggesting that these strains have the same biosynthetic gene cluster for the production of these distinct classes of natural products. Therefore, discovery of new groups of marine bacteria from unexplored or underexploited

habitats, especially, corals, demonstrates this bacterial community as an untapped source of novel natural product.

Actinomycetes are Gram-positive and filamentous bacteria, which represent one of the largest taxonomic groups among the major lineages currently recognized within the bacteria domain and most potentially valuable source of structurally novel bioactive compounds [37]. Almost two-third of clinically relevant molecules was discovered from this diverse class of bacterial source [38]. However, the number of bioactive compounds from marine actinomycetes is comparatively less than the terrestrial counterpart because a large portion remains uncultured for natural product discovery. In marine environment, actinomycetes well are living with marine organisms such as sponges, corals, fish, crab, sea cucumber, mollusks, ascidians, seaweeds, seagrasses, and mangroves [39]. Several numbers of bioactive compounds were discovered from sponge associated actinomycetes, while the remaining are from the actinomycetes associated with mollusk, corals, ascidians, and seaweeds [40]. Among them, coral-associated actinomycetes have received less attention for their natural product. Few compounds have been found from soft coral associated actinomycetes. For example, strepchloritide A [41], octalactin A [42], watasemycin A [43], pulicatin G [44] and aerugine [45] were obtained from soft coral associated actinomycetes (Figure 3-13). In this study, I found new bioactive compounds which are rare in nature from a stony coral-associated actinomycetes. Therefore, stony coral-associated actinomycetes could be a potential source of new bioactive compounds.

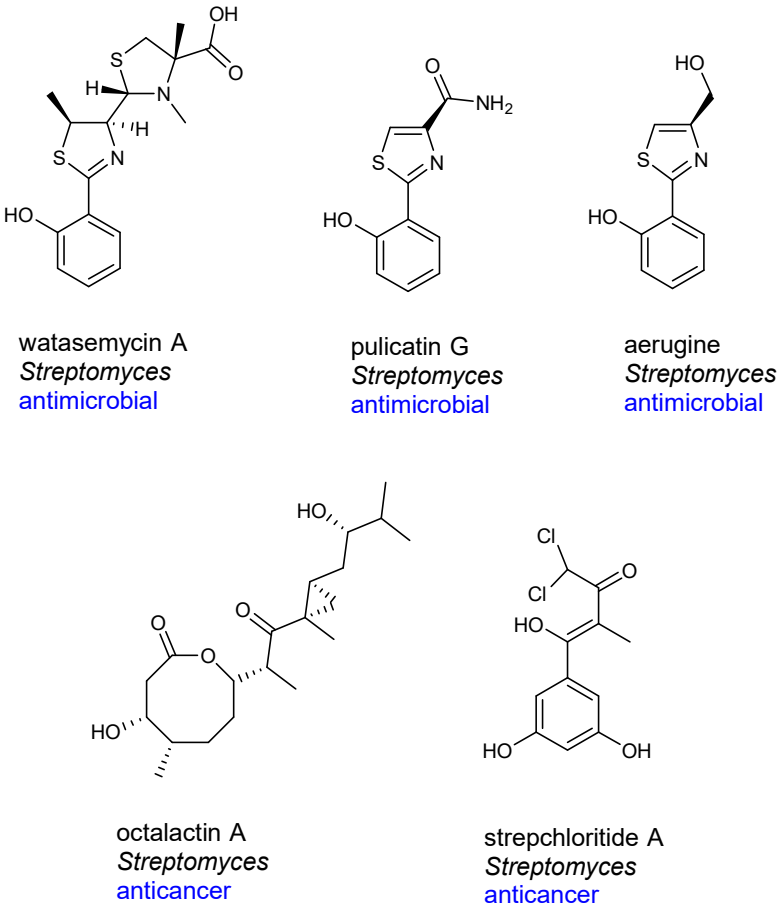

Figure 3-13. Structures of natural products from soft coral-associated actinomycetes.

3-4 Experimental Section

General Experimental Procedures. The specific rotations were measured on a JASCO P-1030 polarimeter. UV and IR spectra were recorded on a Shimadzu UV-1800 spectrophotometer and a PerkinElmer Spectrum 100 spectrophotometer, respectively. NMR spectra were obtained on a Bruker AVANCE II 500 MHz NMR spectrometer in DMSO-d_6 supplemented with a trace amount of trifluoroacetic acid using the signals of the residual solvent protons (δ_H 2.49) and carbon atoms (δ_C 39.5) as internal standards for compounds **1**–**5**, or in $CDCl_3$ using the signals of the residual solvent protons (δ_H 7.27) and carbon atoms (δ_C 77.0) as internal standards for other compounds. HRESITOFMS spectra were recorded on a Bruker micrOTOF focus mass spectrometer. An Agilent HP1200 system equipped with a diode array detector was used for analysis and purification.

Microorganism. The coral sample *Mycedium* sp. was collected depths of 15 to 20 m from Tanjung Gelam, Karimunjawa National Park, Jepara, Central Java, Indonesia with a permission number of 1096/T.34/TU/SIMAKSI/7/2017. The strain T35-5 was isolated according to the method described previously [35] and identified as a member of the genus *Kocuria* on the basis of 100.0% similarity in the 16S rRNA gene sequence (1,381 nucleotides; DDBJ accession number LC556325) to *Kocuria palustris* DSM 11925^T (accession number Y16263).

Fermentation. The strain T35-5 was maintained on Marine Agar 2216 (Difco). A loopful of the strain T35-5 was inoculated into a 500 mL K-1 flask containing 100 mL of Marine Broth 2216 (Difco) as a seed culture. The seed culture was incubated at 30 °C on a rotary shaker at 200 rpm for 2 days. Three mL each of the seed culture were inoculated into 500 mL K-1 flasks containing 100 mL of A11M production medium, which consists of 0.2% glucose, 2.5% soluble starch, 0.5% yeast extract, 0.5% polypeptone (Wako Pure Chemical Industries, Ltd.), 0.5% NZ-amine (Wako Pure Chemical Industries, Ltd.), 0.3% $CaCO_3$, and 1% Diaion HP-20 (Mitsubishi Chemical Co.) in natural seawater (collected from Toyama Bay, Japan). The pH value of the medium was adjusted to 7.0 before sterilization. The inoculated flasks were incubated at 30 °C for 5 days, with rotational shaking at 200 rpm.

Extraction and Isolation. After fermentation, 100 mL of 1-butanol was added to each flask, and the flasks were shaken for 1 h. The emulsified mixture was centrifuged at 6000 rpm for 10 min, and the organic layer was separated from the aqueous layer. Evaporation of the organic solvent gave approximately 3.8 g of extract from 3 L of culture. The extract (3.8 g)

was chromatographed over a silica gel column using a mixture solvent of $CHCl_3$/MeOH (1:0, 20:1, 10:1, 4:1, 2:1, 1:1, and 0:1, v/v). Fraction 3 (10:1) was concentrated to yield 0.38 g of a brown oil, which was further fractionated by ODS column chromatography with a stepwise gradient of a MeCN/0.1% HCO_2H aqueous solution (2:8, 3:7, 4:6, 5:5, 6:4, 7:3, and 8:2, v/v). Fractions 4 (5:5) and 5 (6:4) were separately concentrated in vacuo, and the remaining aqueous layer was extracted with EtOAc. The organic layer was dried over anhydrous Na_2SO_4, filtered, and concentrated to give 40 mg and 45 mg of a semipure material. Final purification was achieved by preparative HPLC (Cosmosil AR-II, Nacalai Tesque Inc., 10 × 250 mm, 4 mL/min, UV detection at 254 nm) with an isocratic elution of MeCN/0.1% HCO_2H (42:58) to afford nocarimidazole C (**4**, 2.4 mg, t_R 8.45 min), nocarimidazole D (**5**, 3.2 mg, t_R 14.9 min), nocarimidazole A (**6**, 3.8 mg, t_R 13.5 min), nocarimidazole B (**7**, 8.0 mg, t_R 17.3 min) from fraction 4, and bulbimidazole A (**1**, 3.2 mg, t_R 11.2 min) from fraction 5.

Nocarimidazole C (**4**): pale yellow amorphous solid; $[\alpha]^{23}_D$ -1.2 (*c* 0.10, MeOH); UV (MeOH) λ_{max} (log ε) 296 (4.27), 226 (3.87), 200 (4.30) nm; IR (ATR) ν_{max} 3127, 2955, 2923, 1664 cm^{-1}; ^1H and ^{13}C NMR data, see Table 1; HR-ESITOFMS *m/z* 224.1763 $[M + H]^+$ (calcd for $C_{12}H_{22}N_3O$, 224.1757).

Nocarimidazole D (**5**): pale yellow amorphous solid; UV (MeOH) λ_{max} (log ε) 296 (4.47), 225 (4.07), 200 (4.52) nm; IR (ATR) ν_{max} 3126, 2954, 2923, 1667 cm^{-1}; ^1H and ^{13}C NMR data, see Table 1; HR-ESITOFMS *m/z* 238.1915 $[M + H]^+$ (calcd for $C_{13}H_{24}N_3O$, 238.1913).

Nocarimidazole A (**6**): UV (MeOH) λ_{max} (log ε) 295 (4.35), 232 (3.91), 200 (4.36) nm; HR-ESITOFMS *m/z* 238.1910 $[M + H]^+$ (calcd for $C_{13}H_{24}N_3O$, 238.1914); ^1H and ^{13}C NMR data in $CDCl_3$ was the same as those reported in reference 21.

Nocarimidazole B (**7**): $[\alpha]^{23}_D$ +1.2 (*c* 0.10, MeOH); UV (MeOH) λ_{max} (log ε) 296 (4.32), 233 (3.89), 200 (4.34) nm; HR-ESITOFMS *m/z* 252.2074 $[M + H]^+$ (calcd for $C_{14}H_{26}N_3O$, 252.2070); ^1H and ^{13}C NMR data in $CDCl_3$ was the same as those reported in reference 21.

Bulbimidazole A (**1**): $[\alpha]^{23}_D$ +1.2 (*c* 0.10, MeOH); HR-ESITOFMS *m/z* 237.1965 $[M + H]^+$ (calcd for $C_{14}H_{25}N_2O$, 237.1961); ^1H and ^{13}C NMR data in DMSO-d_6 with a trace amount of TFA was the same as those reported in reference 22.

Synthesis of 1-(5-amino-1*H*-imidazol-4-yl)ethan-1-one (8)

To a solution of 4-isocyano-1*H*-imidazol-5-amine (100 mg, 92 μmol) in THF (9.2 mL) was added 1.0 M solution of MeMgBr (4.6 mL) at room temperature. After stirring for 2 h, 3 M HCl (10 mL) was added to the reaction mixture. After stirring at 90 °C for 2 h, the reaction mixture was cooled to the ambient temperature and concentrated *in vacuo*. The resulting liquid mixture received a saturated solution of $NaHCO_3$ (100 mL), and then extracted with EtOAc. The organic layer was then washed with water and brine, dried over anhydrous Na_2SO_4, and concentrated *in vacuo* to give 62 mg of crude material. It was then purified by preparative HPLC (XTerra Shield RP18 OBD™ Prep Column, 10 m, 10 x 250 mm, 4 mL/min, Waters) with an isocratic elution MeCN/10 mM NH_4HCO_3 (5:95) to afford 1-(5-amino-1*H*-imidazol-4-yl)ethan-1-one (**8**, 32 mg, 27% yield): ^{1}H NMR (DMSO-d_6 with TFA, 500 MHz) δ_H 2.27 (3H, s), 7.77 (1H, s); ^{13}C NMR (DMSO-d_6 with TFA, 125 MHz) δ_C 187.1, 148.9, 132.4, 113.4, 26.3; HR-ESITOFMS *m/z* 126.0665 $[M + H]^+$ (calcd for $C_5H_8N_3O$ 126.0667).

Synthesis of 1-(2-amino-1*H*-imidazol-4-yl)ethan-1-one (9)

To a solution of pyrimidin-2-amine (100 mg, 105 μmol) in toluene (4 mL) was added 1,1-dimethoxy-*N*,*N*-dimethylmethanamine (200 μL, 157 μmol), and the mixture was stirred at 110 °C for 2 h. After cooling, EtOAc was added to the reaction mixture, and this organic layer was washed with water and brine, dried over anhydrous Na_2SO_4, and concentrated *in vacuo* to afford (*E*)-*N*,*N*-dimethyl-*N*'-(pyrimidin-2-yl)formimidamide (88 mg).

(*E*)-*N*,*N*-Dimethyl-*N*'-(pyrimidin-2-yl)formimidamide (88 mg, 59 μmol) was then treated with 1-chloropropan-2-one (190 μL, 210 μmol) in dry CH_2Cl_2 (4 mL) at room temperature. After stirring for 2 days, EtOAc was added to the reaction mixture, and the organic layer was washed with water and brine, dried over anhydrous Na_2SO_4, and concentrated under reduced pressure to give 3-acetylimidazo[1,2-a]pyrimidine (82 mg).

A solution of 3-acetylimidazo[1,2-a]pyrimidine (82 mg, 50 μmol) was reacted with N_2H_4 (180 μL, 200 μmol) in H_2O (3 mL) at room temperature for 30 min. The reaction mixture was extracted with EtOAc and the organic layer was washed with water and brine, dried over anhydrous Na_2SO_4, and concentrated *in vacuo* to give 78 mg of crude product. The crude material was subjected to preparative HPLC (XTerra Shield RP18 OBD™ Prep Column, 10 m, 10 x 250 mm, 4 mL/min, Waters, MA) with an isocratic elution MeCN/10 mM NH_4HCO_3

(2:98) to yield 1-(5-amino-1*H*-imidazol-4-yl)ethan-1-one (**9**, 65 mg, 56% overall yield): ^{1}H NMR (DMSO-d_6 with TFA, 500 MHz) δ_H 2.34 (3H, s), 8.0 (1H, s); ^{13}C NMR (DMSO-d_6 with TFA, 125 MHz) δ_C 186.6, 148.8, 127.0, 122.8, 25.4; HR-ESITOFMS *m/z* 126.0663 [M + H]$^+$ (calcd for $C_5H_8N_3O$ 126.0667).

Determination of the Absolute Configuration of 4, 7, and 1 by the Ohrui-Akasaka method

Authentic samples for HPLC comparison, (*R*)- and (*S*)-2-(anthracene-2,3-dicarboximido)propyl esters of (*S*)-6-methyloctanoic acid [(*S*)-**10**-(*R*)-2A1P and (*S*)-**10**-(*S*)-2A1P] and (*S*)-8-methyldecanoic acid [(*S*)-**11**-(*R*)-2A1P and (*S*)-**11**-(*S*)-2A1P], were prepared as described in our previous study.

Nocarimidazole C (**4**, 0.5 mg, 2 μmol) was converted to the ester derivative *nat*-**10**-(*R*)-2A1P (1.1 mg) in a similar manner as described previously [22]. Oxidative degradation of nocarimidazole D (**6**, 0.5 mg, 2 μmol) and bulbimidazole A (**1**, 0.5 mg, 2 μmol) and derivatization with (*R*)-2A1P were carried out in a similar manner, yielding the ester derivatives *nat*-**11**-(*R*)-2A1P (0.7 mg) and *nat*-**12**-(*R*)-2A1P (0.7 mg).

nat-**10**-(*R*)-2A1P: HR-ESITOFMS *m/z* 468.2152 [M + Na]$^+$ (calcd for $C_{28}H_{31}NO_4Na$, 468.2145).

nat-**11**-(*R*)-2A1P: HR-ESITOFMS *m/z* 496.2455 [M + Na]$^+$ (calcd for $C_{30}H_{35}NO_4Na$, 496.2458).

nat-**12**-(*R*)-2A1P: HR-ESITOFMS *m/z* 496.2456 [M + Na]$^+$ (calcd for $C_{30}H_{35}NO_4Na$, 496.2458).

nat-**10**-(*R*)-2A1P and synthetic (*S*)-**10**-(*R*)-2A1P and (*S*)-**10**-(*S*)-2A1P were analyzed by HPLC according to the reported protocol [22] with minor modification of conditions. Column: tandemly connected Develosil ODS-HG-3 (3.0 mm i.d. × 250 mm + 3.0 mm i.d. × 150 mm, Nomura Chemical); mobile phase: MeCN/MeOH/THF = 3:1:1; column temperature: −48.0 °C; flow rate: 0.075 mL/min. The column was cooled by using Cryocool CC-100 (Neslab Instruments Inc.). HPLC peaks were detected by monitoring fluorescence intensity at 460 nm with the excitation at 298 nm on an FP-4025 fluorescence detector (JASCO Corporation, Hachioji, Japan). Retention times were 177 min for (*S*)-**10**-(*S*)-2A1P and 184 min for (*S*)-**10**-(*R*)-2A1P, while *nat*-**10**-(*R*)-2A1P gave peaks at 177 and 184 min with an area ratio of 72.9:27.1.

nat-**11**-(*R*)-2A1P derived from nocarimidazoles B (**7**) and synthetic (*S*)-**11**-(*R*)-2A1P and (*S*)-**11**-(*S*)-2A1P were analyzed by HPLC using the same column and solvent system. The column temperature was set at −42.5 °C and the flow rate at 0.10 mL/min. Retention times were 234 min for (*S*)-**11**-(*S*)-2A1P and 244 min for (*S*)-**11**-(*R*)-2A1P, whereas *nat*-**4**-(*R*)-2A1P gave a peak only at 244 min.

nat-**12**-(*R*)-2A1P derived from bulbimidazole A (**1**) and synthetic (*S*)-**11**-(*R*)-2A1P and (*S*)-**11**-(*S*)-2A1P were analyzed by HPLC using the same column and solvent system. The column temperature was set at −42.5 °C and the flow rate at 0.075 mL/min. Retention times were 312 min for (*S*)-**11**-(*S*)-2A1P and 324 min for (*S*)-**11**-(*R*)-2A1P, while *nat*-**12**-(*R*)-2A1P gave peaks at 312 and 324 min in a ratio of 1.4:98.6.

Bioassays

The antimicrobial activity was evaluated in a similar manner as previously reported [24]. The cytotoxicity against P388 murine leukemia cells was examined according to a protocol described in [24].

References

1) Harvey, B. J.; Nash, K. L.; Blanchard, J. L.; Edwards, D. P. *Ecol. Evol*, **2018**, *8*, 6354–6368.
2) Brown, B. E. *Adv. Mar. Biol.* **1997**, *31*, 221-299.
3) Hou, X. –M.; Hai, Y.; Gu, Y. –C.; Chang-Yun Wang, C. –Y.; Chang-Lun Shao, C. –L. *Curr. Med. Chem.* **2019**, *26*, 1-12.
4) Vanwonterghem, I.; Webster, N. S. *iScience*. **2020**, *23*, 100972-100987.
5) Krediet, C. J.; Ritchie, K. B.; Paul, V. J.; Teplitski, M. *Proc. Biol. Sci.* **2013**, *280*, 1755.
6) Paul, V. J.; Puglisi, M. P. *Nat. Prod. Rep.* **2004**, *21*, 189- 209.
7) Paul, V. J.; Puglisi, M. P.; Ritson-Williams, R. *Nat. Prod. Rep*. **2006**, *23*, 153-180.
8) Paul, V. J.; Ritson-Williams, R.; Sharp, K. *Nat. Prod. Rep.* **2011**, *28*, 345-387.
9) Ireland, C. M.; Copp, B. R.; Foster, M. P.; Mcdonald, L. A.; Radisky, D. C.; Swersey, J. C. In: *Technomic Publishing*. **2000**, 641-661.
10) Houa, X. –M.; Xua, R. –F.; Gub, Y. –C. Wanga, C. –Y.; Shaoa, C. –L. *Curr. Med. Chem.* **2015**, *22*, 3707-3762.

11) Shao, C. L.; Wu, H. X.; Wang, C. Y.; Liu, Q. A.; Xu, Y.; Wei, M. Y.; Qian, P. Y.; Gu, Y. C.; Zheng, C. J.; She, Z. G.; Lin, Y. C. *J. Nat. Prod.* **2011**, *74*, 629-633.

12) McDonald, L. A.; Abbanat, D. R.; Barbieri, L. R.; Bernan, V. S.; Discafani, C. M.; Greenstein, M.; Janota, K.; Korshalla, J. D.; Lassota, P.; Tischler, M.; Carter, G. T. *Tetrahedron Lett.* **1999**, *40*, 2489-2492.

13) Zhuang, Y. B.; Teng, X. C.; Wang, Y.; Liu, P. P.; Li, G. Q.; Zhu, W. M. *Org. Lett*. **2011**, *13*, 1130-1133.

14) Sharma, A. R.; Harunari, E.; Oku, N.; Matsuura, N.; Trianto, A.; Igarashi, Y. *Beilstein J. Org. Chem.* **2020**, *16*, 297–304.

15) Tang, J. S.; Gillevet, P. M. *Int. J. Syst. Evol. Microbiol.* **2003**, *53*, 995–997.

16) Seo, Y. B.; Kim, D.-E.; Kim, G.-D.; Kim, H.-W.; Nam, S.-W.; Kim, Y. T.; Lee, J. H. *Int. J. Syst. Evol. Microbiol*. **2009**, *59*, 2769–2772.

17) Li, J.; Zhang, S. *Int. J. Syst. Evol. Microbiol*. **2020**, *70*, 785–789.

18) Kim, S. B.; Nedashkovskaya, O. I.; Mikhailov, V. V.; Han, S. K.; Kim, K.-O.; Rhee, M.-S.; Bae, K. S. *Int. J. Syst. Evol. Microbiol*. **2004**, *54*, 1617–1620.

19) Zhang, L.; Xi, L.; Ruan, J.; Huang, Y. *Int. J. Syst. Evol. Microbiol*. **2017**, *67*, 164–169.

20) AntiSMASH database. https://antismash.secondarymetabolites.org (accessed Apr 29, 2020).

21) Bagley, M. C.; Merritt, E. A. *J. Antibiot*. **2004**, *57*, 829–831.

22) Palomo, S.; González, I.; de la Cruz, M.; Martín, J.; Tormo, J. R.; Anderson, M.; Hill, R. T.; Vicente, F.; Reyes, F.; Genilloud, O. *Mar. Drugs.* **2013**, *11*, 1071–1086.

23) Leutou, A. S.; Yang, I.; Kang, H.; Seo, E. K.; Nam, S.-J.; Fenical, W. *J. Nat. Prod*. **2015**, *78*, 2846–2849.

24) Karim, M. R. U.; Harunari, E.; Oku, N.; Akasaka, K.; Igarashi, Y. *J. Nat. Prod*. **2020**, *83*, 1295–1299.

25) Vila, J. A.; Scheraga, H. A. *J. Mol. Struct*. **2017**, *1134*, 576–581.

26) Wasylishen, R. E.; Tomlinson, G. *Biochem. J.* **1975**, *147*, 605–607.

27) Kick, E. K.; Bodas, M.; Mohan, R.; Valente, M.; Wurtz, N.; Patil, S. *LXR modulators. PCT Int. Pat. Appl.* WO2014144037 A1, Sept 18, **2014**.

28) Rasapalli, S.; Dhawane, A.; Rees, C.; Golen, J. A.; Singh, B. R.; Cai, S.; Jasinski, J.; Kwasny, S. M.; Moir, D. T.; Opperman, T. J.; Bowlin, T. L. *Med. Chem. Comm*. **2013**, *4*, 1467-1472.

29) Love, C.; Van Wauwe, J. P. F.; De Brabander, M.; Cooymans, L.; Vandermaesen, N. 2,4-Disubstituted thiazolyl derivatives. *PCT. Int. Pat. Appl*. WO200164674 A1, Sept 7, **2001.**

30) Lam, F. L.; Parham, J. C. *J. Am. Chem. Soc.* **1975**, *97*, 2839–2844.

31) Akasaka, K.; Meguro, H.; Ohrui, H. *Tetrahedron Lett*. **1997**, *38*, 6853–6856.

32) Kim, Y.; Ogura, H.; Akasaka, K.; Oikawa, T.; Matsuura, N.; Imada, C.; Yasuda, H.; Igarashi, Y. *Mar. Drugs* **2014**, *12*, 4110–4125.

33) Kaneda, T. *Microbiol. Rev*. **1991**, *55*, 288-302.

34) Challis, G. L. *Microbiology* **2008**, *154*, 1555-1569.

35) Akasaka, K.; Shichijyukari, S.; Matsuoka, S.; Murata, M.; Meguro, H.; Ohrui, H. *Biosci. Biotechnol. Biochem*. **2000**, *64*, 1842–1846.

36) Řezanka, T.; Sigler, K.; Dembitsky, V. M. *Tetrahedron* **2006**, *62*, 5937–5943.

37) Jakubiec-krzesniak, K.; Rajnisz-mateusiak, A.; Guspiel, A.; Ziemska, J.; Solecka, J. *Pol J Microbiol.* **2018**, *67*, 259–272.

38) Takahashi, Y.; Nakashima, T. *Antibiotics* **2018**, *7*, 45-61.

39) Valli S, V.; Sugasini, S. S.; Aysha, O. S.; Nirmala, P.; Kumar P. V.; Reena, A. *Asian Pac. J. Trop. Biomed.* **2012**, *2*, 469-473.

40) Abdelmohsen, U. R.; Bayera, K.; Hentschel, U. *Nat. Prod. Rep*. **2014**, *31*, 381–399.

41) Fu, P.; Kong, F. D.; Wang, Y. F.; Wang, Y.; Liu, P. P.; Zuo, G. Y.; Zhu, W. M. *Chin. J. Chem.* **2013**, *31*, 100-104.

42) Tapiolas, D. M.; Roman, M.; Fenical, W.; Stout, T. J.; Clardy, J. *J. Am. Chem. Soc.* **1991**, *113*, 4682-4683.

43) Zuo, G. Y.; Wang, G. C.; Zhao, Y. B.; Xu, G. L.; Hao, X. Y.; Han, J.; Zhao, Q. *J. Ethnopharmacol.* **2008**, *125*, 287-290.

44) Lin, Z.; Antemano, R. R.; Hughen, R. W.; Tianero, M. D. B.; Peraud, O.; Haygood, M. G.; Concepcion, G. P.; Olivera, B. M.; Light, A.; Schmidt, E. W. *J. Nat. Prod.* **2010**, *73*, 1922–1926.

45) Jung Yeop Lee, J. Y.; Moon, S. S.; Byung Kook Hwang, B. K. *Appl. Environ. Microbiol*. **2003**, *69*, 2023–2031.

3-5 Spectral Data

Table of Contents

Figure S38. ^{1}H NMR spectrum of authentic (*S*)-**11**-(*R*)-2A1P (500 MHz, $CDCl_3$)
Figure S39. ^{1}H NMR spectrum of authentic (*S*)-**11**-(*S*)-2A1P (500 MHz, $CDCl_3$)

Figure S1. UV spectrum of nocarimidazole C (**4**)

(MeOH)

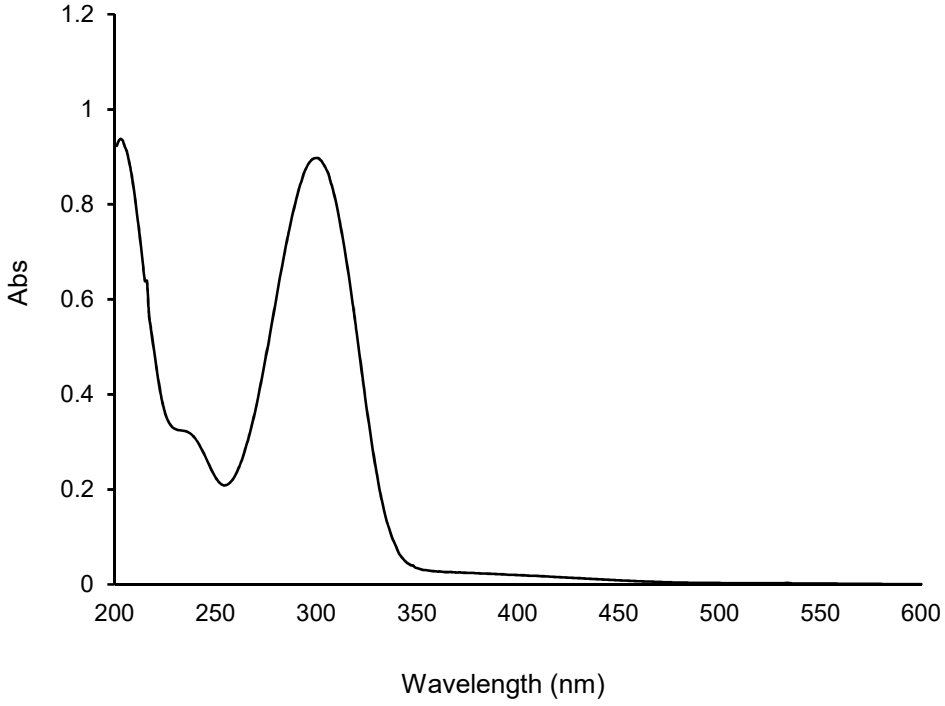

Figure S2. IR spectrum of **4**

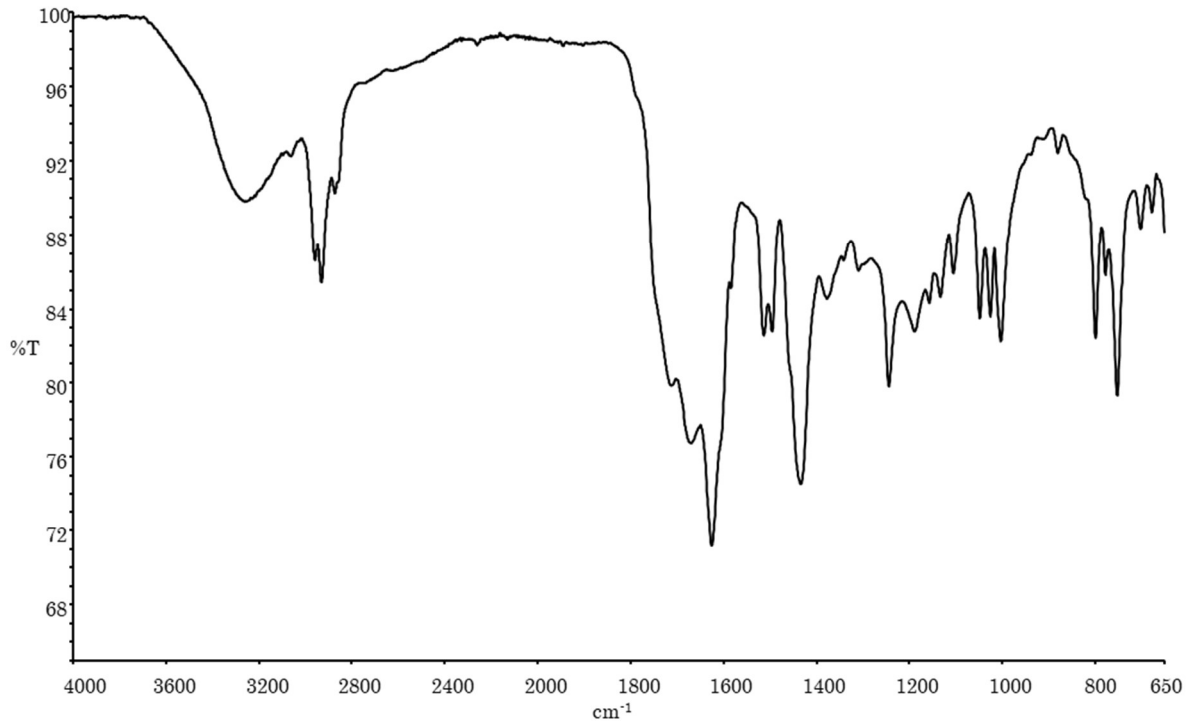

Figure S3. ^{1}H NMR spectrum of **4** (500 MHz, DMSO-d_6 with TFA)

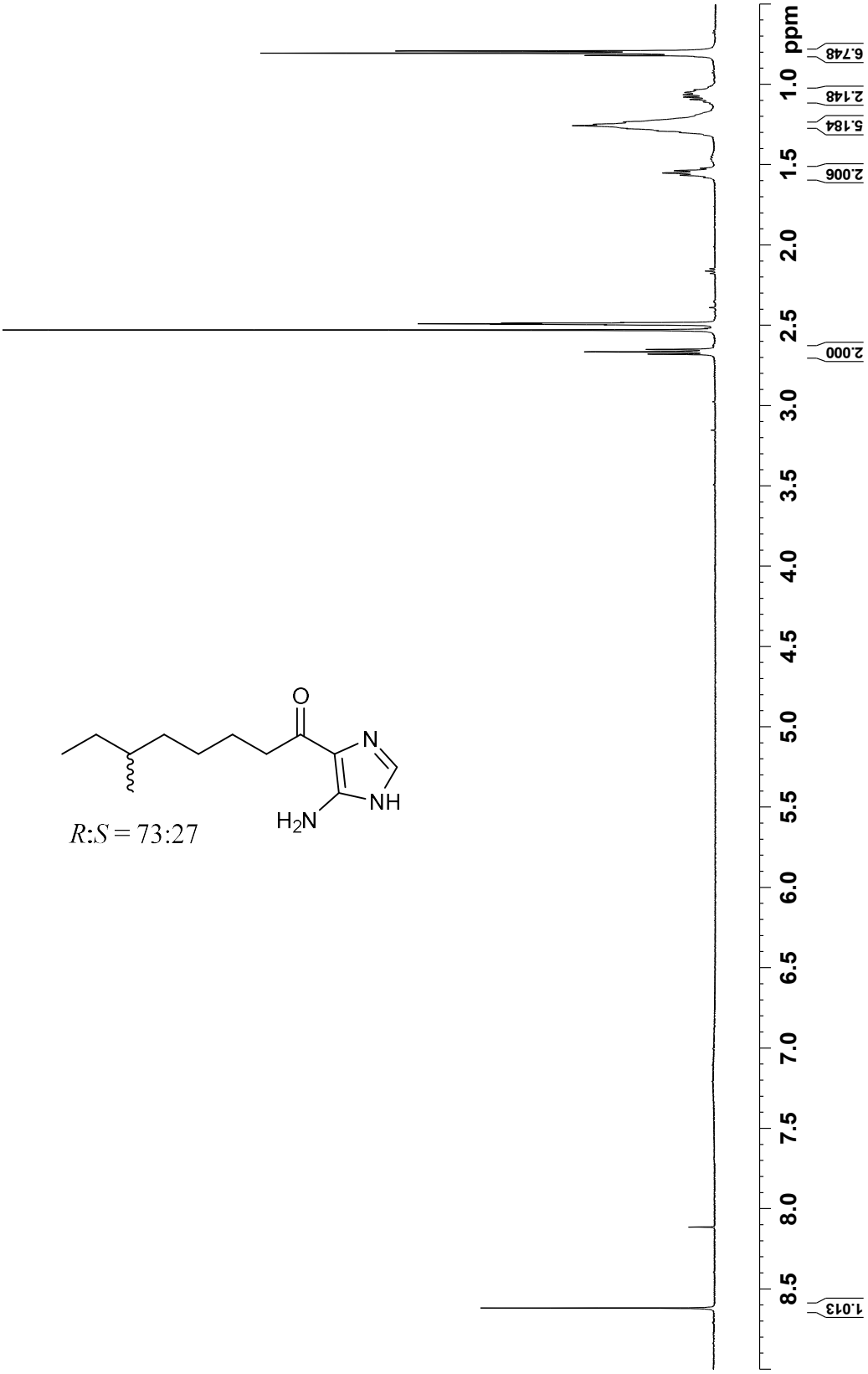

Figure S4. ^{13}C NMR spectrum of **4** (125 MHz, DMSO-d_6 with TFA)

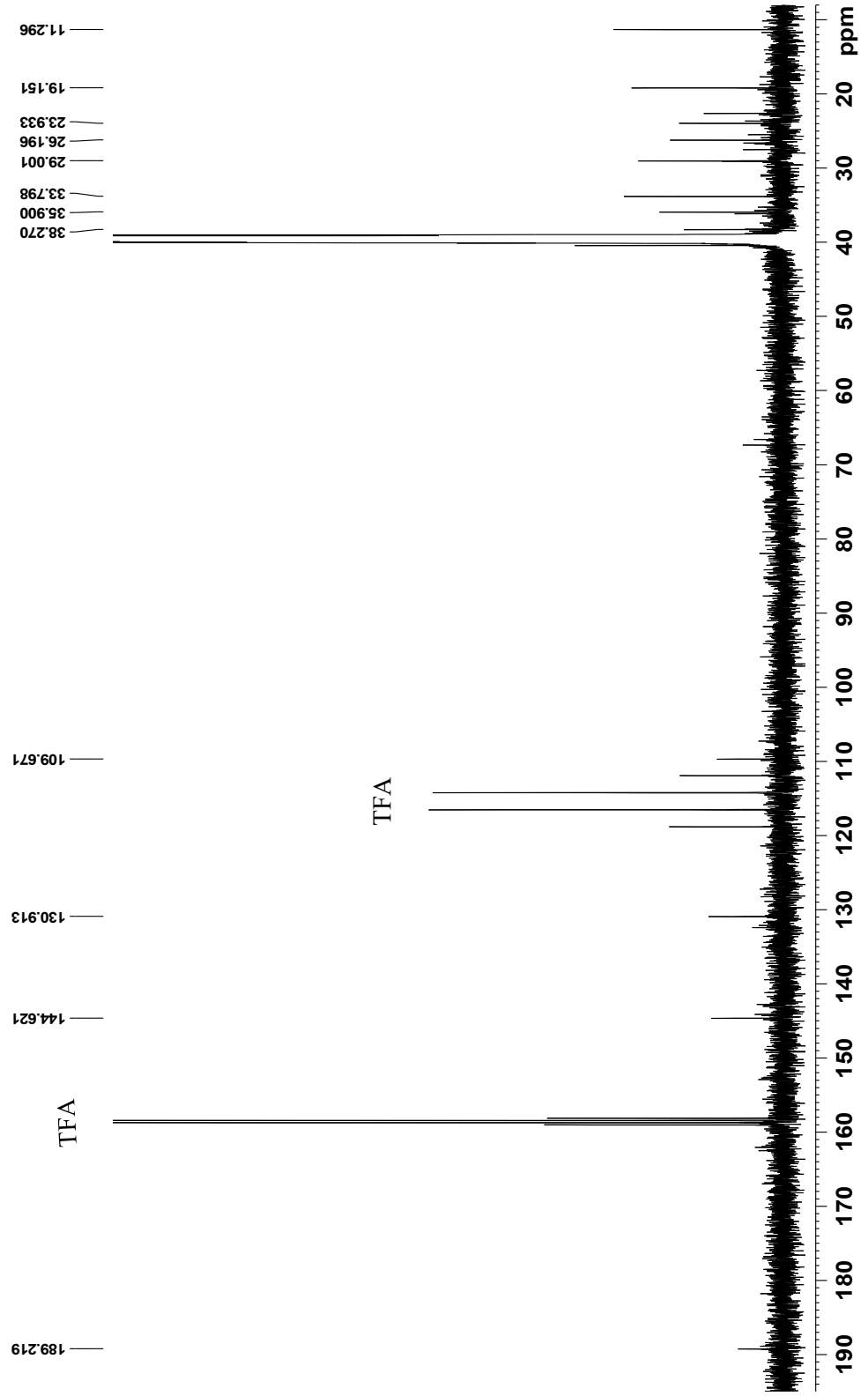

Figure S5. COSY spectrum of **4** (500 MHz, DMSO-d_6 with TFA)

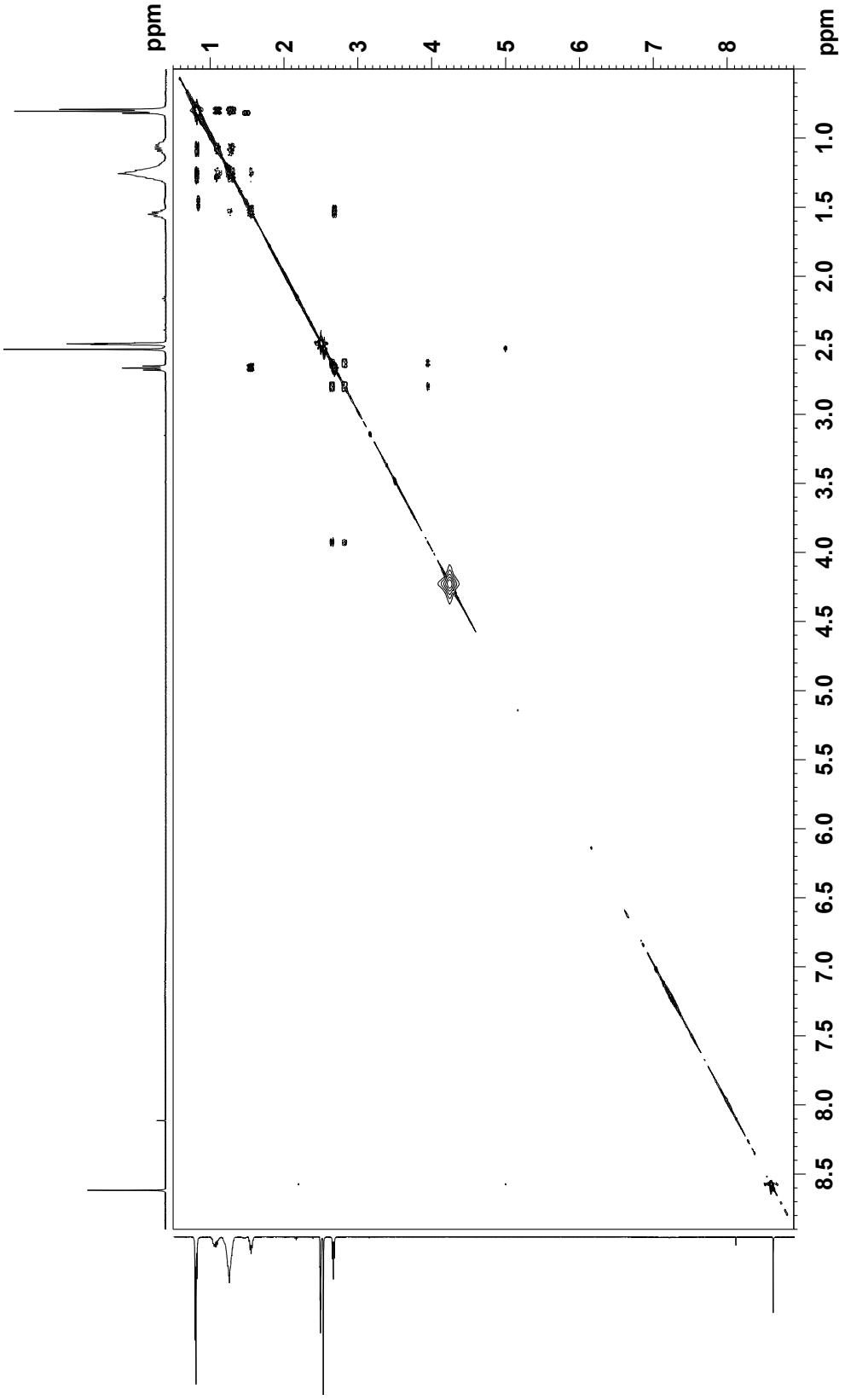

Figure S6. HSQC spectrum of **4** (500 MHz, DMSO-d_6 with TFA)

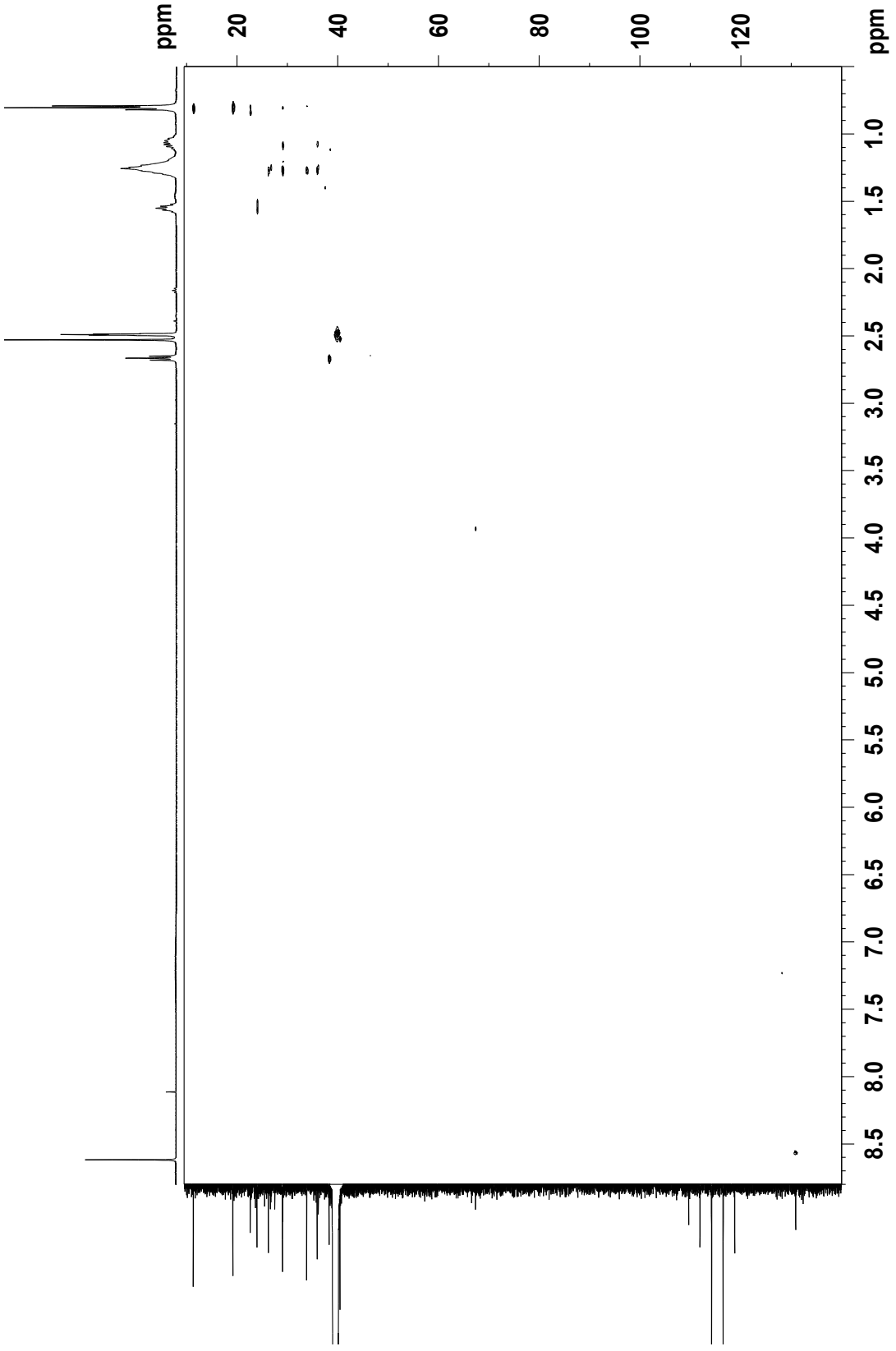

Figure S7. Coupled HSQC spectrum of **4** (500 MHz, DMSO-d_6 with TFA)

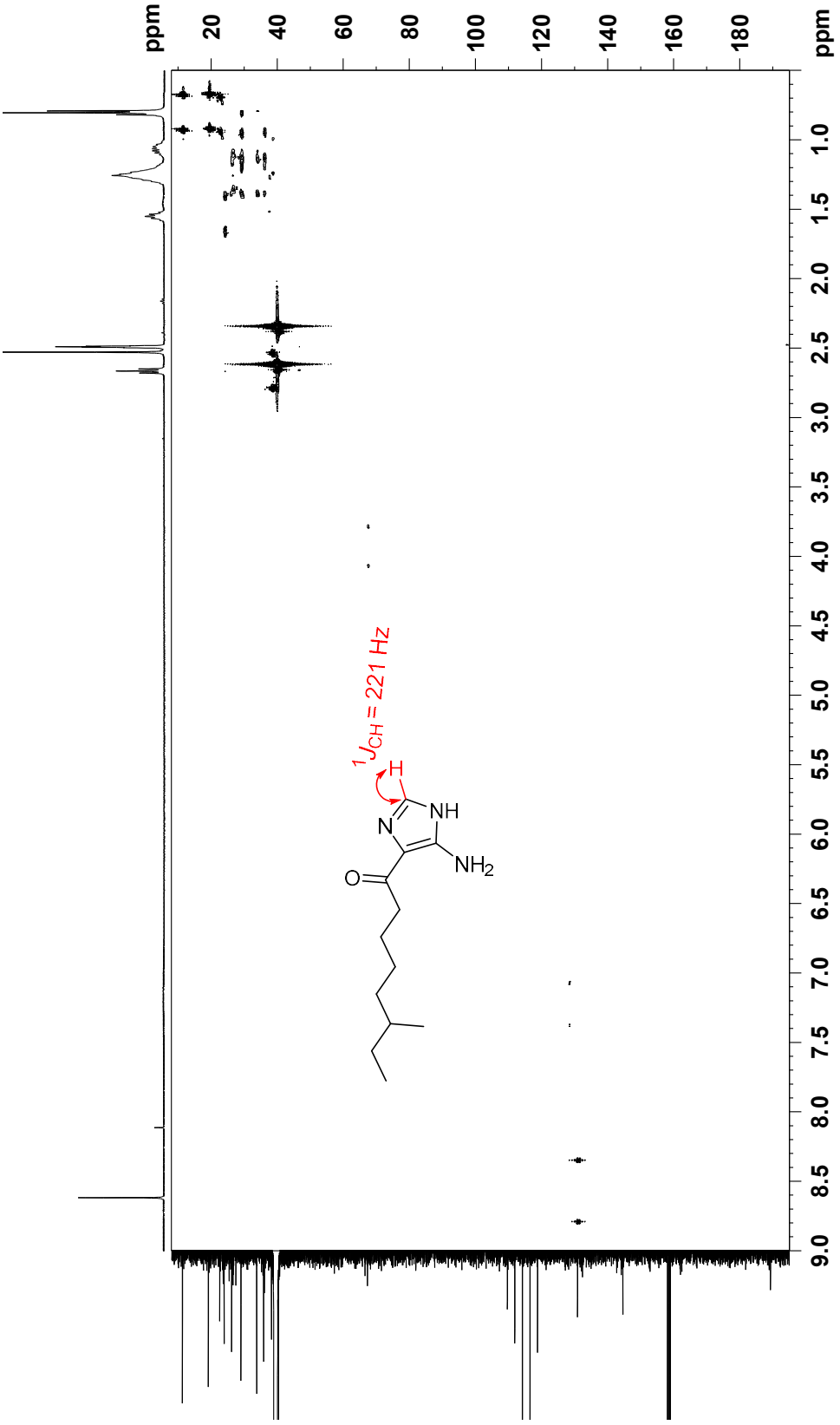

Figure S8. HMBC spectrum of **4** (500 MHz, DMSO-d_6 with TFA)

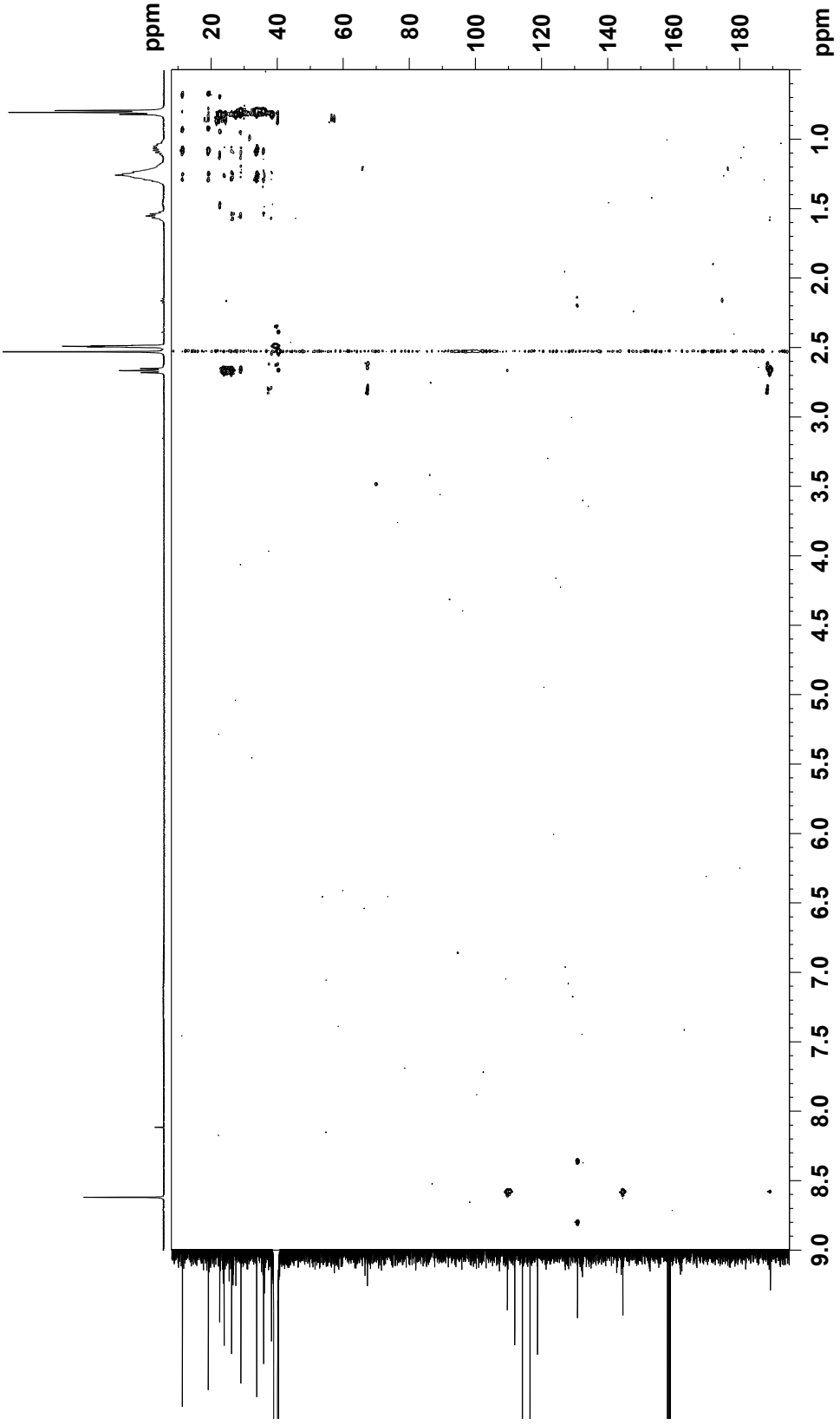

Figure S9. UV spectrum of nocarimidazole D (**5**)

(MeOH)

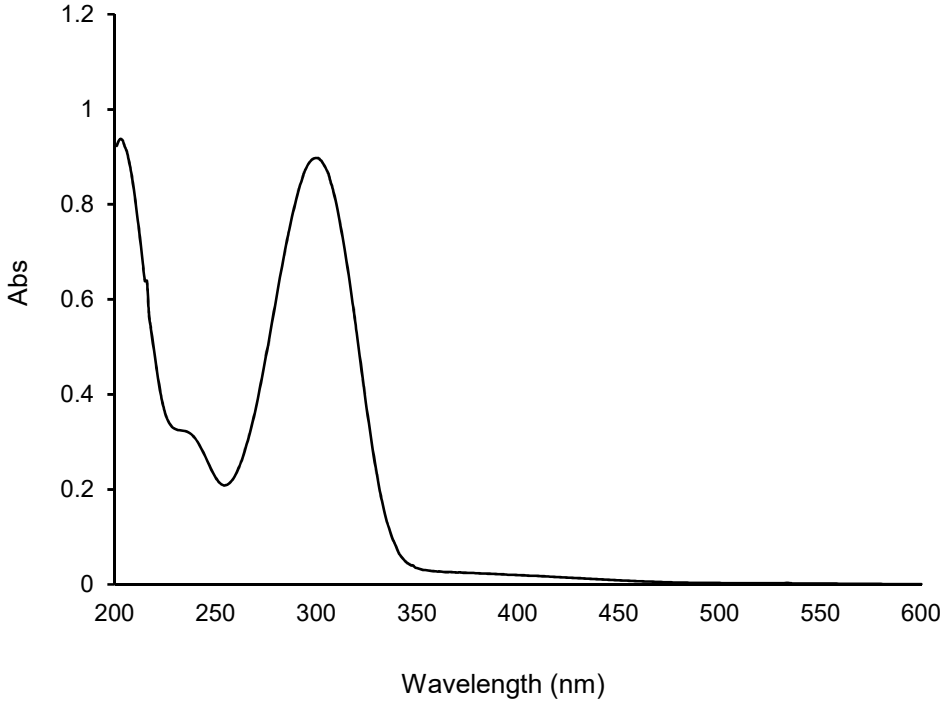

Figure S10. IR spectrum of **5**

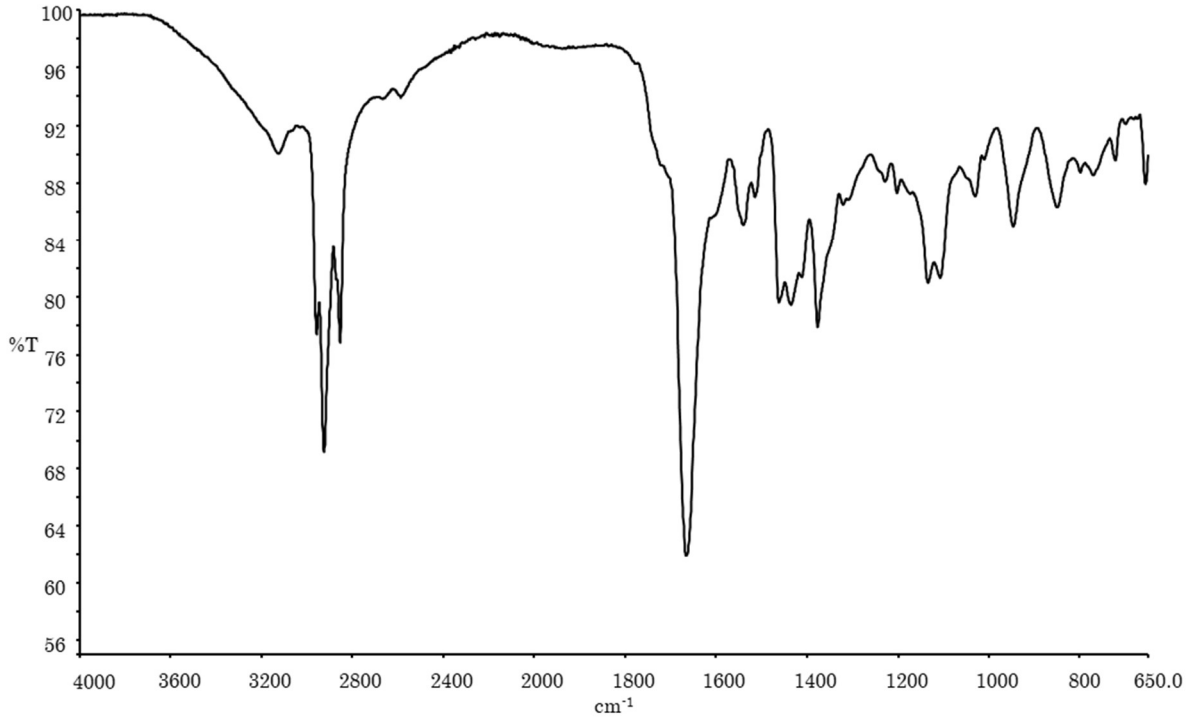

Figure S11. ^{1}H NMR spectrum of **5** (500 MHz, DMSO-d_6 with TFA)

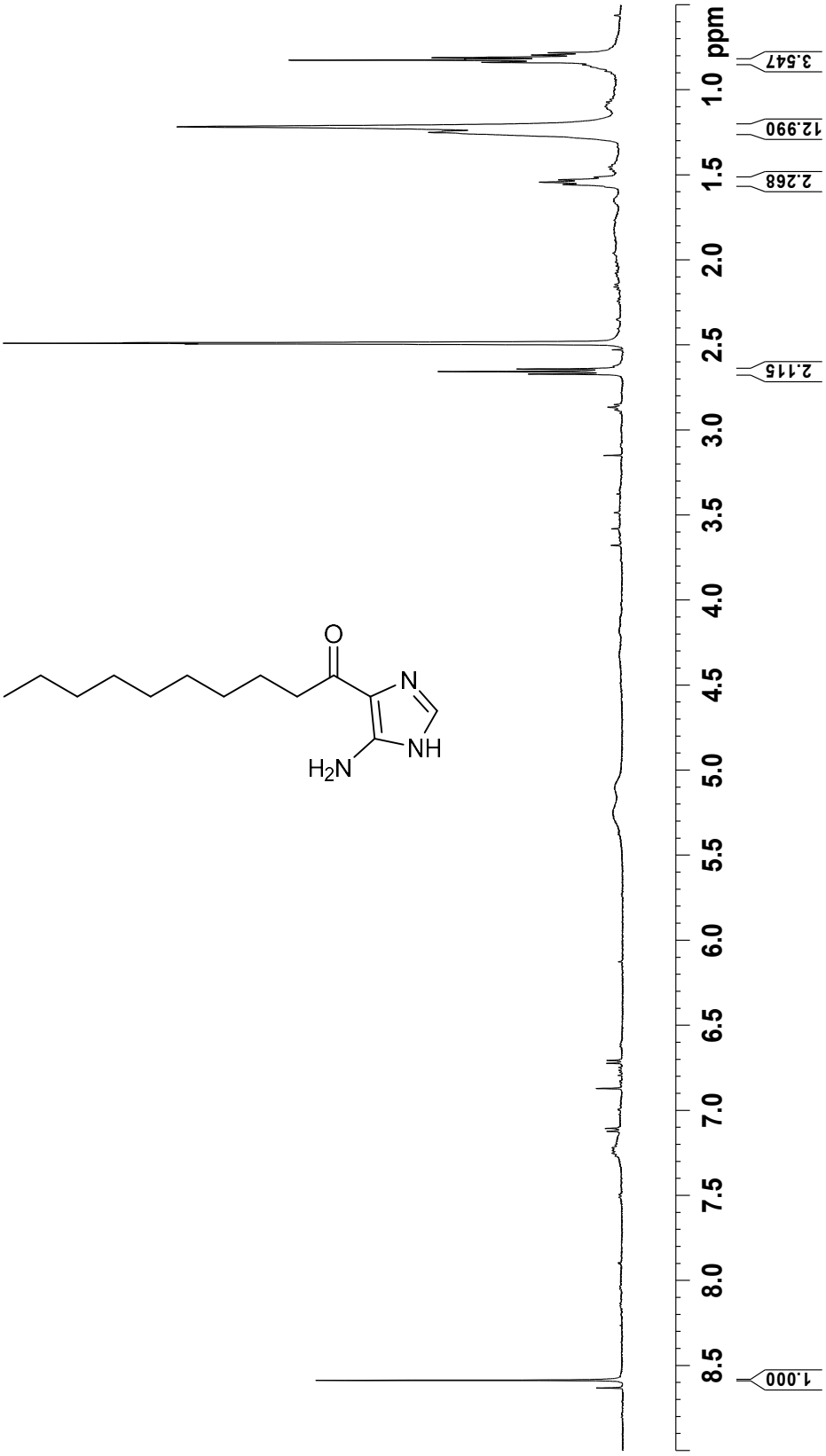

Figure S12. ^{13}C NMR spectrum of **5** (125 MHz, DMSO-d_6 with TFA)

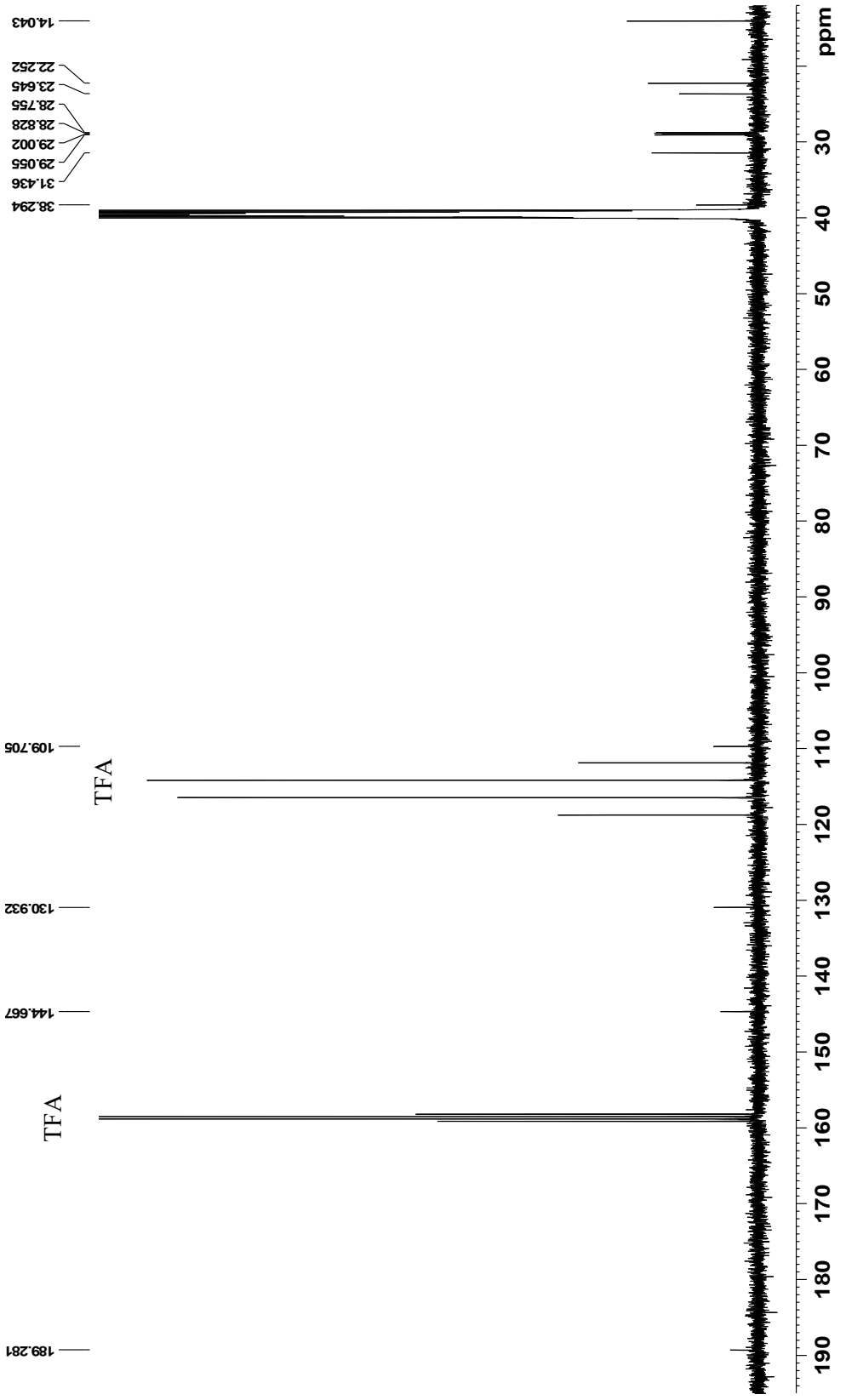

Figure S13. COSY spectrum of **5** (500 MHz, DMSO-d_6 with TFA)

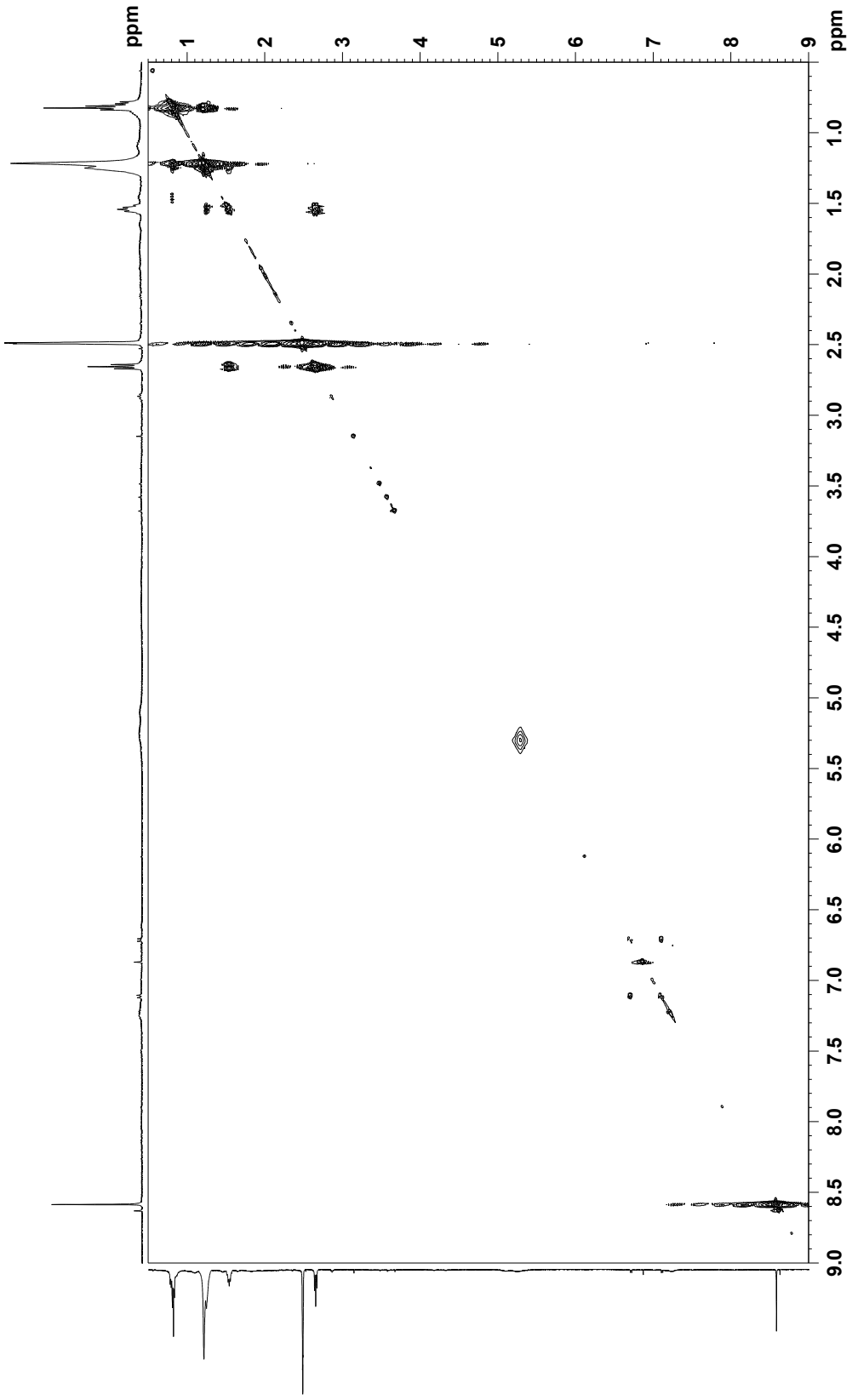

Figure S14. HSQC spectrum of **5** (500 MHz, DMSO-d_6 with TFA)

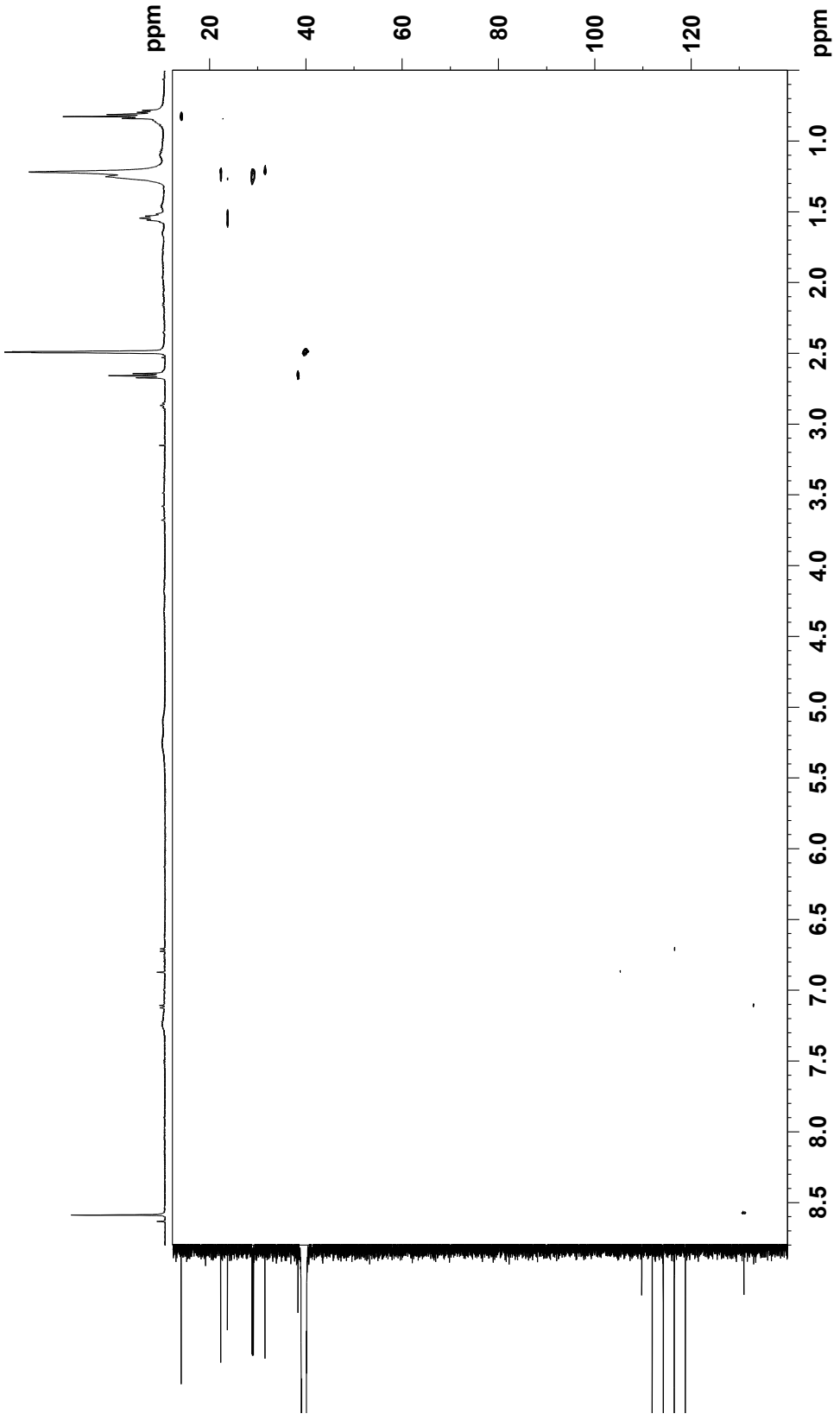

Figure S15. HMBC spectrum of **5** (500 MHz, DMSO-d_6 with TFA)

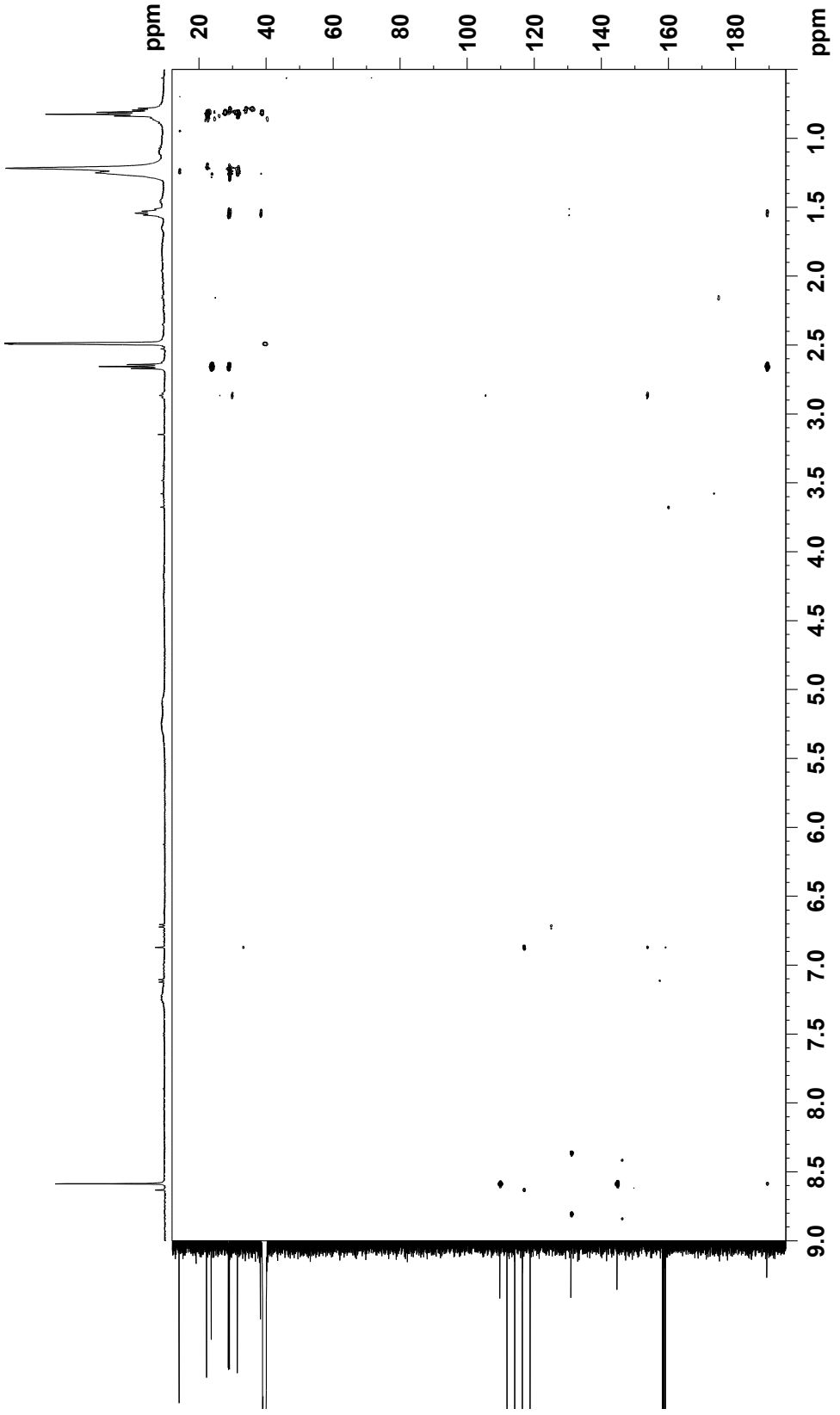

Figure S16. ^{1}H NMR spectrum of **6** (500 MHz, DMSO-d_6 with TFA)

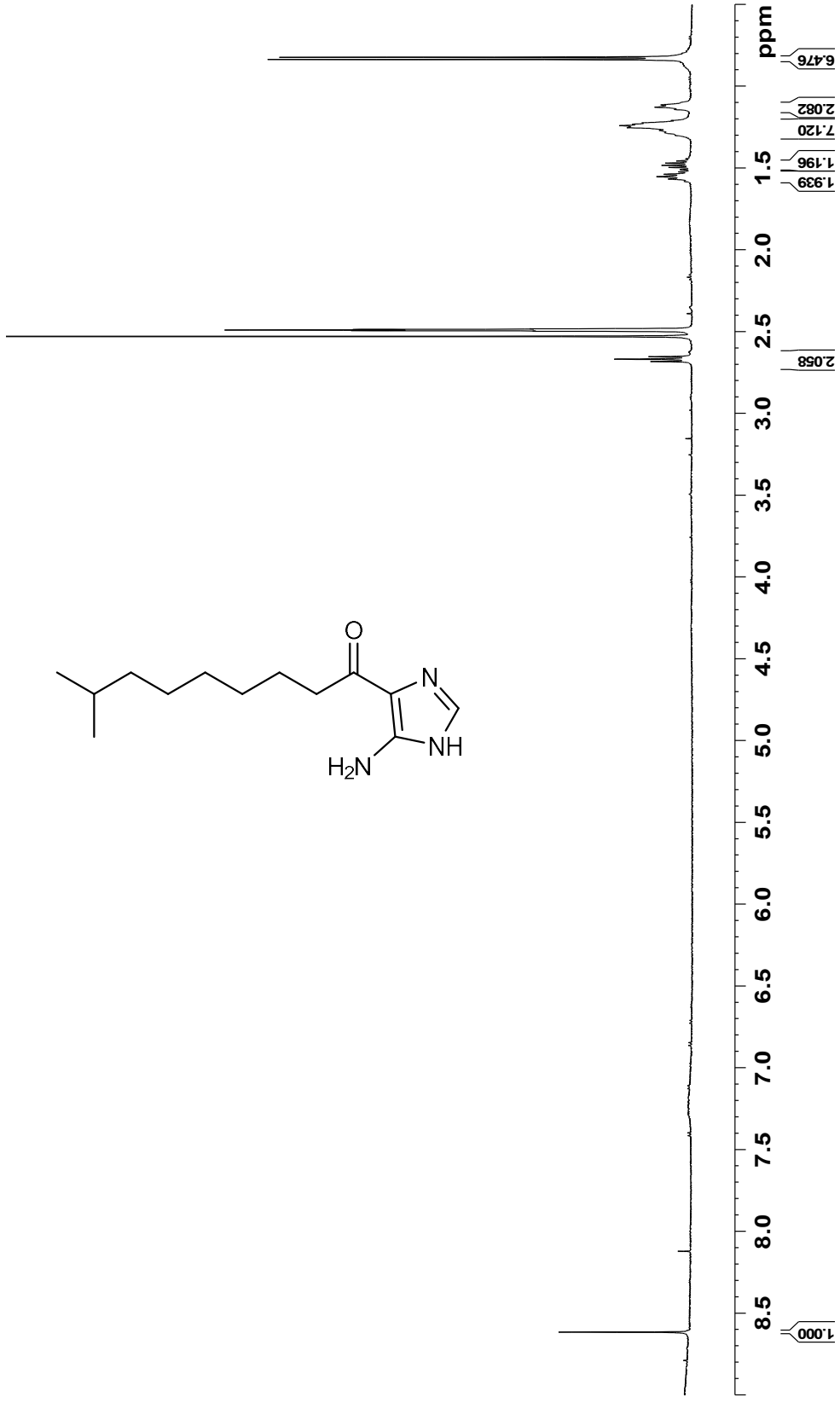

Figure S17. ^{13}C NMR spectrum of **6** (125 MHz, DMSO-d_6 with TFA)

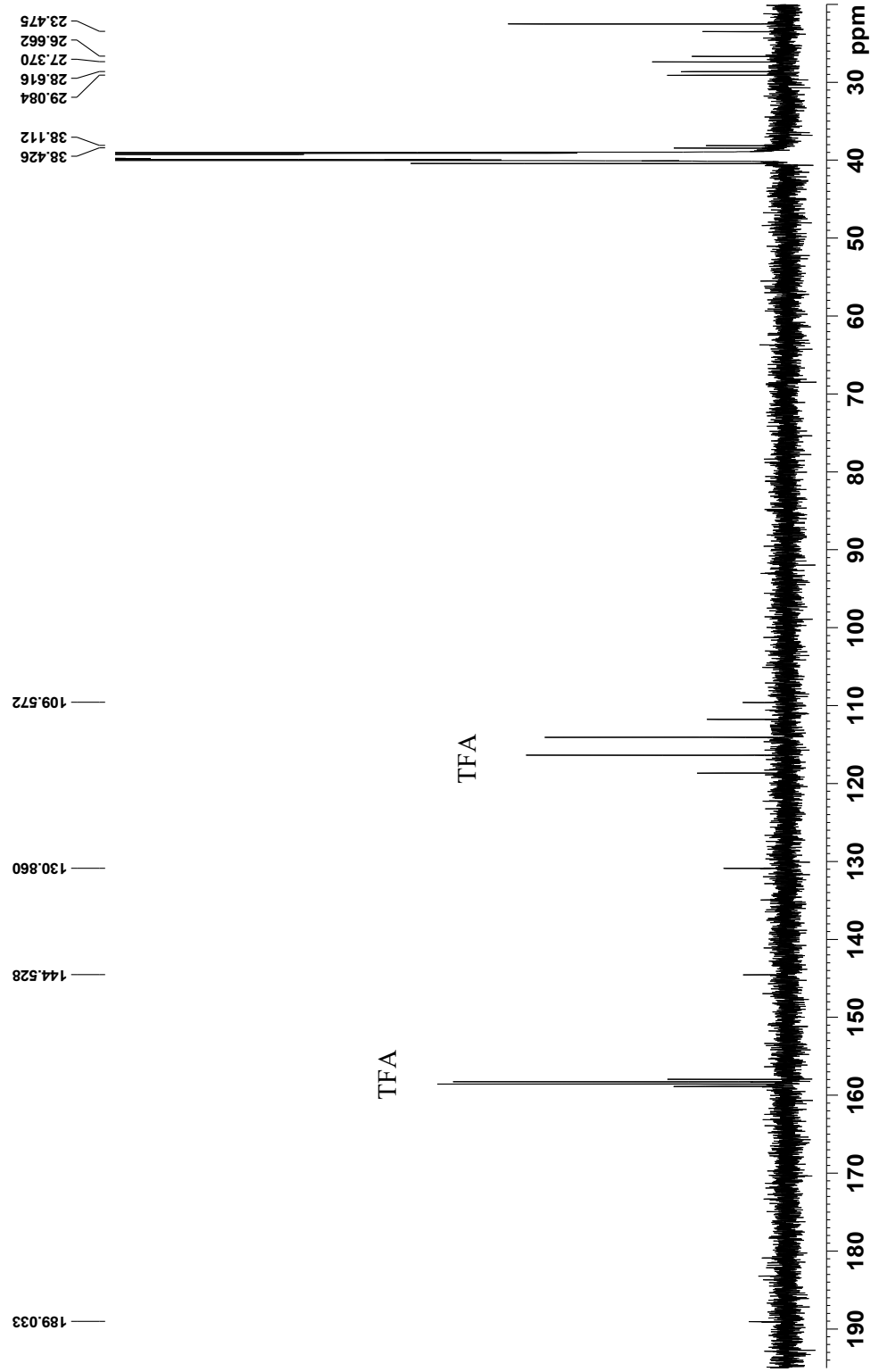

Figure S18. ^{1}H NMR spectrum of **7** (500 MHz, DMSO-d_6 with TFA)

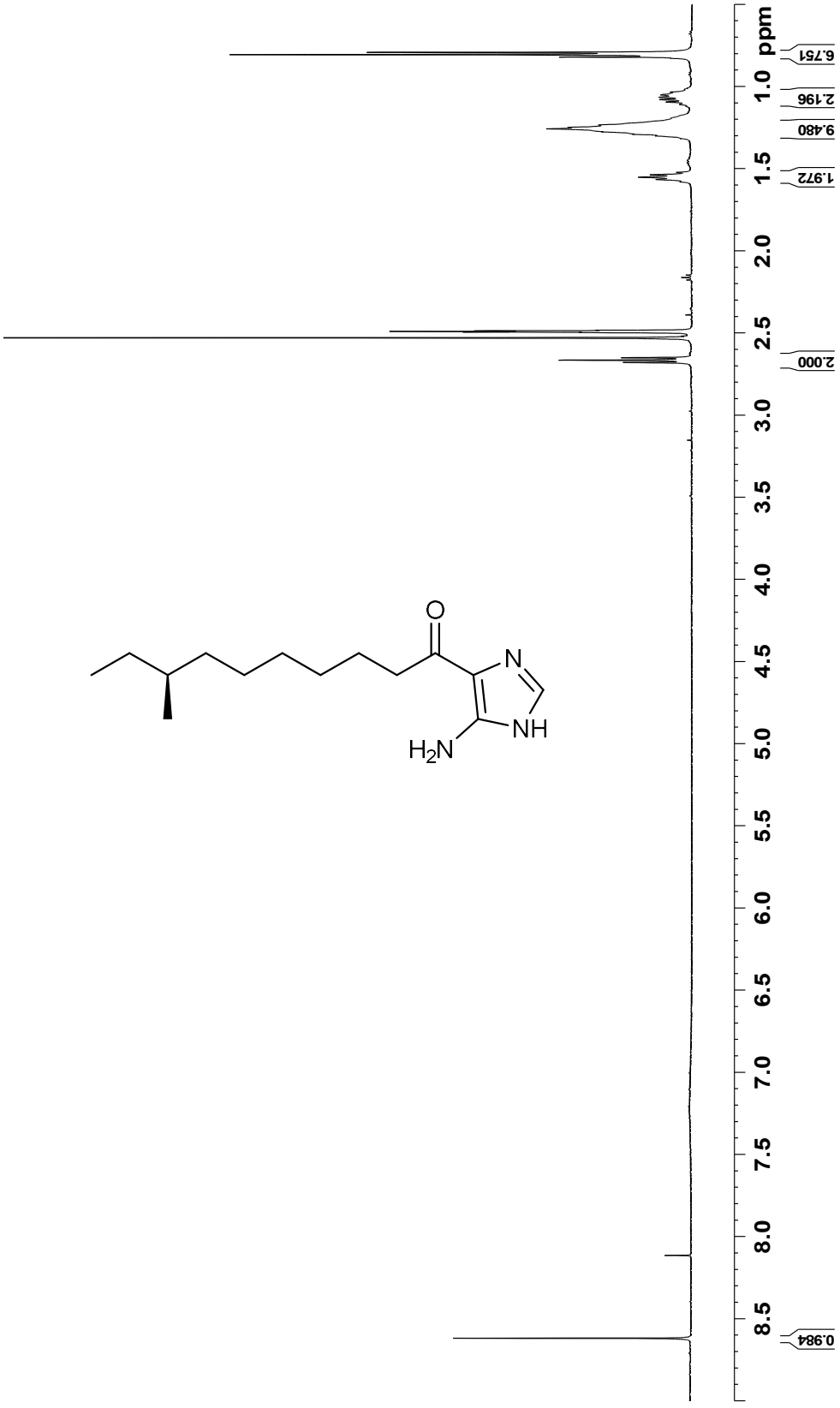

Figure S19. ^{13}C NMR spectrum of **7** (125 MHz, DMSO-d_6 with TFA)

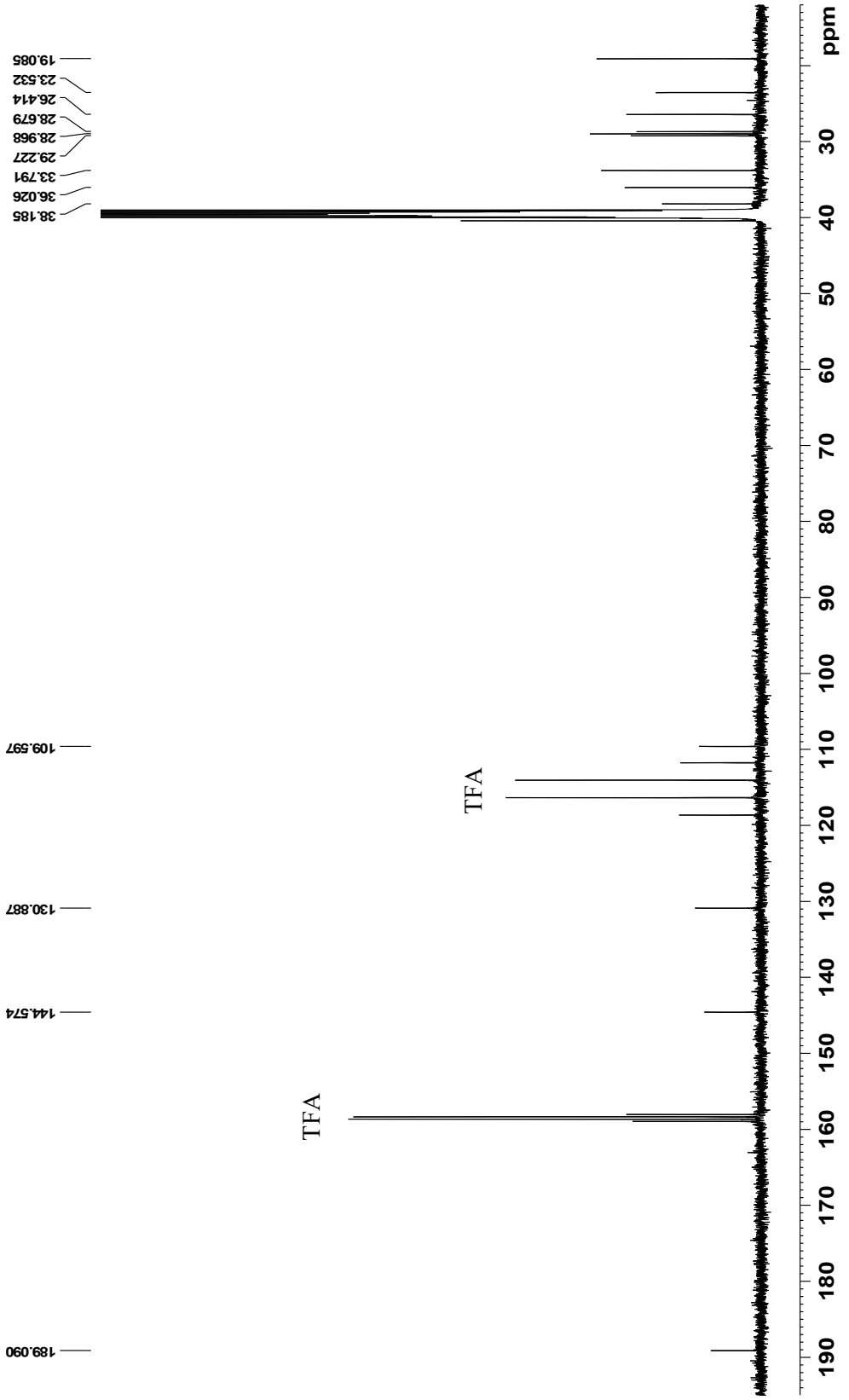

Figure S20. ^{1}H NMR spectrum of **1** (500 MHz, DMSO-d_6 with TFA)

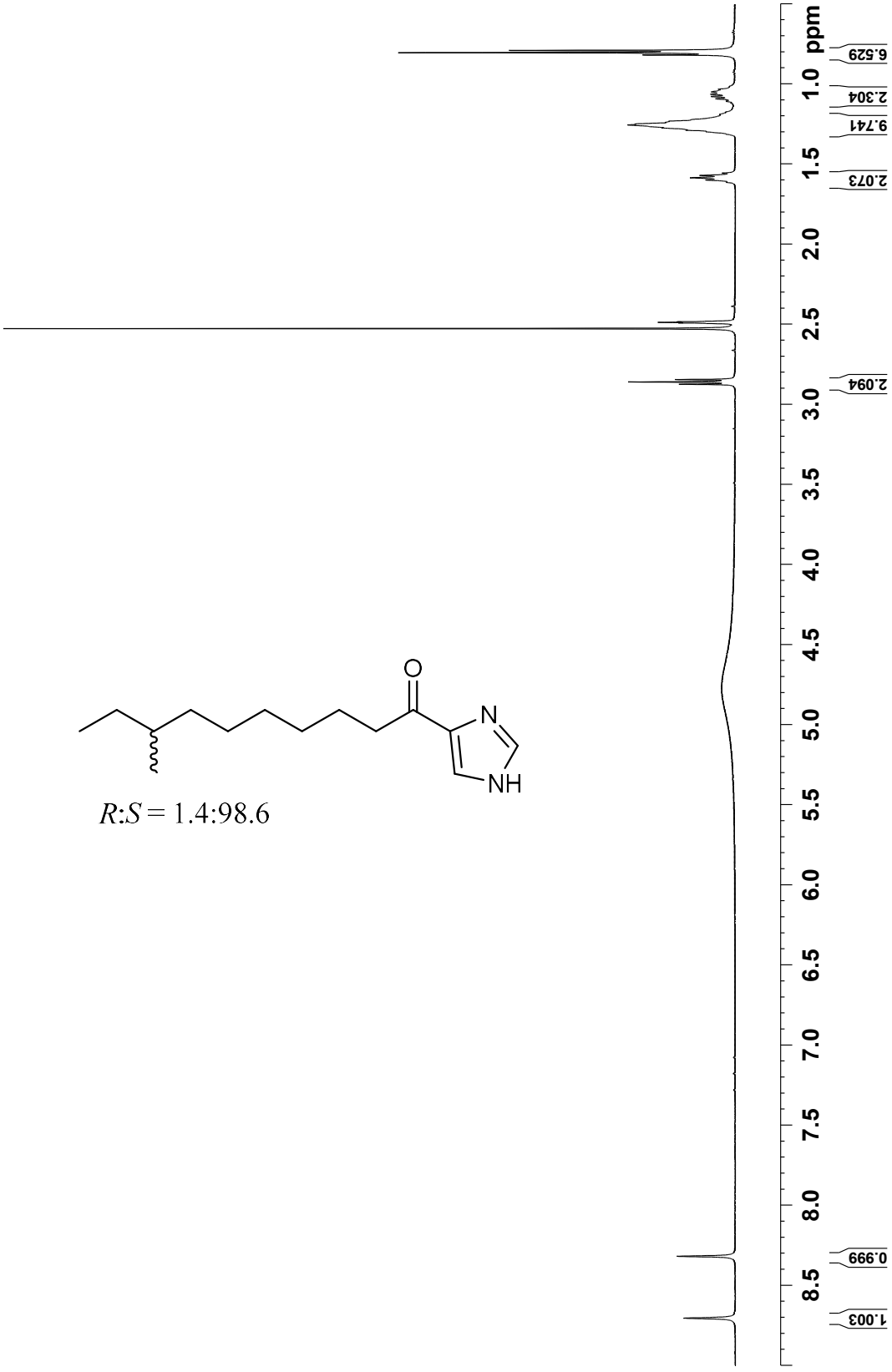

Figure S21. ^{13}C NMR spectrum of **1** (125 MHz, DMSO-d_6 with TFA)

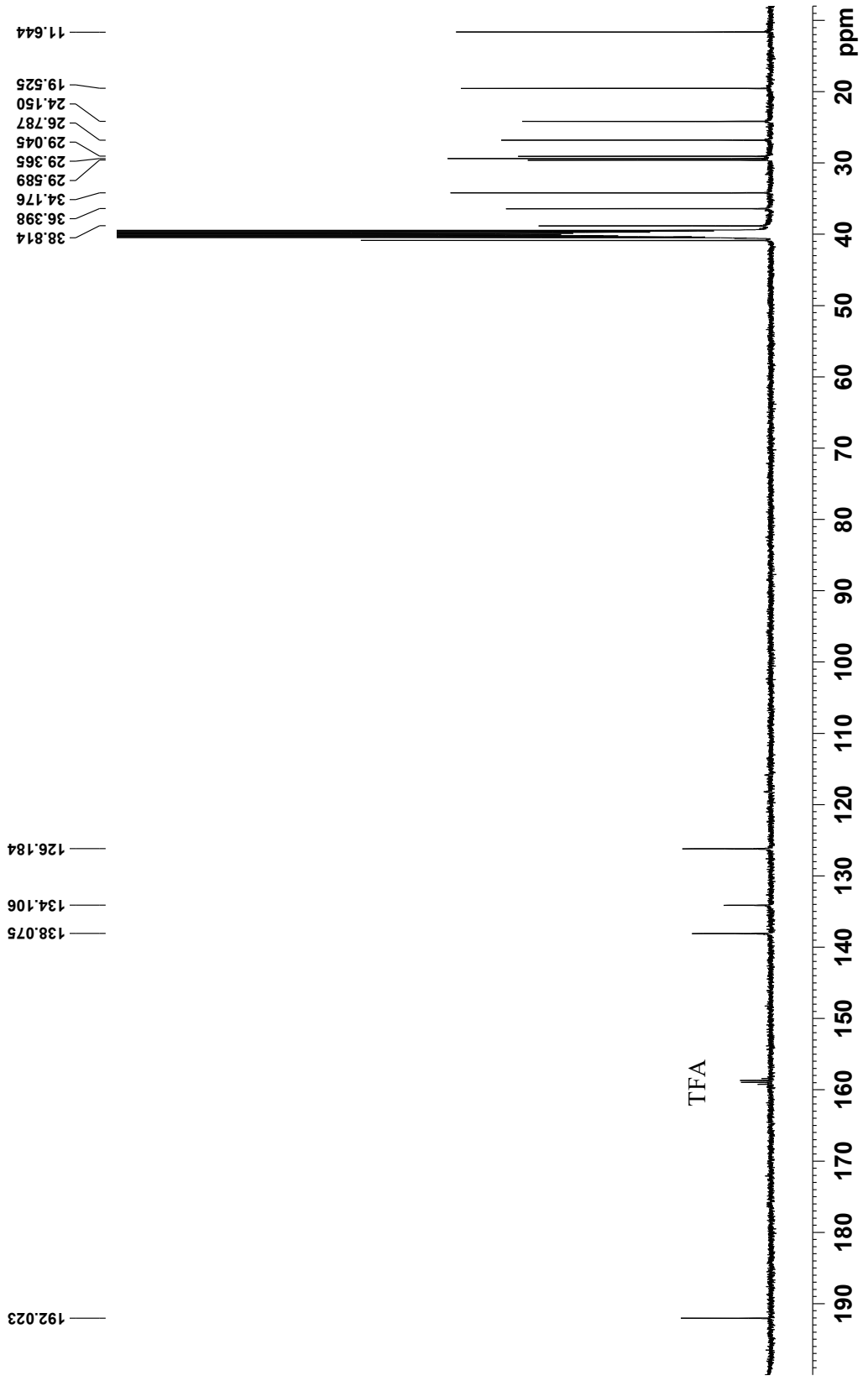

Figure S22. Coupled HSQC spectrum of **1** (500 MHz, DMSO-d_6 with TFA)

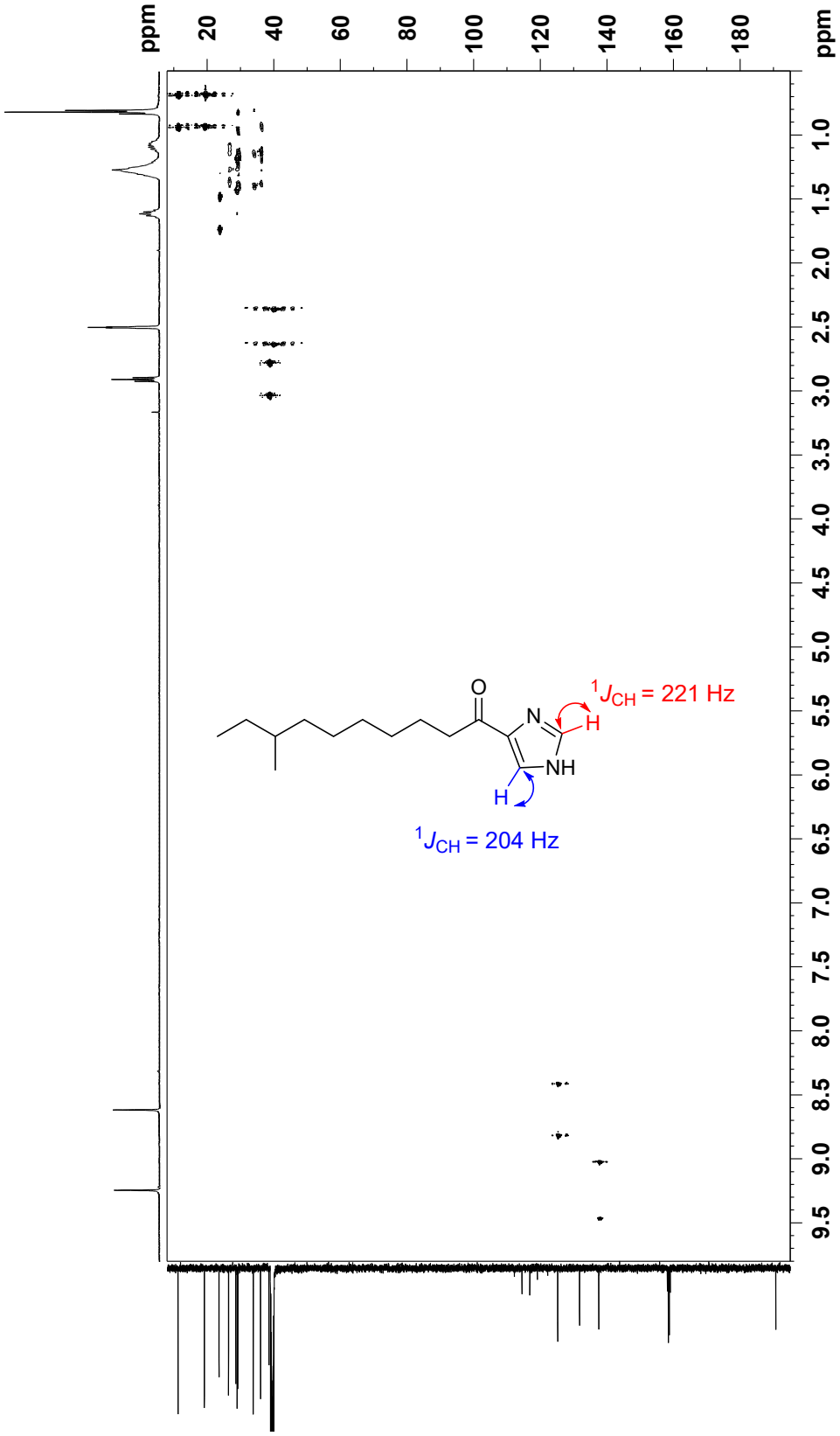

Figure S23. ^{1}H NMR spectrum of **8** (500 MHz, DMSO-d_6 with TFA)

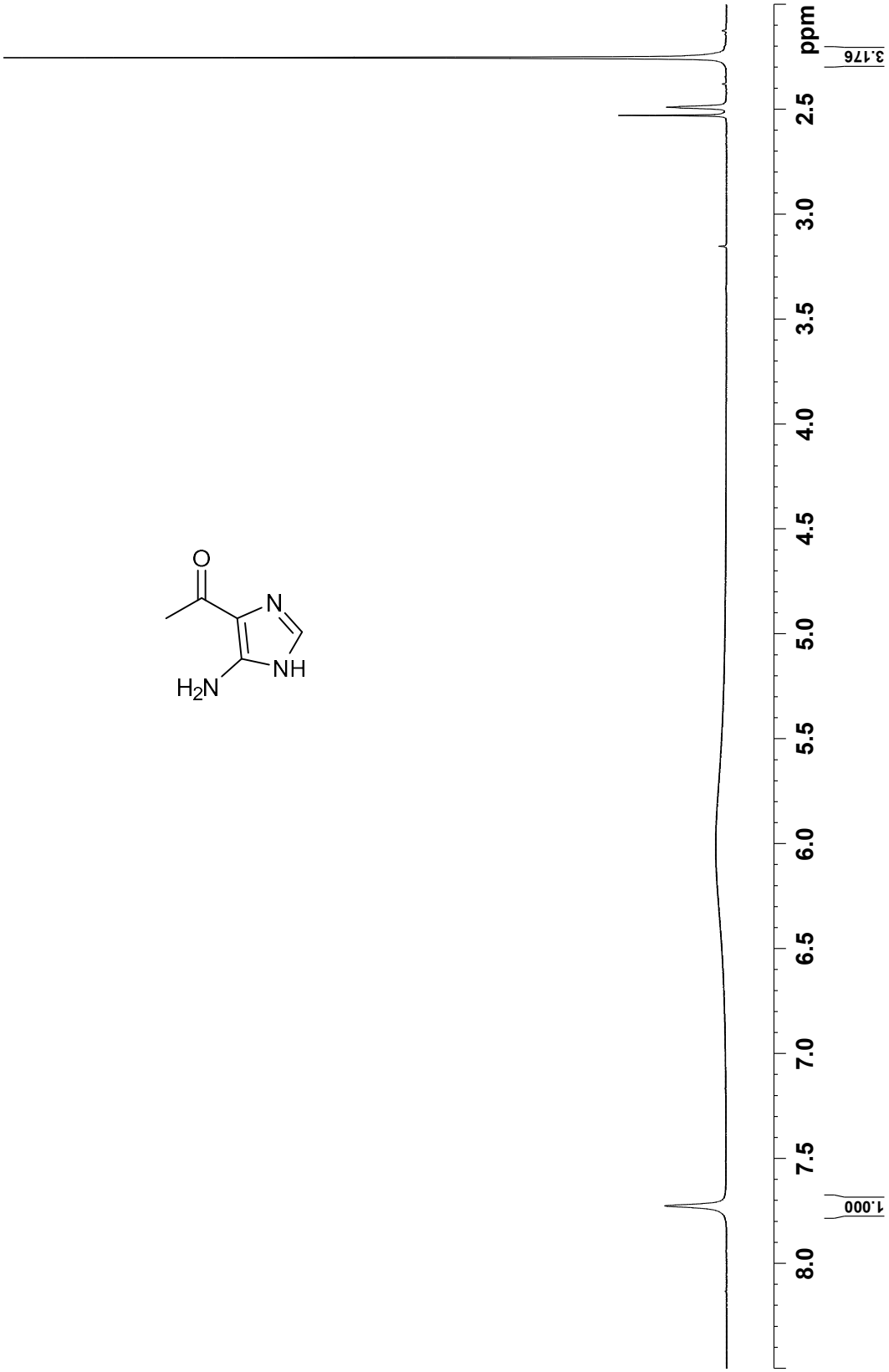

Figure S24. ^{13}C NMR spectrum of **8** (125 MHz, DMSO-d_6 with TFA)

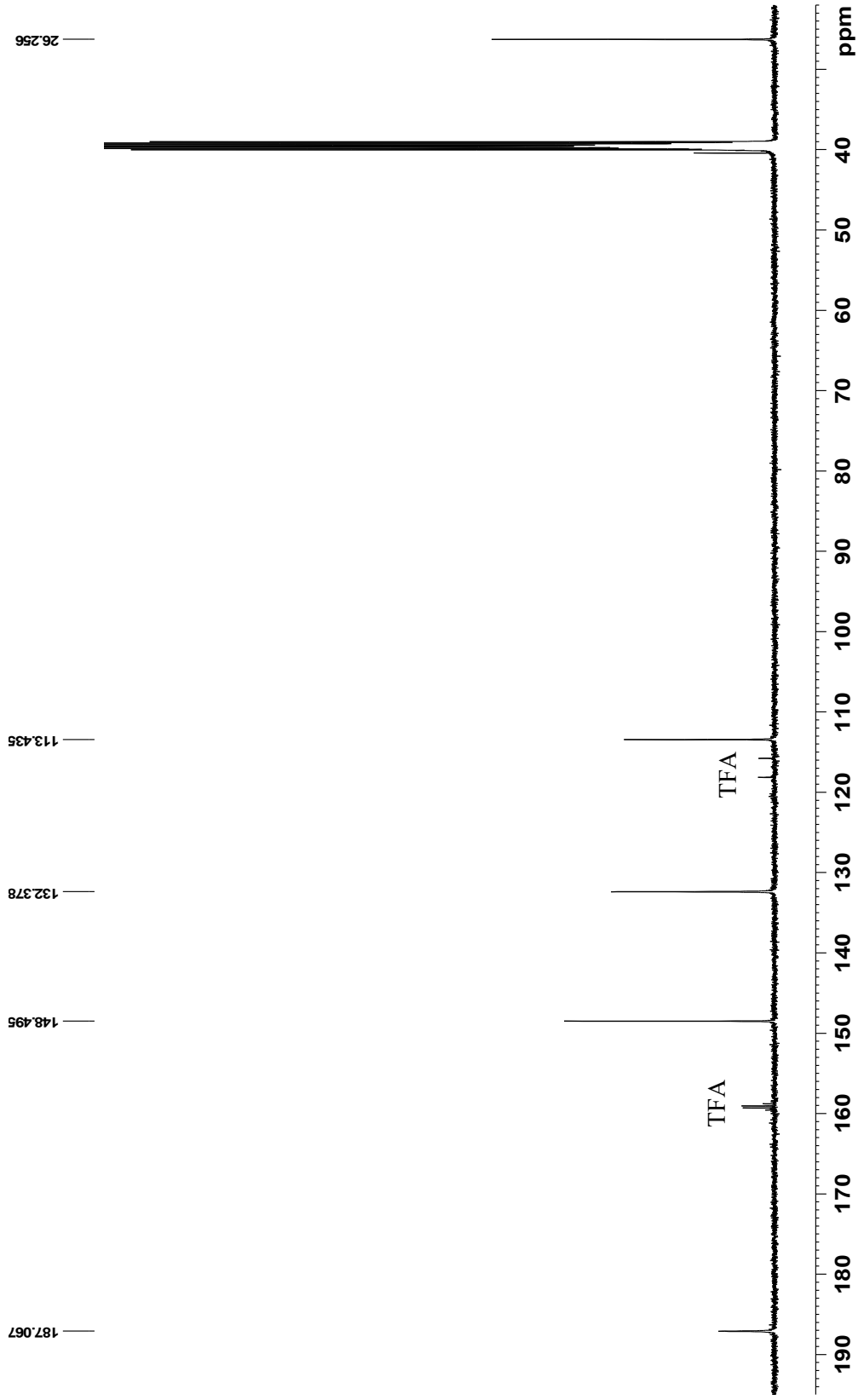

Figure S25. HSQC spectrum of **8** (500 MHz, DMSO-d_6 with TFA)

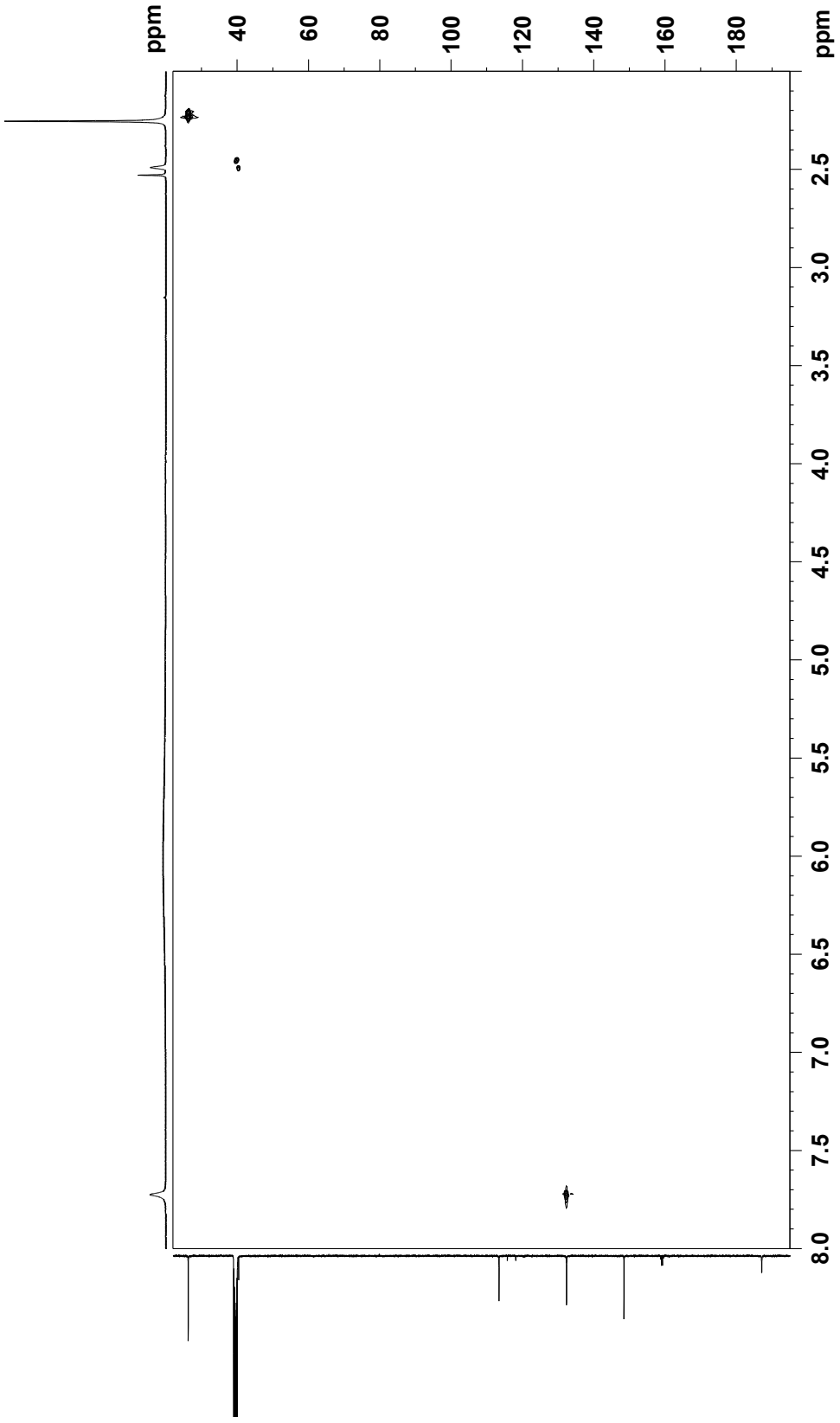

Figure S26. Coupled HSQC spectrum of **8** (500 MHz, DMSO-d_6 with TFA)

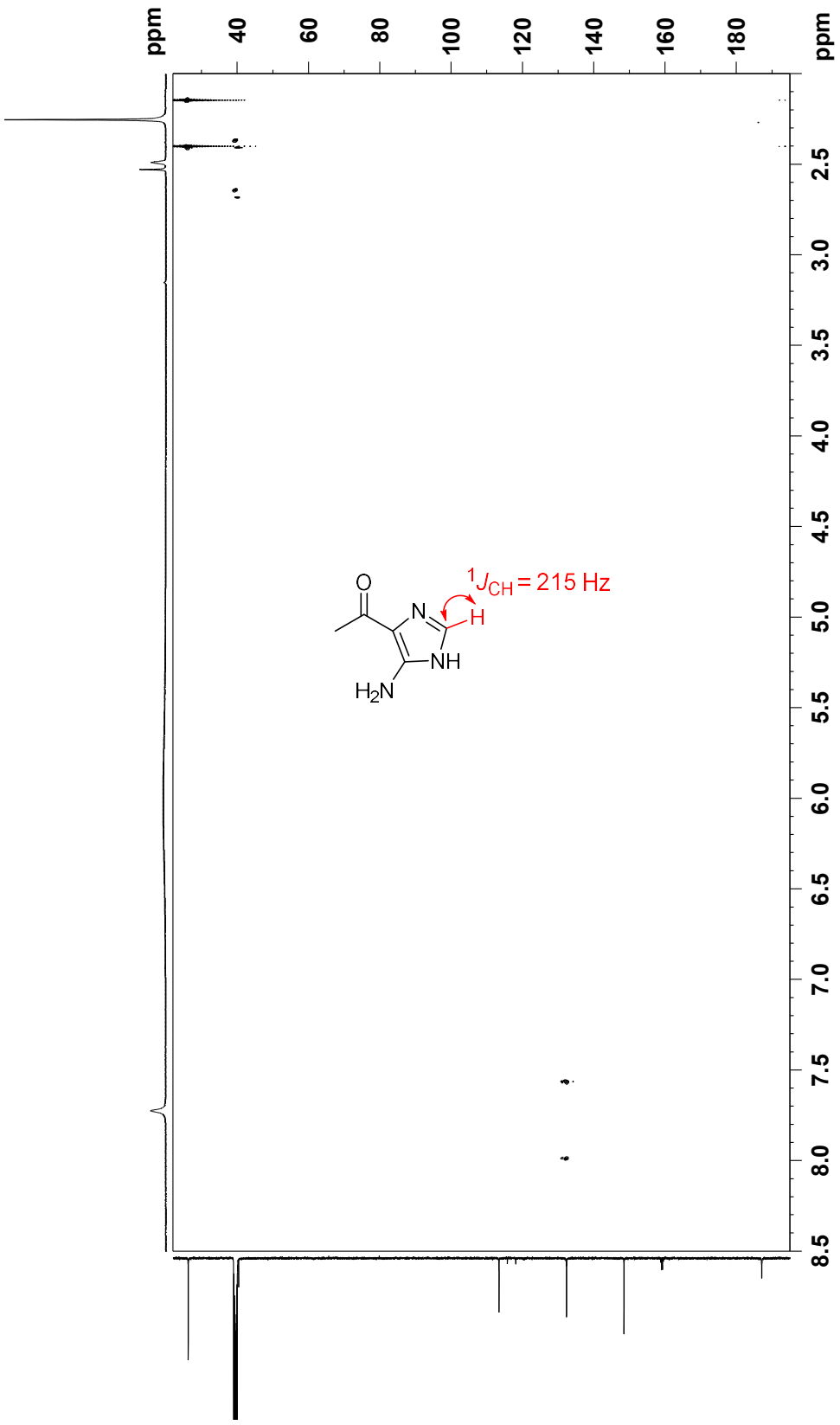

Figure S27. HMBC spectrum of **8** (500 MHz, DMSO-d_6 with TFA)

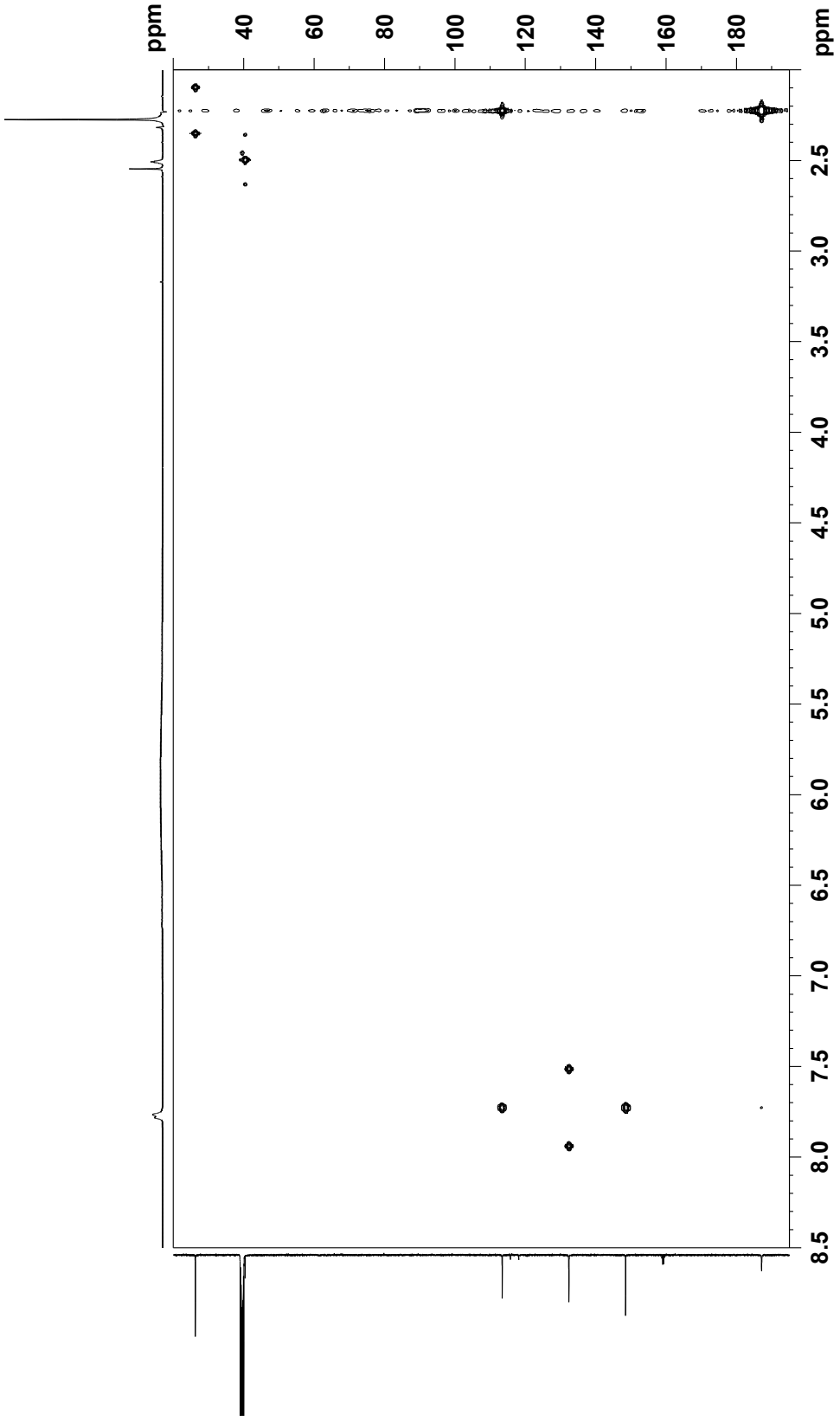

Figure S28. ^{1}H NMR spectrum of **9** (500 MHz, DMSO-d_6 with TFA)

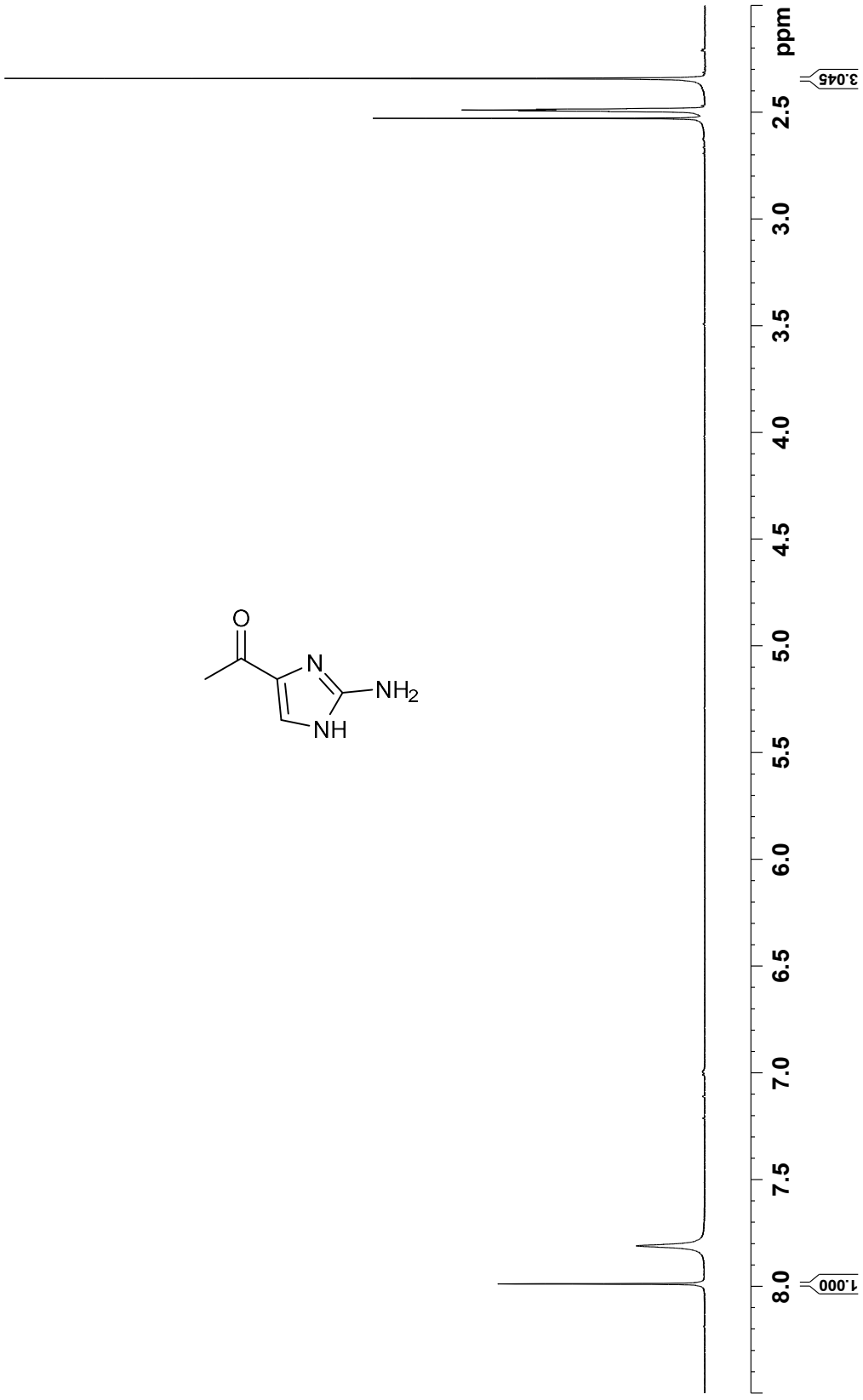

Figure S29. ^{13}C NMR spectrum of **9** (125 MHz, DMSO-d_6 with TFA)

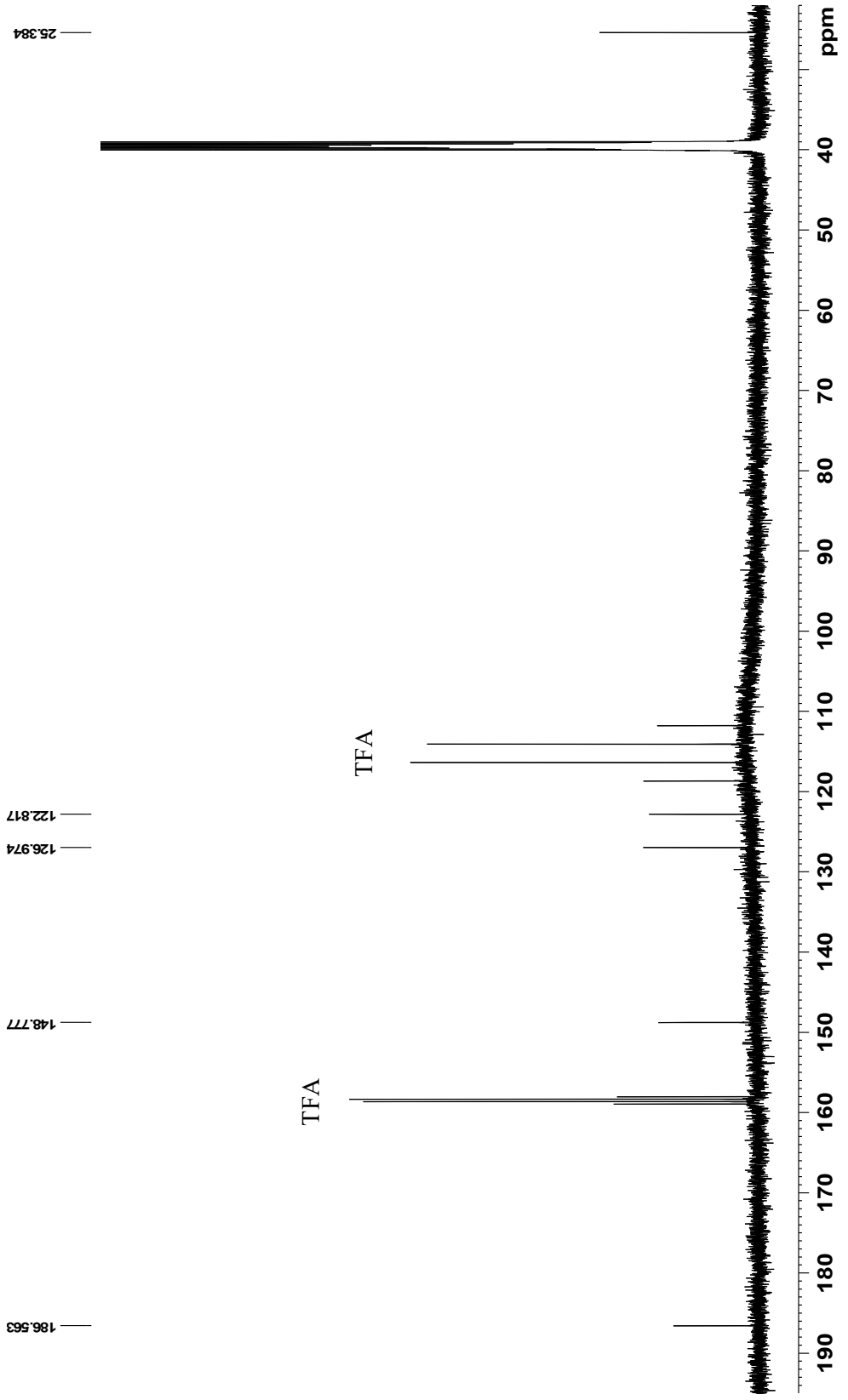

Figure S30. HSQC spectrum of **9** (500 MHz, DMSO-d_6 with TFA)

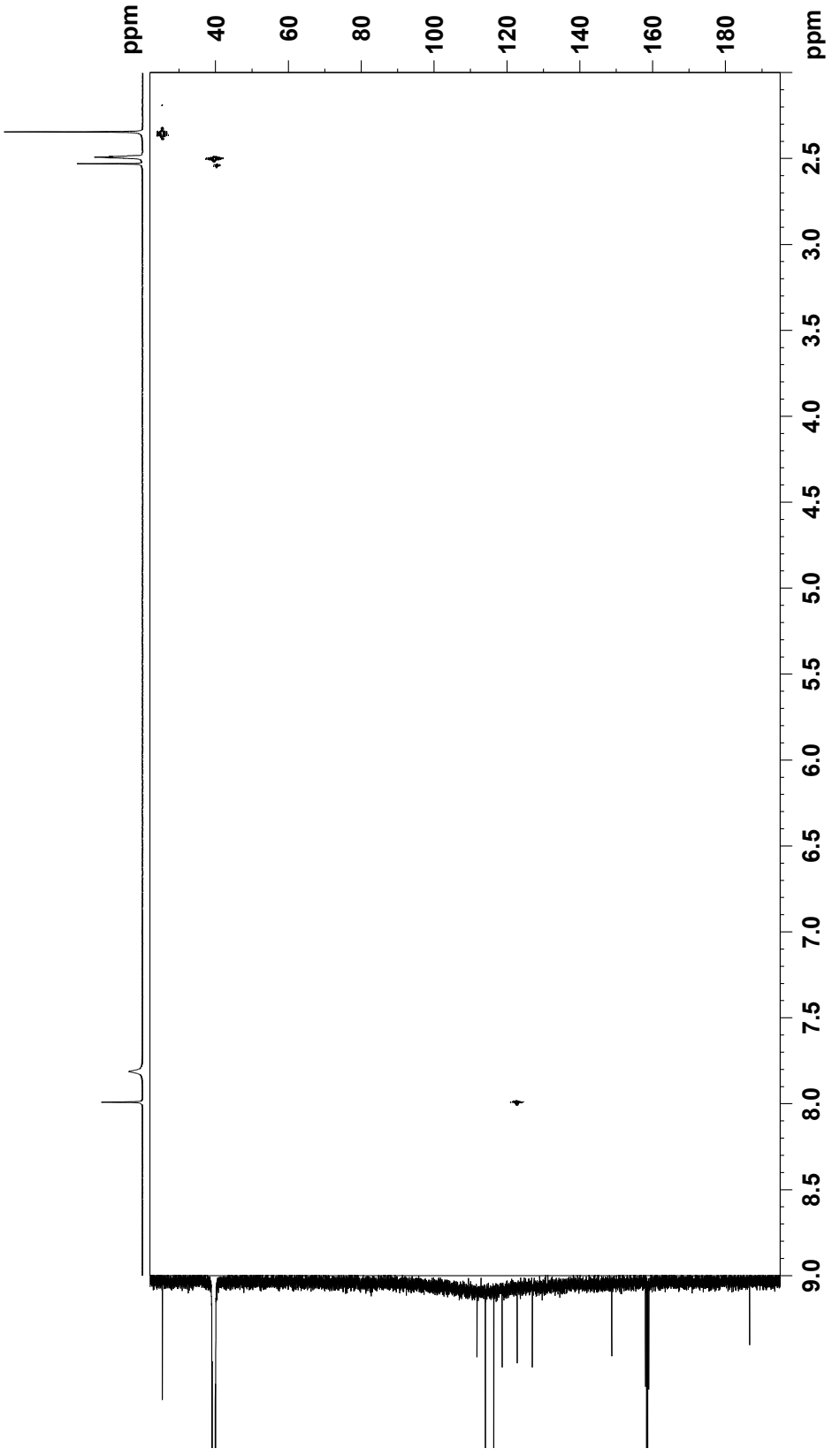

Figure S31. Coupled HSQC spectrum of **9** (500 MHz, DMSO-d_6 with TFA)

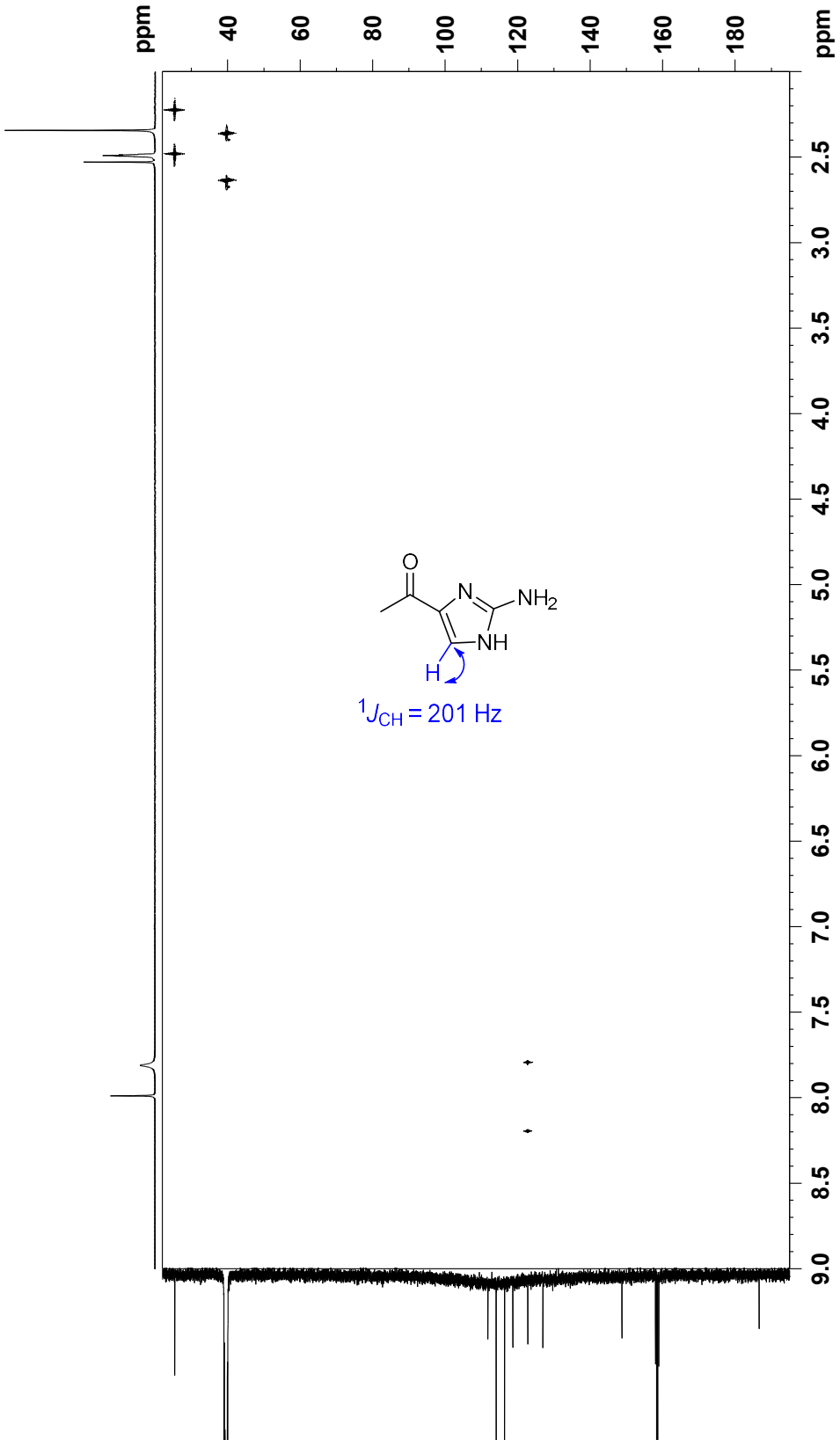

Figure S32. HMBC spectrum of **9** (500 MHz, DMSO-d_6 with TFA)

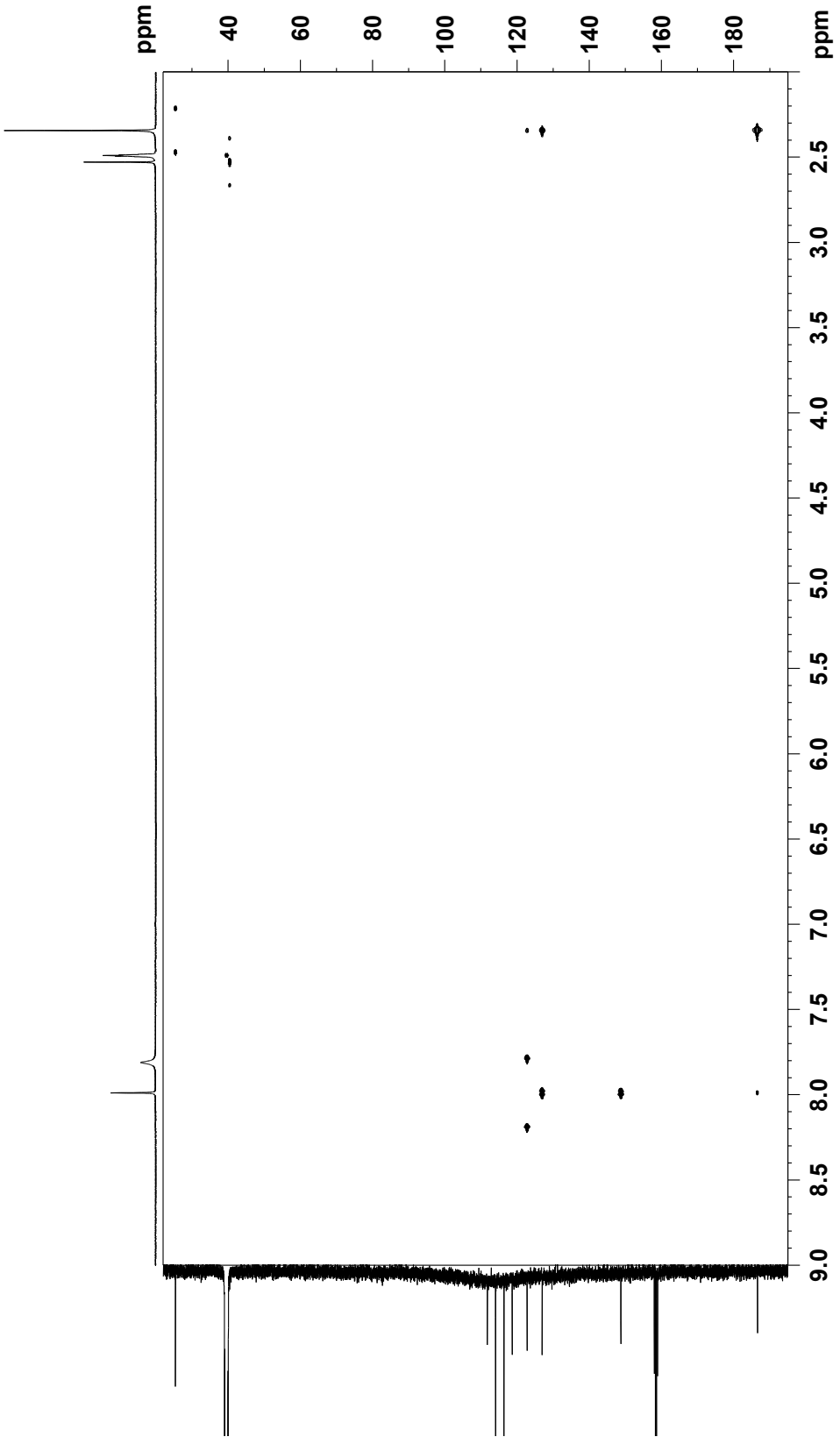

Figure S33. ^{1}H NMR spectrum of *nat*-**10**-(*R*)-2A1P (500 MHz, $CDCl_3$)

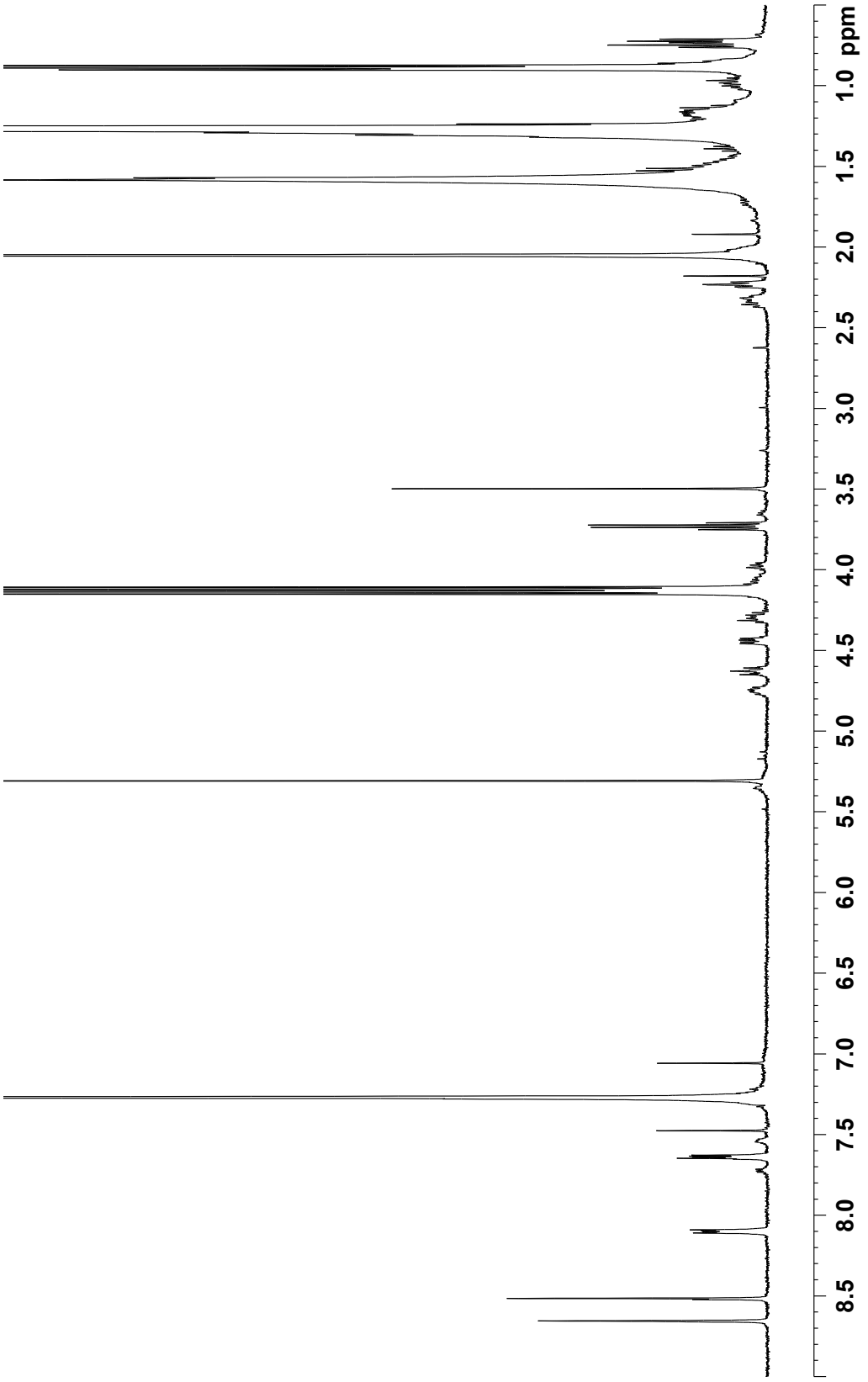

Figure S34. ^{1}H NMR spectrum of authentic (*S*)-**10**-(*R*)-2A1P (500 MHz, $CDCl_3$)

Figure S35. ^{1}H NMR spectrum of authentic (*S*)-**10**-(*S*)-2A1P (500 MHz, $CDCl_3$)

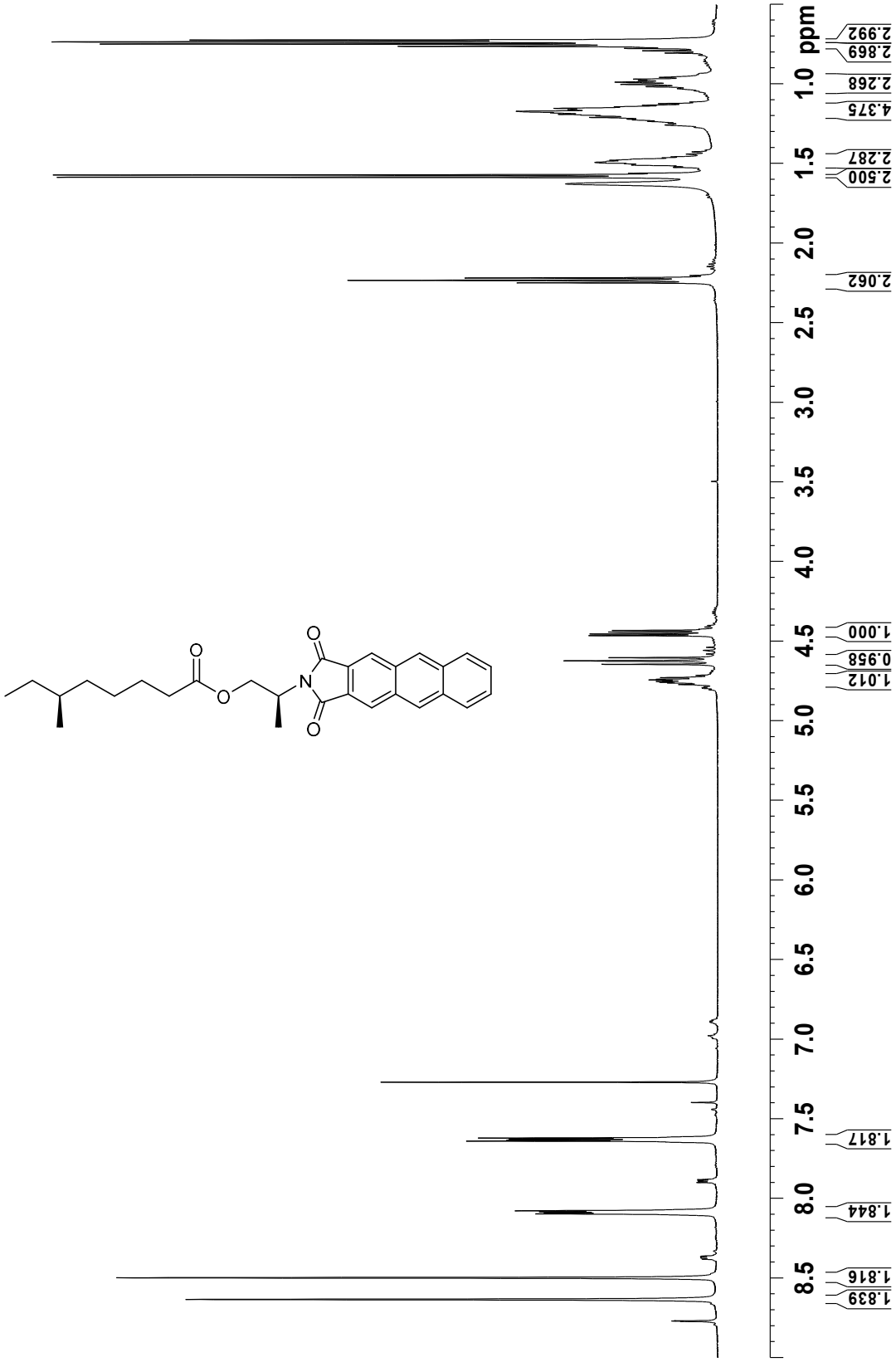

Figure S36. ^{1}H NMR spectrum of *nat*-**11**-(*R*)-2A1P (500 MHz, $CDCl_3$)

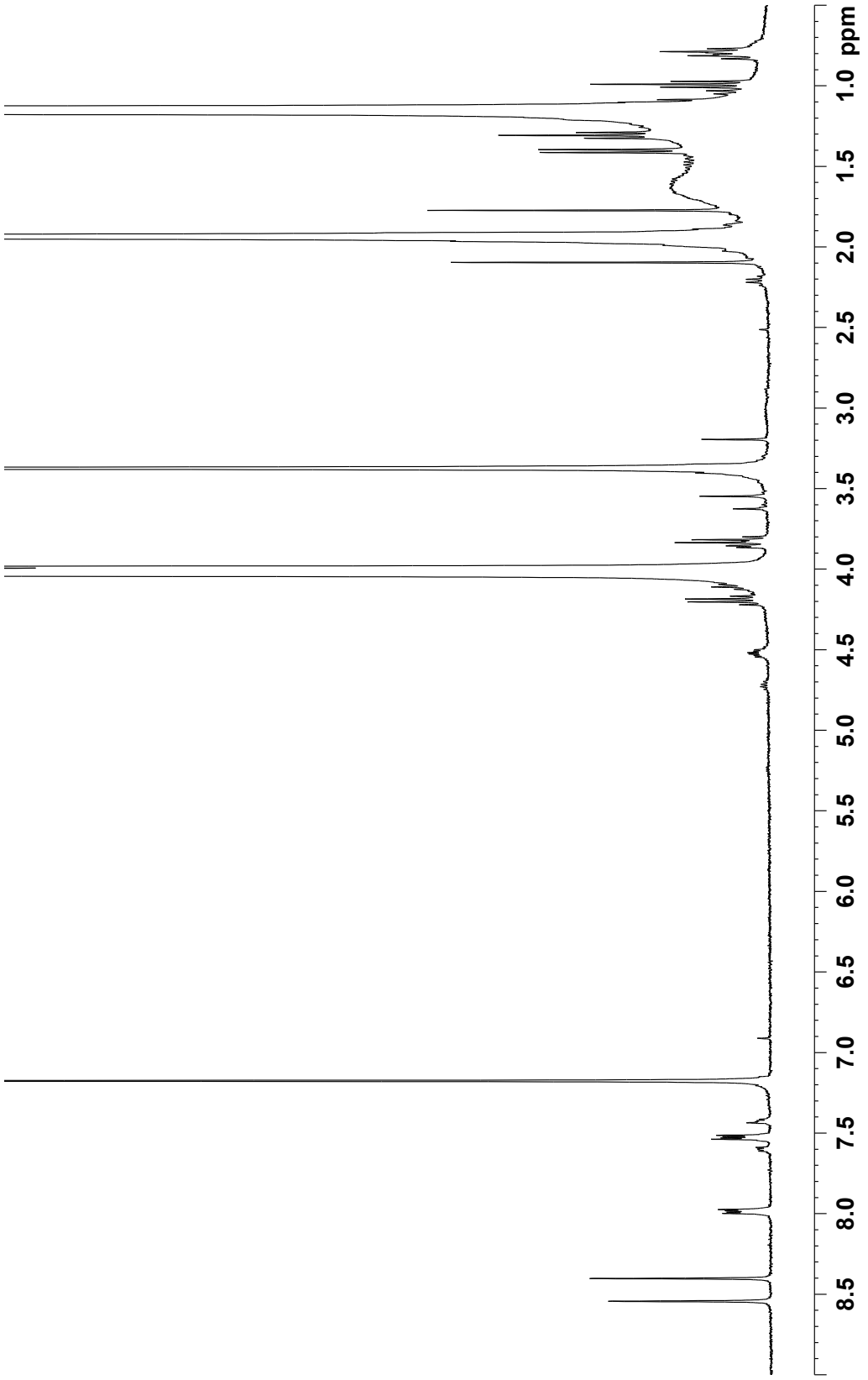

Figure S37. ^{1}H NMR spectrum of *nat*-**12**-(*R*)-2A1P (500 MHz, $CDCl_3$)

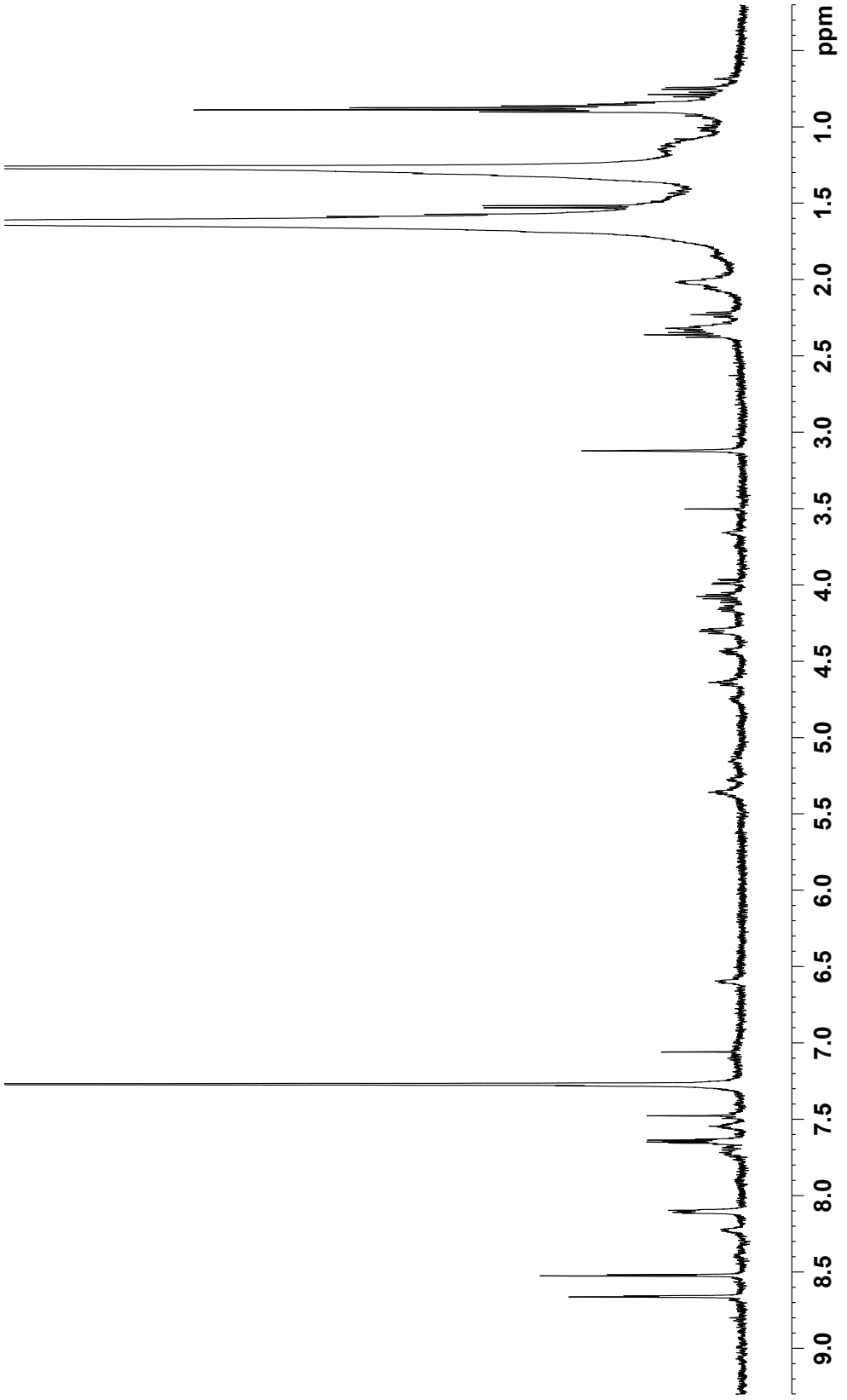

Figure S38. ^{1}H NMR spectrum of authentic (*S*)-**11**-(*R*)-2A1P (500 MHz, $CDCl_3$)

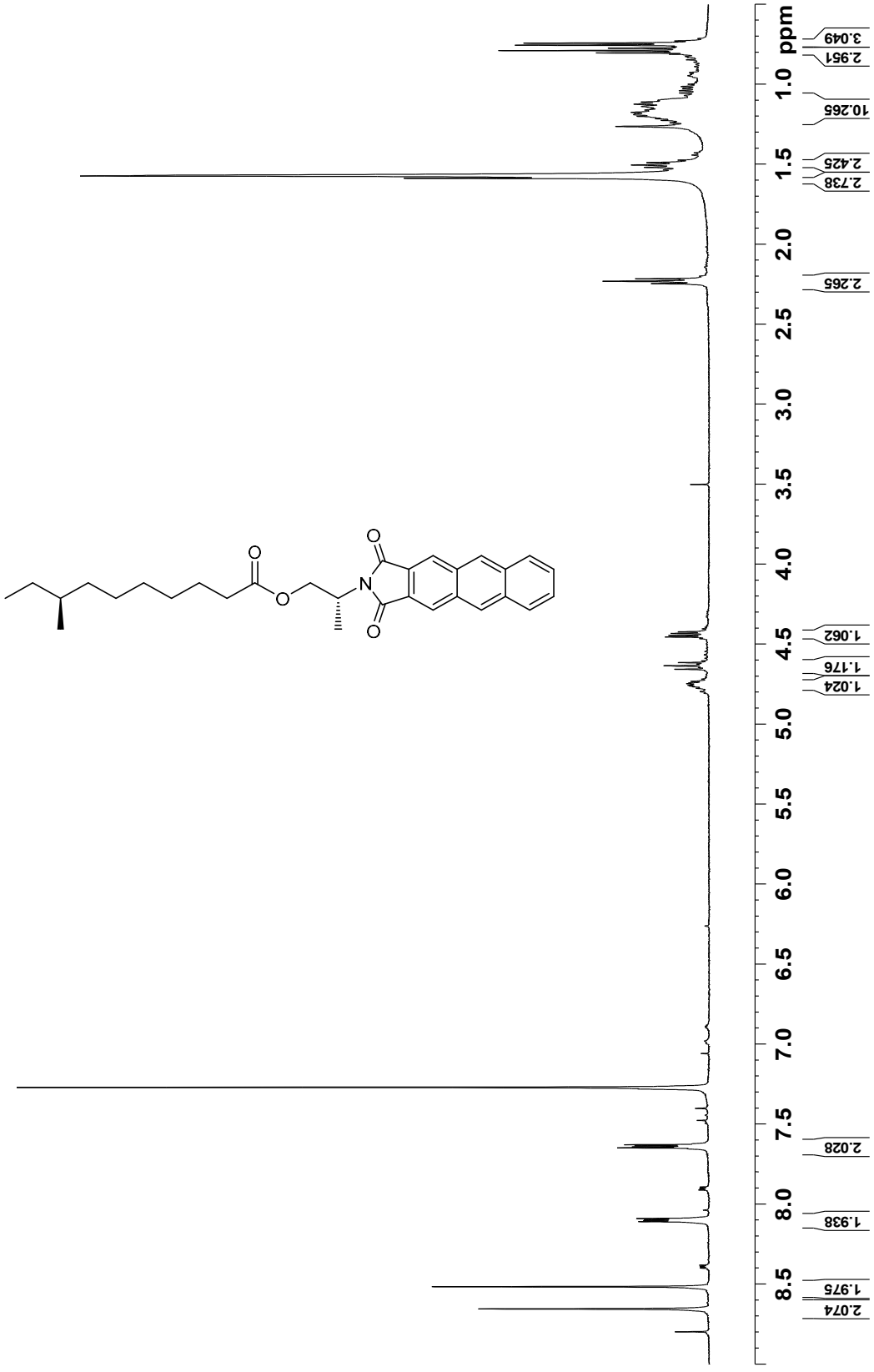

Figure S39. ^{1}H NMR spectrum of authentic (*S*)-**11**-(*S*)-2A1P (500 MHz, $CDCl_3$)

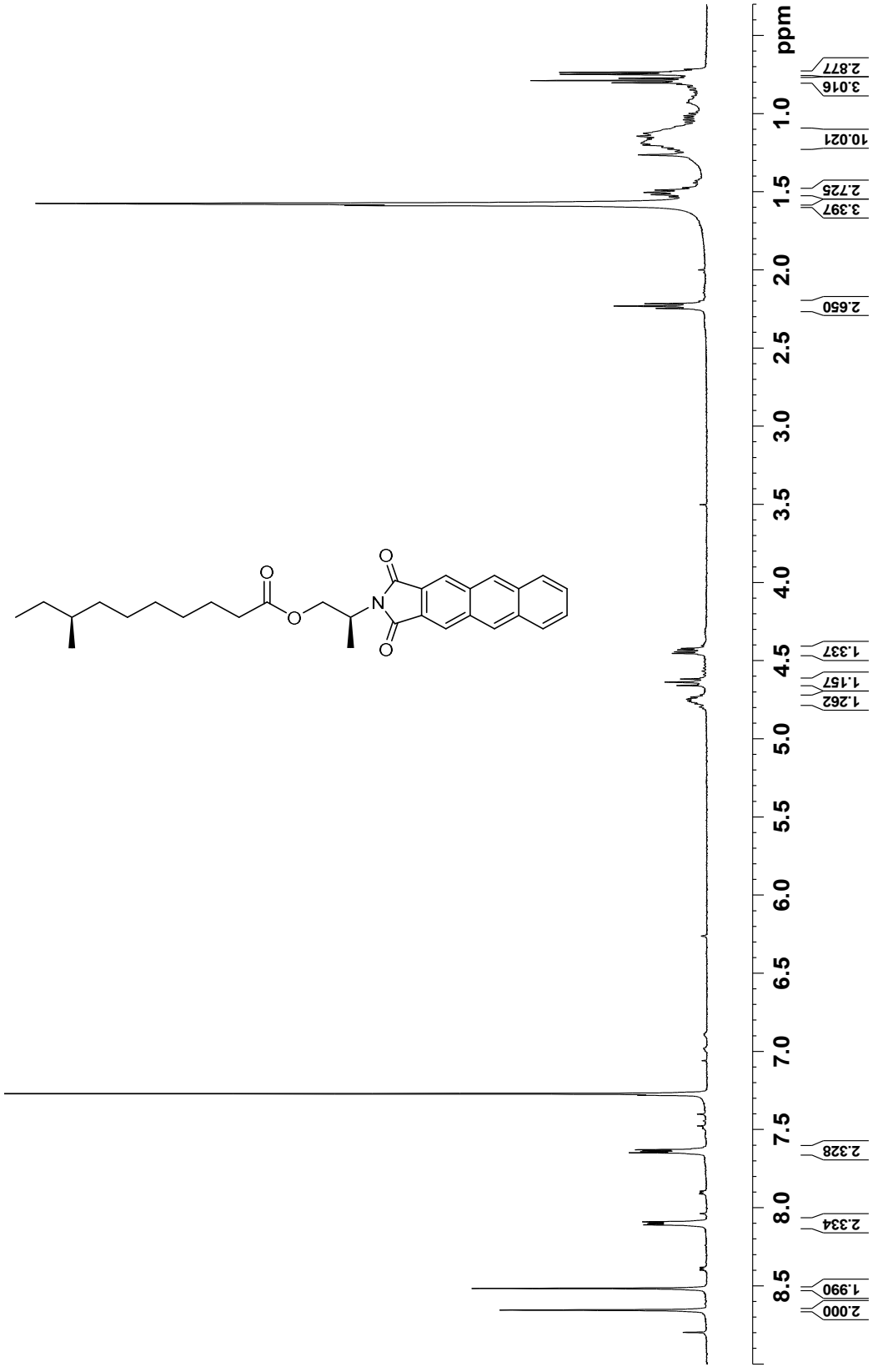

CHAPTER 4

Nyuzenamides A and B, Bicyclic Peptides with Antifungal and Cytotoxic Activity from a Marine-derived *Streptomyces* sp. N11-34

4-1 Background

Successful isolation and characterization of bulbimidazoles A−C and nocarimidazoles C and D from marine bacteria *Microbulbifer* and *Kocuria*, as described in Chapter 2 and Chapter 3, respectively, indicates that marine bacteria are a potential source of structurally unique natural products with diverse biological activity. It also suggested that these marine bacteria possess the same biosynthetic gene cluster, responsible for the production of distinct class of alkanoylimidazoles. Therefore, I selected this underexplored marine bacterial group for further natural product screening, because there still has a chance to get more bioactive compounds with novel structure for new drug discovery.

In this study, I examined one of the most diverse bacterial genera *Streptomyces*, an important group of actinomycetes for natural product discovery program. Recent investigation showed that several structurally unique compounds with potential clinical properties have been discovered from these taxonomically unique populations of marine *Streptomyces*, which add a valuable new dimension to microbial natural product research [1]. The unique adaptation characteristic of this bacterial group to the marine environment may affect secondary metabolite production by altering biosynthetic genes. Amongst the bacterial genera, *Streptomyces* is undoubtedly the most productive genus of new secondary metabolites which were used against new and emerging diseases and antibiotic resistant pathogens. Around 9000 new compounds have been discovered from this genus, which is 80% of the actinomycete natural products reported to date [2]. It should be noticed that the number of natural products is three-times larger than that of secondary metabolites from *Aspergillus* or *Penicillum* [3]. According to the genomic data, members of *Streptomyces* possess biosynthetic gene clusters for the production of polyketides, peptides, isoprenoids and alkaloids [4]. The average genome size of this genus is around 6 to 8 Mbp that is smaller than other organisms such as myxobacteria (~13 Mbp) and cyanobacteria (~9 Mbp) but biosynthetic machinery for secondary metabolites are quite diverse, which makes them most productive bacterial taxa in prokaryotic microbes [5-8]. Several bioactive natural products were discovered from marine *Streptomyces*. For example, borrelidin A, an 18-membered macrolide polyketide, is a potent inhibitor of bacterial and eukaryotic threonyl-tRNA synthetase [9]. Meroindenon is a terpenoid, which exhibits strong antibacterial activities [10]. Chlorizidine, a 5H-pyrrolo [2, 1-a]isoindol-5-one derivative, shows strong cytotoxicity against HCT-116 human colon cancer cells [11] (Figure 4-1).

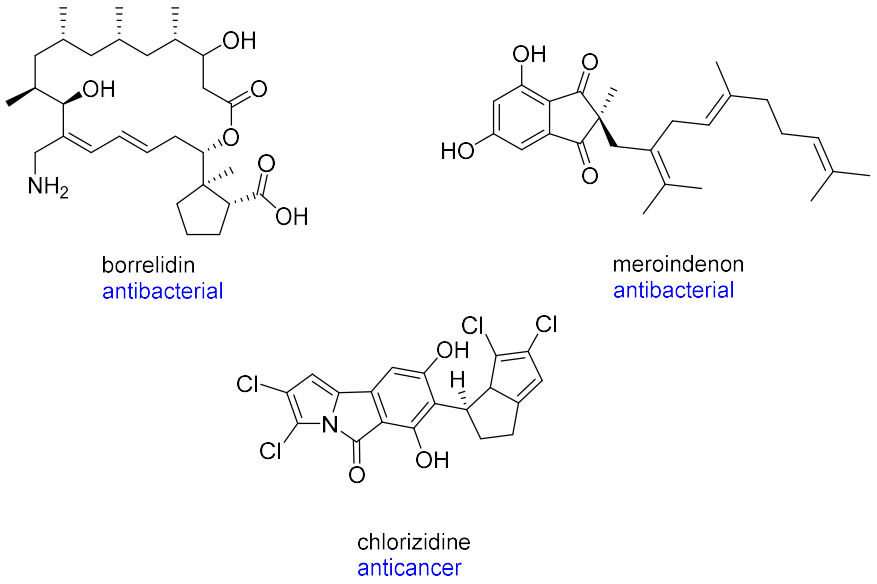

Figure 4-1. Structures of natural products from marine-derived *Streptomyces*.

In our laboratory, actinomycete strains in deep-sea water (DSW) have been analyzed for new bioactive compounds for over 20 years. These bacterial strains were collected from clean deep-sea water by using the membrane filter method. DSW is generally defined as the seawater present below -200 m and is characterized by several unique features, such as low temperature, a high concentration of minerals and nutrients, and homeostasis [12]. There are sixteen pumping stations for DSW in different geographical locations encompassing Japan [13]. DSW has been used in various fields such as aquaculture, food industry, agriculture and medical treatment [14-15]. DSW has also been applied for the production of microorganisms [12] and microalgae [16]. However, only a few reports are available on natural products of microorganisms in DSW. The concentration of microorganisms in DSW are lower compared to SSW (surface sea water). Until now, only, a few portions of microorganisms are able to culture for natural product discovery [17]. However, in recent years, the attentiveness on natural products in marine microorganisms has been increasing, but still a large number of bioactive compounds have yet to be discovered from this unexploited resource. In our laboratory, several structurally unique bioactive compounds were discovered from actinomycetes isolated from DSW of Toyama Bay, Japan. For example, a new member of tetrocarcin class of antibiotics, arisostatin A was obtained from *Micromonospora* [18]. Kosinostatin, a quinocycline antibiotic, was isolated from the culture broth of *Micromonospora* [19]. TPU-0037-C, is a novel lydicamycin congener, isolated from *Streptomyces*. This compound showed antibiotic activity against MRSA [20].

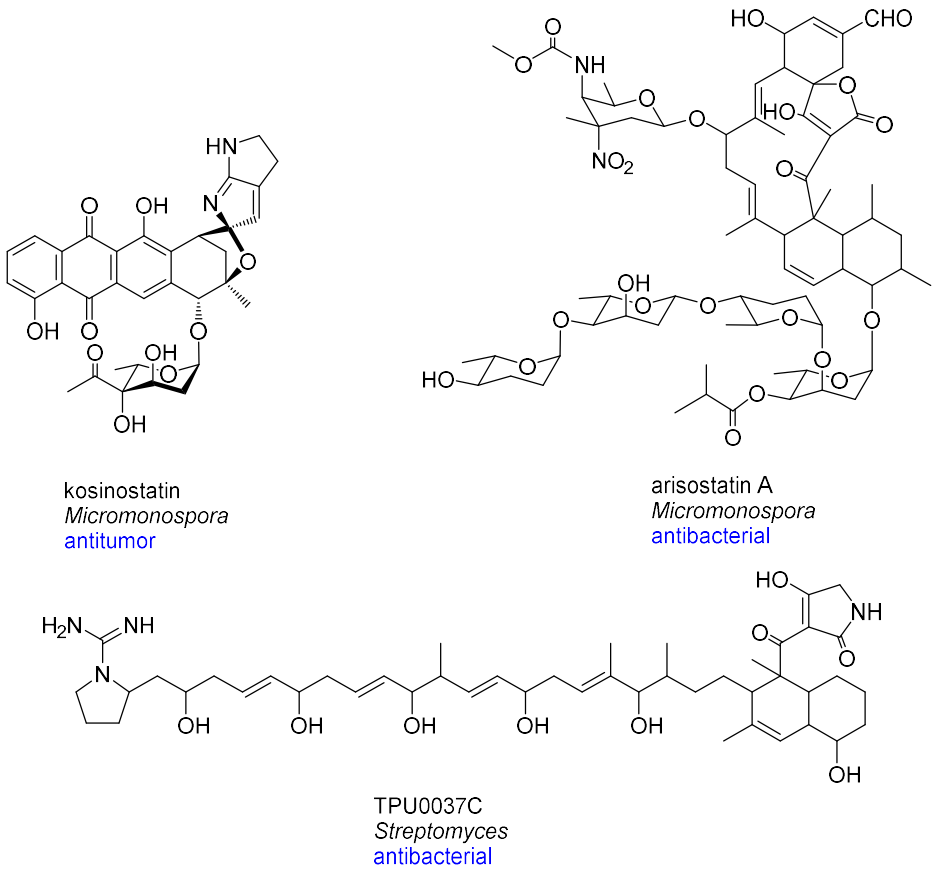

Figure 4-2. Structures of natural products from deep-sea water collected in Toyama Bay, Japan.

In this study, actinomycetes isolated from deep-sea water collected in Toyama Bay, Japan, were used to quest new bioactive compounds by chemical screening. In the previous study, only, 10-20 L of deep-sea water was filtered by using member filter paper. Actinomycetes on agar medium were found very less in number because small amount of DSW was used for this purpose. Therefore, it was difficult to discover new bioactive compounds from those few numbers of actiomycete strains. In this study, around 600,000 L of DSW was filtered by using YSYP filter at Nyuzen DSW facility. The suspended matter was obtained by this filtration, which was cultured on ISP-4 medium. A total of 138 actinomycete strains were isolated from the filter, which were more in number compared to the previous study. Isolated strains were used for searching unknown secondary metabolites by HPLC-UV analysis. The stain N11-34 was found to produce unknown metabolites in their culture broth. Thus, I selected this strain for new bioactive compounds discovery.

The strain N11-34 was characterized as a member of the genus *Streptomyces* on the basis of 99.9% similarity of 16S rRNA gene sequence (1428 nucleotides; DDBJ accession number AB812839) to *Streptomyces hygroscopicus* subsp. *hygroscopicus* NBRC 13472^{T} (accession number BBOX01000593) and isolated from suspended mater in DSW, Toyama, Japan. Bacteria of the genus *Streptomyces* are widely distributed in various marine habitats, such as deep sea sediments [21], sea

sands [22] and sea water [23]. The number of natural products from marine *Streptomyces* is less than terrestrial counterpart because relatively little work has been done on this marine bacterial group and only a small portion has been directed at examining for natural product screening program. Therefore, marine *Streptomyces* sp. N11-34 was selected as a candidate strain to search unknown secondary metabolites after HPLC-UV chemical screening analysis. Several known compounds were isolated from strain N11-34 including terfestatin C [24], abierixin [25], alchivemycin A [26], nocardamine [27] and 6-prenylindole [28] (Figure 4-3). However, I decided to work with this candidate strain because this diverse bacterial strain was collected from an unexploited marine source. Since environmental conditions of the ocean are extremely harsh in terms of nutrients, light, oxygen concentration, hydrostatic pressure, salinity, and temperature, compared with terrestrial conditions [29]. It is expectd that the strain N11-34 may have different characteristics such as unique biochemical metabolic and physiological abilites, which not only ensure their survival in this habitat but also provide potential ability to alter the biosynthetic gene cluster or activate the silent gene for the production of novel metabolites absent in terrestrial microorganisms [30, 31].

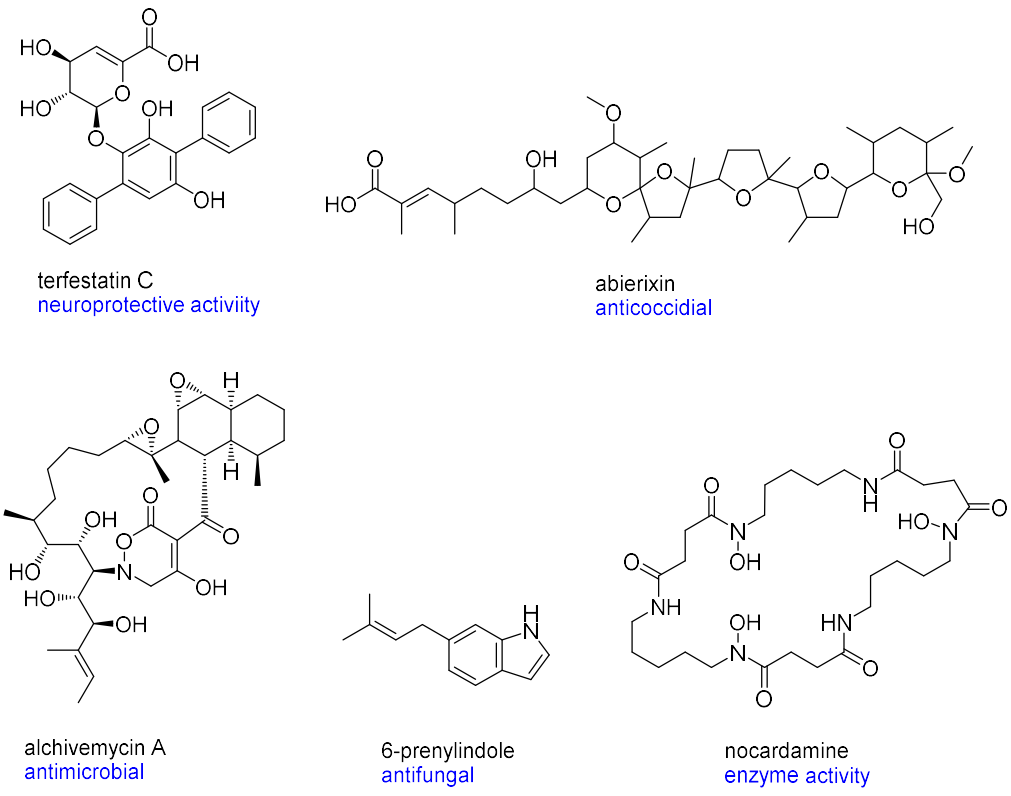

Figure 4-3. Structures of natural products produced by the candidate strain

Streptomyces sp. N11-34

In this study, chemical investigation for structurally novel secondary metabolites from marine actinomycetes led to the discovery of two bicyclic peptides nyuzenamides A (**13**) and B (**14**) possessing several unusual structural features. In this chapter, I will describe the isolation, structure determination, and bioactivity of **13** and **14**.

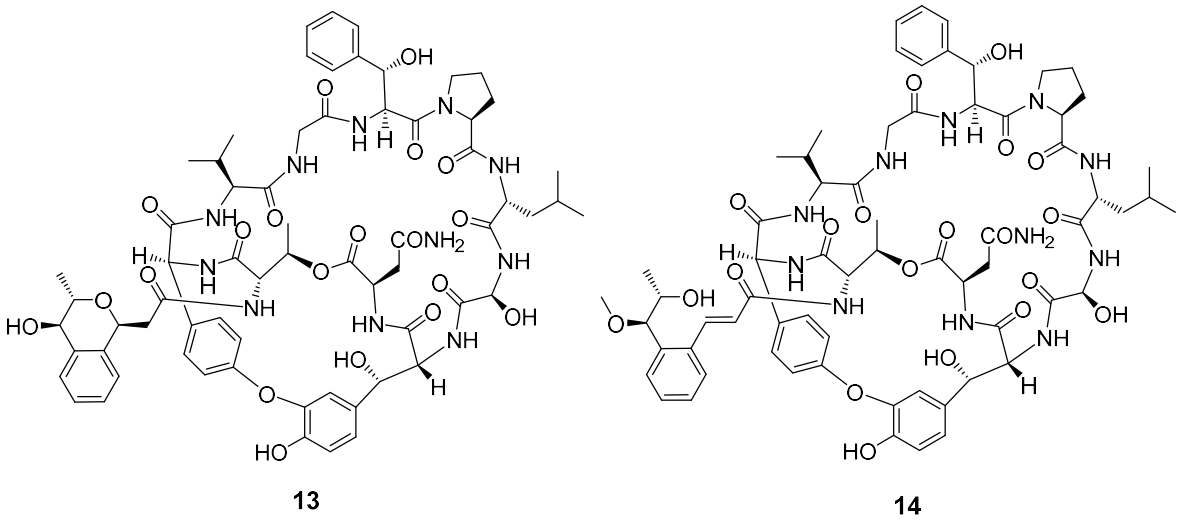

Figure 4-4. Structures of nyuzenamides A (**13**) and B (**14**)

4-2 Results and Discussion

In this study, marine actinomycete of the genus *Streptomyces* sp. N11-34 was isolated from suspended mater collected from DSW and selected as a candidate strain to discover structurally novel bioactive compounds. The secondary metabolites produced by this strain were analyzed by HPLC/UV-based spectroscopy analysis. For this purpose, three types of production media (A3M, A11M and A16) composed of different nutritional ingredient were used for secondary metabolites analysis. Strain N11-34 produced metabolites only in A16 medium that was confirmed after UV-chemical screening of three production media. Therefore, the whole culture broth of *Streptomyces* sp. N11-34, cultured in A16 seawater medium at 30 °C for five days, was extracted with 1-butanol, and the extract was subjected to chromatographic purification. HPLC/UV spectroscopy analysis of the crude extract from this producing strain showed several peaks in A16 medium. Most of the peaks were belonging to the secondary metabolites isolated as known compounds in previous study. However, this strain also had a few unknown peaks in the culture extract. These secondary metabolites showed UV absorption maximum at 273 nm. The extract was fractionated by

solvent/solvent partitioning. Following silica gel column chromatography and isocratic reversed-phase preparative HPLC, I collected seven peaks indicated as A, B, C, D, E, F and G (Figure 4-6). In my study, peaks B and E were selected for structure determination and bioassay. The UV spectra of peaks B and E were similar each other with absorption maxima at 200 and 273 nm, respectively. These peaks eluted at 10.5 and 17.5 min, respectively (Figure 4-6).

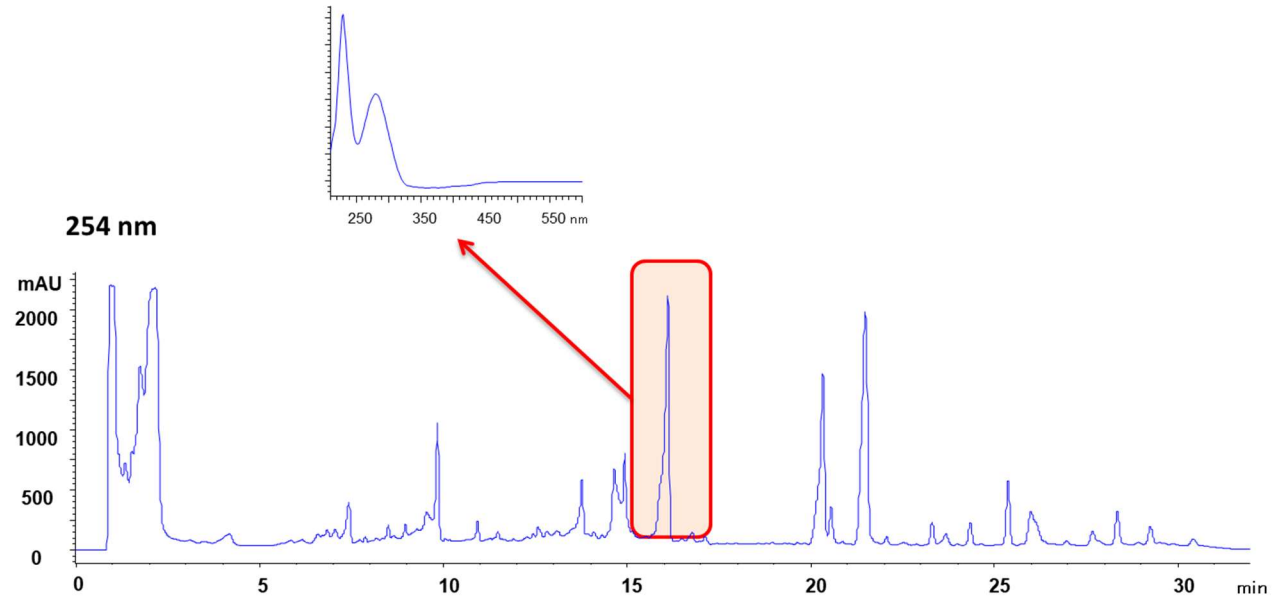

Figure 4-5. HPLC analysis of 1-butanol extract of *Streptomyces* sp. N11-34

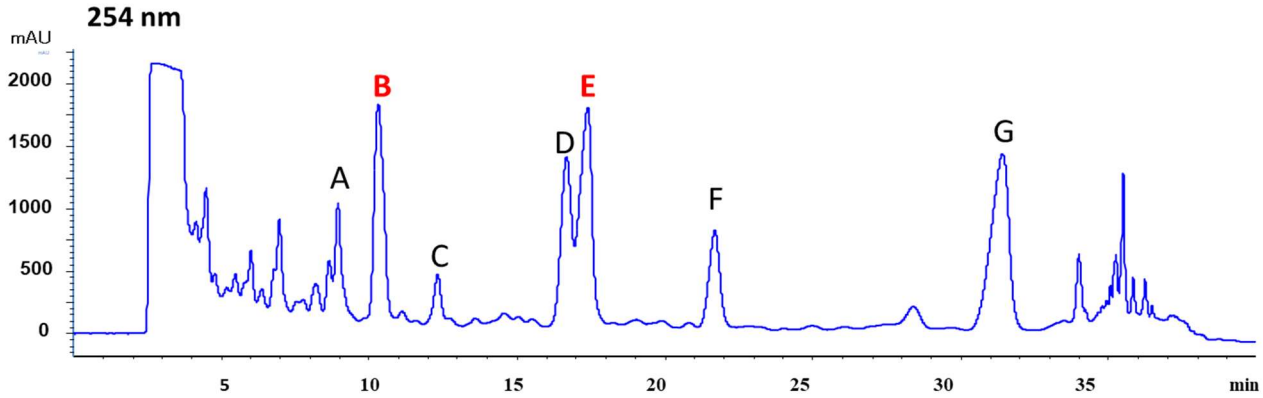

Figure 4-6. HPLC chromatogram of silica Fraction 2:1.

The producing strain N11-34 readily grows on ISP-2 agar and its colony morphology is shown in Figure 4-7.

Figure 4-7. Colony morphology of *Streptomyces* sp. N11-34 on ISP-2.

4-2-1 Fermentation and Isolation

The producing strain N11-34 was isolated from suspended matter collected from -311 m in depth at the Nyuzen DSW pumping facility, Toyama, Japan [32]. This strain was identified as a member of the genus *Streptomyces* based on the 16S rRNA gene sequence analysis. The whole fermentation broth of strain N11-34 cultured in A16 liquid medium was extracted with 1-butanol. After evaporation, the solvent extract was fractionated by silica gel, eluting with a stepwise gradient of $CHCl_3$−MeOH to concentrate metabolites of interest in a fraction that eluted with $CHCl_3$−MeOH = 2:1. Careful investigation of these silica fractions by HPLC-DAD spectroscopy displayed the production of unknown metabolites showing UV spectra characteristic of non-conjugated benzene rings. UV-guided purification by reverse-phase HPLC afforded nyuzenamides A (**13**, 12.3 mg) and B (**14**, 14.5 mg) from 3 L of culture (Scheme 4-1).

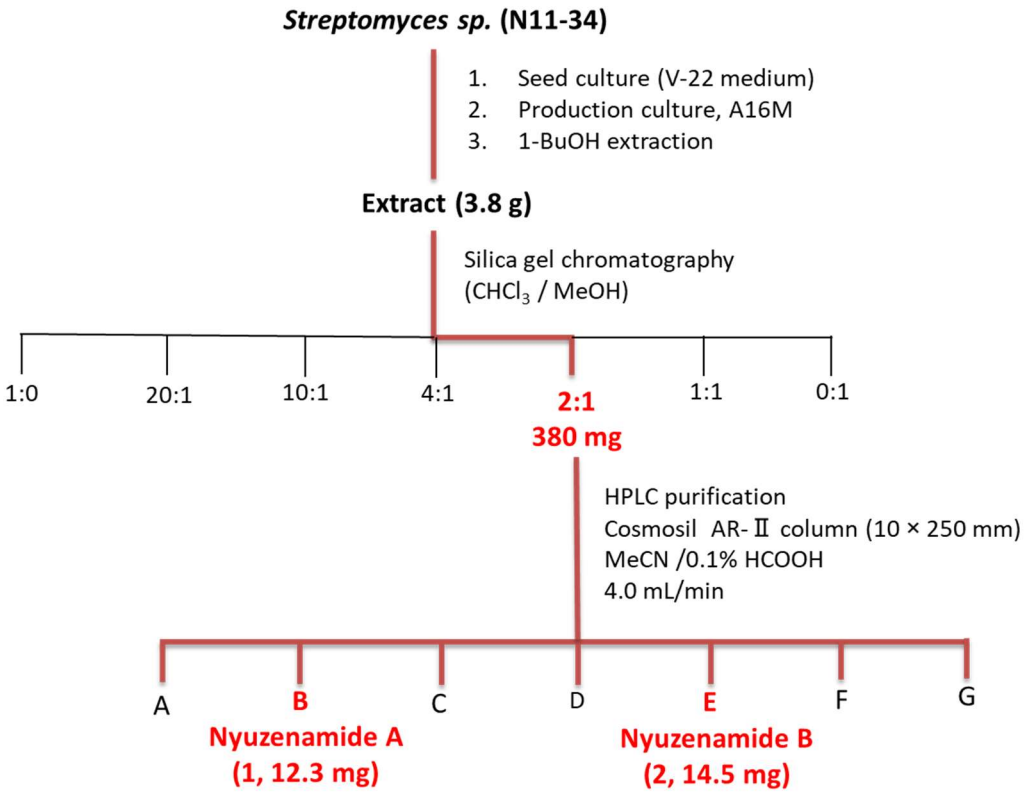

Scheme 4-1. Isolation of nyuzenamides A (**13**) and B (**14**).

4-2-2 Structure Determination

Nyuzenamide A (**13**) was obtained as a pale yellow, amorphous powder. The molecular formula was deduced as $C_{66}H_{81}N_{11}O_{20}$ on the basis of HRESITOFMS that gave a sodium adduct ion $[M + Na]^+$ at *m/z* 1370.5554 (Δ +0.2 mmu). The UV spectrum in methanol, displaying absorption bands at 203 nm and 273 nm, implying the presence of benzene ring(s) in the molecule. The IR spectrum showed absorption bands at 3291 cm^{-1} and 1644 cm^{-1}, suggesting the existence of NH group(s) and a carbonyl functionality, respectively. Analysis of the 1D and 2D NMR spectra revealed the presence of multiple aromatic protons/carbons (δ_H 6.40~7.39; δ_C 116.0~131.6), 12 carbonyl carbons (δ_C 168.4~175.9), and nine amide protons (δ_H 7.51~9.10), respectively connecting to α-methines/methylenes (δ_H 3.21~5.77; δ_C 42.7~71.4), indicating the peptidic nature of this compound (Table 4-1).

Analysis of COSY, HSQC, and HMBC spectral data permitted the establishment of six standard amino acids, Asx, Gly, Leu, Pro, Thr/*allo*-Thr, and Val (Figure 4-7), which accounted for five out of the nine signatures of α-amino acids. In parallel with the NMR analysis, chiral GC-MS analysis was conducted to establish the amino acid composition and their absolute configurations. Chiral-phase

GC-MS analysis determined the existence of D-Asx, D-Leu, L-Pro, L-Thr, and L-Val (Figure S15). The remaining four pairs of amide protons and α-methines, on the other hand, were all determined to be fragments of oxygenated unusual α-amino acids, namely, hydroxyglycine (Hgy), β-hydroxyphenylalanine (Hpa), 4-hydroxyphenylglycine (Hpg), and β-hydroxytyrosine (Htr). Hydroxylation at the α- or β-positions of Hgy, Hpa, and Htr were apparent from sequences of COSY cross peaks from amide protons to hydroxy protons (δ_H 5.73, 6.21, and 7.15), while the existence of an aromatic ring in Hpa, Hpg, and Htr was determined by HMBC correlations from *ortho*-aromatic protons to benzylic carbons (Figure 4-8). Oxygenation of the aromatic rings in Hpg and Htr was deduced by downfilded chemical shifts of carbons at the *para*- and *meta*-positions (δ_H 147.5, 147.8, and 160.3). Because both of the proton pairs symmetrically positioned on the phenoxy ring of Hpg (H4/H8 and H5/H7) were magnetically unequivalent, the ring rotation emerged to be severely restricted, which suggested a connection of the phenolic oxygen to some other fragment of the compound.

In addition to these amino acid residues, another component, a methyl- and hydroxy-substituted 2-(isochroman-1-yl)acetyl moiety (Ica), was connected from the remaining three spin-coupled parts and two nonprotonated aromatic carbons (δ_C 138.4, Ica-C4; 136.7, Ica-C9). Based on the HMBC spectrum analysis, a bundle of four aromatic protons (δ_H 7.12, 5.71, 6.92, and 7.29) had a doublet-triplet-triplet-doublet coupling pattern and correlated with both of these nonprotonated carbons, displaying a typical signature of a 1,2-disubstituted benzene ring. The two substituents on this ring were an oxymethine (Ica-3) paired with a deshielded methylene (δ_H 2.64, 3.22/δ_C 41.5, Ica-2) and a hydroxy-substituted methine (Ica-10) connecting to a methyl-substituted oxymethine (Ica-11), as supported by HMBC correlations from protons at both ends of the aromatic fragments to these methine carbons. An ether-bridge was confirmed between Ica-C3 and Ica-C11 based on HMBC correlation from Ica-H11 to Ica-C3, thus establishing an isochroman core. Furthermore, HMBC correlations were displayed from the deshielded methylene and neighboring oxymethine protons to a carbonyl carbon (δ_C 175.9, Ica-C1), which showed a connection of the Ica unit to hydroxy or amino functionalities in the peptide chain. Tow sequences of the amino acid residues, revealing Pro-Leu-Hgy-Htr-Asx and Thr-Hpg-Val-Gly-Hpa, were established by HMBC correlations from amide protons to the adjacent amide carbons. HMBC correlation was found from the Thr β-proton to a carboxyl carbon of Asx, which joined two fragments of peptide via an ester linkage, while a connection from Thr α-proton to the Ica carbonyl carbon corroborated acylation of the Thr amino group by the Ica unit.

Table 4-1. ^{1}H and ^{13}C NMR data for nyuzenamide A (**13**) in DMSO-d_6

unit	C/H no.	δ_C[a], type	δ_H mult (*J* in Hz)[b]	HMBC[b,c]
Ica	1	175.9, C		
	2	41.5, CH_2	2.64[e]; 3.22[e]	1, 3, 4
	3	67.4, CH	5.17[e]	1, 2
	4	138.4, C		
	5	123.8, CH	7.12, d (7.7)	3, 7, 9
	6	127.9, CH	5.71, t (7.4)	4, 8
	7	126.1, CH	6.92, t (7.5)	5, 9
	8	125.5, CH	7.29, d (7.5)	4, 6, 10
	9	136.7, C		
	10	68.8, CH	3.97[e]	4, 8, 9, 11, 12
	11	71.8, CH	3.35[e]	3, 9, 10
	12	17.21,[d] CH_3	0.82, d (6.4)	10, 11
	10-O*H*		5.46, d (5.4)	9, 10, 11
Thr	1	173.5, C		
	2	61.1, CH	4.60[e]	1, Ica-1
	3	68.7, CH	5.16[e]	1, 4, Asn-1
	4	17.24,[d] CH_3	1.21, d (6.8)	2, 3
	N*H*		9.10, s	3, Ica-1
Hpg	1	169.5, C		
	2	60.3, CH	4.87, d (2.5)	1, 3, 4, 8
	3	131.7, C		
	4	128.0, CH	6.87, dd (8.5, 1.7)	2, 6, 8
	5	124.0, CH	6.70, dd (8.4, 2.2)	3, 6, 7
	6	160.3, C		
	7	122.9, CH	7.36, dd (8.1, 2.3)	3, 5, 6
	8	131.6, CH	7.39, dd (8.1, 1.8)	2, 4, 6
	N*H*		7.83, d (2.4)	2, 3, Thr-1
Val	1	170.3, C		
	2	56.8, CH	4.44, dd (10.2, 3.9)	1, 3, 4, 5, Hpg-1
	3	28.7, CH	2.47[e]	2, 4, 5
	4	19.9, CH_3	0.713, d (6.8)	2, 3, 5
	5	17.26,[d] CH_3	0.707, d (6.7)	2, 3, 4
	N*H*		7.71, d (10.0)	2, Hpg-1
Gly	1	168.4, C		
	2	42.7, CH_2	3.26, dd (17.5, 5.2); 3.93, dd (17.4, 7.9)	1, Val-1
	N*H*		7.51, t (6.2)	Val-1
Hpa	1	169.1, C		
	2	56.7, CH	4.68, t, (9.5)	1, 3, 4
	3	73.7, CH	4.53, brd (10.0)	2, 4, 5
	4	141.5, C		
	5/9	126.8, CH	7.40[e]	3, 7, 9/5
	6/8	127.5, CH	7.22[e]	4, 5, 7, 8/6
	7	127.2, CH	7.22[e]	5

	N*H*		7.65, d (9.2)	2, 3, Gly-1
	3-O*H*		5.73, d (1.5)	2, 3, 4
Pro	1	171.2, C		
	2	60.5, CH	4.37, t (7.3)	1, 3, 4, 5
	3	30.2, CH_2	1.63, m; 2.30, m	1, 2, 4, 5
	4	24.8, CH_2	1.83, m; 1.88, m	2, 3
	5	47.9, CH_2	3.62, m; 3.96[e]	3, 4
Leu	1	171.6, C		
	2	50.4, CH	4.58[e]	1, 3, 4, Pro-1
	3	42.6, CH_2	1.43, m; 1.31, m	1, 2, 4, 5, 6
	4	24.2, CH	1.50, m	3, 5, 6
	5	22.0, CH_3	0.85, d (5.9)	3, 4, 6
	6	23.3, CH_3	0.85, d (5.9)	3, 4, 5
	N*H*		8.37, d (9.6)	Pro-1
Hgy	1	170.5, C		
	2	71.4, CH	5.77, d (9.5)	1, Leu-1
	N*H*		8.89, d (9.5)	Leu-1
	2-O*H*		7.15, brs	
Htr	1	170.7, C		
	2	62.7, CH	3.21[e]	1, 3
	3	69.7, CH	4.62[e]	
	4	132.4, C		
	5	121.2, CH	6.40, brs	3, 6, 7, 9
	6	147.5, C		
	7	147.8, C		
	8	116.0, CH	7.01, s	4, 6
	9	120.4, CH	7.01, s	3, 5
	N*H*		7.95, brs	Hgy-1
	3-O*H*		6.21, brs	
	7-O*H*		9.63, br	
Asn	1	169.9, C		
	2	49.1, CH	4.22, m	1, 3, Htr-1
	3	35.1, CH_2	2.60[e]; 2.70, dd (15.7, 3.1)	1, 2, 4
	4	170.8, C		
	N*H*		8.28, d (6.9)	2, 3, Htr-1

[a] Measured at 500 MHz.

[b] Measured at 125 HMz.

[c] From proton(s) to stated carbon(s).

[d] Interchangeable.

[e] Signal overlapping.

A peptolide sequence thus assembled was one oxygen excess and fewer by H_3N compared to the molecular formula, with six open termini of Pro-N, Htr-6-O, Htr-7-O, Asx-C4, Hpg-6-O, and Hpa-C1 remained to be connected. A ROESY spectrum was partially supported the possible connectivities among those termini (Figure S6). First, an amide linkage was formed between Pro-N and Hpa-C1, suggesting by ROESY correlations from Pro-H5 to Hpa-H2 and Pro-H5 to Hpa-H3 (Figure 4-8). In addition, an ether bridge was established between Hpg and Htr by a series of ROESY correlations from Hpg-H5 to Htr-H5 and Hpg-H7 to Htr-H5, which eliminated the excessive oxygen as assumed previously.

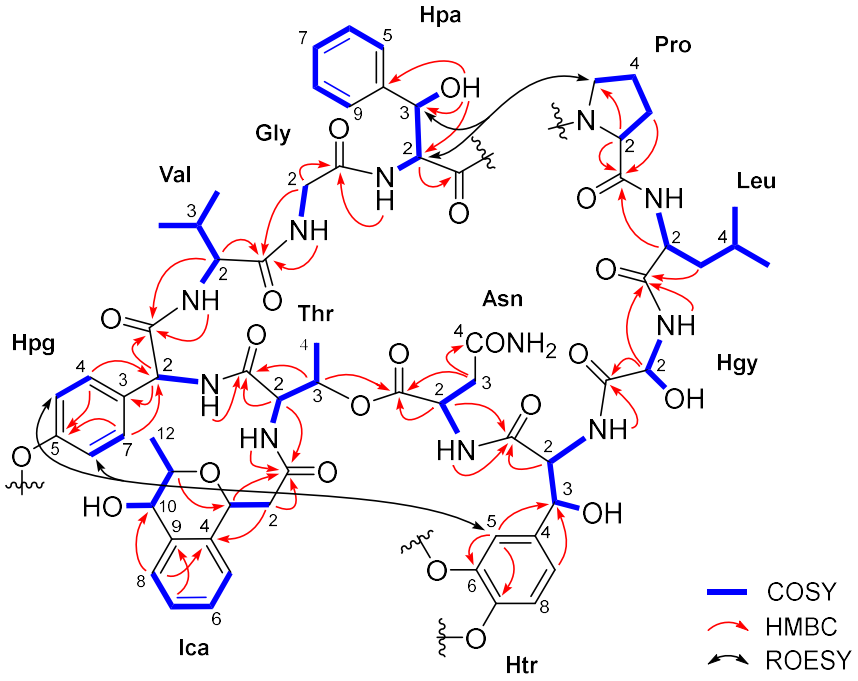

Figure 4-8. Key 2D NMR correlations for nyuzenamide A (**13**).

Based on the 2D NMR spectra, no COSY or HMBC correlation was observed from an exchangeable proton at δ_H 9.63, was accordingly attributable to a phenolic proton at Htr-7-O, and the rest atoms, NH_2, were likely the components of a carboxamide blockade at the Asx-C4 terminus. No further information was available in the NMR data to validate these speculations. To our delight, however, crystalline particles of **13** were formed during the storage of the NMR sample in a refrigerator. These crystal particles were then recovered and recrystallized from a mixture of MeOH-CH_2Cl_2 to provide colorless needles and subjected to single-crystal X-ray analysis determined the gross structure of **13**. The crystal structure of **13** displayed that Pro and Hpa were connected through an amide bond and Hpg and Htr through an ether bridge at Hpg-C6 and Htr-C6, while a carboxamide group was present on Asx to form Asn (CCDC accession No. 2026824, Figure

3). The Flack parameter (0.01) was small enough to verify the results from the chiral-phase GC-MS analysis and establish the remaining stereochemistry for the unusual amino acids and a non-peptidic unit to be (*S*) for Hpg, (2*S*, 3*S*) for Hpa, (*S*) for Hgy, (2*R*, 3*S*) for Htr, and (3*S*, 10*S*, 12*R*) for Ica (Figure 4-9).

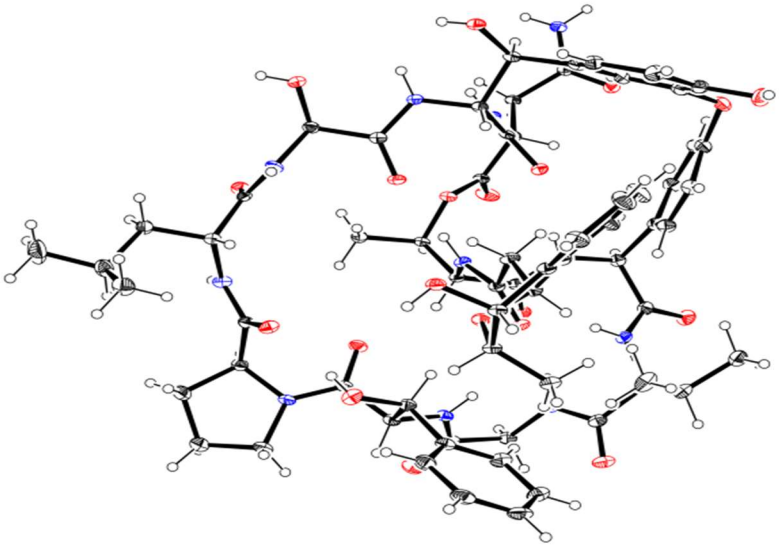

Figure 4-9. X-ray crystal structure of nyuzenamide A (**13**).

Nyuzenamide B (**14**) was also obtained as a pale yellow amorphous powder. The molecular formula of **14** was determined as $C_{67}H_{83}N_{11}O_{20}$ on the basis of HR-ESITOFMS that gave a protonated molecular ion $[M + Na]^+$ at *m/z* 1384.5706. The molecular weight of **14** was 14 amu (corresponding to the increment of a CH_2 fragment) larger than **14**. The UV and IR spectra displayed almost the same absorption bands as **14**. Detailed analysis of 2D NMR spectra of **14,** including COSY, HSQC and HMBC experiments revealed that the ten amino acid residues, including four unusual amino acids, were totally similar to those in **14**, indicating a structural difference in the N-acyl substituent on Thr. Further Analysis of an HMBC correlations confirmed the amino acid sequence was identical in **13** and **14** (Table 4-2).The connectivity between Pro and Hpa and Hpg and Htr were not supported by HMBC correlations. The same set of ROESY correlations observed for **13** was also present in **14**. The amide linkage between Pro and Hpa and the ether linkage between Hpg and Htr in **14** was confirmed by a series of ROESY correlations (Figure S12).

Table 4-2. ^{1}H and ^{13}C NMR data for nyuzenamide B (**14**) in DMSO-d_6

unit	C/H no.	δ_C[a]	δ_H mult (*J* in Hz)[b]	HMBC[b,c]
Ppa	1	168.8, C		
	2	126.3, CH	6.84, d (15.7)	1, 3, 4
	3	138.2, CH	8.03, d (15.6)	1, 2, 4, 5, 9
	4	135.4, C		
	5	127.1, CH	7.10, d (7.5)	3, 7, 9
	6	127.7, CH	6.99, t (7.4)	4, 8
	7	128.8, CH	7.30, t (7.5)	5, 9
	8	129.0, CH	7.25[e]	4, 6, 10
	9	138.7, C		
	10	85.3, CH	3.74, d (7.0)	4, 8, 9, 11, 12, 13
	11	68.3, CH	3.45, m	9, 10
	12	20.1, CH_3	0.73, d (6.0)	10, 11
	13	56.0, CH_3	2.69, s	10
	11-O*H*		4.35, d (5.6)	10, 11, 12
Thr	1	173.0, C		
	2	60.7, CH	4.94, d (3.8)	1, 3, 4, Ppa-1
	3	69.1, CH	5.21, q (6.7)	1, 2, 4, Asn-1
	4	17.5, CH_3	1.27, d (6.7)	2, 3
	N*H*		8.89, d (3.8)	1, 2, 3, Ppa-1
Hpg	1	169.2, C		
	2	60.3, CH	4.75, d (2.8)	1, 3, 4, 8
	3	131.6, C		
	4	128.0, CH	7.04, dd (8.7, 2.2)	2, 6, 8
	5	123.5, CH	6.49, dd (8.6, 2.1)	3, 6, 7
	6	159.8, C		
	7	122.3, CH	7.23, dd (8.2, 2.5)	3, 5, 6
	8	131.2, CH	7.43, dd (8.4, 2.2)	2, 4, 6
	N*H*		7.66, d (2.5)	1, 2, 3, Thr-1
Val	1	170.5, C		
	2	56.8, CH	4.53[e]	1, 3, 4, 5, Hpg-1
	3	29.1, CH	2.59[e]	4, 5
	4	19.9, CH_3	0.814, d (6.7)	2, 3, 5
	5	17.7, CH_3	1.13, d (6.8)	2, 3, 4
	N*H*		7.88, d (10.0)	2, Hpg-1
Gly	1	168.8, C		
	2	42.7, CH_2	3.29, dd (17.9, 4.7); 4.00, dd (17.8, 8.1)	1, Val-1
	N*H*		7.52, dd (7.3, 5.8)	2, Val-1
Hpa	1	169.1, C		
	2	57.6, CH	4.51[e]	1, 3, 4, Gly-1
	3	73.2, CH	4.33, brd (9.8)	4, 5/9
	4	141.6, C		
	5/9	126.4, CH	7.46[e]	3, 5/9, 7
	6/8	127.9, CH	7.27[e]	4, 6/8
	7	127.3, CH	7.26[e]	5/9

	N*H*		7.86, d (8.8)	Gly-1
	3-O*H*		5.61, d (1.8)	3, 4
Pro	1	171.5, C		
	2	60.4, CH	4.39, t (7.4)	1, 3, 4
	3	30.0, CH_2	1.62, m; 2.25, m	1, 2, 4, 5
	4	24.8, CH_2	1.83, m; 1.88, m	2, 3, 5
	5	47.6, CH_2	3.66, m; 3.92[e]	3, 4
Leu	1	171.4, C		
	2	50.4, CH	4.60, ddd (9.6, 9.6, 5.0)	1, 3, 4, Pro-1
	3	42.3, CH_2	1.27[e]; 1.44[e]	1, 4, 5, 6
	4	24.1, CH	1.45[e]	2, 3, 5, 6
	5	23.1, CH_3	0.84, d (6.2)	3, 4, 6
	6	21.8, CH_3	0.807, d (5.7)	3, 4, 5
	N*H*		8.49, d (9.7)	1, Pro-1
Hgy	1	171.0, C		
	2	71.2, CH	5.76, dd (8.8, 4.9)	1, Leu-1
	N*H*		9.15, d (9.5)	Leu-1
	2-O*H*		7.10[e]	1, 2
Htr	1	170.75, C		
	2	64.1, CH	3.57, dd (10.2, 3.4)	1, 3, 4
	3	69.5, CH	4.71, dd (10.3, 5.8)	1, 2, 4, 5, 9
	4	132.7, C		
	5	120.5, CH	6.30, d (2.1)	3, 6, 7, 9
	6	147.2, C		
	7	147.5, C		
	8	116.1, CH	6.93, d (8.4)	4,9
	9	120.1, CH	7.19, dd (8.4, 2.0)	3, 5, 7
	N*H*		8.16, d (3.5)	2, 3, Hgy-1
	3-O*H*		6.21, d (6.2)	2, 3
	7-O*H*		9.45, brs	
Asn	1	169.6, C		
	2	49.0, CH	3.93[e]	1, 3, 4, Htr-1
	3	35.0, CH_2	2.60[e]; 2.68[e]	1, 2, 4
	4	170.7, C		
	N*H*		8.26, d (7.3)	2, 3, Htr-1

[a] Measured at 500 MHz.

[b] Measured at 125 HMz.

[c] From proton(s) to stated carbon(s).

[d] Interchangeable.

[e] Signal overlapping.

The remaining molecular fragments for the non-peptidic moiety, which eventually were connected into a 2-(2-hydroxy-1-methoxypropyl)phenylpropenoyl group (Ppa), lacked an oxymethine and a methylene units exit in **8** and instead added a methoxy (δ_H 2.69, s/δ_C 56.0) and a disubstitued *E*-olefin (δ_H 6.84, d, J = 15.7 Hz; 8.03, d, J = 15.6 Hz) groups, suggesting alteration of the substituents on the benzene ring (Figure 4-10). In fact, both of the double bond protons showed HMBC correlations to a carbonyl carbon at δ_C 168.8 (Ppa-C1) and a nonprotonated aromatic carbon at δ_C 135.4 (Ppa-C4), determining a 2-propenoyl unit coupled with a phenyl ring. The β-proton (Ppa-H3) of the acyl unit further connected with another two aromatic carbons, one protonated (δ_C 127.1, Ppa-C5) and the other nonprotonated (δ_C 138.7, Ppa-C9), which, together with a four proton sequence traced in the COSY spectrum, suggested a 1,2-disubstituted benzene moiety. Finally, analysis of the COSY and HMBC correlations, 2-hydroxy-1-methoxypropyl group was allocated at Ppa-C9 as the other substituent on the ring to establish the modified cinnamoyl unit as well as the gross structure of **14**. Chiral-phase GC-MS analysis revealed that the absolute configurations of the common amino acids were identical to those in **8**, and the same conclusion might be applicable to the rest of amino acids in consideration of the global resemblance of the NMR spectra and biogenetic identity. The two chiral centers in the Ppa group were tentatively determined to be 10*R* and 11*S*, based on an interconvertible relationship of Ica and Ppa through β-elimination or Michael addition.

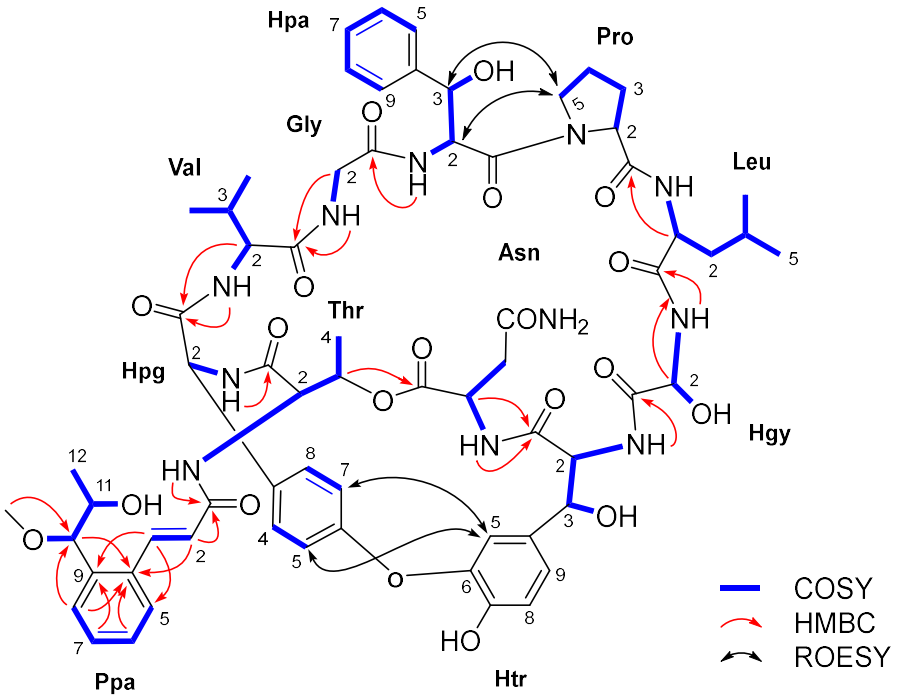

Figure 4-10. Key 2D NMR correlations for nyuzenamide B (**14**).

4-2-3 Absolute Configuration

Chiral GC-MS analysis is one of method for determining the absolute configurations of hydrolytically accessible amino acid residues present in polypeptide [33]. Four steps are performed to analysis enantiomer of amino acids by this method, (i) the polypeptide is subjected to acid hydrolysis (6 N HCl) to release free amino acid residues, (ii) the free amino acid is derivatized to methyl esters by esterification in the presence of hydrochloric methanol. (iii) The methyl esters of amino acid are derivatized to TFA amide by reacting with trifluoroacetic acid anhydride. (iv) the TFA amide methyl esters of amino acid are subjected to chiral GC-MS analysis on Chirasil-L-Val column, and (iv) GC-MS retention times of derivatized amino acid residues in the analyte is compared with TFA amide methyl esters of standards L and D- amino acid.

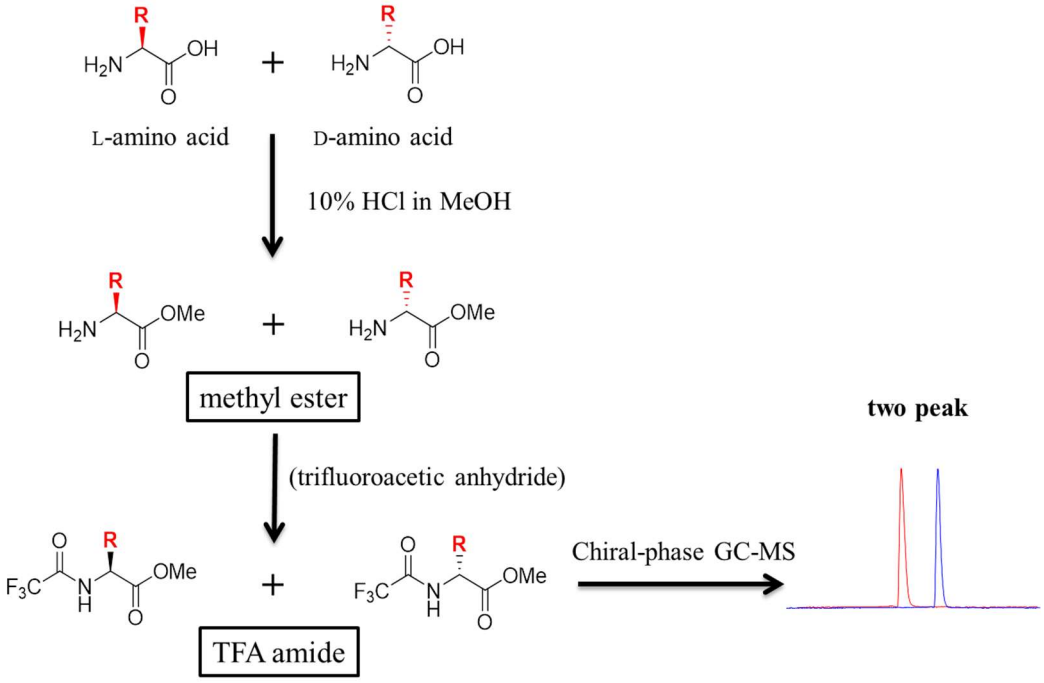

Scheme 4-2. Principle of chiral GC-MS analysis

In order to determine the absolute configuration of common amino acid residues in **13** and **14**, chiral GC-MS analysis was utilized. Following acid-catalyzed hydrolysis in HCl, free amino acids in the hydrolysate of **13** and **14** were derivatized to TFA amide methyl esters by esterification in hydrochloric methanol, followed by the treatment with trifluoroacetic acid anhydride. The derivatized hydrolysates were analyzed by chiral-phase GC-MS on a Chirasil-L-Val capillary column. The retention times of the *N*-trifluoroacetic ester derivatives of the amino acids were compared with those of authentic D- and L-amino acids that had been derivatized in the same

manner, which established the presence of D-Asx, D-Leu, L-Pro, L-Thr, and L-Val (Figure 4-10). Retention times for standard amino acids were D-Val 6.54 min, D/L-Val 6.60 and 6.97 min, D-Thr 7.07 min, L-Thr 7.54 min, D-allo-Thr 8.99 min, L-allo-Thr 9.47 min, D-Pro 8.19 min, L-Pro 8.52 min, D-Leu 8.82 min, L-Leu 9.39 min, D-Asp 10.32 min, and L-Asp 9.58 min, respectively. The hydrolysate of nyuzenamide A gave peaks for L-Val (6.95 min), L-Thr (7.57 min), L-Pro (8.57 min), D-Leu (8.82 min), and D-Asp (10.37 min), while that of nyuzenamide B gave L-Val (6.96 min), L-Thr (7.59 min), L-Pro (8.56 min), D-Leu (8.84 min), and D-Asp (10.36 min) (Figure S15).

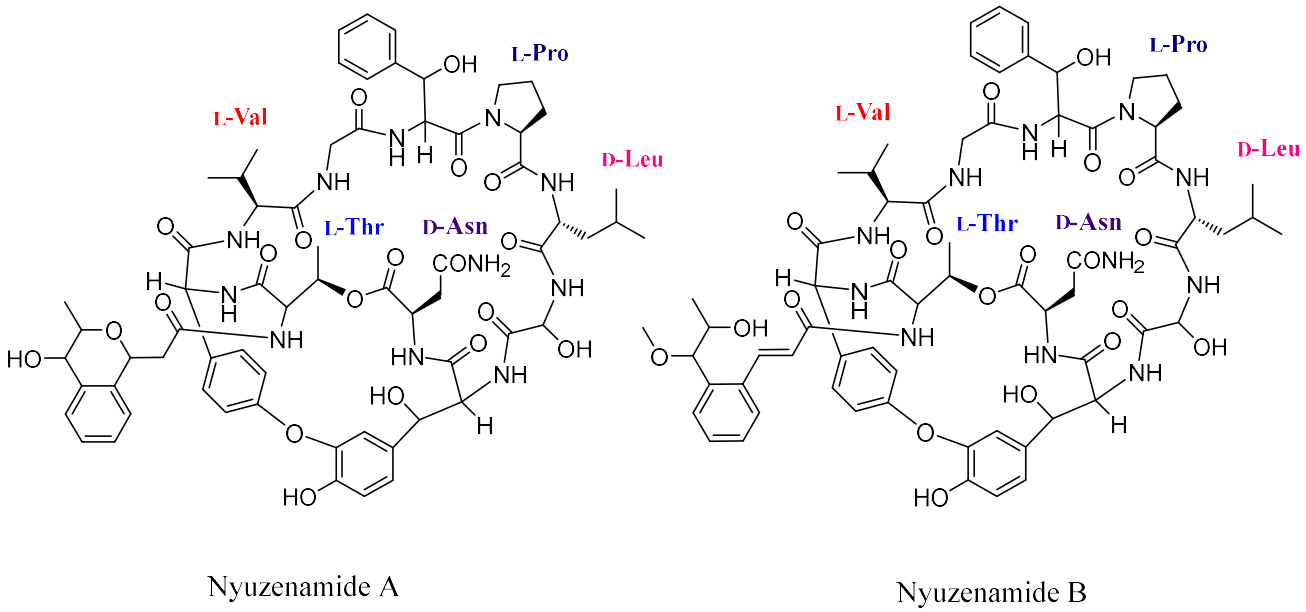

Nyuzenamide A　　Nyuzenamide B

Figure 4-11. Absolute configurations of common amino acids in nyuzenamides A (**13**) and B (**14**)

4-2-4 Bioactivity

Nyuzenamides A (**13**) and B (**14**) were tested against two Gram-positive bacteria (*Kocuria rhizophila* ATCC9341 and *Staphylococcus aureus* FDA209P JC-1), three Gram-negative bacteria (*Escherichia coli* NIHJ JC-2, *Rhizobium radiobacter* NBRC14554, and *Tenacibaculum maritimum* NBRC16015), and three fungi (*Candida albicans* NBRC0197, *Glomerella cingulata* NBRC5907, and *Trichophyton rubrum* NBRC5467). Compounds **13** and **14** were not active against Gram-positive and -negative bacteria and a yeast, but exhibited selectively antifungal activity by inhibiting the growth of filamentous fungi (Table 4-3). Compound **13** was more potent than **14** against plant and human pathogens, *Glomerella cingulata* NBRC5907 and *Trichophyton rubrum* NBRC5467, with MIC 3.1 and 6.3 μg/mL, respectively. The MIC values of **13** against these fungi were 25 μg/mL. In addition, **13** and **14** exhibited cytotoxicity against P388 murine leukemia cells with IC_{50} values 4.9 and 6.2 μM (6.6 and 8.4 μg/mL, respectively).

Table 4-3. Antimicrobial activity of **13** and **14**.

Microoraganisms	MIC (μg/mL)			
	13	**14**	kanamycin sulfate	amphotericin B
Kocuria rhizophila ATCC9341	>100	>100	0.78	NT
Staphylococcus aureus FDA209P JC-1	>100	>100	0.78	NT
Escherichia coli NIHJ JC-2	>100	>100	1.25	NT
Rhizobium radiobacter NBRC14554	>100	>100	0.78	NT
Tenacibaculum maritinum NBRC16015	>100	>100	1.25	NT
Candida albicans NBRC0197	>100	>100	NT	0.78
Glomerella cingulata NBRC5907	3.1	25	NT	1.25
Trichophyton rubrum NBRC5467	6.3	25	NT	0.78

NT: not tested

4.3 Conclusion

In summary, chemical investigation of secondary metabolites from a marine-derived *Streptomyces* strain N11-34 led to the discovery of two novel bicyclic peptides with unusual skeleton, namely, nyuzenamides A (**13**) and B (**14**). Recently, bicyclic peptides have acquired much attention for the development of next generation therapeutics. Bicyclic peptides have showed greater potentiality, compared with linear and monocyclic peptides in terms of conformational rigidity and metabolic stability. These properties make them capable of binding to challenging drug targets [34]. A search for novel drug candidates to target the undruggable proteins, several macrocyclic peptides from natural products such as vancomycin [35], cyclosporine [36] and daptomycin [37] showed potential clinical properties (Figure 4-12). These peptides inspired researchers to explore synthetic bicyclic peptides from natural bicyclic peptides as next generation drugs.

In nature, like monocyclic peptides, bicyclic peptide exhibits diverse biological activities [38]. For example, a bicyclic octapeptide known as moroidin isolated from the seeds of *Celosia argentea*, shows anti-mitotic activity by preventing eukaryotic cell division by inhibiting tubulin polymerization (Figure 4-13) [39]. Other bioactive bicyclic peptides reported from nature known as phallotoxins and amatoxins, were obtained from poisonous mushrooms of the genus *Amanita phalloides*. Phallotoxins are bicyclic heptapeptides that inhibit cytokinesis and cytotaxis by preventing the depolarization of actin filaments (Figure 4-12) [40].

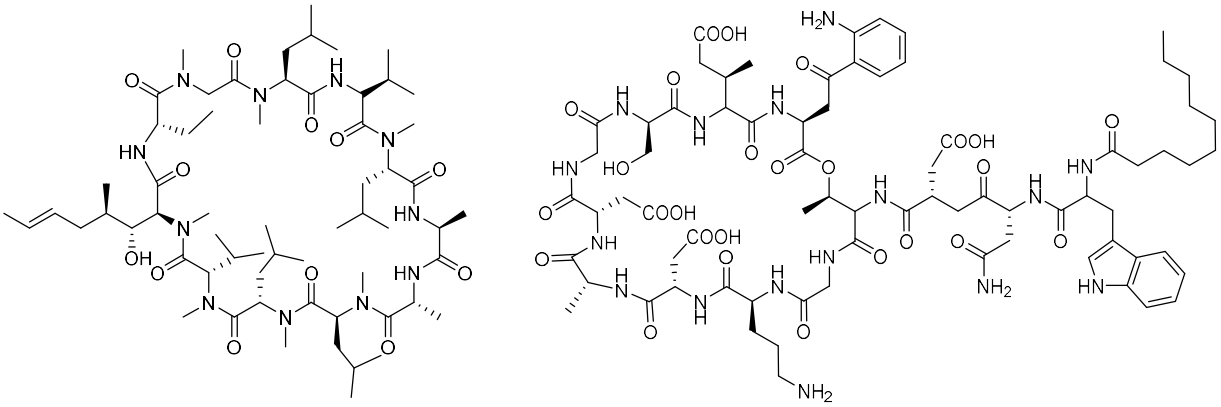

cyclosporin
Tolypocladium
immunosurppressive

daptomycin
Streptomyces
antimicrobial

Figure 4-12. Structures of cyclosporine and daptomycin

Amatoxins are bicyclic octapeptides, shown cytotoxicity by inhibiting mammalian RNA polymerase II [41]. Another class of sterol-binding bicyclic peptides known as theonellamides A-G isolated from marine sponge, exhibit both cytotoxic and antifungal activities [42]. Only a few bicyclic peptides were reported from marine ecosystem. Therefore, there have still a chance to get more structurally unique bicyclic peptides from marine-derived organisms.

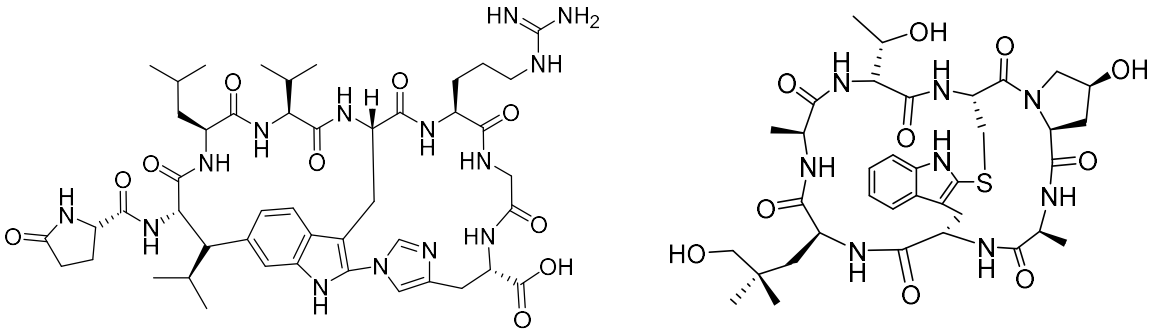

moroidin
Celosia
antimitotic

phalloidin
Amanita
antimicrobial

Figure 4-13. Chemical structures of moroidin and phalloidin

In this study, nyuzenamides A (**13**) and B (**14**) were discovered from the strain *Streptomyces*, possessing several unique components and exhibiting antifungal activity as well as cytotoxic activity. Four unusual amino acids were found in **13**. Hgy is a component of an antitumor antibiotic

spergualin from *Bacillus* [43], and cyclic peptides dolyemycins from *Streptomyces* [44] (Figure 4-13). Another nonstandard amino acid Hpa is a part of several cyclic peptides including dolyemycins [44], RP-1776 [45], and ohmyungsamycins [46], atratumycin [47], and atrovimycin [48] (Figure 4-13). All of those are cyclic peptides from *Streptomyces*. Htr is a component of an antibiotic drug vancomycins from *Amycolatopsis* [35] and ralstonins from *Ralstonia solanacearum* [49]. Hpg is also a building block of vancomycin [35] (Figure 4-13). The most rare structural feature in **13** is the diphenyl ether bridge to be a component of some cyclic peptides such as vancomycins [35] and seongsanamides [50], but the linkage pattern between aromatic amino acids Htr and Hpg is not reported before. The non-peptidic units which are named as Ica and Ppa in **13** and **14,** are also rare in nature, but these oxygenated moieties are reported as an acyl decoration unit in RP-1776 [45], atratumycin [47], atrovimycin [48], cinnapeptin [51] and eudistamides [52], all of which are monocyclic depsipeptides from Streptomyces (Figure 4-14). Although many bicyclic peptides such as anti-inflammatory depsipeptides salinamides from marine *Streptomycete* and seongsamides [53] are known in nature. In overall, **13** and **14** have no structural resemblance to any of the known natural peptides. Discovery of **13** and **14** expands the structural diversity of microbial peptides and provides new scaffolds for the discovery and development of new therapeutic agents for treating various diseases. Literature survey showed several cyclic peptides with unique structural feature and potential biological activity discovered from marine actinomycetes. In this study, two structurally unique bicyclic peptides were isolated from a marine derived *Streptomyces*. Both compounds exhibited selective antifungal activity against pathogenic filamentous fungi. From this study, I concluded that common bacterial taxa such as *Streptomyces* from unique, extreme, underexploited marine ecosystem can be a potential source of new compounds useful for drug lead discovery.

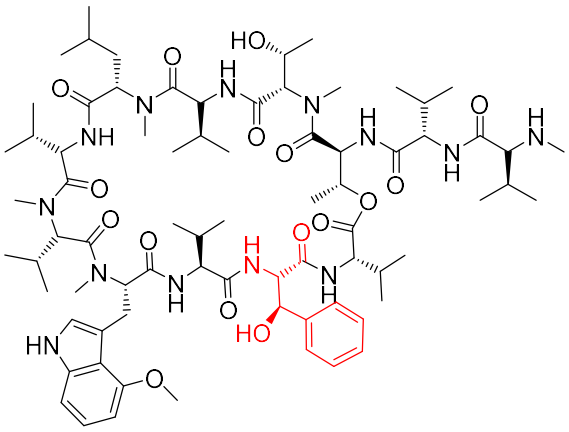

ohmyungsamycin A
Streptomyces
antibacterial

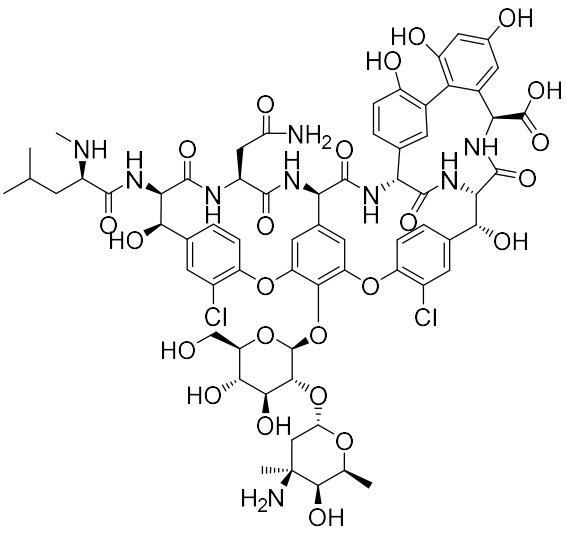

vancomycin
Streptomyces orientalis
antibacterial

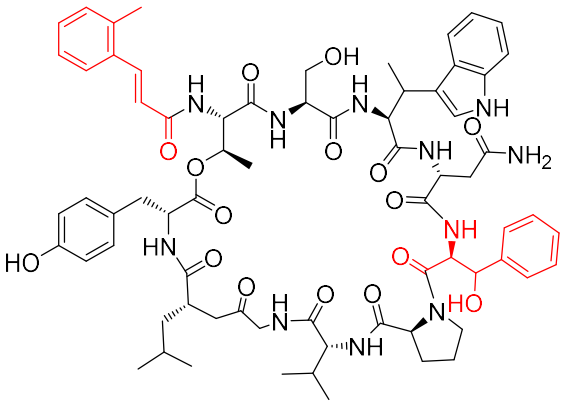

atratumycin
Streptomyces
antituberculosis

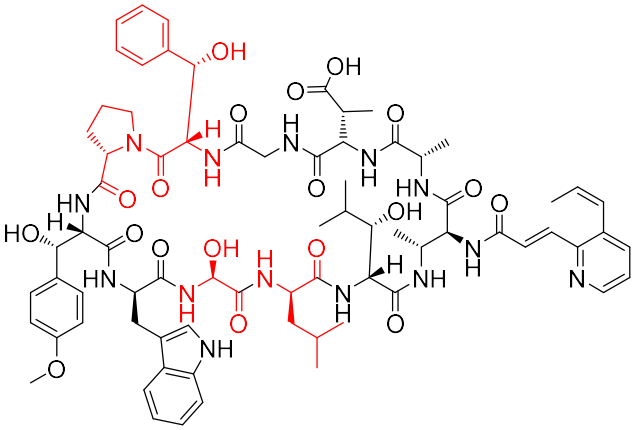

dolyemycin A
Streptomyces
anticancer

Figure 4-14. Structures of ohmyungsamycin A, vancomycins, atratumycin and dolyemycin A

Experimental Section

General. Optical rotations were measured on a JASCO P-1030 polarimeter. UV and IR spectra were recorded on a Shimadzu UV-1800 and a Perkin Elmer Spectrum 100 spectrophotometers, respectively. NMR spectra were recorded on a Bruker AVANCE II spectrometer using residual solvent peaks of DMSO-d_6 at δ_H 2.49 and δ_C 39.5 as internal standards. HRESITOFMS were measured on a Bruker micrOTOF focus mass spectrometer. Chiral-phase GC-MS analysis was executed on a Shimadzu GC-17A chromatograph coupled with QP-5000 mass spectrometer. X-ray crystallographic analysis was performed on an HPC diffractometer (Rigaku XtaLAB P200). HPLC analysis and purification were conducted on an Agilent HP1200 system.

Microorganism. Strain N11-34 was isolated from deposits on a spent filter used for filtration of DSW taken at the depth of -311 m at Nyuzen Deep-sea Water Park, Toyama, Japan. The deposits were spread on a plate of ISP4 agar medium (Difco Laboratories). After cultivation at 23 °C for 14 days, a single colony was transferred onto ISP2 agar medium (Difco Laboratories) to obtain a pure isolate. The strain was characterized as a member of the genus *Streptomyces* on the basis of 99.9% similarity of 16S rRNA gene sequence (1428 nucleotides; DDBJ accession number AB812839) to *Streptomyces hygroscopicus* subsp. *hygroscopicus* NBRC 13472^T (accession number BBOX01000593).

Fermentation. Strain N11-34 cultured on a Bn-2 slant [soluble starch 0.5%, glucose 0.5%, meat extract (Kyokuto Pharmaceutical Industrial Co., Ltd.) 0.1%, yeast extract (Difco Laboratories) 0.1%, NZ-case (Wako Chemicals USA, Inc.) 0.2%, NaCl 0.2%, $CaCO_3$ 0.1%, and agar 1.5% in distilled water] was inoculated into 500-mL K-1 flasks each containing 100 mL of V-22 seed medium [soluble starch 1%, glucose 0.5%, NZ-case 0.3%, yeast extract 0.2%, Tryptone (Difco Laboratories) 0.5%, K_2HPO_4 0.1%, $MgSO_4 \cdot 7H_2O$ 0.05%, and $CaCO_3$ 0.3% (pH 7.0) in distilled water]. The flasks were shaken on a rotary shaker (200 rpm) at 30 °C for 4 days. Aliquots (3 mL) of the resulting seed culture were transferred into 500-mL K-1 flasks each containing 100 mL of A-16 production medium [glucose 2%, Pharmamedia (Traders Protein) 1%, $CaCO_3$ 0.5%, and Diaion HP-20 (Mitsubishi Chemical Co.) in distilled water]. The pH of the medium was adjusted to 7.0 before sterilization. The inoculated flasks were placed on a rotary shaker (200 rpm) at 30 °C for 7 days.

Extraction and isolation. At the end of the fermentation period, 100 mL of 1-butanol was added to each flask, and they were shaken for 1 h. The mixture was centrifuged at 6,000 rpm for 10 min and

the organic layer was separated from the aqueous layer containing the biomass. Evaporation of the solvent gave 4.6 g of the extract from 2 L-culture. The extract (4.6 g) was subjected to silica gel column chromatography with a step gradient of $CHCl_3$-MeOH (1:0, 20:1, 10:1, 4:1, 2:1, 1:1, and 0:1 v/v). The fifth fraction (2:1) was concentrated to provide 475 mg of brown oily material. Further purification was achieved by preparative HPLC (Cosmosil AR-II, Nacalai Tesque Inc., 10 × 250 mm, 4 mL/min, UV detection at 254 nm) with 40% MeCN in 0.1% formic acid to give nyuzenamides A (**13**, 12.3 mg, t_R 10.0 min) and B (**14**, 14.5 mg, t_R 15.0 min).

Nyuzenamide A (13): colorless needles; mp 237~240˚C; $[\alpha]^{23}_D$ +27 (*c* 0.10, MeOH); UV (MeOH) λ_{max} (log ε) 203 (4.96), 273 (4.10) nm; IR (ATR) ν_{max} 3291, 1644, 1564, 1509 cm^{-1}; ^1H and ^{13}C NMR data, see Table S1; HRESITOFMS *m*/*z* 1370.5554 $[M + Na]^+$ (calcd for $C_{66}H_{81}N_{11}NaO_{20}$, 1370.5552).

Nyuzenamide B (14): pale yellow amorphous solid ; $[\alpha]^{23}_D$ +32 (*c* 0.10, MeOH); UV (MeOH) λ_{max} (log ε) 203 (5.12), 276 (4.31) nm; IR (ATR) ν_{max} 3284, 1650, 1556, 1505 cm^{-1}; ^1H and ^{13}C NMR data, see Table S2; HRESITOFMS *m*/*z* 1384.5706 $[M + Na]^+$ (calcd for $C_{67}H_{83}N_{11}NaO_{20}$, 1384.5708).

Amino acid analysis by chiral GC-MS. Compounds **13** and **14** (0.1 mg each) were respectively dissolved in 6 M HCl (100 μl) and heated at 105 °C for overnight in a sand bath. The reaction mixtures were dried by a stream of N_2, and then methylated in 10% HCl in MeOH (0.3 mL) at 100 °C for 30 min in a pressure vial. After removing the solvent and reagent with a N_2 stream, and the residues were acylated with trifluoroacetic anhydride (0.3 mL) in CH_2Cl_2 (0.3 mL) at 100 °C for 5 min. The reaction mixture was brought to dryness and dissolved in CH_2Cl_2. For preparation of analytical standards, authentic amino acids were derivatized in the same manner. The prepared analytes were dissolved in CH_2Cl_2 to make 1 mg/mL solutions, and aliquots (0.3 μL) were chromatographed on a Chirasil-L-Val capillary column (Agilent Technologies, 25 m × 0.25 mm i.d., 0.12 μm film thickness) with a split ratio of 1:50. Temperatures were set to 250 °C at the injection port and 230 °C at the transfer line to the detector. The oven temperature program was 60 °C for 3 min, 10 °C/min heat ramp to 200 °C, and the same temperature held for 5 min. Peaks for *N*-trifluoroacetyl methyl ester derivatives of the amino acids were identified by checking the EI mass fragmentation pattern against NIST/EPA/NIH mass spectral library, and compared the retention times with those of analytical standards for chirality determination. Retention times for standard amino acids were D-Val 6.54 min, D/L-Val 6.60 and 6.97 min, D-Thr 7.07 min, L-Thr 7.54 min, D-*allo*-Thr 8.99 min, L-*allo*-Thr 9.47 min, D-Pro 8.19 min, L-Pro 8.52 min, D-Leu 8.82 min, L-Leu

9.39 min, D-Asp 10.32 min, and L-Asp 9.58 min. The hydrolysate of nyuzenamide A gave peaks for L-Val (6.95 min), L-Thr (7.57 min), L-Pro (8.57 min), D-Leu (8.82 min), and D-Asp (10.37 min), while that of nyuzenamide B gave L-Val (6.96 min), L-Thr (7.59 min), L-Pro (8.56 min), D-Leu (8.84 min), and D-Asp (10.36 min).

X-ray crystallographic analysis

During the storage of the NMR sample solution of **13** in a refrigerator, crystalline particles were formed, which were recovered and recrystallized from a mixture of MeOH-CH_2Cl_2 to provide colorless needles. Some crystals appeared, and for single crystal parsing, crystals were selected with sizes of 0.28 mm × 0.15 mm × 0.06 mm. All diffraction data were obtained on a HPC diffractometer (Rigaku XtaLAB P200) equipped with graphite-monochromated Cu Kα radiation. CCDC-2026824 (nyuzenamide A) contains the supplementary crystallographic data. These data can be obtained free of charge from the Cambridge Crystallographic Data Centre (http://www.ccdc.cam.ac.uk/). Thermal ellipsoids are shown at the 30% level.

Bioassays

Antimicrobial activity was evaluated in a similar manner previously reported in ref 1, for *Kocuria rhizophila* ATCC9341, *Staphylococcus aureus* FDA209P JC-1, *Escherichia coli* NIHJ JC-2, *Rhizobium radiobacter* NBRC14554, *Tenacibaculum maritimum* NBRC16015 and non-filamentous *Candida albicans* NBRC0197 were used as indication strains. As for filamentous fungi, the antimicrobial activity was tested described in ref 1 after inoculum preparation of pathogen stains *Glomerella cingulata* NBRC5907 and *Trichophyton rubrum* NBRC5467. Filamentous fungi were subcultured from the stock water suspensions on Sabouraud dextrose agar and incubated at 25 °C. After 5 to 7 days, freshly cultured fungi colonies were used for preparing the inoculum suspensions. The colonies were covered with 5 ml of sterized distilled water and the inoculum was obtained by carefully scraping the colonies with a sterile loop and withdrawing the resulting suspension with a sterile Pasteur pipette. Then, the suspensions obtained were filtered through sterile gauze to remove the majority of hyphae, producing an inoculum mainly composed of spores. The suspension collected in a sterile tube and inoculum size was adjusted by adding sterile distilled water to a concentration of 1×10^5 cfu/ml by microscopic enumeration with a hemacytometer cell counting chamber. These inoculum suspensions were used to evaluate the antifungal activity of compounds **13** and **14**.

Cytotoxicity against P388 murine leukemia cells were examined according to a protocol described in ref 54. The positive control, doxorubicin, displayed IC_{50} of 0.06 μM.

References

1) Subramani, R.; Aalbersberg, W. *Microbiol. Res.* **2012**, *167*, 571-580.
2) Sivalingam, P.; Hong, K.; Pote, J.; Prabakar, K. *Int J Microbiol.* **2019**, *2019*, 20-39.
3) Dictionary of Natural Products 27.2. CRC Press, *Taylor & Francis Group*; **2018**. http://dnp.chemnetbase.com/ (accessed May 2, 2021)
4) Dang, T.; Süssmuth, R. D. *Acc. Chem. Res.* **2017**, *50*, 1566-1576.
5) Harrison, J.; Studholm, D. J. *Microb. Biotechnol.* **2014**, *7*, 373-380.
6) Lee, N.; Kim, W.; Hwang, S.; Lee, Y.; Cho, S.; Palsson, B.; Cho, B-K. *Sci. Data* **2020**, *7*, 55-62.
7) Calteau, A.; Fewer, D. P.; Latifi, A.; Coursin, T.; Laurent, T.; Jokela, J.; Kerfeld, C. A.; Sivonen, K.; Piel, J.; Gugger, M. *BMC Genom.* **2014**, *15*, 977-990.
8) Gregory, K.; Salvador, L. A.; Akbar, S.; Adaikpoh, B. I.; Stevens, D. C. *Microorganisms* **2019**, *7*, 181-190.
9) Gao, Y. –M.; Wang, X. –J.; Zhang, J.; Li, M.; Liu, C. –X.; An, J.; Jiang, L.; Xiang, W. –S. *J. Agric. Food Chem.* **2012**, *60*, 9874–9881.
10) Ryu, M. –J.; Hwang, S.; Kim, S.; Yang, I.; Oh, D. –C. Sang-Jip Nam, S. –J.; Fenical, W. *Org. Lett.* **2019**, *21*, 5779–5783.
11) Alvarez-Mico, X.; Jensen, P. R.; Fenical, W.; Hughes, C. C. *Org. Lett.* **2013**, *15*, 988–991.
12) Nakasone, T.; Akeda, S. 1999. *UJNR Technical Report*. **1999**, *28*, 69–75.
13) DeepOcean Water Applications Society:http://www.dowas.net/facilities/index.html[In Japanese]
14) Hataguchi, Y.; Tai, H.; Nakajima, H.; Kimata, H. *Eur. J. Clin. Nutr*. **2005**, *59*, 1093–1096.
15) Katsuda, S. I.; Yasukawa, T.; Nakagawa, K.; Miyake, M.; Yamasaki, M.; Katahira, K.; Mohri, M.; Shimizu, T.; Hazama, *A. Biol. Pharm. Bull*. **2008**, *31*, 38–44.
16) Ikeda, T.; Hayashi, M.; Otsuka, K. *International Society of Offshore and Polar Engineers* **2002**, 480–485.
17) Imada, C. *Mar. Biol*, **2013**, 21–31.
18) Furumai, T.; Takagi, K.; Igarashi, Y.; Saito, N.; Oki, T. *J. Antibiot*. **2000**, *53*, 227-232.
19) Furumai, T.; Igarashi, Y.; Higuchi, H.; Saito, N.; Oki, T. *J. Antibiot*. **2002**, *55*, 128-133.
20) Furumai, T.; Eto, K.; Sasaki, T.; Higuchi, H.; Onaka, H.; Saito, N.; Fujita, T.; Naoki, H.; Igarashi, Y. *J. Antibiot*. **2002**, *55*, 873-80.
21) Zhang, G.; Zhang, Y.; Yin, X.; Wang, S. *Int. J. Syst. Evol. Microbiol.* **2015**, *65*, 516–521.

22) Hong, S. G.; Lee, Y. K.; Yim, J. H.; Chun, J.; Lee, H. K. *Int. J. Syst. Evol. Microbiol.* **2008**, *58*, 50–52.

23) Zhang, L.; Xi, L.; Ruan, J.; Huang, Y. *Syst. Appl. Microbiol.* **2012**, *35*, 81–85.

24) Wang, X.; Reynolds, A. R.; Elshahawi, S. I.; Shaaban, K. A.; Ponomareva, L. V.; Saunders, M. A.; Elgumati, I. S.; Zhang, Y.; Copley, G. C.; Hower, J. C.; Sunkara, M.; Morris, A. J.; Kharel, M. K.; Van, Lanen S. G.; Prendergast, M. A.; Thorson, J. S. *Org. Lett.* **2015**, *17*, 2796–2799.

25) David, L.; Ayala, H. L.; Tabet, J. C. *J. Antibio*. **1985**, *38*, 1655-63.

26) Igarashi, Y.; Kim, Y.; In, Y.; Ishida, T.; Kan, Y.; Fujita, T.; Iwashita, T.; Tabata, H.; Onaka, H.; Furumai, T. *Org Lett.* **2010**, *12*, 3402-3405.

27) Lee, H. S.; Shin, H. J.; Jang, K. H.; Kim, T. S.; Oh, K. B.; Shin, J. *J. Nat. Prod*. **2005**, *68*, 623-625

28) Sasaki, T.; Igarashi, Y.; Ogawa, M.; Furumai, T. *J. Antibiot*. **2002**, *55*, 1009-1012.

29) Fenical, W. *Chem. Rev.* **1993**, *93*, 1673–1683.

30) Bull, A. T.; Ward, A. C.; Goodfellow, M. *Microbiol. Mol. Biol. Rev*. **2000**, *64*, 573–606.

31) Skropeta, D.; Wei, L. *Nat. Prod. Rep.* **2014**, *31*, 999–1025.

32) Deep Ocean Water Application Society. http://www.dowas.net/english/index.html.

33) Zampolli, M.; Meunier, D.; Sternberg, R.; Raulin, F.; Szopa, C.; Pietrogrande M. C.; Dondi, F. *Chirality*. **2006**, *18*, 279-295.

34) Rhodes, C. A.; Pei, D. *Chem. Eur. J.* **2017**, *23*, 12690–12703.

35) Kahne, D.; Leimkuhler, C.; Lu, W.; Walsh, C. *Chem. Rev*. **2005**, *105*, 425-448.

36) Li, F.; Ma, L.; Zhang, X.; Chen, J.; Qi, F.; Huang, Y.; Qu, Z.; Yao, L.; Zhang, W.; Kim E. S.; Li, S. *Synth Syst Biotechnol*. **2020**, *5*, 236-243.

37) Steenbergen, J. N.; Alder, J.; Thorne G. M.; Tally F. P. *J Antimicrob Chemother*. **2005**, *55*, 283-288.

38) Chung, B. K. W.; Yudin, A. K.; *Org. Biomol. Chem*. **2015**, *13*, 8768–8779.

39) Morita, H.; Shimbo, K.; Shigemori, H.; Kobayashi, J. *Bioorg. Med. Chem. Lett*. **2000**, *10*, 469–471.

40) Lengsfeld, A. M.; Lçw, I.; Wieland, T.; Dancker, P.; Hasselbach, W.; *Proc. Natl. Acad. Sci. USA* **1974**, *71*, 2803–2807.

41) Hallen, E.; Luo, H.; J. S. Scott-Craig, J. S.; Walton, J. D. *Proc. Natl. Acad. Sci. USA* **2007**, *104*, 19097–1910.

42) Matsunaga, S.; Fusetani, N.; Hashimoto, K.; Walchli, M. *J. Am. Chem.Soc*. **1989**, *111*, 2582–2588.

43) Umezawa, H.; Kondo, S.; Iinuma, H.; Kunimoto, S.; Ikeda, Y.; Iwasawa, H.; Ikeda, D.; Takeuchi, T. *J. Antibiot.* **1981**, *34*, 1622-1624.

44) Liu, X-D.; Gu, K-B.; X. S-S.; Zhang, D-J.; Li, Y-G. *J. Antibiot*. **2018**, *71*, 838-845.

45) Toki, S.; Agatsuma, T.; Ochiai, K.; Saitoh, Y.; Ando, K.; Nakanishi, S.; Lokker, N. A.; Giese, N. A.; Matsuda, Y. *J. Antibiot*. **2001**, *54*, 405-414.

46) Um, S.; Choi, T. J.; Kim, H.; Kim, B. Y.; Kim, S-H.; Lee, S. K.; Oh, K-B.; Shin, J.; Oh, D-C. *J. Org. Chem.* **2013**, *78*, 12321-12329.

47) Sun, C.; Yang, Z.; Zhang, C.; Liu, Z., He, J.; Liu, Q.; Zhang, T.; Ju, J.; Ma, J. *Org. Lett*. **2019**, *21*, 1453-1457.

48) Liu, Q.; Liu, Z.; Sun, C.; Shao, M.; Ma, J.; Wei, X.; Zhang, T.; Li, W.; Ju, J. *Org. Lett*. **2019**, *21*, 2634-2638.

49) Murai, Y.; Mori, S.; Konno, H.; Hikichi, Y.; Kai, K. *Org. Lett*. **2017**, *19*, 4175-4178.

50) Kim, G. J.; Li, X.; Kim, S-H.; Yang, I.; Hahn, D.; Chin, J.; Nam, S.-J.; Nam, J.-W.; Nam, D. H.; Oh, D.-C.; Chang, H. W.; Choi, H. *Org. Lett*. **2018**, *20*, 7539-7543.

51) Zhang, C.; Seyedsayamdost, M. R. *Angew. Chem. Int. Ed*. **2020**, *59*, 23005−23009.

52) Zhang, F.; Adnani, N.; Vazquez-Rivera, E.; Braun, D. R.; Tonelli, M.; Andes, D. R.; Bugni, T. S. *J. Org. Chem*. **2015**, *80*, 8713− 8719.

53) Trischman, J. A.; Tapiolas, D. M.; Jensen, P. R.; Dwight, R.; Fenical, W.; McKee, T. C.; Ireland, C. M.; Stout, T. J.; Clardy, J. *J. Am. Chem. Soc*. **1994**, *116*, 757−758.

54) Sharma, A. R.; Zhou, T.; Harunari, E.; Oku, N.; Trianto, A.; Igarashi, Y. *J. Antibiot*. **2019**, *72*, 634–639.

4-5 Spectral Data

Table of Contents

Figure S1. High resolution ESI-TOF mass spectra of **13** and **14**

Nyuzenamide A (**13**)

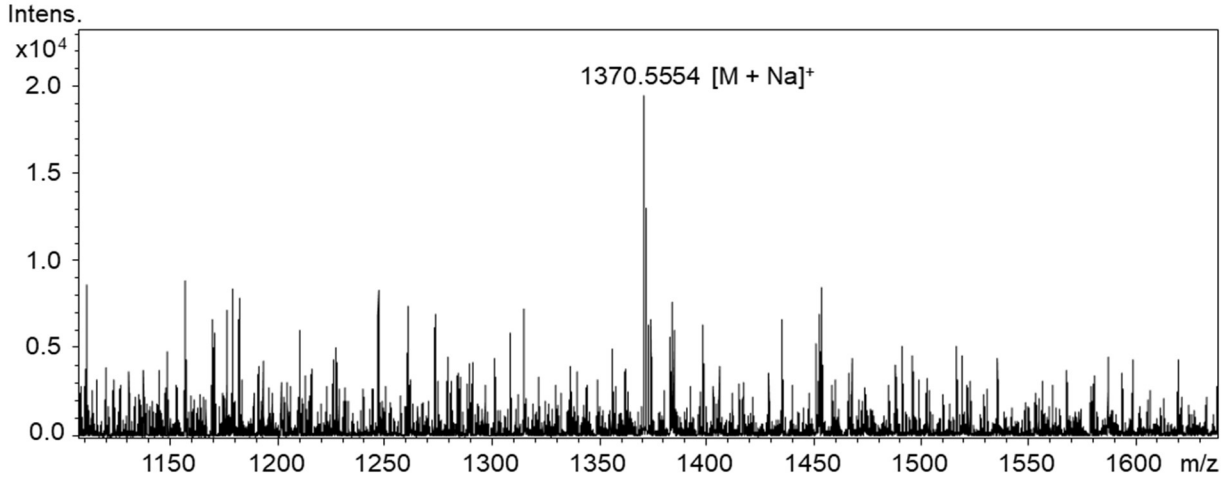

Nyuzenamide B (**14**)

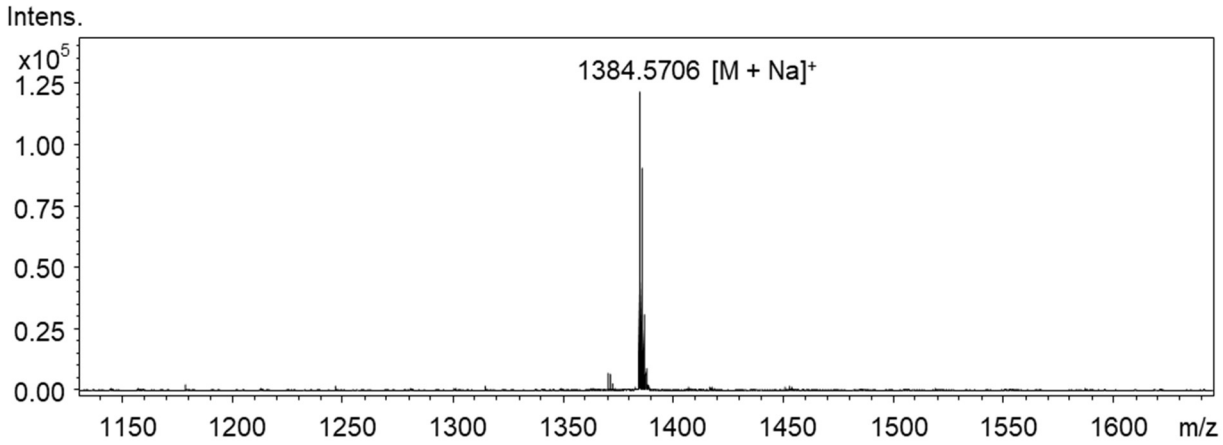

Figure S2. UV spectra of **13** and **14**

Nyuzenamide A (**13**)

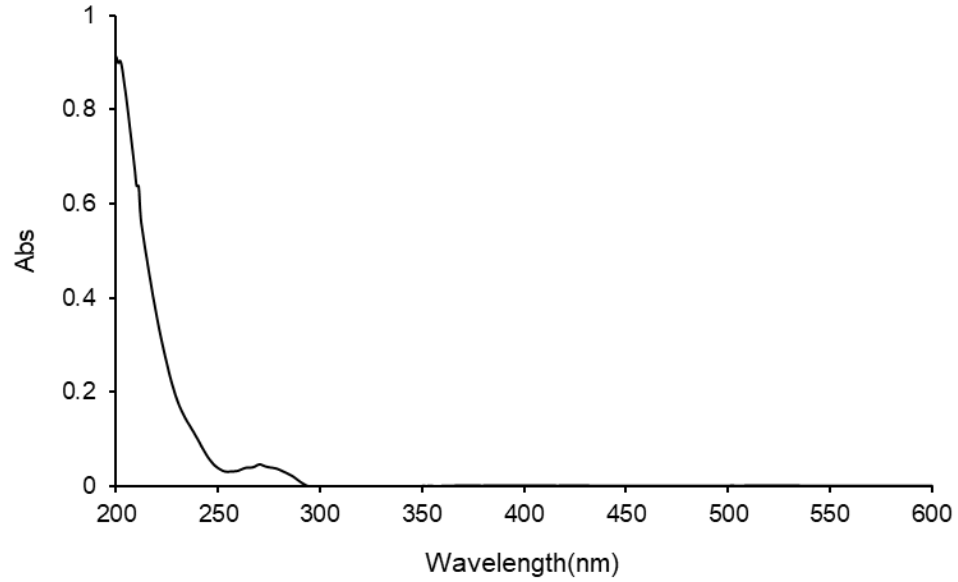

Nyuzenamide B (**14**)

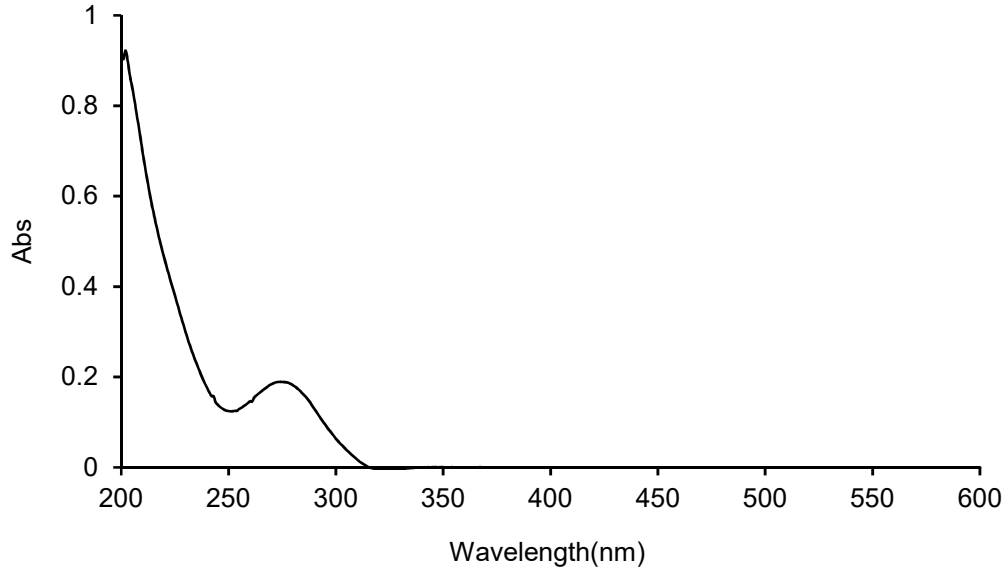

Figure S3. IR spectra of **13** and **14**

Nyuzenamide A (**13**)

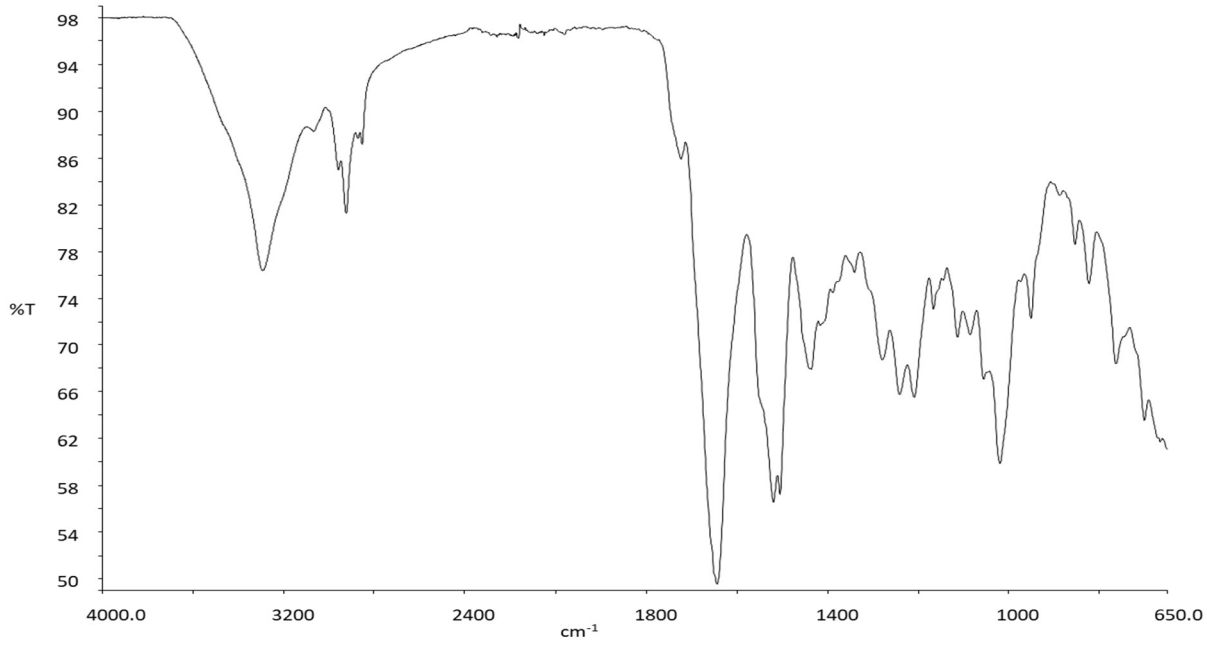

Nyuzenamide B (**14**)

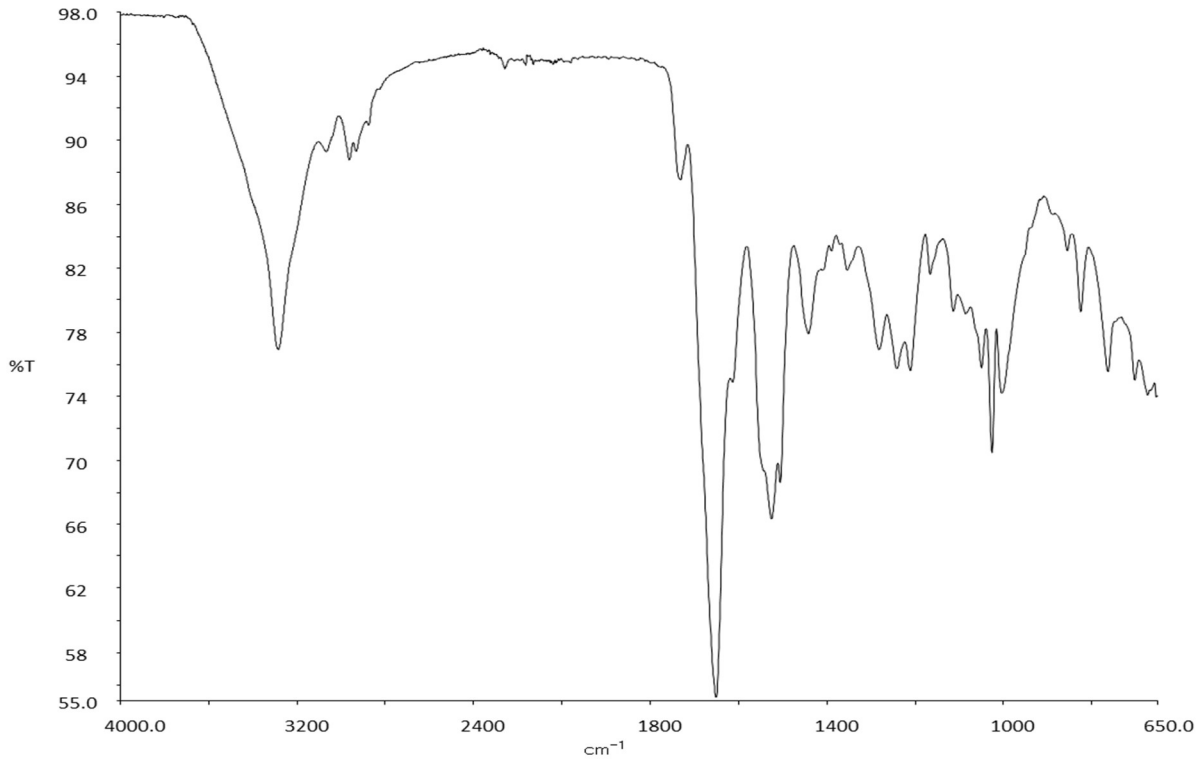

Figure S4. ^{1}H NMR spectrum of **13** (500 MHz, DMSO-d_6)

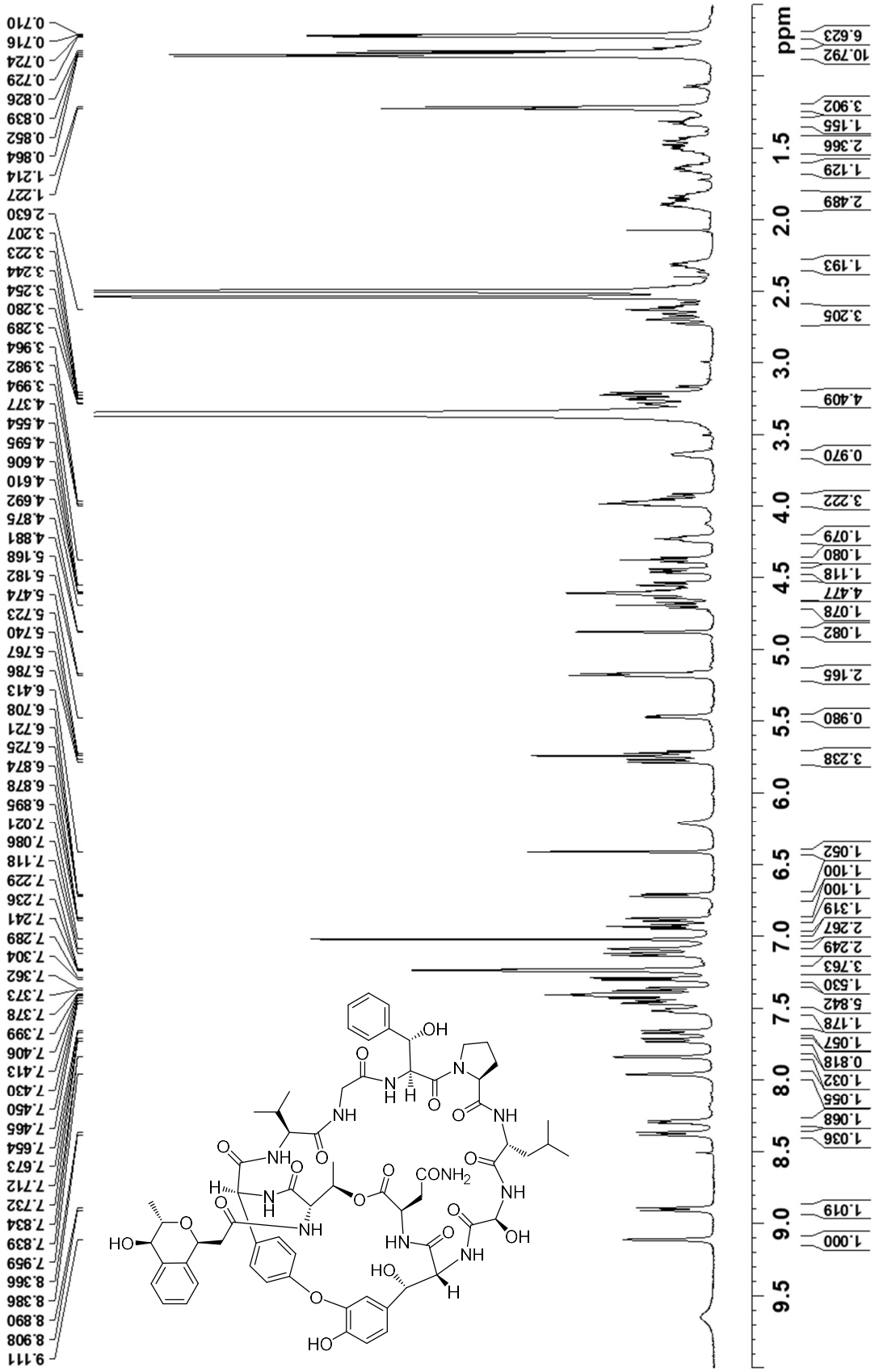

Figure S5. ^{13}C NMR spectrum of **13** (125 MHz, DMSO-d_6)

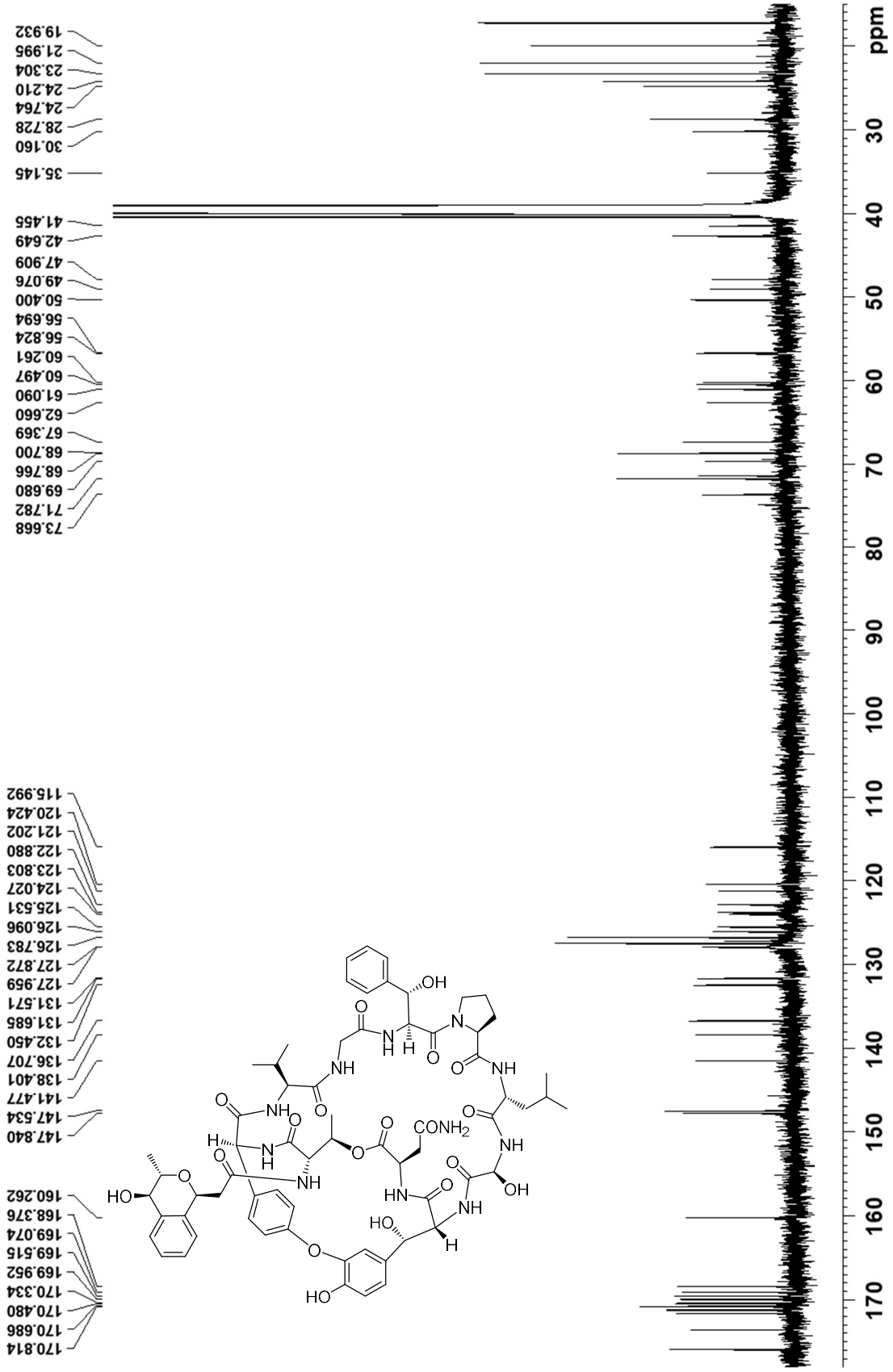

Figure S6. COSY spectrum of **13** (500 MHz, DMSO-d_6)

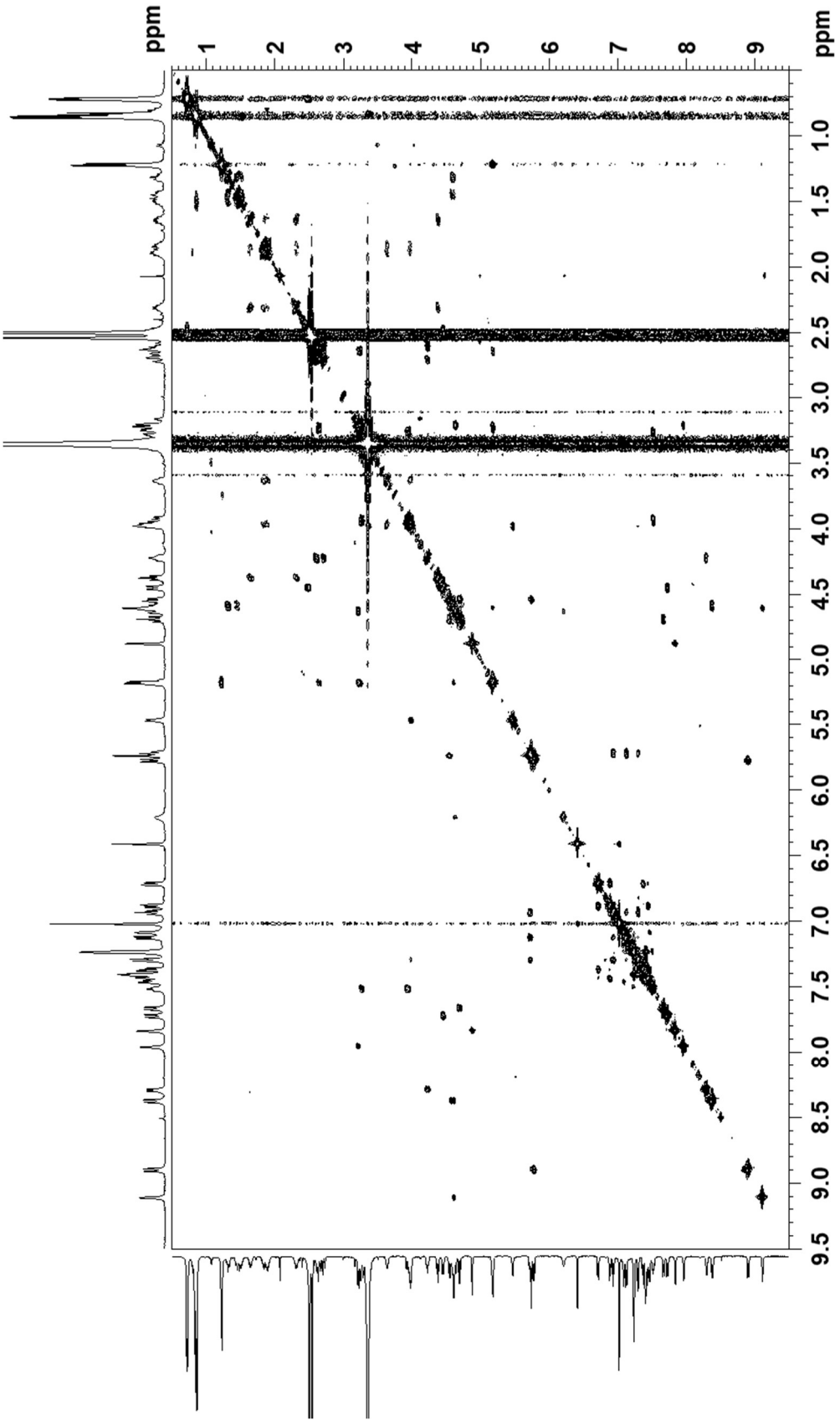

Figure S7. ROESY spectrum of **13** (500 MHz, DMSO-d_6)

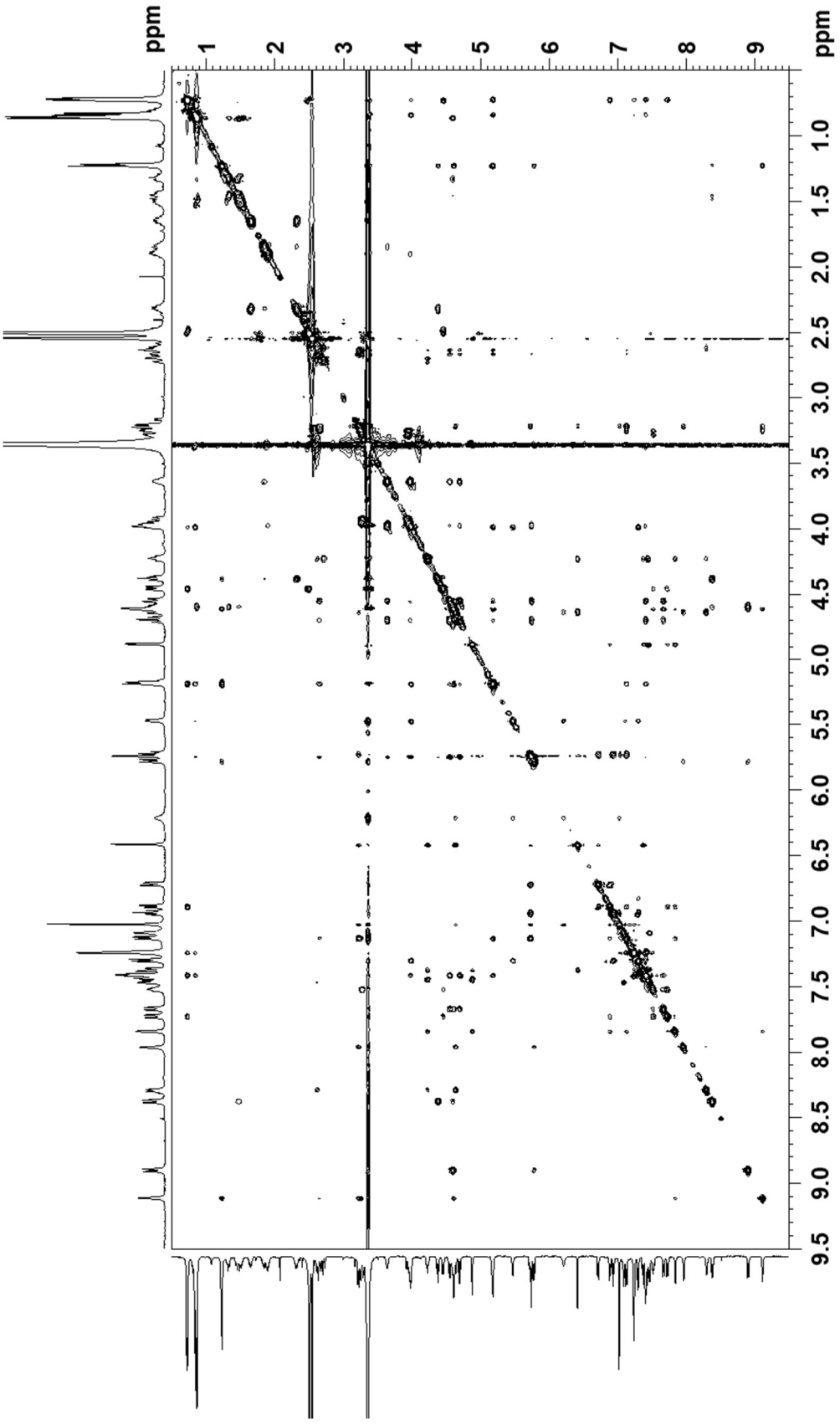

Figure S8. HSQC spectrum of **13** (500 MHz, DMSO-d_6)

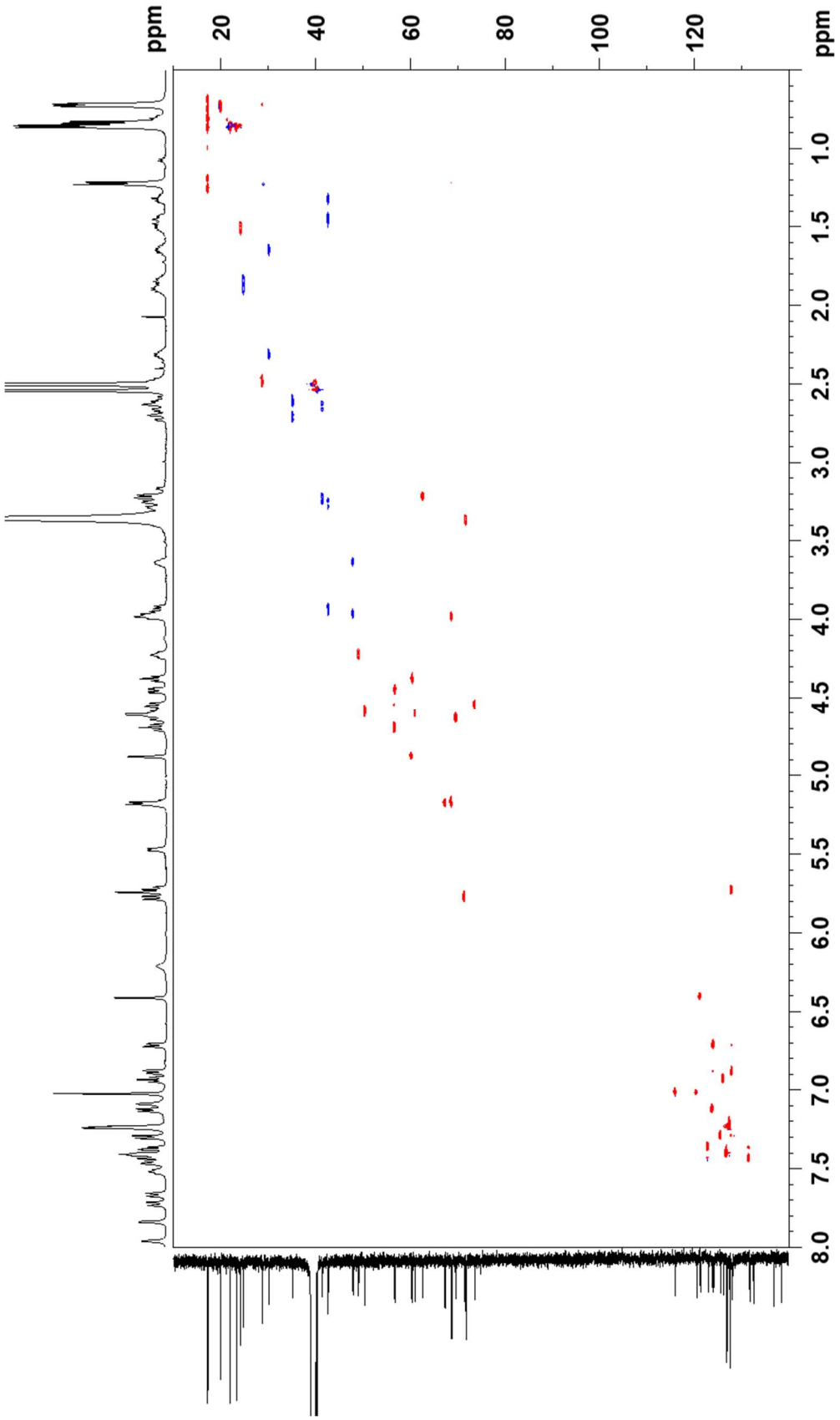

Figure S9. HMBC spectrum of **13** (500 MHz, DMSO-d_6)

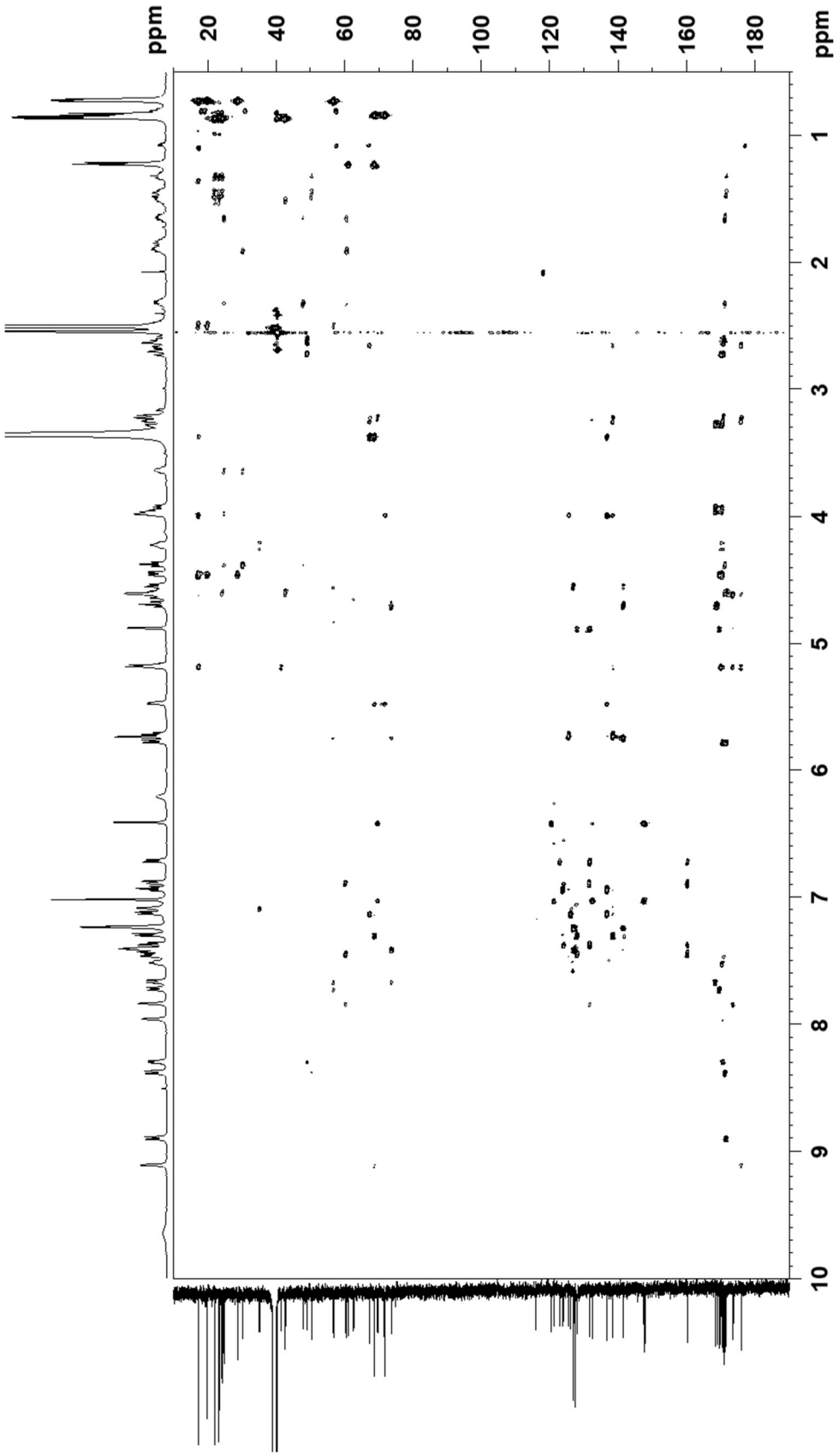

Figure S10. ^{1}H NMR spectrum of **14** (500 MHz, DMSO-d_6)

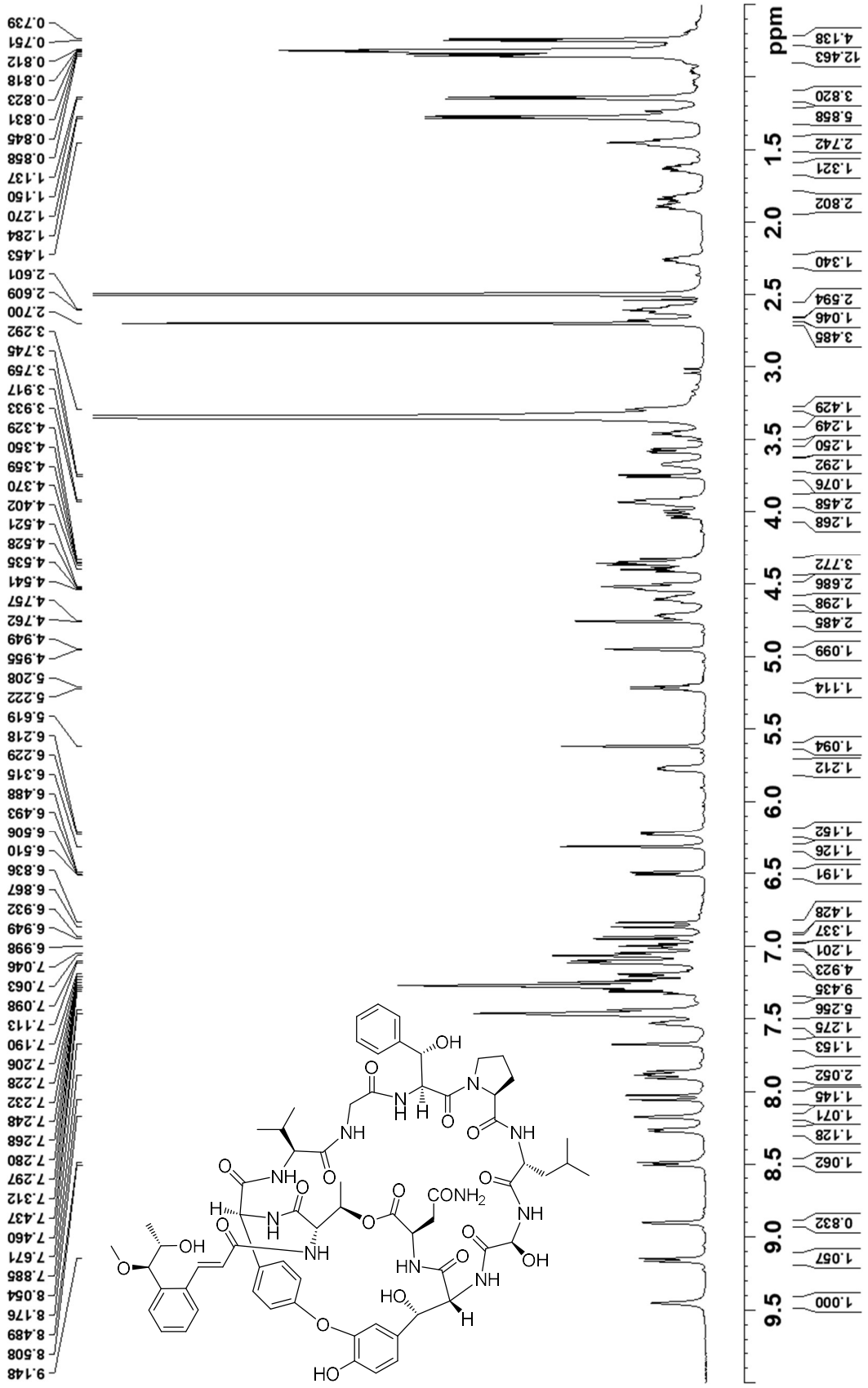

Figure S11. ^{13}C NMR spectrum of **14** (125 MHz, DMSO-d_6)

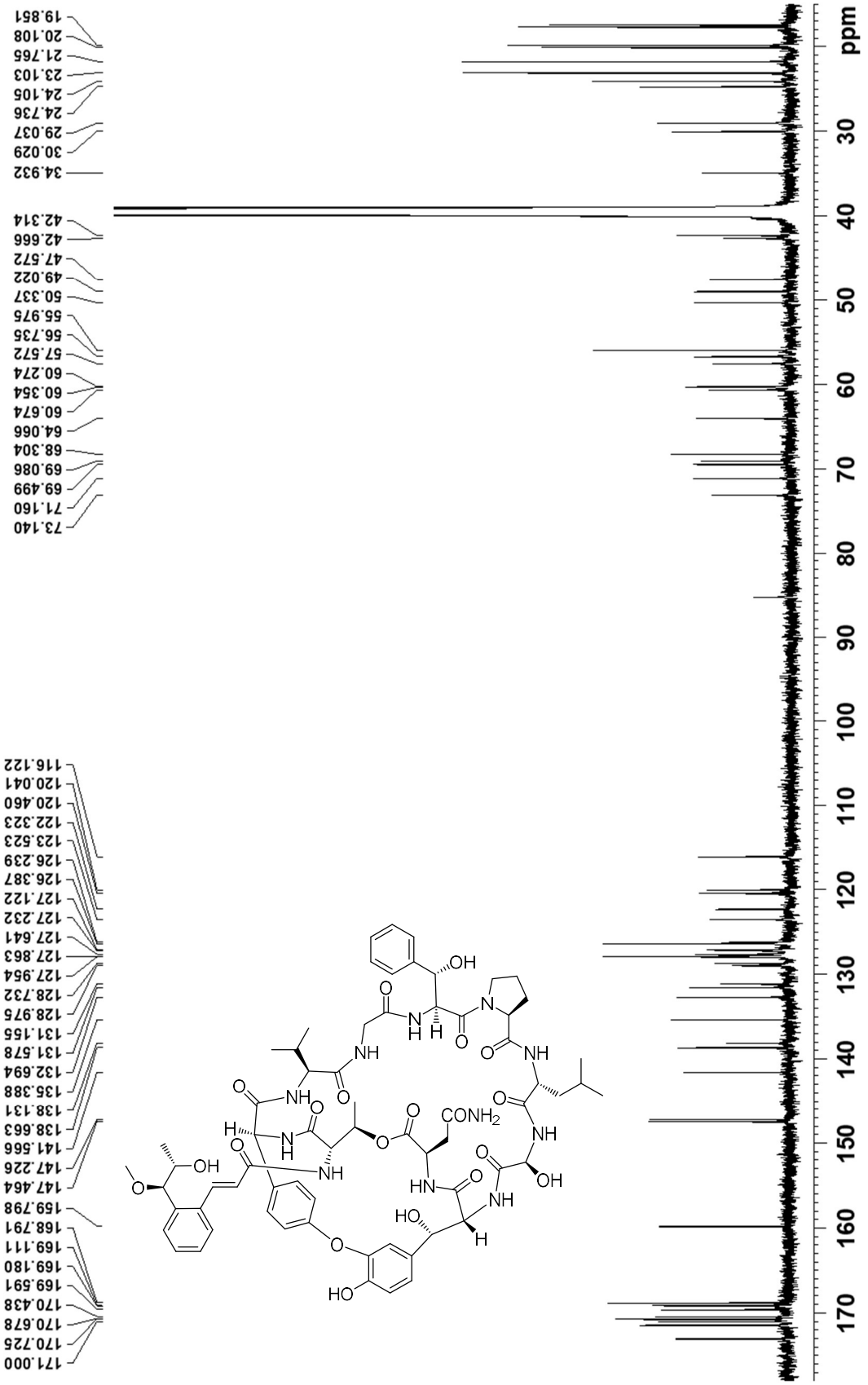

Figure S12. COSY spectrum of **14** (500 MHz, DMSO-d_6)

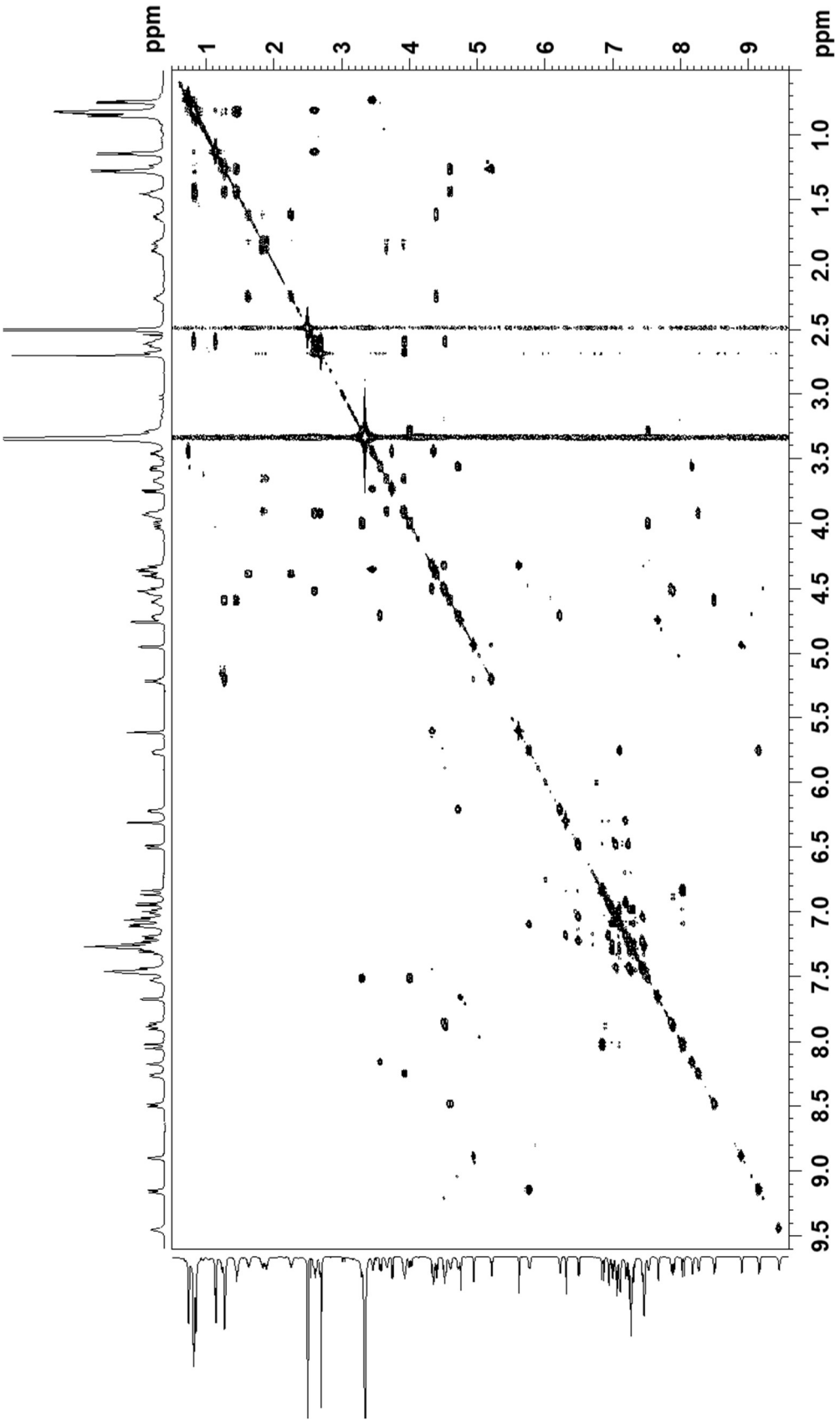

Figure S13. ROESY spectrum of **14** (500 MHz, DMSO-d_6)

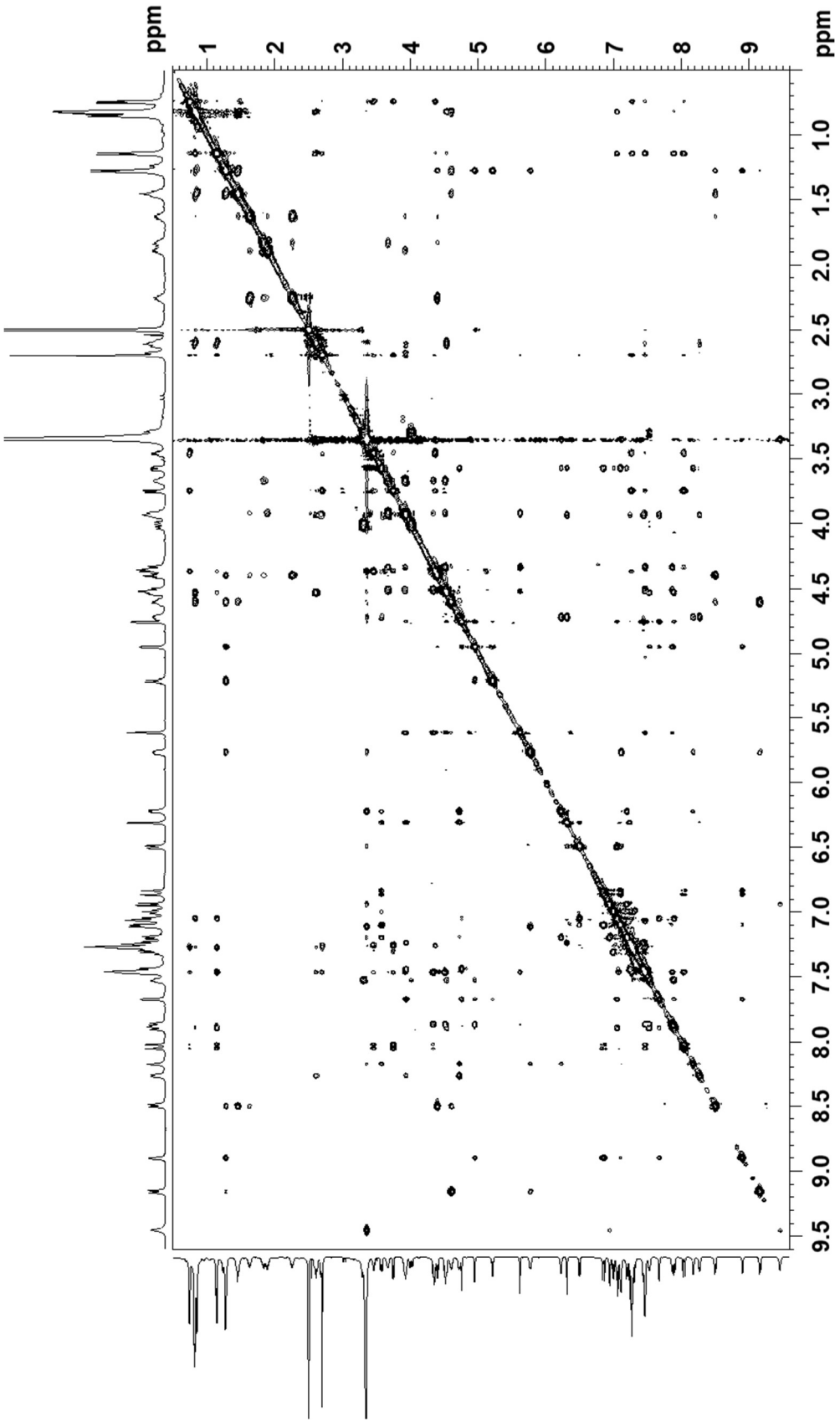

Figure S14. HSQC spectrum of **14** (500 MHz, DMSO-d_6)

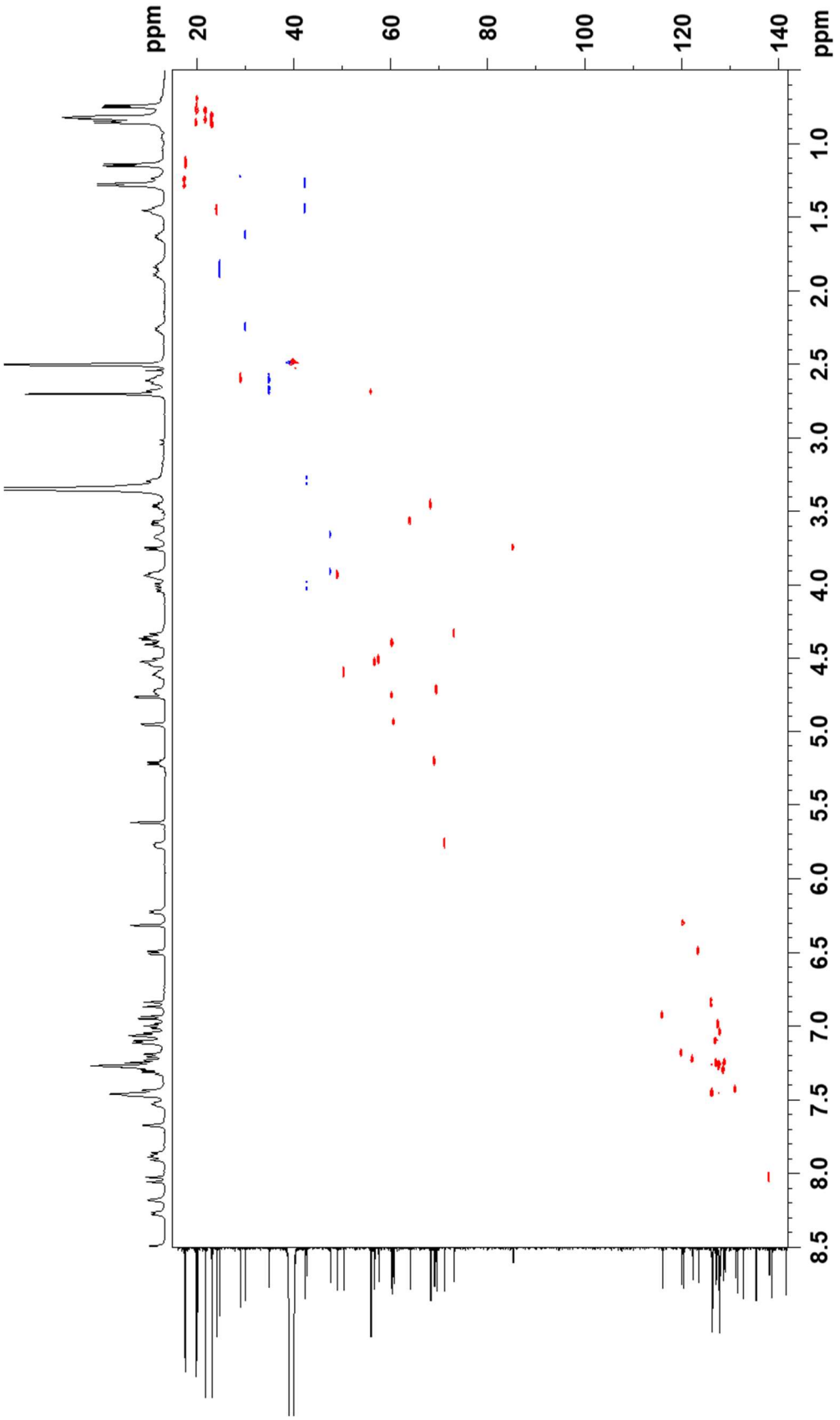

Figure S15. HMBC spectrum of **14** (500 MHz, DMSO-d_6)

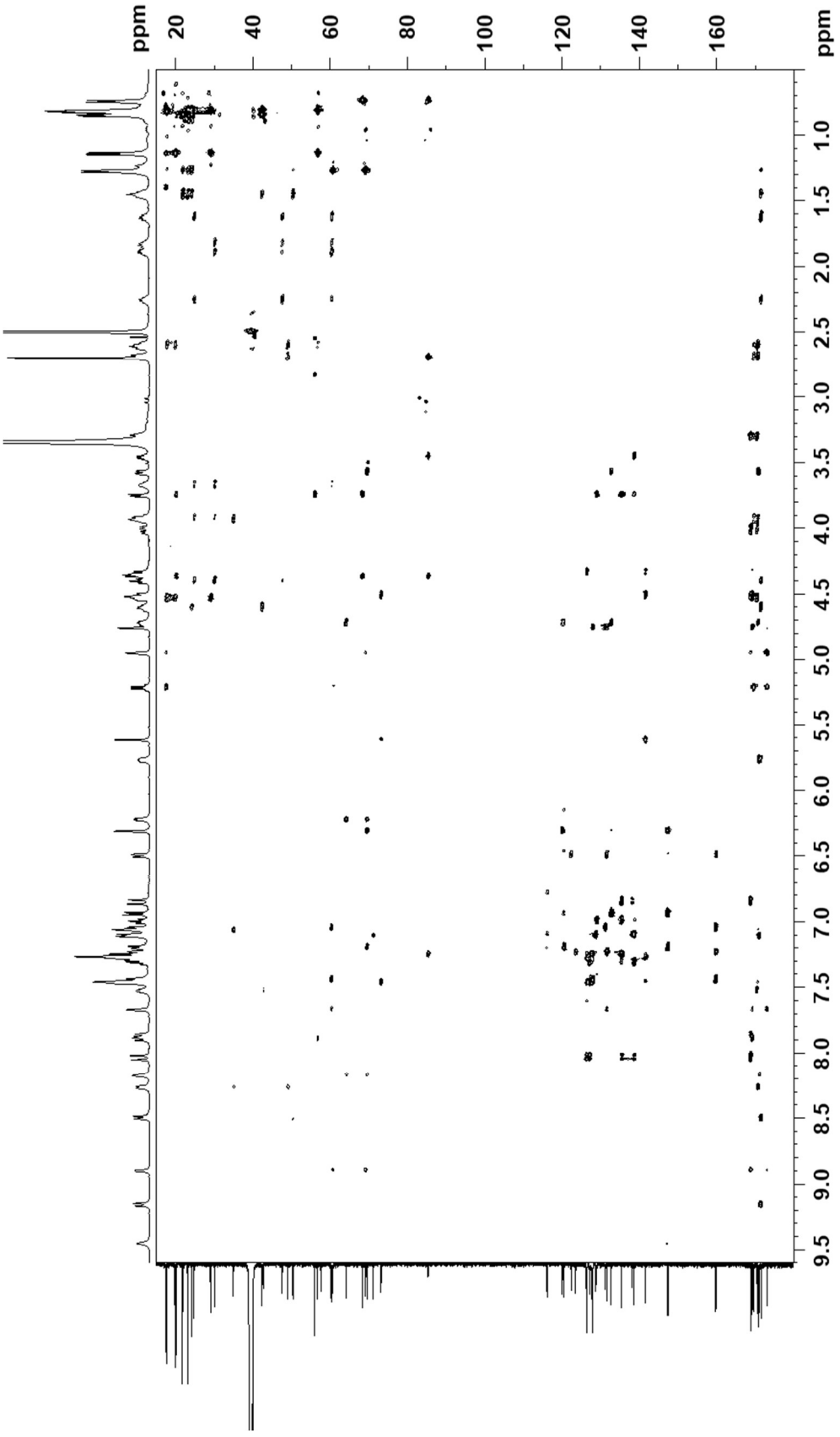

Figure S16. Chiral-phase GC-MS analyses of acid-hydrolysates of **13** and **14**

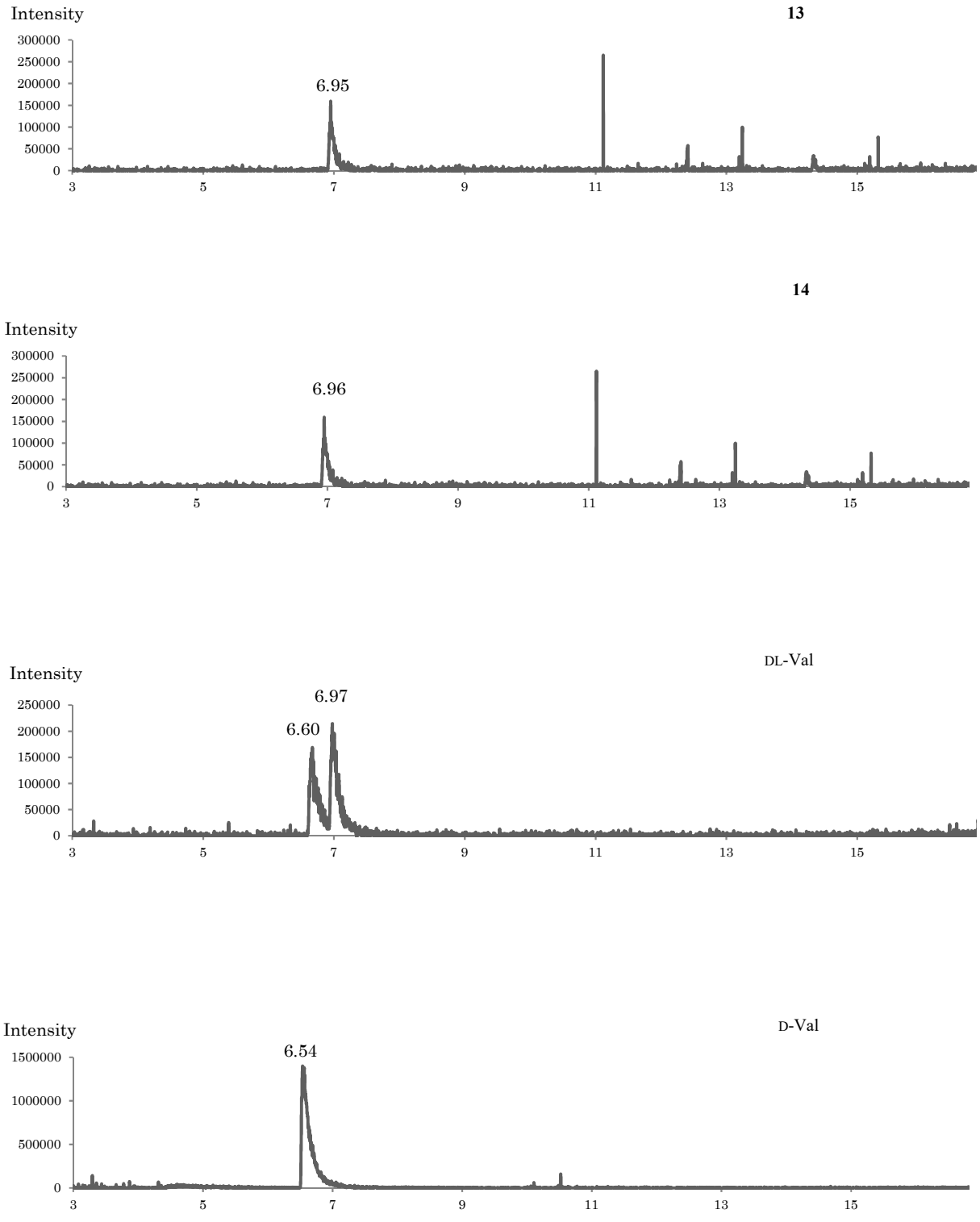

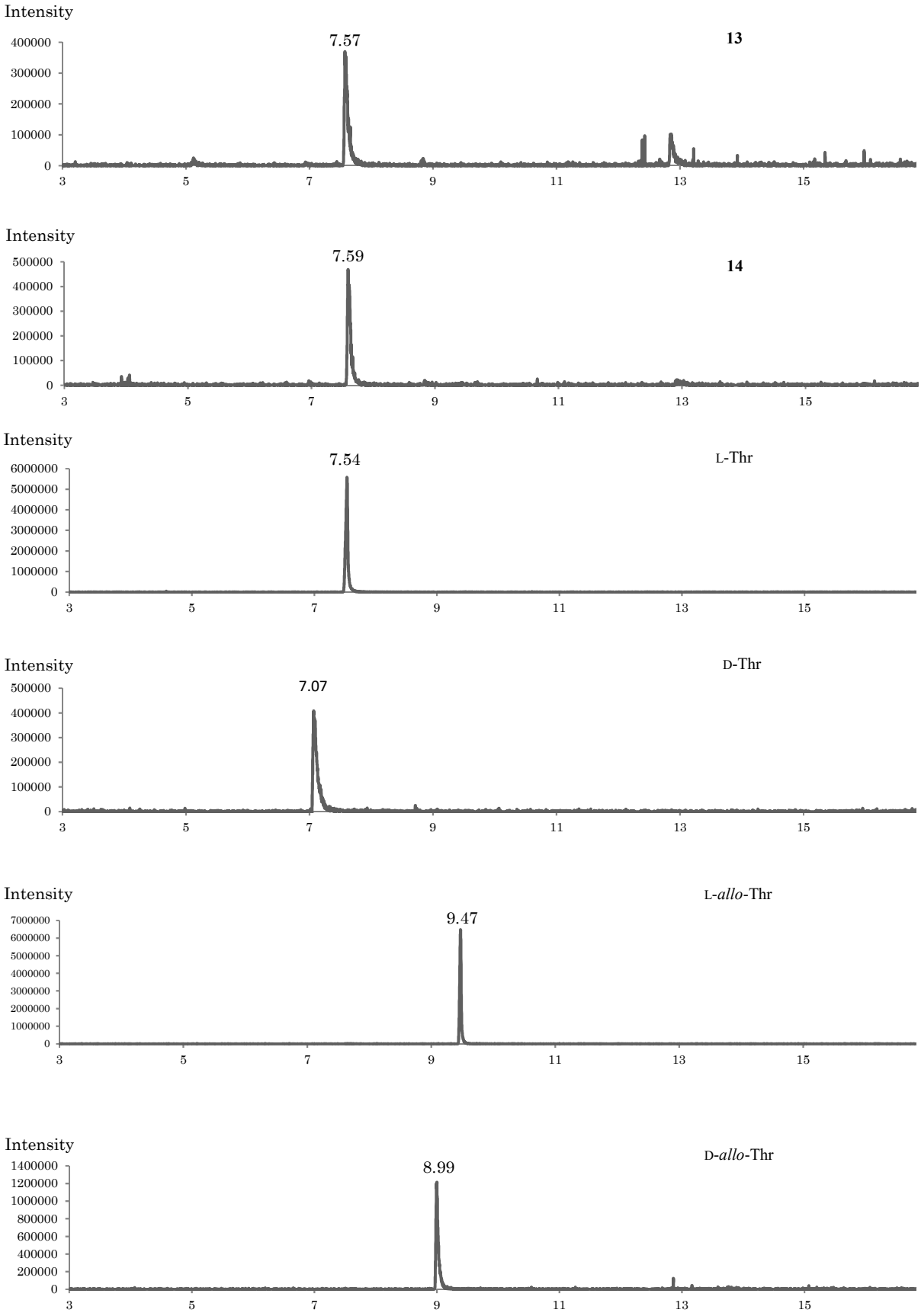
Intensity
7.57
13
Intensity
7.59
14
Intensity
7.54
L-Thr
Intensity
7.07
D-Thr
Intensity
9.47
L-*allo*-Thr
Intensity
8.99
D-*allo*-Thr

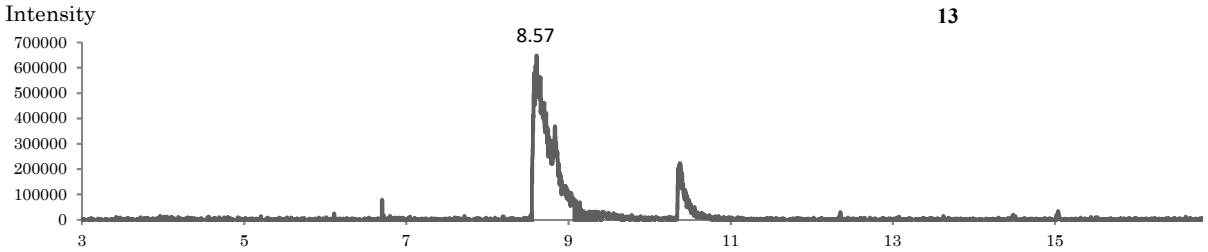
Intensity
13
8.57
700000
600000
500000
400000
300000
200000
100000
0
3
5
7
9
11
13
15

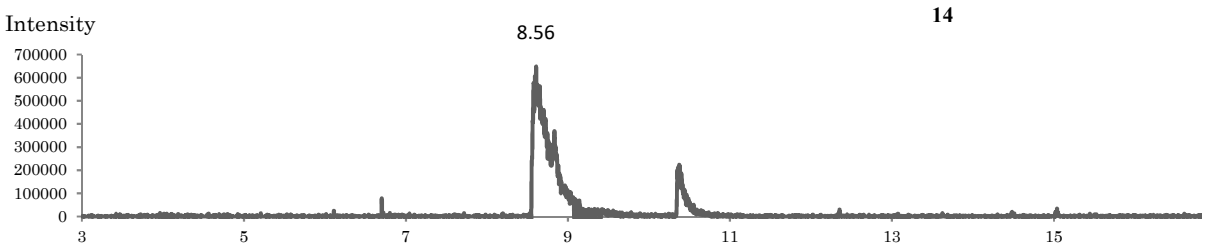
Intensity
14
8.56
700000
600000
500000
400000
300000
200000
100000
0
3
5
7
9
11
13
15

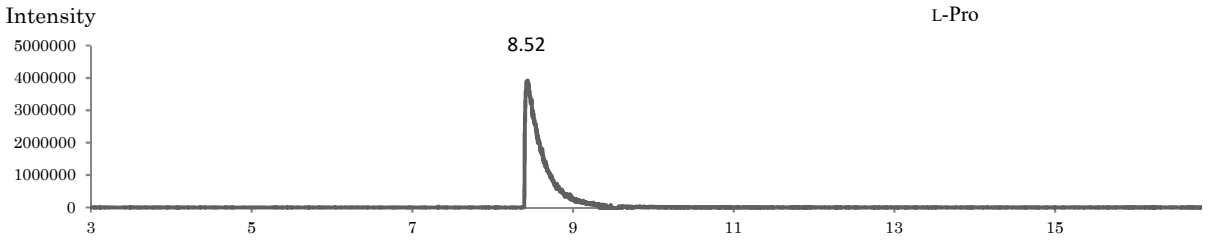
Intensity
L-Pro
8.52
5000000
4000000
3000000
2000000
1000000
0
3
5
7
9
11
13
15

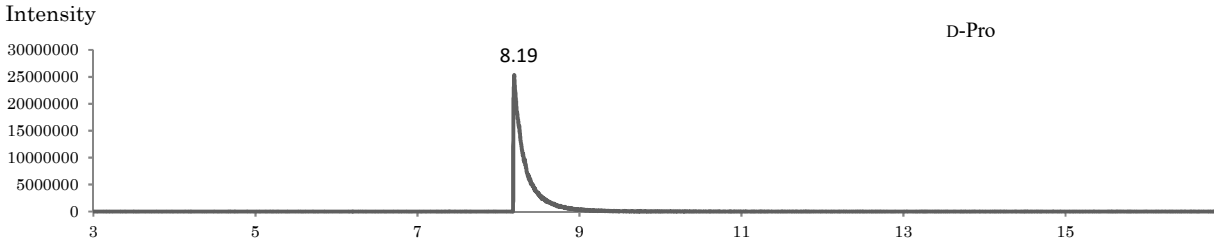
Intensity
D-Pro
8.19
30000000
25000000
20000000
15000000
10000000
5000000
0
3
5
7
9
11
13
15

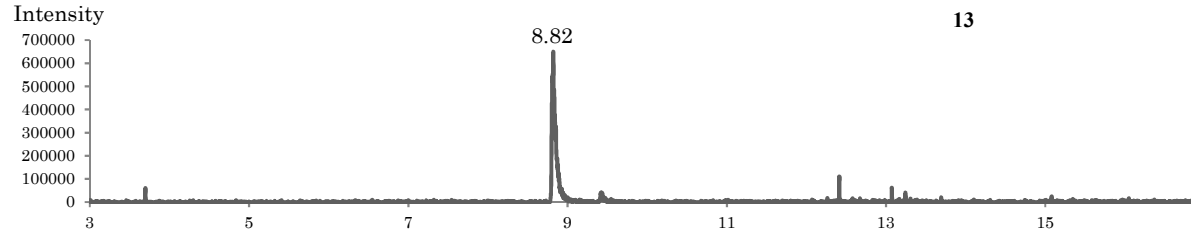
Intensity
13
8.82
700000
600000
500000
400000
300000
200000
100000
0
3
5
7
9
11
13
15

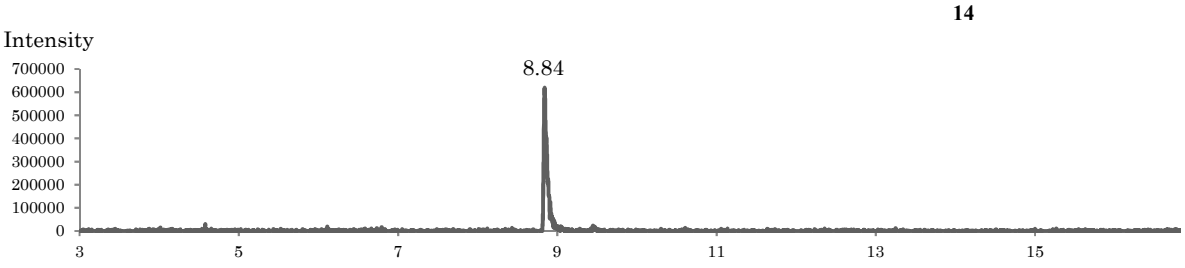
14
Intensity
8.84
700000
600000
500000
400000
300000
200000
100000
0
3
5
7
9
11
13
15

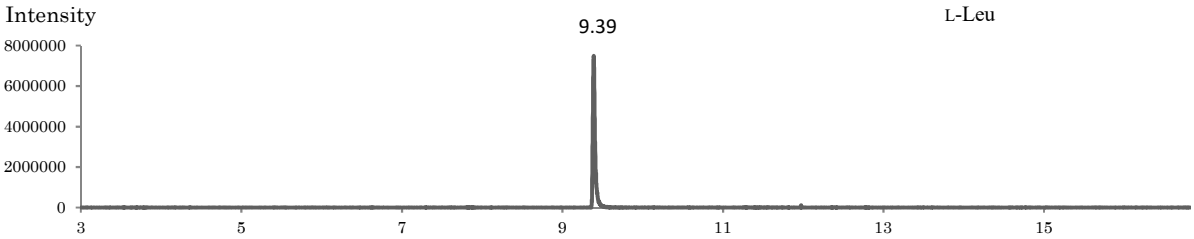
Intensity
L-Leu
9.39
8000000
6000000
4000000
2000000
0
3
5
7
9
11
13
15

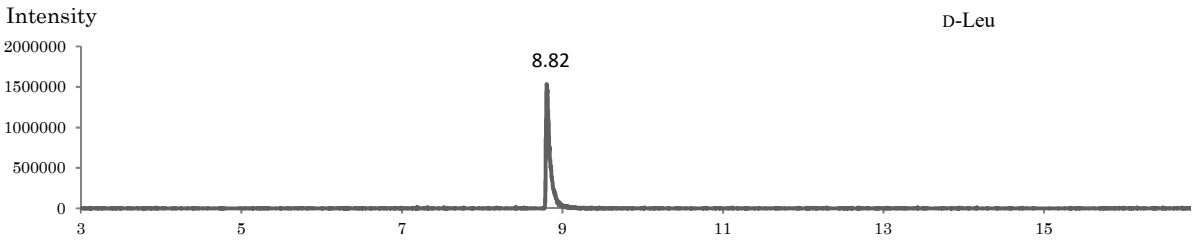
Intensity
D-Leu
8.82
2000000
1500000
1000000
500000
0
3
5
7
9
11
13
15

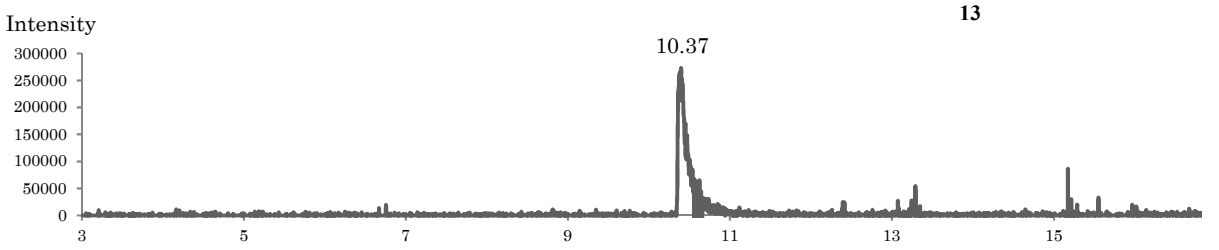
13
Intensity
10.37
300000
250000
200000
150000
100000
50000
0
3
5
7
9
11
13
15

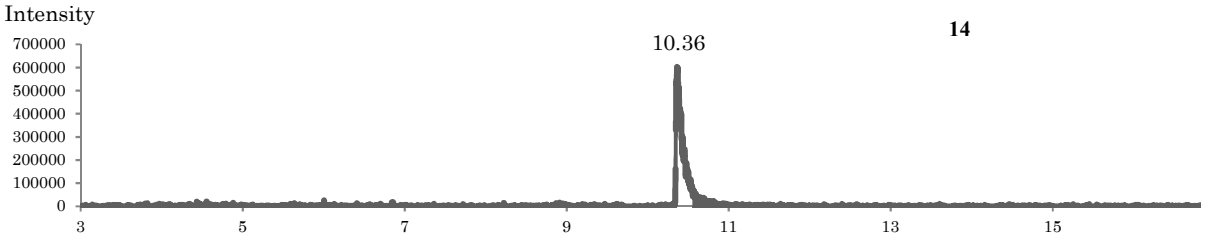
Intensity
14
10.36
700000
600000
500000
400000
300000
200000
100000
0
3
5
7
9
11
13
15

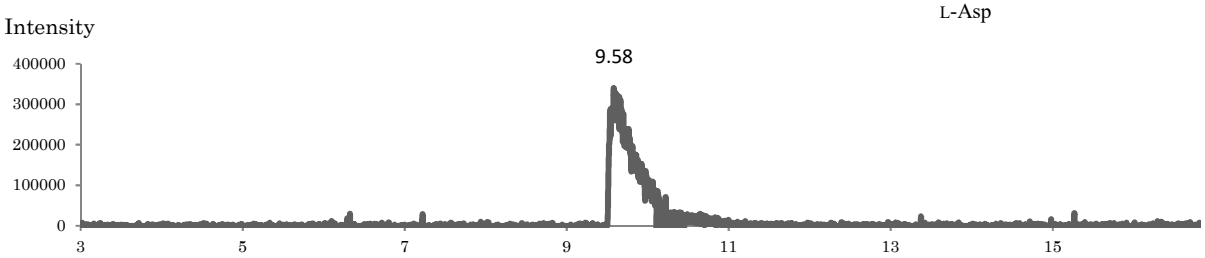
L-Asp
Intensity
9.58
400000
300000
200000
100000
0
3
5
7
9
11
13
15

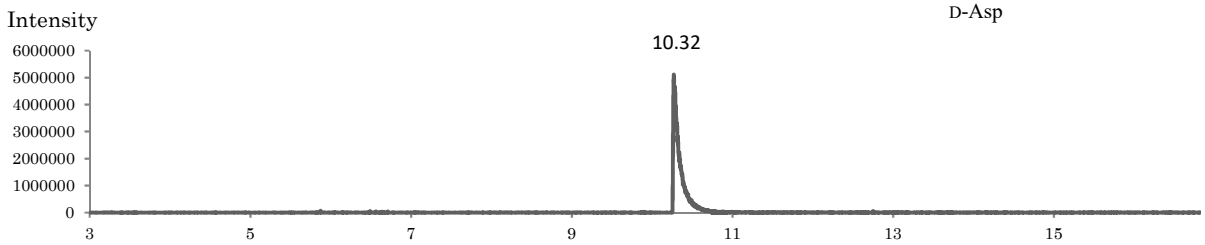
D-Asp
Intensity
10.32
6000000
5000000
4000000
3000000
2000000
1000000
0
3
5
7
9
11
13
15

Figure S17. ORTEP drawing of **13**

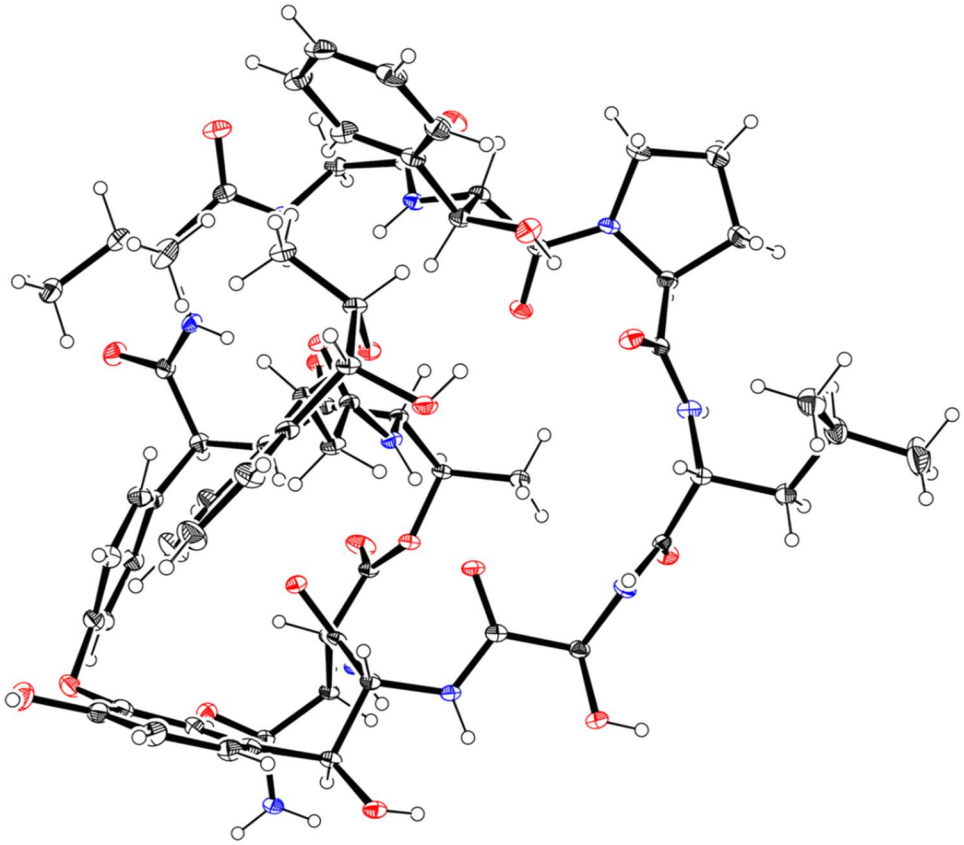

Displacement ellipsoids are drawn at the 30% probability level.

Table S1. X-ray experimental details for **13**

Crystal data	
Chemical formula	$C_{132}H_{190}N_{22}O_{54}$
M_r	2949.05
Crystal system, space group	Monoclinic, $P2_1$
Temperature (K)	143
a, b, c (Å)	18.3426 (1), 16.5391 (1), 23.8979 (1)
β (°)	92.20
V (Å^3)	7244.55 (7)
Z	2
Radiation type	Cu $K\alpha$
μ (mm^{-1})	0.89
Crystal size (mm)	0.28 × 0.15 × 0.06
Data collection	
Diffractometer	X-ray crystallographic analysis was performed on a HPC diffractometer (Rigaku XtaLAB P200)
Absorption correction	Multi-scan *CrysAlis PRO* 1.171.39.20a (Rigaku Oxford Diffraction, 2015) Empirical absorption correction using spherical harmonics, implemented in SCALE3 ABSPACK scaling algorithm
T_{min}, T_{max}	0.817, 1
No. of measured, independent and observed [$I > 2\sigma(I)$] reflections	28536, 28536, 27156
R_{int}	0.028
$(\sin \theta/\lambda)_{max}$ (Å^{-1})	0.625
Refinement	
$R[F^2 > 2\sigma(F^2)]$, $wR(F^2)$, S	0.049, 0.141, 1.03
No. of reflections	28536
No. of parameters	1902
No. of restraints	31
H-atom treatment	H-atom parameters constrained
$\Delta\rho_{max}$, $\Delta\rho_{min}$ (e Å^{-3})	1.23, −0.48
Absolute structure	Flack x determined using 12071 quotients [(I+)-(I-)]/[(I+)+(I-)] (Parsons, Flack and Wagner, Acta Cryst. B69 (2013) 249-259)
Absolute structure parameter	0.01 (2)

Computer programs: *CrysAlis PRO* 1.171.39.20a (Rigaku OD, 2015), *SHELXL2018*/3 (Sheldrick, 2018), *ORTEP* for Windows (Farrugia, 2012), *WinGX* publication routines (Farrugia, 2012).

Table S2. Selected bond lengths (Å) of **13**

O1A—C4A	1.226 (4)	O3B—C10B	1.232 (4)
O2A—C7A	1.236 (4)	O4B—C13B	1.234 (4)
O3A—C10A	1.231 (4)	O5B—C16B	1.228 (4)
O4A—C13A	1.235 (4)	O6B—C22B	1.230 (4)
O5A—C16A	1.232 (4)	O7B—C25B	1.221 (4)
O6A—C22A	1.230 (4)	O8B—C27B	1.396 (4)
O7A—C25A	1.224 (4)	O9B—C28B	1.236 (4)
O8A—C27A	1.402 (4)	O10B—C31B	1.232 (4)
O9A—C28A	1.229 (4)	O11B—C34B	1.211 (4)
O10A—C31A	1.229 (4)	O12B—C37B	1.245 (4)
O11A—C34A	1.212 (4)	O13B—C39B	1.431 (4)
O12A—C37A	1.237 (4)	O13B—C47B	1.449 (4)
O13A—C39A	1.433 (4)	O14B—C46B	1.436 (4)
O13A—C47A	1.450 (4)	O15B—C58B	1.415 (4)
O14A—C46A	1.435 (4)	O16B—C69B	1.417 (4)
O15A—C58A	1.418 (4)	O17B—C73B	1.373 (4)
O16A—C69A	1.416 (4)	O18B—C77B	1.230 (4)
O17A—C73A	1.378 (4)	O19B—C52B	1.394 (4)
O18A—C77A	1.234 (4)	O19B—C72B	1.395 (4)
O19A—C52A	1.395 (4)	C1B—C2B	1.516 (4)
O19A—C72A	1.396 (4)	C2B—O35B	1.471 (3)
C1A—C2A	1.517 (4)	C2B—C3B	1.531 (4)
C2A—O35A	1.468 (3)	C3B—N36B	1.453 (4)
C2A—C3A	1.533 (4)	C3B—C4B	1.538 (4)
C3A—N36A	1.453 (4)	C4B—N5B	1.347 (4)
C3A—C4A	1.536 (4)	N5B—C6B	1.457 (4)
C4A—N5A	1.348 (4)	C6B—C49B	1.518 (5)
N5A—C6A	1.456 (4)	C6B—C7B	1.537 (4)
C6A—C49A	1.523 (4)	C7B—N8B	1.330 (4)
C6A—C7A	1.536 (4)	N8B—C9B	1.463 (4)
C7A—N8A	1.332 (4)	C9B—C10B	1.528 (5)
N8A—C9A	1.458 (4)	C9B—C55B	1.537 (5)
C9A—C10A	1.529 (5)	C10B—N11B	1.349 (5)
C9A—C55A	1.541 (5)	N11B—C12B	1.454 (4)
C10A—N11A	1.349 (4)	C12B—C13B	1.512 (5)
N11A—C12A	1.451 (4)	C13B—N14B	1.335 (4)
C12A—C13A	1.516 (5)	N14B—C15B	1.457 (4)
C13A—N14A	1.336 (4)	C15B—C16B	1.529 (4)
N14A—C15A	1.452 (4)	C15B—C58B	1.562 (4)
C15A—C16A	1.524 (4)	C16B—N17B	1.343 (4)
C15A—C58A	1.564 (4)	N17B—C21B	1.468 (4)
C16A—N17A	1.338 (4)	N17B—C18B	1.472 (4)
N17A—C21A	1.467 (4)	C18B—C19C	1.490 (12)

N17A—C18A	1.478 (4)	C18B—C19B	1.584 (7)
C18A—C19A	1.513 (5)	C19B—C20B	1.420 (8)
C19A—C20A	1.525 (5)	C19C—C20B	1.635 (12)
C20A—C21A	1.539 (5)	C20B—C21B	1.526 (5)
C21A—C22A	1.529 (4)	C21B—C22B	1.536 (4)
C22A—N23A	1.338 (4)	C22B—N23B	1.334 (4)
N23A—C24A	1.465 (4)	N23B—C24B	1.458 (4)
C24A—C65A	1.527 (4)	C24B—C65B	1.525 (4)
C24A—C25A	1.532 (4)	C24B—C25B	1.537 (4)
C25A—N26A	1.350 (4)	C25B—N26B	1.353 (4)
N26A—C27A	1.440 (4)	N26B—C27B	1.446 (4)
C27A—C28A	1.532 (4)	C27B—C28B	1.536 (4)
C28A—N29A	1.345 (4)	C28B—N29B	1.338 (4)
N29A—C30A	1.455 (4)	N29B—C30B	1.454 (4)
C30A—C31A	1.537 (4)	C30B—C31B	1.536 (4)
C30A—C69A	1.559 (4)	C30B—C69B	1.560 (4)
C31A—N32A	1.350 (4)	C31B—N32B	1.343 (4)
N32A—C33A	1.443 (4)	N32B—C33B	1.449 (4)
C33A—C76A	1.525 (4)	C33B—C76B	1.519 (4)
C33A—C34A	1.524 (4)	C33B—C34B	1.529 (4)
C34A—O35A	1.323 (4)	C34B—O35B	1.323 (4)
N36A—C37A	1.341 (4)	N36B—C37B	1.338 (4)
C37A—C38A	1.523 (4)	C37B—C38B	1.515 (4)
C38A—C39A	1.523 (4)	C38B—C39B	1.521 (4)
C39A—C40A	1.520 (4)	C39B—C40B	1.525 (4)
C40A—C41A	1.396 (5)	C40B—C45B	1.395 (4)
C40A—C45A	1.398 (5)	C40B—C41B	1.401 (5)
C41A—C42A	1.390 (6)	C41B—C42B	1.378 (6)
C42A—C43A	1.386 (6)	C42B—C43B	1.391 (6)
C43A—C44A	1.390 (5)	C43B—C44B	1.387 (5)
C44A—C45A	1.391 (5)	C44B—C45B	1.401 (5)
C45A—C46A	1.509 (4)	C45B—C46B	1.509 (4)
C46A—C47A	1.517 (4)	C46B—C47B	1.508 (4)
C47A—C48A	1.515 (4)	C47B—C48B	1.518 (5)
C49A—C50A	1.392 (4)	C49B—C54B	1.391 (5)
C49A—C54A	1.394 (5)	C49B—C50B	1.396 (4)
C50A—C51A	1.390 (5)	C50B—C51B	1.386 (5)
C51A—C52A	1.387 (5)	C51B—C52B	1.381 (5)
C52A—C53A	1.397 (5)	C52B—C53B	1.390 (5)
C53A—C54A	1.376 (5)	C53B—C54B	1.386 (5)
C55A—C57A	1.526 (5)	C55B—C56B	1.525 (5)
C55A—C56A	1.529 (5)	C55B—C57B	1.524 (5)
C58A—C59A	1.522 (4)	C58B—C59B	1.511 (4)
C59A—C64A	1.379 (5)	C59B—C64B	1.393 (5)
C59A—C60A	1.396 (5)	C59B—C60B	1.394 (5)

C60A—C61A	1.383 (5)	C60B—C61B	1.389 (5)
C61A—C62A	1.379 (6)	C61B—C62B	1.382 (6)
C62A—C63A	1.392 (6)	C62B—C63B	1.391 (5)
C63A—C64A	1.391 (5)	C63B—C64B	1.385 (5)
C65A—C66A	1.540 (5)	C65B—C66B	1.518 (5)
C66A—C68A	1.505 (5)	C66B—C68B	1.416 (8)
C66A—C67A	1.507 (6)	C66B—C68C	1.404 (12)
C69A—C70A	1.516 (4)	C66B—C67B	1.546 (6)
C70A—C71A	1.389 (5)	C69B—C70B	1.522 (4)
C70A—C75A	1.391 (5)	C70B—C71B	1.392 (5)
C71A—C72A	1.387 (5)	C70B—C75B	1.397 (4)
C72A—C73A	1.390 (5)	C71B—C72B	1.392 (5)
C73A—C74A	1.398 (5)	C72B—C73B	1.386 (5)
C74A—C75A	1.389 (5)	C73B—C74B	1.391 (5)
C76A—C77A	1.518 (4)	C74B—C75B	1.384 (5)
C77A—N78A	1.327 (4)	C76B—C77B	1.520 (4)
O1B—C4B	1.229 (4)	C77B—N78B	1.333 (4)
O2B—C7B	1.235 (4)		

Table S3. Selected bond angles (°) of **13**

C39B—O13B—C47B	113.6 (2)	N32A—C33A—C34A	114.2 (2)
C39A—O13A—C47A	113.6 (2)	N32A—C33A—C76A	109.8 (2)
C52B—O19B—C72B	112.2 (2)	C76A—C33A—C34A	111.3 (2)
C52A—O19A—C72A	110.8 (2)	O11B—C34B—O35B	124.9 (3)
C34B—O35B—C2B	120.5 (2)	O11B—C34B—C33B	122.6 (3)
C34A—O35A—C2A	120.2 (2)	O35B—C34B—C33B	112.3 (2)
C4B—N5B—C6B	122.3 (3)	O11A—C34A—O35A	125.0 (3)
C4A—N5A—C6A	122.4 (3)	O11A—C34A—C33A	122.7 (3)
C7B—N8B—C9B	122.6 (3)	O35A—C34A—C33A	112.2 (2)
C7A—N8A—C9A	122.9 (3)	O12B—C37B—N36B	122.4 (3)
C10B—N11B—C12B	122.0 (3)	O12B—C37B—C38B	123.7 (3)
C10A—N11A—C12A	123.0 (3)	N36B—C37B—C38B	113.6 (3)
C13B—N14B—C15B	119.8 (3)	O12A—C37A—N36A	122.5 (3)
C13A—N14A—C15A	121.2 (3)	O12A—C37A—C38A	123.1 (3)
C16B—N17B—C18B	127.9 (3)	N36A—C37A—C38A	114.1 (3)
C16B—N17B—C21B	119.0 (3)	C37B—C38B—C39B	116.0 (3)
C21B—N17B—C18B	112.8 (3)	C37A—C38A—C39A	115.7 (2)
C16A—N17A—C18A	127.8 (3)	O13B—C39B—C38B	107.0 (3)
C16A—N17A—C21A	119.5 (2)	O13B—C39B—C40B	111.3 (2)
C21A—N17A—C18A	112.6 (3)	C38B—C39B—C40B	112.2 (3)
C22B—N23B—C24B	122.0 (3)	O13A—C39A—C38A	106.3 (3)
C22A—N23A—C24A	122.8 (3)	O13A—C39A—C40A	112.0 (2)
C25B—N26B—C27B	123.3 (3)	C40A—C39A—C38A	113.2 (3)
C25A—N26A—C27A	122.5 (3)	C41B—C40B—C39B	120.9 (3)
C28B—N29B—C30B	120.1 (2)	C45B—C40B—C39B	120.3 (3)
C28A—N29A—C30A	119.3 (2)	C45B—C40B—C41B	118.8 (3)
C31B—N32B—C33B	123.2 (2)	C41A—C40A—C39A	120.8 (3)
C31A—N32A—C33A	122.8 (2)	C41A—C40A—C45A	118.6 (3)
C37B—N36B—C3B	122.9 (2)	C45A—C40A—C39A	120.5 (3)
C37A—N36A—C3A	121.9 (2)	C42B—C41B—C40B	121.0 (4)
O35B—C2B—C1B	105.3 (2)	C42A—C41A—C40A	120.9 (4)
O35B—C2B—C3B	106.4 (2)	C41B—C42B—C43B	120.5 (4)
C1B—C2B—C3B	114.2 (3)	C43A—C42A—C41A	120.6 (4)
O35A—C2A—C1A	105.3 (2)	C44B—C43B—C42B	119.0 (3)
O35A—C2A—C3A	106.6 (2)	C42A—C43A—C44A	118.7 (4)
C1A—C2A—C3A	114.5 (3)	C43B—C44B—C45B	121.0 (3)
N36B—C3B—C2B	109.8 (2)	C43A—C44A—C45A	121.3 (3)
N36B—C3B—C4B	112.1 (3)	C40B—C45B—C44B	119.7 (3)
C2B—C3B—C4B	110.1 (2)	C40B—C45B—C46B	121.5 (3)
N36A—C3A—C2A	110.1 (2)	C44B—C45B—C46B	118.8 (3)
N36A—C3A—C4A	111.8 (3)	C40A—C45A—C46A	121.2 (3)
C2A—C3A—C4A	110.1 (2)	C44A—C45A—C40A	119.9 (3)
O1B—C4B—N5B	122.8 (3)	C44A—C45A—C46A	118.9 (3)

O1B—C4B—C3B	120.6 (3)	O14B—C46B—C45B	106.7 (2)
N5B—C4B—C3B	116.6 (3)	O14B—C46B—C47B	112.3 (3)
O1A—C4A—N5A	122.8 (3)	C45B—C46B—C47B	110.2 (3)
O1A—C4A—C3A	120.9 (3)	O14A—C46A—C45A	107.1 (2)
N5A—C4A—C3A	116.2 (3)	O14A—C46A—C47A	112.1 (3)
N5B—C6B—C7B	113.6 (3)	C45A—C46A—C47A	110.1 (3)
N5B—C6B—C49B	106.7 (2)	O13B—C47B—C46B	108.8 (2)
C49B—C6B—C7B	111.2 (3)	O13B—C47B—C48B	113.5 (3)
N5A—C6A—C7A	113.8 (3)	C46B—C47B—C48B	112.1 (3)
N5A—C6A—C49A	106.6 (2)	O13A—C47A—C46A	108.7 (2)
C49A—C6A—C7A	110.5 (3)	O13A—C47A—C48A	113.2 (3)
O2B—C7B—N8B	124.4 (3)	C48A—C47A—C46A	111.9 (3)
O2B—C7B—C6B	118.6 (3)	C50B—C49B—C6B	120.0 (3)
N8B—C7B—C6B	117.0 (3)	C54B—C49B—C6B	119.7 (3)
O2A—C7A—N8A	123.8 (3)	C54B—C49B—C50B	119.5 (3)
O2A—C7A—C6A	118.7 (3)	C50A—C49A—C6A	120.1 (3)
N8A—C7A—C6A	117.4 (3)	C50A—C49A—C54A	119.3 (3)
N8B—C9B—C10B	111.0 (3)	C54A—C49A—C6A	119.9 (3)
N8B—C9B—C55B	111.8 (3)	C51B—C50B—C49B	120.0 (3)
C10B—C9B—C55B	114.6 (3)	C51A—C50A—C49A	120.5 (3)
N8A—C9A—C10A	111.4 (3)	C52B—C51B—C50B	119.6 (3)
N8A—C9A—C55A	111.9 (3)	C52A—C51A—C50A	118.8 (3)
C10A—C9A—C55A	113.8 (3)	C51B—C52B—O19B	118.8 (3)
O3B—C10B—N11B	122.1 (3)	C51B—C52B—C53B	120.9 (3)
O3B—C10B—C9B	121.4 (3)	C53B—C52B—O19B	120.3 (3)
N11B—C10B—C9B	116.3 (3)	O19A—C52A—C53A	120.1 (3)
O3A—C10A—N11A	122.5 (3)	C51A—C52A—O19A	118.5 (3)
O3A—C10A—C9A	120.8 (3)	C51A—C52A—C53A	121.4 (3)
N11A—C10A—C9A	116.5 (3)	C54B—C53B—C52B	119.1 (3)
N11B—C12B—C13B	116.5 (3)	C54A—C53A—C52A	118.7 (3)
N11A—C12A—C13A	116.6 (3)	C53B—C54B—C49B	120.5 (3)
O4B—C13B—N14B	122.3 (3)	C53A—C54A—C49A	121.0 (3)
O4B—C13B—C12B	118.9 (3)	C56B—C55B—C9B	113.0 (3)
N14B—C13B—C12B	118.8 (3)	C56B—C55B—C57B	110.7 (3)
O4A—C13A—N14A	122.7 (3)	C57B—C55B—C9B	110.5 (3)
O4A—C13A—C12A	119.2 (3)	C56A—C55A—C9A	112.5 (3)
N14A—C13A—C12A	118.0 (3)	C57A—C55A—C9A	109.8 (3)
N14B—C15B—C16B	109.6 (3)	C57A—C55A—C56A	110.7 (3)
N14B—C15B—C58B	109.4 (3)	O15B—C58B—C15B	110.9 (3)
C16B—C15B—C58B	108.1 (2)	O15B—C58B—C59B	107.3 (3)
N14A—C15A—C16A	109.8 (2)	C59B—C58B—C15B	113.2 (2)
N14A—C15A—C58A	109.1 (3)	O15A—C58A—C15A	110.7 (3)
C16A—C15A—C58A	107.5 (2)	O15A—C58A—C59A	107.4 (3)
O5B—C16B—N17B	121.8 (3)	C59A—C58A—C15A	113.0 (2)
O5B—C16B—C15B	120.0 (3)	C60B—C59B—C58B	119.8 (3)

N17B—C16B—C15B	117.9 (3)	C64B—C59B—C58B	121.9 (3)
O5A—C16A—N17A	121.7 (3)	C64B—C59B—C60B	118.2 (3)
O5A—C16A—C15A	120.0 (3)	C60A—C59A—C58A	119.6 (3)
N17A—C16A—C15A	117.8 (3)	C64A—C59A—C58A	122.1 (3)
N17B—C18B—C19C	105.0 (5)	C64A—C59A—C60A	118.1 (3)
N17B—C18B—C19B	99.0 (3)	C61B—C60B—C59B	121.0 (3)
N17A—C18A—C19A	102.1 (3)	C61A—C60A—C59A	120.7 (4)
C18B—C19C—C20B	99.8 (6)	C62B—C61B—C60B	120.2 (3)
C20B—C19B—C18B	105.5 (5)	C62A—C61A—C60A	120.9 (4)
C18A—C19A—C20A	103.6 (3)	C61B—C62B—C63B	119.4 (3)
C19B—C20B—C21B	104.4 (4)	C61A—C62A—C63A	118.8 (3)
C21B—C20B—C19C	105.9 (5)	C64B—C63B—C62B	120.3 (3)
C19A—C20A—C21A	103.9 (3)	C64A—C63A—C62A	120.0 (4)
N17B—C21B—C20B	103.1 (3)	C63B—C64B—C59B	120.9 (3)
N17B—C21B—C22B	110.0 (3)	C59A—C64A—C63A	121.4 (3)
C20B—C21B—C22B	112.0 (3)	C66B—C65B—C24B	116.3 (3)
N17A—C21A—C20A	103.1 (3)	C24A—C65A—C66A	114.8 (3)
N17A—C21A—C22A	110.8 (3)	C65B—C66B—C67B	110.1 (4)
C22A—C21A—C20A	110.4 (3)	C68C—C66B—C65B	124.9 (6)
O6B—C22B—N23B	122.7 (3)	C68C—C66B—C67B	121.9 (6)
O6B—C22B—C21B	120.9 (3)	C68B—C66B—C65B	120.0 (5)
N23B—C22B—C21B	116.2 (3)	C68B—C66B—C67B	111.1 (4)
O6A—C22A—N23A	123.4 (3)	C67A—C66A—C65A	108.7 (3)
O6A—C22A—C21A	121.3 (3)	C68A—C66A—C65A	114.1 (3)
N23A—C22A—C21A	115.1 (3)	C68A—C66A—C67A	111.2 (4)
N23B—C24B—C25B	109.7 (3)	O16B—C69B—C30B	110.3 (2)
N23B—C24B—C65B	112.7 (3)	O16B—C69B—C70B	113.7 (2)
C65B—C24B—C25B	110.1 (2)	C70B—C69B—C30B	110.1 (2)
N23A—C24A—C25A	110.2 (3)	O16A—C69A—C30A	110.6 (2)
N23A—C24A—C65A	111.4 (3)	O16A—C69A—C70A	114.3 (3)
C65A—C24A—C25A	108.5 (2)	C70A—C69A—C30A	108.9 (2)
O7B—C25B—N26B	123.9 (3)	C71B—C70B—C69B	120.0 (3)
O7B—C25B—C24B	122.2 (3)	C71B—C70B—C75B	118.6 (3)
N26B—C25B—C24B	113.9 (3)	C75B—C70B—C69B	121.4 (3)
O7A—C25A—N26A	123.9 (3)	C71A—C70A—C69A	119.4 (3)
O7A—C25A—C24A	121.8 (3)	C71A—C70A—C75A	118.7 (3)
N26A—C25A—C24A	114.2 (3)	C75A—C70A—C69A	121.8 (3)
O8B—C27B—N26B	113.7 (3)	C72B—C71B—C70B	120.4 (3)
O8B—C27B—C28B	107.8 (2)	C72A—C71A—C70A	120.5 (3)
N26B—C27B—C28B	110.3 (2)	C71B—C72B—O19B	120.4 (3)
O8A—C27A—N26A	114.0 (3)	C73B—C72B—O19B	118.8 (3)
O8A—C27A—C28A	107.7 (3)	C73B—C72B—C71B	120.7 (3)
N26A—C27A—C28A	109.6 (2)	C71A—C72A—O19A	120.6 (3)
O9B—C28B—N29B	122.6 (3)	C71A—C72A—C73A	120.8 (3)
O9B—C28B—C27B	120.4 (3)	C73A—C72A—O19A	118.7 (3)

N29B—C28B—C27B	116.9 (2)	O17B—C73B—C72B	118.1 (3)
O9A—C28A—N29A	122.3 (3)	O17B—C73B—C74B	123.0 (3)
O9A—C28A—C27A	121.0 (3)	C72B—C73B—C74B	118.8 (3)
N29A—C28A—C27A	116.6 (3)	O17A—C73A—C72A	117.2 (3)
N29B—C30B—C31B	110.2 (2)	O17A—C73A—C74A	123.9 (3)
N29B—C30B—C69B	109.6 (2)	C72A—C73A—C74A	118.9 (3)
C31B—C30B—C69B	110.8 (2)	C75B—C74B—C73B	120.7 (3)
N29A—C30A—C31A	110.5 (2)	C75A—C74A—C73A	119.9 (3)
N29A—C30A—C69A	109.7 (2)	C74B—C75B—C70B	120.7 (3)
C31A—C30A—C69A	111.2 (2)	C74A—C75A—C70A	121.1 (3)
O10B—C31B—N32B	123.4 (3)	C33B—C76B—C77B	110.8 (3)
O10B—C31B—C30B	122.3 (3)	C77A—C76A—C33A	111.2 (3)
N32B—C31B—C30B	114.4 (2)	O18B—C77B—N78B	122.6 (3)
O10A—C31A—N32A	123.4 (3)	O18B—C77B—C76B	120.0 (3)
O10A—C31A—C30A	122.3 (3)	N78B—C77B—C76B	117.3 (3)
N32A—C31A—C30A	114.3 (2)	O18A—C77A—N78A	123.0 (3)
N32B—C33B—C34B	113.8 (2)	O18A—C77A—C76A	119.7 (3)
N32B—C33B—C76B	109.9 (2)	N78A—C77A—C76A	117.2 (3)
C76B—C33B—C34B	111.3 (2)		

Table S4. Selected torsion angles (°) of **13**

O35A—C2A—C3A—N36A	52.0 (3)	N36B—C3B—C4B—O1B	147.7 (3)
C1A—C2A—C3A—N36A	−64.0 (3)	C2B—C3B—C4B—O1B	−89.7 (3)
O35A—C2A—C3A—C4A	−71.8 (3)	N36B—C3B—C4B—N5B	−30.9 (4)
C1A—C2A—C3A—C4A	172.2 (2)	C2B—C3B—C4B—N5B	91.7 (3)
N36A—C3A—C4A—O1A	148.2 (3)	O1B—C4B—N5B—C6B	0.4 (5)
C2A—C3A—C4A—O1A	−89.1 (3)	C3B—C4B—N5B—C6B	178.9 (3)
N36A—C3A—C4A—N5A	−30.7 (4)	C4B—N5B—C6B—C49B	178.2 (3)
C2A—C3A—C4A—N5A	92.0 (3)	C4B—N5B—C6B—C7B	−59.0 (4)
O1A—C4A—N5A—C6A	0.1 (5)	N5B—C6B—C7B—O2B	160.4 (3)
C3A—C4A—N5A—C6A	178.9 (3)	C49B—C6B—C7B—O2B	−79.3 (4)
C4A—N5A—C6A—C49A	179.1 (3)	N5B—C6B—C7B—N8B	−21.4 (4)
C4A—N5A—C6A—C7A	−58.9 (4)	C49B—C6B—C7B—N8B	98.9 (3)
N5A—C6A—C7A—O2A	162.8 (3)	O2B—C7B—N8B—C9B	−3.8 (5)
C49A—C6A—C7A—O2A	−77.3 (4)	C6B—C7B—N8B—C9B	178.2 (3)
N5A—C6A—C7A—N8A	−18.9 (4)	C7B—N8B—C9B—C10B	−122.7 (3)
C49A—C6A—C7A—N8A	101.0 (3)	C7B—N8B—C9B—C55B	108.1 (4)
O2A—C7A—N8A—C9A	−2.5 (5)	N8B—C9B—C10B—O3B	−158.2 (3)
C6A—C7A—N8A—C9A	179.2 (3)	C55B—C9B—C10B—O3B	−30.4 (4)
C7A—N8A—C9A—C10A	−123.7 (3)	N8B—C9B—C10B—N11B	26.3 (4)
C7A—N8A—C9A—C55A	107.5 (4)	C55B—C9B—C10B—N11B	154.1 (3)
N8A—C9A—C10A—O3A	−162.1 (3)	O3B—C10B—N11B—C12B	−7.1 (5)
C55A—C9A—C10A—O3A	−34.4 (4)	C9B—C10B—N11B—C12B	168.4 (3)
N8A—C9A—C10A—N11A	22.9 (4)	C10B—N11B—C12B—C13B	94.2 (4)
C55A—C9A—C10A—N11A	150.7 (3)	N11B—C12B—C13B—O4B	−178.3 (3)
O3A—C10A—N11A—C12A	−6.3 (5)	N11B—C12B—C13B—N14B	1.1 (4)
C9A—C10A—N11A—C12A	168.5 (3)	O4B—C13B—N14B—C15B	2.0 (5)
C10A—N11A—C12A—C13A	100.1 (4)	C12B—C13B—N14B—C15B	−177.4 (3)
N11A—C12A—C13A—O4A	179.4 (3)	C13B—N14B—C15B—C16B	−87.2 (3)
N11A—C12A—C13A—N14A	−2.5 (4)	C13B—N14B—C15B—C58B	154.5 (3)
O4A—C13A—N14A—C15A	4.3 (5)	N14B—C15B—C16B—O5B	−37.7 (4)
C12A—C13A—N14A—C15A	−173.7 (3)	C58B—C15B—C16B—O5B	81.5 (4)
C13A—N14A—C15A—C16A	−88.1 (3)	N14B—C15B—C16B—N17B	148.5 (3)
C13A—N14A—C15A—C58A	154.3 (3)	C58B—C15B—C16B—N17B	−92.3 (3)
N14A—C15A—C16A—O5A	−41.1 (4)	O5B—C16B—N17B—C21B	−8.3 (5)
C58A—C15A—C16A—O5A	77.5 (4)	C15B—C16B—N17B—C21B	165.5 (3)
N14A—C15A—C16A—N17A	146.3 (3)	O5B—C16B—N17B—C18B	178.6 (4)
C58A—C15A—C16A—N17A	−95.1 (3)	C15B—C16B—N17B—C18B	−7.7 (5)
O5A—C16A—N17A—C21A	−7.7 (5)	C16B—N17B—C18B—C19C	−157.6 (6)
C15A—C16A—N17A—C21A	164.7 (3)	C21B—N17B—C18B—C19C	28.9 (6)
O5A—C16A—N17A—C18A	176.2 (3)	C16B—N17B—C18B—C19B	158.0 (4)
C15A—C16A—N17A—C18A	−11.3 (5)	C21B—N17B—C18B—C19B	−15.5 (5)
C16A—N17A—C18A—C19A	−163.7 (3)	N17B—C18B—C19B—C20B	34.2 (5)
C21A—N17A—C18A—C19A	20.0 (4)	N17B—C18B—C19C—C20B	−35.3 (7)

N17A—C18A—C19A—C20A	−35.1 (4)	C18B—C19B—C20B—C21B	−39.8 (5)
C18A—C19A—C20A—C21A	38.0 (4)	C18B—C19C—C20B—C21B	32.2 (8)
C16A—N17A—C21A—C22A	−55.2 (4)	C16B—N17B—C21B—C20B	179.1 (3)
C18A—N17A—C21A—C22A	121.4 (3)	C18B—N17B—C21B—C20B	−6.7 (4)
C16A—N17A—C21A—C20A	−173.3 (3)	C16B—N17B—C21B—C22B	−61.3 (4)
C18A—N17A—C21A—C20A	3.3 (4)	C18B—N17B—C21B—C22B	112.9 (3)
C19A—C20A—C21A—N17A	−25.3 (4)	C19B—C20B—C21B—N17B	29.2 (5)
C19A—C20A—C21A—C22A	−143.6 (3)	C19C—C20B—C21B—N17B	−16.0 (6)
N17A—C21A—C22A—O6A	−29.5 (4)	C19B—C20B—C21B—C22B	−89.1 (4)
C20A—C21A—C22A—O6A	84.0 (4)	C19C—C20B—C21B—C22B	−134.2 (6)
N17A—C21A—C22A—N23A	155.3 (3)	N17B—C21B—C22B—O6B	−19.6 (4)
C20A—C21A—C22A—N23A	−91.2 (4)	C20B—C21B—C22B—O6B	94.5 (4)
O6A—C22A—N23A—C24A	−7.9 (5)	N17B—C21B—C22B—N23B	164.7 (3)
C21A—C22A—N23A—C24A	167.1 (3)	C20B—C21B—C22B—N23B	−81.2 (4)
C22A—N23A—C24A—C65A	−115.4 (3)	O6B—C22B—N23B—C24B	1.3 (5)
C22A—N23A—C24A—C25A	124.2 (3)	C21B—C22B—N23B—C24B	176.9 (3)
N23A—C24A—C25A—O7A	45.5 (4)	C22B—N23B—C24B—C65B	−123.1 (3)
C65A—C24A—C25A—O7A	−76.6 (4)	C22B—N23B—C24B—C25B	113.8 (3)
N23A—C24A—C25A—N26A	−137.4 (3)	N23B—C24B—C25B—O7B	38.9 (4)
C65A—C24A—C25A—N26A	100.4 (3)	C65B—C24B—C25B—O7B	−85.8 (4)
O7A—C25A—N26A—C27A	−8.8 (5)	N23B—C24B—C25B—N26B	−143.4 (3)
C24A—C25A—N26A—C27A	174.3 (3)	C65B—C24B—C25B—N26B	91.9 (3)
C25A—N26A—C27A—O8A	126.7 (3)	O7B—C25B—N26B—C27B	−6.1 (5)
C25A—N26A—C27A—C28A	−112.4 (3)	C24B—C25B—N26B—C27B	176.2 (3)
O8A—C27A—C28A—O9A	151.6 (3)	C25B—N26B—C27B—O8B	125.7 (3)
N26A—C27A—C28A—O9A	27.0 (4)	C25B—N26B—C27B—C28B	−113.1 (3)
O8A—C27A—C28A—N29A	−31.1 (4)	O8B—C27B—C28B—O9B	153.7 (3)
N26A—C27A—C28A—N29A	−155.6 (3)	N26B—C27B—C28B—O9B	29.1 (4)
O9A—C28A—N29A—C30A	−3.5 (4)	O8B—C27B—C28B—N29B	−29.2 (4)
C27A—C28A—N29A—C30A	179.2 (3)	N26B—C27B—C28B—N29B	−153.8 (3)
C28A—N29A—C30A—C31A	65.3 (3)	O9B—C28B—N29B—C30B	−2.6 (4)
C28A—N29A—C30A—C69A	−171.8 (3)	C27B—C28B—N29B—C30B	−179.6 (3)
N29A—C30A—C31A—O10A	−131.6 (3)	C28B—N29B—C30B—C31B	64.4 (3)
C69A—C30A—C31A—O10A	106.4 (3)	C28B—N29B—C30B—C69B	−173.4 (2)
N29A—C30A—C31A—N32A	49.7 (3)	N29B—C30B—C31B—O10B	−129.9 (3)
C69A—C30A—C31A—N32A	−72.4 (3)	C69B—C30B—C31B—O10B	108.5 (3)
O10A—C31A—N32A—C33A	0.7 (4)	N29B—C30B—C31B—N32B	51.7 (3)
C30A—C31A—N32A—C33A	179.4 (3)	C69B—C30B—C31B—N32B	−69.8 (3)
C31A—N32A—C33A—C76A	−155.6 (3)	O10B—C31B—N32B—C33B	0.2 (4)
C31A—N32A—C33A—C34A	78.5 (4)	C30B—C31B—N32B—C33B	178.5 (3)
N32A—C33A—C34A—O11A	169.7 (3)	C31B—N32B—C33B—C76B	−155.5 (3)
C76A—C33A—C34A—O11A	44.6 (4)	C31B—N32B—C33B—C34B	79.0 (4)
N32A—C33A—C34A—O35A	−13.5 (4)	N32B—C33B—C34B—O11B	169.2 (3)
C76A—C33A—C34A—O35A	−138.5 (3)	C76B—C33B—C34B—O11B	44.4 (4)
O11A—C34A—O35A—C2A	7.3 (5)	N32B—C33B—C34B—O35B	−14.5 (4)

C33A—C34A—O35A—C2A	−169.5 (2)	C76B—C33B—C34B—O35B	−139.3 (3)
C1A—C2A—O35A—C34A	−135.0 (3)	O11B—C34B—O35B—C2B	6.4 (5)
C3A—C2A—O35A—C34A	103.0 (3)	C33B—C34B—O35B—C2B	−169.8 (2)
C2A—C3A—N36A—C37A	−174.9 (3)	C1B—C2B—O35B—C34B	−134.0 (3)
C4A—C3A—N36A—C37A	−52.1 (4)	C3B—C2B—O35B—C34B	104.4 (3)
C3A—N36A—C37A—O12A	−7.2 (5)	C2B—C3B—N36B—C37B	−174.0 (3)
C3A—N36A—C37A—C38A	166.5 (3)	C4B—C3B—N36B—C37B	−51.2 (4)
O12A—C37A—C38A—C39A	−23.9 (4)	C3B—N36B—C37B—O12B	−7.7 (5)
N36A—C37A—C38A—C39A	162.5 (3)	C3B—N36B—C37B—C38B	166.5 (3)
C47A—O13A—C39A—C40A	−47.2 (3)	O12B—C37B—C38B—C39B	−19.9 (5)
C47A—O13A—C39A—C38A	−171.3 (2)	N36B—C37B—C38B—C39B	166.0 (3)
C37A—C38A—C39A—O13A	−71.0 (3)	C47B—O13B—C39B—C38B	−171.7 (2)
C37A—C38A—C39A—C40A	165.7 (3)	C47B—O13B—C39B—C40B	−48.8 (3)
O13A—C39A—C40A—C41A	−170.6 (3)	C37B—C38B—C39B—O13B	−73.1 (3)
C38A—C39A—C40A—C41A	−50.5 (4)	C37B—C38B—C39B—C40B	164.6 (3)
O13A—C39A—C40A—C45A	13.4 (4)	O13B—C39B—C40B—C45B	15.1 (4)
C38A—C39A—C40A—C45A	133.5 (3)	C38B—C39B—C40B—C45B	134.9 (3)
C45A—C40A—C41A—C42A	−1.3 (6)	O13B—C39B—C40B—C41B	−167.4 (3)
C39A—C40A—C41A—C42A	−177.4 (4)	C38B—C39B—C40B—C41B	−47.5 (4)
C40A—C41A—C42A—C43A	0.4 (7)	C45B—C40B—C41B—C42B	−0.9 (5)
C41A—C42A—C43A—C44A	0.9 (7)	C39B—C40B—C41B—C42B	−178.5 (3)
C42A—C43A—C44A—C45A	−1.2 (6)	C40B—C41B—C42B—C43B	0.8 (6)
C43A—C44A—C45A—C40A	0.3 (5)	C41B—C42B—C43B—C44B	−0.2 (6)
C43A—C44A—C45A—C46A	179.2 (3)	C42B—C43B—C44B—C45B	−0.3 (6)
C41A—C40A—C45A—C44A	0.9 (5)	C41B—C40B—C45B—C44B	0.4 (5)
C39A—C40A—C45A—C44A	177.1 (3)	C39B—C40B—C45B—C44B	178.0 (3)
C41A—C40A—C45A—C46A	−177.9 (3)	C41B—C40B—C45B—C46B	−180.0 (3)
C39A—C40A—C45A—C46A	−1.8 (5)	C39B—C40B—C45B—C46B	−2.3 (5)
C44A—C45A—C46A—O14A	80.2 (4)	C43B—C44B—C45B—C40B	0.2 (5)
C40A—C45A—C46A—O14A	−101.0 (3)	C43B—C44B—C45B—C46B	−179.5 (3)
C44A—C45A—C46A—C47A	−157.7 (3)	C40B—C45B—C46B—O14B	−101.7 (3)
C40A—C45A—C46A—C47A	21.2 (4)	C44B—C45B—C46B—O14B	77.9 (4)
C39A—O13A—C47A—C48A	−56.4 (3)	C40B—C45B—C46B—C47B	20.5 (4)
C39A—O13A—C47A—C46A	68.6 (3)	C44B—C45B—C46B—C47B	−159.9 (3)
O14A—C46A—C47A—O13A	67.1 (3)	C39B—O13B—C47B—C46B	69.3 (3)
C45A—C46A—C47A—O13A	−52.0 (3)	C39B—O13B—C47B—C48B	−56.3 (3)
O14A—C46A—C47A—C48A	−167.1 (3)	O14B—C46B—C47B—O13B	67.7 (3)
C45A—C46A—C47A—C48A	73.8 (3)	C45B—C46B—C47B—O13B	−51.1 (3)
N5A—C6A—C49A—C50A	−108.1 (3)	O14B—C46B—C47B—C48B	−165.9 (3)
C7A—C6A—C49A—C50A	127.8 (3)	C45B—C46B—C47B—C48B	75.3 (3)
N5A—C6A—C49A—C54A	62.3 (4)	N5B—C6B—C49B—C54B	60.8 (4)
C7A—C6A—C49A—C54A	−61.8 (4)	C7B—C6B—C49B—C54B	−63.5 (4)
C54A—C49A—C50A—C51A	−4.1 (5)	N5B—C6B—C49B—C50B	−109.4 (3)
C6A—C49A—C50A—C51A	166.3 (3)	C7B—C6B—C49B—C50B	126.3 (3)
C49A—C50A—C51A—C52A	−0.2 (5)	C54B—C49B—C50B—C51B	−4.1 (5)

C50A—C51A—C52A—O19A	−173.0 (3)	C6B—C49B—C50B—C51B	166.1 (3)
C50A—C51A—C52A—C53A	4.7 (5)	C49B—C50B—C51B—C52B	−0.6 (5)
C72A—O19A—C52A—C51A	122.5 (3)	C50B—C51B—C52B—C53B	5.3 (5)
C72A—O19A—C52A—C53A	−55.3 (4)	C50B—C51B—C52B—O19B	−173.4 (3)
C51A—C52A—C53A—C54A	−4.8 (5)	C72B—O19B—C52B—C51B	123.9 (3)
O19A—C52A—C53A—C54A	172.9 (3)	C72B—O19B—C52B—C53B	−54.8 (4)
C52A—C53A—C54A—C49A	0.3 (5)	C51B—C52B—C53B—C54B	−5.2 (5)
C50A—C49A—C54A—C53A	4.1 (5)	O19B—C52B—C53B—C54B	173.4 (3)
C6A—C49A—C54A—C53A	−166.4 (3)	C52B—C53B—C54B—C49B	0.5 (5)
N8A—C9A—C55A—C57A	−61.8 (4)	C50B—C49B—C54B—C53B	4.1 (5)
C10A—C9A—C55A—C57A	170.7 (3)	C6B—C49B—C54B—C53B	−166.1 (3)
N8A—C9A—C55A—C56A	62.0 (4)	N8B—C9B—C55B—C56B	65.6 (4)
C10A—C9A—C55A—C56A	−65.5 (4)	C10B—C9B—C55B—C56B	−61.8 (4)
N14A—C15A—C58A—O15A	165.3 (2)	N8B—C9B—C55B—C57B	−59.0 (4)
C16A—C15A—C58A—O15A	46.2 (3)	C10B—C9B—C55B—C57B	173.6 (3)
N14A—C15A—C58A—C59A	−74.1 (3)	N14B—C15B—C58B—O15B	164.6 (2)
C16A—C15A—C58A—C59A	166.8 (3)	C16B—C15B—C58B—O15B	45.3 (3)
O15A—C58A—C59A—C64A	179.7 (3)	N14B—C15B—C58B—C59B	−74.9 (3)
C15A—C58A—C59A—C64A	57.2 (4)	C16B—C15B—C58B—C59B	165.9 (3)
O15A—C58A—C59A—C60A	−4.5 (4)	O15B—C58B—C59B—C64B	176.6 (3)
C15A—C58A—C59A—C60A	−126.9 (3)	C15B—C58B—C59B—C64B	54.0 (4)
C64A—C59A—C60A—C61A	1.0 (5)	O15B—C58B—C59B—C60B	−6.9 (4)
C58A—C59A—C60A—C61A	−175.0 (3)	C15B—C58B—C59B—C60B	−129.5 (3)
C59A—C60A—C61A—C62A	−1.7 (6)	C64B—C59B—C60B—C61B	1.8 (5)
C60A—C61A—C62A—C63A	0.8 (6)	C58B—C59B—C60B—C61B	−174.8 (3)
C61A—C62A—C63A—C64A	0.7 (5)	C59B—C60B—C61B—C62B	−1.8 (5)
C60A—C59A—C64A—C63A	0.5 (5)	C60B—C61B—C62B—C63B	0.6 (5)
C58A—C59A—C64A—C63A	176.4 (3)	C61B—C62B—C63B—C64B	0.7 (5)
C62A—C63A—C64A—C59A	−1.3 (5)	C62B—C63B—C64B—C59B	−0.7 (5)
N23A—C24A—C65A—C66A	57.7 (4)	C60B—C59B—C64B—C63B	−0.6 (5)
C25A—C24A—C65A—C66A	179.2 (3)	C58B—C59B—C64B—C63B	176.0 (3)
C24A—C65A—C66A—C68A	56.4 (4)	N23B—C24B—C65B—C66B	78.7 (4)
C24A—C65A—C66A—C67A	−179.0 (4)	C25B—C24B—C65B—C66B	−158.4 (4)
N29A—C30A—C69A—O16A	41.2 (3)	C24B—C65B—C66B—C68B	−62.7 (6)
C31A—C30A—C69A—O16A	163.8 (2)	C24B—C65B—C66B—C68C	6.1 (10)
N29A—C30A—C69A—C70A	167.6 (2)	C24B—C65B—C66B—C67B	166.4 (4)
C31A—C30A—C69A—C70A	−69.8 (3)	N29B—C30B—C69B—O16B	42.5 (3)
O16A—C69A—C70A—C71A	−153.5 (3)	C31B—C30B—C69B—O16B	164.3 (2)
C30A—C69A—C70A—C71A	82.2 (3)	N29B—C30B—C69B—C70B	168.8 (2)
O16A—C69A—C70A—C75A	29.3 (4)	C31B—C30B—C69B—C70B	−69.3 (3)
C30A—C69A—C70A—C75A	−94.9 (3)	O16B—C69B—C70B—C71B	−158.2 (3)
C75A—C70A—C71A—C72A	2.7 (5)	C30B—C69B—C70B—C71B	77.5 (3)
C69A—C70A—C71A—C72A	−174.5 (3)	O16B—C69B—C70B—C75B	24.2 (4)
C70A—C71A—C72A—C73A	−3.5 (5)	C30B—C69B—C70B—C75B	−100.1 (3)
C70A—C71A—C72A—O19A	175.5 (3)	C75B—C70B—C71B—C72B	2.6 (4)

C52A—O19A—C72A—C71A	−63.3 (4)	C69B—C70B—C71B—C72B	−175.1 (3)
C52A—O19A—C72A—C73A	115.7 (3)	C70B—C71B—C72B—C73B	−2.5 (5)
C71A—C72A—C73A—O17A	−177.0 (3)	C70B—C71B—C72B—O19B	176.5 (3)
O19A—C72A—C73A—O17A	4.0 (5)	C52B—O19B—C72B—C73B	120.4 (3)
C71A—C72A—C73A—C74A	1.9 (5)	C52B—O19B—C72B—C71B	−58.6 (4)
O19A—C72A—C73A—C74A	−177.1 (3)	C71B—C72B—C73B—O17B	−178.8 (3)
O17A—C73A—C74A—C75A	179.2 (3)	O19B—C72B—C73B—O17B	2.2 (5)
C72A—C73A—C74A—C75A	0.4 (5)	C71B—C72B—C73B—C74B	0.4 (5)
C73A—C74A—C75A—C70A	−1.1 (5)	O19B—C72B—C73B—C74B	−178.6 (3)
C71A—C70A—C75A—C74A	−0.4 (5)	O17B—C73B—C74B—C75B	−179.4 (3)
C69A—C70A—C75A—C74A	176.7 (3)	C72B—C73B—C74B—C75B	1.5 (5)
N32A—C33A—C76A—C77A	80.7 (3)	C73B—C74B—C75B—C70B	−1.3 (5)
C34A—C33A—C76A—C77A	−151.8 (3)	C71B—C70B—C75B—C74B	−0.7 (5)
C33A—C76A—C77A—O18A	39.1 (4)	C69B—C70B—C75B—C74B	176.9 (3)
C33A—C76A—C77A—N78A	−143.8 (3)	N32B—C33B—C76B—C77B	79.8 (3)
O35B—C2B—C3B—N36B	52.6 (3)	C34B—C33B—C76B—C77B	−153.3 (3)
C1B—C2B—C3B—N36B	−63.1 (3)	C33B—C76B—C77B—O18B	41.6 (4)
O35B—C2B—C3B—C4B	−71.3 (3)	C33B—C76B—C77B—N78B	−141.3 (3)
C1B—C2B—C3B—C4B	173.0 (2)		

CHAPTER 5

Conclusion

Marine microorganisms are not over exploited in respect with terrestrial microorganisms for natural product screening. This study was conducted to evaluate the productivity of structurally new natural products by marine bacteria. Marine bacteria were isolated from two different unexploited sources, stony corals and deep-sea water. Around 110 bacterial strains from different stony corals were screened for analyzing the production of unknown secondary metabolites. In addition, one strain from deep sea water was analyzed for new bioactive compounds. HPLC-UV chemical screening was employed to find structurally novel bioactive compounds from these marine bacterial strains. For the screening purpose, three types of seawater-based fermentation media (A3M, A11M and A16M) were used. In this study, I selected nine as candidate stains for the isolation of unknown secondary metabolites on the basis of their HPLC-UV chromatogram profile.

In this study, among nine bacterial species, three candidate strains produced seven structurally unique new compounds with potent biological activity. Three strains, first from *Microbulbifer*, isolated from a stony coral *Tubastraea*, and second from *Kocuria*, isolated from a stony coral *Mycedium*, and third from *Streptomyces*, isolated from suspended matter in deep sea water, were selected and subjected to metabolite analysis. The first candidate strain, *Microbulbifer* sp. DC3-6, isolated from a scleractinian (stony) coral *Tubastraea* sp. collected as fishery waste at −10 to −15 m near the coast of Minami-Ise, Mie Prefecture, Japan, was subjected to secondary metabolites screening. This strain was selected after a spectroscopic screening process using HPLC/UV analysis of 264 culture broths obtained by fermentation in three different media of 88 coral-associated bacteria. The 16S rRNA gene sequence analysis showed that strain DC3-6 belongs to the genus *Microbulbifer*. *Microbulbifer* is an unexplored genus of marine natural products. The genus *Microbulbifer* is marine obligate bacteria and cannot grow in culture media without NaCl. Chemical screening of fermentation broth of this stain DC3-6 led to the isolation of three new alkanoyl imidazoles, designated, bulbimidazoles A–C (**1**–**3**). These compounds are structurally quite rare and the second member of imidazole-containing natural products in which an alkyl chain and an imidazole ring are coupled through a ketone group. These compounds are also the third example of natural products discovered from marine Gammaproteobacterium *Microbulbifer*. According to the biosynthetic gene cluster database, bacteria belonging to this genus possess biosynthetic genes for the production of polyketide, non-ribosomal peptide, and terpenoid. But up to date, only three classes of natural products were reported from this unexploited bacterial taxon. Structures of bulbimidazoles were established on the basis of spectroscopic analysis including NMR and MS. The absolute configuration of the *anteiso*-methyl substituent of bulbimidazole A was determined by Ohrui-Akasaka method. All compounds showed strong antimicrobial activity against human pathogens *S. aureus*, *C. albicans*, and *T. rubrum*, a fish pathogen *T. maritinum*, and a plant

pathogen *G. cingulate*, with MICs in the ranges of 0.78 to 12.5 μg/mL. In addition, bulbimidazoles A–C exhibited moderate cytotoxicity against P388 murine leukemia cells with IC_{50} of 5.0, 5.8 and 7.0 μM, respectively. From this study, it can be concluded that phylogenetically distinct species such as *Microbulbifer* have ability to produce unique compounds with broad-spectrum of bioactivities for developing new drugs.

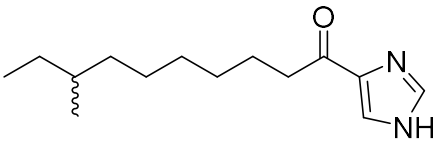

Bulbimidazole A (**1**) (*R*:*S* = 9:91)

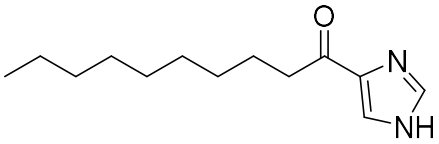

Bulbimidazole B (**2**)

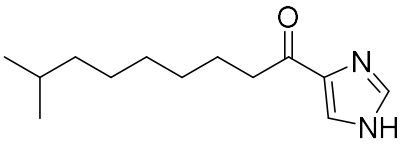

Bulbimidazol C (**3**)

The second candidate stran, *Kocuria* sp. T35-5, isolated from a scleractinian coral of the genus *Mycedium* sp. collected at −15 to −20 m from Tanjung Gelam, Karimunjawa National Park, Jepara, Central Java, Indonesia, was subjected to metabolite analysis. This strain was chosen through an HPLC-UV chemical screening of 78 culture broths obtained by fermentation in three different media of 26 bacteria associated with stony corals. The producing strain T35-5 was identified as a member of the genus *Kocuria* by phylogenetic analysis based on 16S rRNA gene sequence similarity. Similarly, chemical investigation of secondary metabolites from this marine-derived actinomycete strain led to discovery of two new alkanoyl imidazoles named as nocarimidazoles C and D, 4-acylated imidazoles of varying chain length and terminal branching, as well as three known compounds such as nocarimidazoles A and B, and bulbimidazole A. These alkanoyl imidazoles are distinct class of marine-derived natural products discoverd from common bacterial taxa. To the best of our knowledge, nocarimidazoles C and D are the third example of this class of rare alkanoyl imidazole natural products. Previously, the first two members in this class, nocarimidazoles A and B were obtained from a marine actinomycete *Nocardiopsis*, bulbimidazoles A–C were isolated from a marine gammaproteobacterium *Microbulbifer*. The structure of nocarimidazoles C and D established by NMR and MS data showed the presence of amino group

attached to the imidazole ring. The position of amino group was unequivocally established by application of $^{1}J_{CH}$ coupling constants. The absolute configurations of the anteiso-alkanoyl group present in nocarimidazole C, nocarimidazole B, and bulbimidazole A were determined by low-temperature HPLC analysis, demonstrating stereochemical diversity of anteiso-alkyl chains present in microbial natural products. All compounds exhibited moderate antimicrobial activity against Gram-positive bacteria and fungi, with MICs in the ranges of 6.25 to 12.5 μg/mL but were inactive against Gram-negative bacteria. In addition, nocarimidazoles B and C exhibited weak cytotoxicity against P388 murine leukemia cells with the IC_{50} of 38 and 33 μM, respectively. In this study, marine actinomycete strain of the genus *Kocuria* showed the ability to produce structurally rare class of natural products as well as stereochemical diversity of anteiso-alkyl branching. Therefore, there is still a chance to get more bioactive natural products even from common bacterial taxa collected from marine environment.

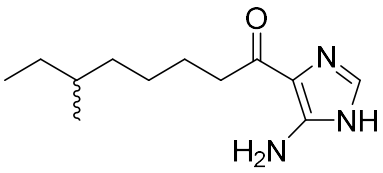

Nocarimidazole C (**4**) (*R*:*S* = 73:27)

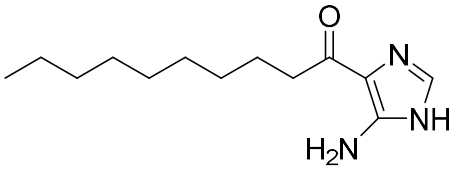

Nocarimidazole D (**5**)

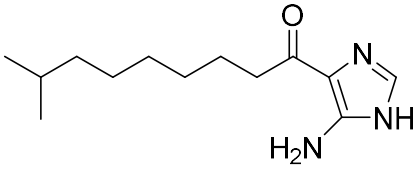

Nocarimidazole A (**6**)

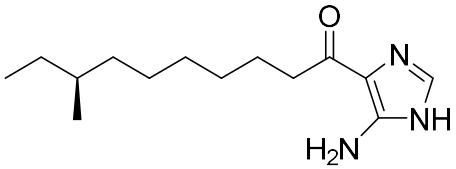

Nocarimidazole B (**7**) (*R*:*S* = 0:100)

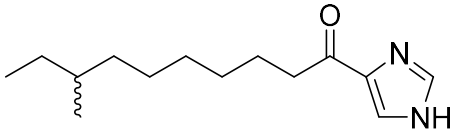

Bulbimidazole A (**1**) (*R*:*S* = 1:99)

The third candidate strain, *Streptomyces* sp. N11-34, isolated from suspended matter in deep-sea water of Toyama Bay, Japan, was subjected to metabolite analysis. The 16S rRNA gene sequence

analysis showed that strain N11-34 belongs to the genus *Streptomyces*. Chemical investigation for structurally novel secondary metabolites from this marine actinomycetes led to the discovery of two bicyclic peptides designated nyuzenamides A (**13**) and B (**14**). Their structures were established through the interpretation of NMR and MS data, which revealed eleven structural parts consisting of six standard amino acids, four unusual amino acids and one non-peptidic unit. The four unusual amino acids including β-hydroxyphenylalanine, β-hydroxytyrosine, 4-hydroxyphenylglycine, and α-hydroxyglycine in **13** and **14** are quite rare in nature. In addition to these amino acid residues, the non-peptidic units, 2-(isochroman-1-yl)acetyl moiety (Ica) and 2-(2-hydroxy-1-methoxypropyl)phenylpropenoyl group (Ppa), are also structurally rare in nature. The linkage pattern between two phenyl groups is unreported to date. Overall, no structurally similar compounds with these bicyclic peptides is reported. Both compounds showed selective antifungal activity against plant and human pathogens, *Glomerella cingulata* NBRC5907 and *Trichophyton rubrum* NBRC5467, with MIC ranging from 3.1 to 25 μg/mL, respectively. In addition, **13** and **14** exhibited moderate cytotoxicity against P388 murine leukemia cells with IC_{50} 4.9 and 6.2 μM. These structurally unprecedented bicyclic peptides was isolated from DSW derived *Streptomyces*. This most productive genus possesses the average genome size of 6 to 8 Mbp and biosynthetic machineries for secondary metabolites in *Streptomyces* are much more diverse than other prokaryotic organisms. Based on this study, it should be noticed that even from common type of diverse bacterial taxa, collected from most extreme ecosystem such as marine source, there still have a high chance to get bioactive compounds with unique structure. In addition, the structural diversity of nyuzenamides provides new scaffolds for the discovery and development of next generation drugs for treating various human diseases.

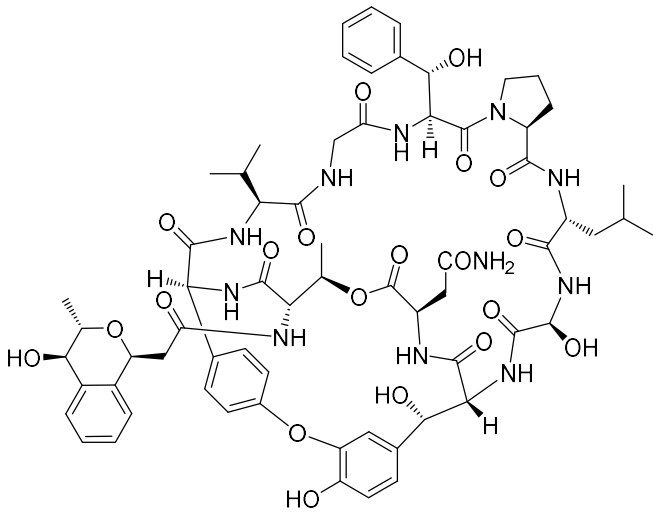

Nyuzenamide A (**13**)

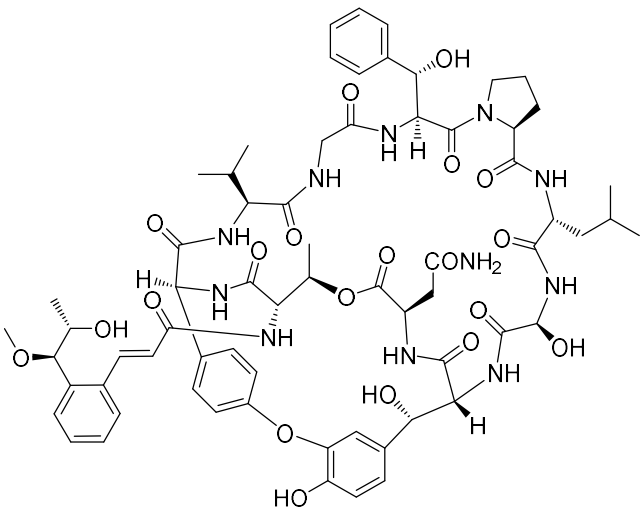

Nyuzenamide B (**14**)

In summary, three bacterial strains, *Microbulbifer*, *Kocuria* and *Streptomyces*, were used to analyze the secondary metabolites. Chromatographic separation of the fermented products and NMR-based structure analysis led to the discovery of seven structurally novel bioactive compounds, including three structurally rare antimicrobial alkanoyl imidazoles, designated bulbimidazoles A–C (**1–3**) from unexploited bacterial genus *Microbulbifer* collected from stony coral, another two new members of alkanoyl imidazoles, namely, nocarimidazoles C(**4**) and D (**5**) and three related known metabolites nocarimidazoles A–B (**6–7**) and bulbimidazole A (**1**) with the antimicrobial activity from *Kocuria* obtained from stony coral, and two new antifungal bicyclic peptides, nyuzenamides A (**13**) and B (**14**) possessing several unusual structural features from *Streptomyces* sp. isolated from suspended matter in deep sea water. All of these structurally rare compounds were discovered from marine bacteria. My research results displayed that finding of structurally new bioactive compounds needs to be concentrated on unique, extreme, underexplored sources. For new bioactive compounds discovery, researchers should consider to work underestimated sources such as marine ecosytem. In my study, the results substantiate that marine bacterium are promising resource for screening for new drug lead discovery.

Acknowledgments

I would like to express my deepest appreciation for my advisor Professor Yasuhiro Igarashi, Toyama Prefectural University, for his guidance, supervision, continuous encouragement, and valuable advice in completing this work.

In addition, I would like to express my gratitude to Lecturer Naoya Oku and Assistant Professor Enjuro Harunari, Professor Daisuke Urabe, Dr. Tao Zhou, and Dr. Amit Raj Sharma, Toyama Prefectural University, for their valuable advice and warm encouragement throughout this work.

Acknowledgments are also made to co-authors: Assoc. Prof. Yasuko In, Osaka University of Pharmaceutical Sciences, and Prof. Kazuaki Akasaka, Shokei Gakuin University and Dr. Mada Triandala Sibero, Diponegoro University, Indonesia.

I greatly appreciate all members of Laboratory of Microbial Engineering, Department of Biotechnology, Toyama Prefectural University.

I would like to thank the Ministry of Education, Culture, Sports, Science and Technology (MEXT) of Japan for the Japanese government (Monbukagakusho) scholarship, which supported my stay at Toyama Prefectural University.

Finally, I extend my gratitude to my parents and family members for their prolonged inspiration, continue support, love, and patience, which made this work possible and successful.

Publication List

1. Bulbimidazoles A−C, antimicrobial and cytotoxic alkanoyl imidazoles from a marine gammaproteobacterium *Microbulbifer* species.
   Md. Rokon Ul Karim, Enjuro Harunari, Naoya Oku, Kazuaki Akasaka, and Yasuhiro Igarashi
   Journal of Natural Products **2020**, *83*, 1295-1299
2. Nocarimidazoles C and D, antimicrobial alkanoylimidazoles from a coral-derived actinomycete *Kocuria* sp.: application of $^{1}J_{C,H}$ coupling constants for the unequivocal determination of substituted imidazoles and stereochemical diversity of anteisoalkyl chains in microbial metabolites.
   Md. Rokon Ul Karim, Enjuro Harunari, Amit Raj Sharma, Naoya Oku, Kazuaki Akasaka, Daisuke Urabe, Mada Triandala Sibero, and Yasuhiro Igarashi
   Beilstein Journal of Organic Chemistry **2020**, *16*, 2719-2727
3. Nyuzenamides A and B, bicyclic peptides with anti-fungal and cytotoxic activity from a marine-derived *Streptomyces* sp.
   Md. Rokon Ul Karim, Yasuko In, Tao Zhou, Enjuro Harunari, Naoya Oku, and Yasuhiro Igarashi
   Organic Letters **2021**, *23*, 2109–2113